Doctoral theses at NTNU, 2016:110

Tonje Husby Haukaas

Metabolic profiling of breast cancer using *ex vivo* MR spectroscopy

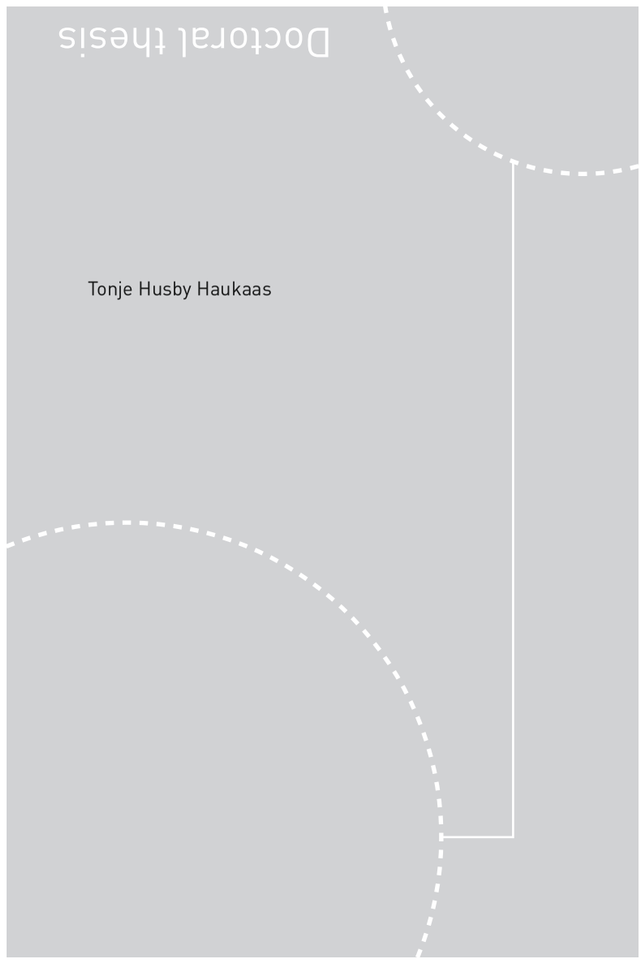

ISBN 978-82-326-1558-2 (printed ver.)
ISBN 978-82-326-1559-9 (electronic ver.)
ISSN 1503-8181

NTNU
Norwegian University of
Science and Technology

NTNU
Norwegian University of
Science and Technology
Thesis for the Degree of
Philosophiae Doctor
Faculty of Medicine
Department of Circulation
and Medical Imaging

Doctoral theses at NTNU, 2016:110

NTNU
Norwegian University of
Science and Technology

NTNU

Tonje Husby Haukaas

Metabolic profiling of breast cancer using *ex vivo* MR spectroscopy

Thesis for the Degree of Philosophiae Doctor

Trondheim, April 2016

Norwegian University of Science and Technology
Faculty of Medicine
Department of Circulation and Medical Imaging

NTNU
Norwegian University of
Science and Technology

NTNU
Norwegian University of Science and Technology

Thesis for the Degree of Philosophiae Doctor

Faculty of Medicine
Department of Circulation and Medical Imaging

ISBN 978-82-326-1558-2 (printed ver.)
ISBN 978-82-326-1559-9 (electronic ver.)
ISSN 1503-8181

Doctoral theses at NTNU, 2016:110

Printed by NTNU Grafisk senter

Metabolsk profilering av brystkreft ved hjelp av *ex vivo* MR spektroskopi

Til tross for tidligere oppdagelse og forbedret behandling er brystkreft fortsatt den nest hyppigste årsaken til kreftrelatert død blant kvinner på verdensbasis. Årlig blir over 3000 kvinner diagnostisert med brystkreft i Norge. Det forskes mye for å finne underliggende mekanismer som bidrar til den komplekse heterogeniteten observert i brystkreft. Dette har ført til oppdagelsen av flere subtyper av brystkreft, inkludert histologiske og genetiske subtyper, med forskjellige egenskaper og prognose, noe som forsterker hypotesen om at brystkreft ikke er én, men en samling av flere sykdommer.

Kreftceller må være i stand til å omdanne næringsstoffer til biomasse samtidig som energi produseres, noe som krever reprogrammering av sentrale metabolske prosesser i cellene. Dette fenomenet er foreslått som et potensielt mål for behandling, samtidig som det kan være en kilde til biomarkører som kan forutsi prognose og risiko og brukes til å overvåke behandlingsrespons. MR metabolomikk er et mye brukt verktøy som kan identifisere klinisk relevante metabolske markører og gi ny forståelse for den molekylære biologien i svulstene. *Ex vivo* proton høy-oppløsning MR spektroskopi (HR MAS MRS) er en ikke-destruktiv metode som gir høyoppløselige MR spektra fra biologisk vev: Prøven forblir intakt for videre analyser som genetiske analyser, genuttrykksanalyser og/eller histopatologi. HR MAS MRS er mye brukt til å studere sentrale metabolske prosesser som er relatert til kreftprogresjon, inkludert fosfolipidmetabolisme, glykolyse og metabolismen av aminosyrer og polyaminer. Mer enn 30 metabolitter kan detekteres samtidig i et HR MAS spektrum fra brystkreftvev og de metabolske profilene målt ved hjelp av denne metoden har blitt vist å korrelere med tumorgrad, lymfeknute- og hormonreseptorstatus, behandlingsrespons og pasientoverlevelse.

For å oppnå robuste data med høy kvalitet krever MR metabolomikk bevissthet rundt eksperimentelle detaljer. Det er svært viktig at prøvene behandles og prepareres på en optimal måte for å oppnå kvalitetssikre resultater. I artikkel I ble tumorvev fra xenograftmodeller brukt for å vurdere de metabolske endringene forårsaket av tidsintervallet fra tumorene fjernes frem til de hurtigfryses for lagring (frysetid-forsinkelse). Studien viste at de metabolske profilene var robuste for forsinkelser på opp til 30 minutter. Videre viste den metabolske effekten av

langvarig MR analyse viktigheten av standardiserte protokoller og begrensning i analysetid.

I artikkel II avslørte analyse av metabolske profiler tre naturlige metabolske grupper av brystkrefttumorer. Når gruppene ble kombinerte med data fra genuttrykk- og proteinuttrykksanalyser, viste de i tillegg forskjeller i nivået av gener og proteiner involvert i ekstracellulær matrix. Forskjellene i genuttrykk kunne også forklare noen av de metabolske forskjellene observert mellom gruppene. De etablerte genetiske subtypene var jevnt fordelt blant de tre gruppene, noe som dermed betyr at de metabolske gruppene kan bidra med tilleggsinformasjon som kan forklare noe av heterogeniteten observert i brystkreft.

I artikkel III ble de metabolske effektene av neoadjuvant kjemoterapi med eller uten angiogenesehemmeren bevacizumab undersøkt hos brystkreftpasienter. Tydelige metabolske endringer som et resultat av behandlingen ble observert. I tillegg kunne de metabolske profilene i tumorene ved operasjon skille pasienter som hadde oppnådd patologisk minimal residual sykdom fra pasienter med ikke-responderende tumorer. Selv om administrering av bevacizumab ikke viste noe tydelig metabolsk endring ble det observert at metabolismen av glutation antakelig ble påvirket. Samlet viser dette at metabolske profiler kan komplementere andre molekylære nivå for kartlegging av underliggende mekanismer som påvirker patologisk respons, og i tillegg gi informasjon om tumorens metabolske respons på behandling.

Totalt sett har arbeidet i denne avhandlingen vist at metabolske profiler bestemt ved hjelp av MR spektroskopi av tumorvev kan bidra til å karakterisere heterogenitet utover genetiske subtyper, så vel som å bidra med verdifull informasjon under overvåkning av respons på neoadjuvant behandling. Ved å kombinere metabolsk data med andre plattformer (f.eks. genuttrykk- og proteinuttrykksanalyser) kan man finne nye molekylære mål som kan brukes til å utvikle behandlingsstrategier som angriper på flere molekylære nivå.

Kandidat: Tonje Husby Haukaas
Institutt: Institutt for sirkulasjon og bildediagnostikk
Veiledere: Prof. Tone Frost Bathen og Dr. Guro Fanneløb Giskeødegård
Finansieringskilde: K. G. Jebsen-senter for brystkreftforskning

Ovennevnte avhandling er funnet verdig til å forsvares offentlig for graden Philosophiae Doctor i medisinsk teknologi.
Disputas finner sted i Auditoriet MTA, Medisinsk-Teknisk Forskningssenter, Torsdag 28. April 2016 kl. 12:15.

Acknowledgement

The work presented in this thesis is based on work carried out in the MR Cancer group, Department of Circulation and Medical imaging, Norwegian University of Science and Technology (NTNU), between January 2012 and January 2016. The financial support of my work was provided by K. G. Jebsen Center for Breast Cancer Research.

I would like express gratitude to all the women who have contributed with tumor material for research used in this study.

There are so many people that have helped and supported me in achieving this thesis. First of all I would like to thank my main supervisor Prof. Tone Frost Bathen for believing in me and for always taking the time to give feedback to my work and discuss different subjects. You have encouraged me and given excellent guidance throughout my period as a PhD student. Thank you so much! Second, I would like to thank my co-supervisor Dr. Guro F. Giskeødegård for your positive attitude and for always contributing with great input, especially with your expertise in multivariate analysis. I would also like to thank Prof Ingrid Gribbestad for founding the MR Cancer group and believing that I could contribute to it. I hope this thesis have made you all proud.

A special acknowledgement goes to all my former and current coworkers in the MR Cancer group. Torill, Tina, Øystein, Trygve, Marius, Kirsten, Riyas, Mattijs, Morteza, Eugene, Debbie, Guro, May-Britt, Siver, Tone, Maria, Jana, Brage, Gabriel, Hanna Maja, Liv, Mingshu, Jose, Igor, Ioanna, Torfinn, Saurabh, Maria Karoline, Ailin, Leslie, Elise and Marie, I feel privileged to be part of such a friendly and resourceful research group and I have enjoyed working with all of you. Thank you Leslie for always taking the time to help me and for all your support before and during the submission process. Thank you Marie and Debbie for valuable feedback on my thesis. A special thanks goes to my office mates and to Jana and Shalini for all the friendly discussions, your positive encouragements and many helpful advice.

I would also like to thank my coauthors, especially my collaborators in Oslo. Thank you, Prof. Anne-Lise Børresen-Dale, Dr. Kristine K. Sahlberg, Dr. Miriam R. Aure and Eldri U. Due for valuable suggestions and interesting discussions.

Finally, this thesis could not have been completed without the love and support from my dear family and friends. My mom and dad, Mary-Ann and Tor, have always

supported me and encouraged me to fulfill my dream of taking a PhD. My sister Iselin has made me confident by telling me how proud she is of me and motivated me to keep up the hard work. The greatest inspiration though, has been my dear husband Johnny and my daughter Mila. Thank you both for your love and patience and for making me want to work efficiently so that I could spend as much time as possible with you two.

Tonje Husby Haukaas
Trondheim, April 2016

Summary

Despite progress in early detection and therapeutic strategies, breast cancer remains the second leading cause of cancer-related death among women globally. Annually, more than 3000 women are diagnosed with breast cancer in Norway. Much effort has been made to find underlying mechanisms contributing to the complex heterogeneity observed in breast cancer. This has led to the discovery of several subtypes of breast cancer, for example histological and genetic subtypes, with different traits and prognosis, supporting that breast cancer is not one disease but in fact multiple diseases.

Cancer cells must be able to convert nutrients to biomass while maintaining energy production, which requires reprogramming of central metabolic processes in the cells. This phenomenon is increasingly recognized as a potential target for treatment, but also as a source for biomarkers that can be used for prognosis, risk stratification and therapy monitoring. MR metabolomics is a widely used approach in translational research, aiming to identify clinically relevant metabolic biomarkers or generate novel understanding of the molecular biology of tumors. *Ex vivo* proton high-resolution magic angle spinning (HR MAS) MR spectroscopy is a non-destructive and high-throughput technique that provides highly resolved MR spectra from biological tissue, leaving the sample intact for further analysis, such as genomics, transcriptomics and/or histopathology. HR MAS MRS is widely used to study central metabolic processes related to cancer progression, including choline phospholipids metabolism, glycolysis and metabolism of amino acids, lipids and polyamines. More than 30 metabolites can be detected and assigned simultaneously in a HR MAS spectrum of breast cancer tissue. The metabolic profiles acquired by HR MAS MRS have shown to correlate to tumor grade, lymph node and hormone receptor status, treatment response and patient survival in breast cancer.

Generating robust and valid data using MR metabolomics requires close attention to experimental details. For valid interpretation of the results, consistent sample collection and preparation is crucial. In paper I, tumor tissue from xenograft models were used to evaluate the metabolic changes caused by the time interval from surgical removal of a tumor until it is snap-frozen for storage (freezing delay time). The study showed that the metabolic profile was robust to freezing delay times up to 30 minutes. Furthermore, the metabolic effect of prolonged MR analysis demon-

strated the importance of using standardized protocols and limiting the analytical time.

In paper II, analysis of tumor metabolic profiles revealed three naturally occurring metabolic clusters of breast cancer tumors. When combined with transcriptomic and proteomic data, the clusters showed differences in expression of genes and proteins involved in the extracellular matrix. Additional gene expression differences explaining some of the observed metabolic differences between the clusters were also observed. Interestingly, genetic subtypes were evenly distributed among the three metabolic clusters, which therefore could contribute additional information beyond the intrinsic gene sets for understanding breast cancer heterogeneity.

In paper III, the metabolic effects of neoadjuvant chemotherapy with or without the antiangiogenic agent bevacizumab in breast cancer patients were explored. Distinct metabolic alterations due to treatment could be observed. In addition, tumor metabolic profiles at surgery could discriminate patients achieving pathologcal minimal residual disease from non-responders. Although bevacizumab administration did not show any prominent metabolic differences, glutathione metabolism was found to possibly be affected. Together, this shows that metabolic profile may complement other molecular levels for the elucidation of the underlying mechanisms affecting pathological response, and may additionally provide information on tumor metabolic response to treatment.

In conclusion, MR determined metabolic profiles of tumor tissue have been shown to characterize breast cancer heterogeneity beyond genetic subtypes as well as to provide valuable information when monitoring response to neoadjuvant chemotherapy. The approach of combining metabolic data with other platforms (e.g. transcriptomics and proteomics) may further provide targets for investigation of new treatment strategies at different molecular levels.

Symbols & Abbreviations

Symbol	Description	Page
2DG	2-deoxy-D-glucose	59
μ	Magnetic momentum of a precessing nucleus	13
γ	Gyromagnetic ratio	13
B_0	External static magnetic field	13
ATP	Adenosine triphosphate	10
CHKA	Choline kinase alpha	54
CDP	Cytidyldiphosphate	11
CPMG	Carr-Purcell-Meiboom-Gill pulse sequence	15
CT	Computed tomography	62
DAG	Diacylglycerol	11
ECM	Extracellular matrix	57
ER	Estrogen receptor	5
HER2	Human epidermal growth factor 2	5
HES	Hematoxylin-Eosin-Safron	34
HKs	Hexokinases	59
GLS	Glutaminase	55
GPC	Glycerophosphocholine	11
GR	Good response	37
GSEA	Gene set enrichment analysis	41
I	Nuclear spin number	13
IDC	Invasive ductal carcinoma	4
ILC	Invasive lobular carcinoma	4
LMM	Linear mixed model	29
LV	Latent variable	25
MAS	Magic angle spinning	17
MICE	Multivariate imputation by chained equation	40
MRI	Magnetic resonance imaging	37
MRS	Magnetic resonance spectroscopy	13
MS	Mass spectrometry	63
NOESY	Nuclear Overhauser effect spectroscopy	15
NR	No response	37

FFT	Fast fourier transformation	20
FID	Free induction decay	14
PBS	Phosphate buffered saline	38
PCA	Principal component analysis	23
PCho	Phosphocholine	11
pCR	pathological complete response	37
PET	Positron emission tomography	52
PgR	Progesteron receptor	5
PLD	PtdCho-spesific phospholipase D	54
PLS-DA	Partial least squares	25
pMRD	pathological minimal residual disease	37
pNR	pathological non-responder	37
PtdCho	Phosphatidylcholine	11
ppm	Parts per million	14
PQN	Probabilistic quotient normalization	20
RECIST	Response evaluation criteria for solid tumours	6
RF	Radio frequency	14
ROS	Reactive oxygen species	56
RPPA	Reverse phase protein array	9
SAM	Significance analysis of microarrays	41
T_1	Longitudinal relaxation	14
T_2	Transverse relaxation	14
TCA	Tricarboxylic acid	10
tCho	Total-choline	54
TNBC	Triple negative breast cancer	8
TNM	Tumor size (T), degree of spread to lymph nodes (N), distant metastasis (M)	4
TSP	Trimethylsilyl propionic acid	38
VEGF	Vascular endothelial growth factor	6

List of Papers

Paper I

Impact of freezing delay time on tissue samples for metabolomic studies.

Haukaas TH*, Moestue SA*, Vettukattil R, Sitter B, Lamichhane S, Segura R, Giskeødegård GF, Bathen TF (2016). *Shared first authorship

Frontiers in Oncology 6(17): doi: 10.3389/fonc.2016.00017

Paper II

Metabolic clusters of breast cancer in relation to gene- and protein expression subtypes.

Haukaas TH, Euceda LR, Giskeødegård GF, Lamichhane S, Krohn M, Jernströ m S, Aure MR, Lingærde OC, Schlichting E, Garred Ø, Due EU, OSBREAC, Mills GB, Sahlberg KK, Børresen-Dale A-L, Bathen, TF

Submitted to Cancer & Metabolism 2016.

Paper III

Evaluation of metabolomic changes during neoadjuvant chemotherapy combined with bevacizumab in breast cancer using MR spectroscopy.

Euceda LR, Haukaas TH, Giskeødegård GF, Vettukattil R, Engel J, Silwal-Pandit L, Lundgren S, Postma G, Buydens LMC, Børresen-Dale A-L, Bathen TF

Submitted to Neoplasia 2016

Contents

List of Figures

List of Tables

1 Introduction

1.1 Cancer

Cancer is a collection of over 100 diseases where genetic alterations (mutations) cause cells to grow and divide uncontrollably and lose regulation of important cellular processes. These characteristics and accumulating mutations can potentially lead to cancer cells invading nearby or distant areas from the cancer's primary site [1]. Invasion of distant locations, also known as metastasis, can happen through blood or lymph vessels and is the main reason for cancer death due to disruption of important and essential functions of the organs it metastasizes to. Based on the most recently reported cancer statistics, it was estimated that 14.1 million new cancer cases were diagnosed in 2012 world wide [2]. The same year, cancer was the leading cause of 8.2 million deaths.

Although there is huge complexity and variety in characteristics among the different cancer types as well as within distinct cancer types, there has been proposed six essential alterations necessary for malignant growth [1] illustrated in Figure 1.1a. During tumor development cancer cells establish characteristics of avoiding apoptosis (programmed cell death), they become self-sufficient of growth signals and insensitive to anti-growth signals, they can potentially invade tissue and metastasize, they have limitless replicative potential and they sustain angiogenesis (blood vessel supply). More recently, two emerging hallmarks were suggested including deregulation of cellular energetics and avoiding immune destruction as illustrated in Figure 1.1b [3].

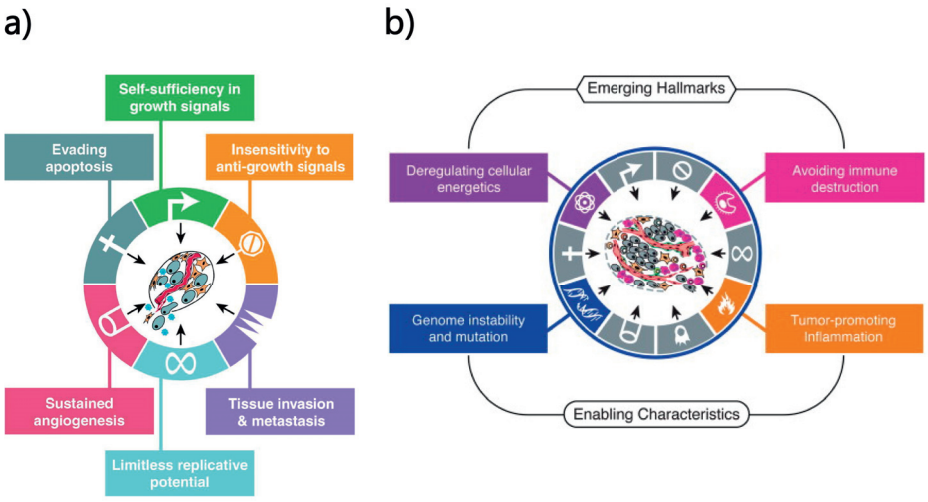

Figure 1.1: Hallmarks and enabling characteristics of cancer. a) The six biological characteristics of cancers acquired during development of human tumors. b) The two emerging hallmarks and enabling characteristics of cancer. The figure is adapted from [1] and [3] with permission.

1.2 Breast Cancer

Breast cancer is the most frequently diagnosed cancer among women worldwide [4] and in Norway it has been estimated that one out of twelve women will develop this disease by the age of 75 [5]. Although trends show decreasing mortality in several countries [4] and almost 90 % of women diagnosed in Norway still are alive 5 years after the diagnosis [5], it is difficult to predict each breast cancer patient's outcome. Patients with the same diagnosis of breast cancer may have different response to treatment, underpinning the need to further characterize breast cancer heterogeneity.

1.2.1 Etiology and screening

Although there still is a lack of knowledge regarding the direct etiology for developing breast cancer, known risk factors are hereditary, age, hormonal circumstances (early menarche, late first-time birth, nulliparity, late menopause, estrogen use before the age of 35, longterm post-menopausal estrogen therapy), obesity and alcohol consumption. Factors reducing the risk include early first pregnancy, multiple pregnancies, breastfeeding and regular exercise [6, 7]. In addition, there are higher incidence rates in developed countries, believed to be due to environmental factors [4] as well as increased screening [5]. In Norway, all women in the age of 50-69 are advised to take part in a program with mammography screening every second year aiming to detect breast cancer at an early stage and thereby reducing the mortality. This program was gradually implemented within the years of 1995-2005. Based on a prospective cohort study evaluating the effectiveness of mammography screening, it was reported that such a program could reduce breast cancer mortality by about 28% [8].

1.2.2 Anatomy and pathology

The female breast consists of fatty tissue, connective tissue, lobes, lobules, ducts and lymph nodes (Figure 1.2). Each of the 15 to 20 lobes is made up by several small lobules, the functional unit of the breast which produce milk in nursing women. These lobes are connected to ducts that transport the milk from the lobule to the nipple. Lymph nodes and lymph vessels containing immune system cells surround the breast and contribute to removing waste products.

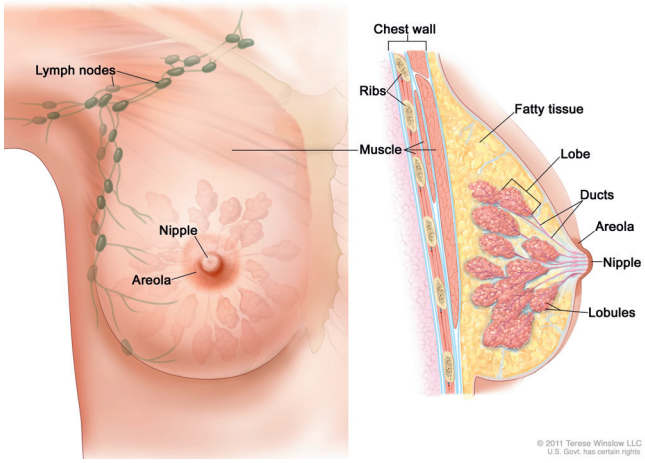

Figure 1.2: The anatomy of the female breast. The female breast consists of nipple, areola and lymph nodes (left) and fatty tissue, lobe, ducts and lobules (right). Reproduced with permission from Terese Winslow LLC.

In some rare cases (less than 1%) the cancer arises from stromal components (connective tissue) within the breast (i.e. sarcomas) [9], however, breast cancer normally originates from epithelial cells and are thus called breast carcinomas. The premalignant changes where the epithelial cells have not broken through the basement membrane, are classified into hyperplasia (atypical or non-atypical) or carcinoma in situ. If cancer cells have broken the basement membrane and invaded surrounding tissue, it is classified as invasive carcinoma [10]. Invasive carcinomas are the most common type of breast cancer [11], where between 72-80% are invasive ductal carcinomas (IDC) and 5-15% are invasive lobular carcinomas (ILC) [12]. Other important subtypes of invasive breast carcinomas include medullary carcinoma, mucinous carcinoma, intracystic and tubular carcinoma [11].

1.2.3 Diagnosis and treatment

During the diagnostic process, breast cancer patients in Norway are examined by three main strategies [10]; clinical examination, image diagnostics and needle biopsy. This is followed by classification into stage I-IV using the TNM-system where tumor size (T), degree of spread to lymph nodes (N) and existence of distant metastasis (M) are considered. T0 is used for cases where no primary tumor is classified, Tis represents carcinoma in situ and T1-T4 reports increasing size of the tumor. N0-

N3 report the number and location of detected lymph node metastasis and finally, the status of detected distant metastasis is reported as either M0 (no apparent metastasis) or M1 (metastasis). Based on the TNM classification, the tumor is defined as primary operable or inoperable [10].

In addition to finding anatomical features of the tumor, histopathological grade gives information of the tumor cells degree of differentiation, a measure that has well-established prognostic value [13]. Grade 1-3 tumors consist of well, moderately and poorly differentiated cancer cells, respectively. The growth and function of the tumor is a result of several factors. Thus, histopathological examination also include assessment of the tumor's expression of estrogen receptor (ER), progesterone receptor (PgR), human epidermal growth factor 2 (HER2) and, in some cases, proliferation (by the Ki67 marker). The hormone receptors ER and PgR are transcription factors depending on binding of their ligand (the hormones estrogen and progesterone, respectively) for activation of important proliferation processes and production of growth factors [14]. As ER activation also regulates the PgR-gene, less than 1% of PgR-positive (PgR+) cases are ER-negative (ER−) [15]. Over-expression of ER and/or PgR are found in approximately 70-80% of all breast cancer cases [16, 17], which due to their dependency of hormonal stimuli can be treated with validated treatment targets, and have a better prognosis than hormone receptor negative patients [16]. Over-expression of the tyrosine kinase associated receptor HER2, and amplification of its gene *ERBB2*, is found in 15-23% of all breast cancers [18]. HER2 over-expression is associated with aggressiveness and poorer prognosis, however, targeted anti-HER2 treatment improves the progression free survival and overall survival [19]. In addition to these well-establish molecular characteristics, Ki67 is an emerging biomarker for proliferation, present in cells preparing for division [15].

The main treatment strategy for patients with primary operable tumors is surgical removal of the tumor followed by adjuvant treatment according to clinical findings. Patients undergoing breast conserving surgery, that have unclear margins after mastectomy or findings of lymph node involvement are recommended to be treated with local radiotherapy. Depending on age, hormone receptor-, HER2- and Ki67 status, the treatment regimen can also include systemic treatment in form of endocrine treatment for receptor positive cancers, anti-HER2 treatment for HER2-positive (HER2+) and chemotherapy. Tamoxifen is a well-established anti-estrogen treatment where an antagonist of estrogen will compete with estrogen for receptor

binding, and thereby inhibit its activation. For post-menopausal women with ER+ tumors, aromatase inactivator or inhibitor is given, to block the formation of estrogen. Patients with HER2+ tumors are given treatment with monoclonal antibody Herceptin®(trastuzumab). This antibody binds to the extracellular domain of the HER2-receptor resulting in inhibition of cell growth.

Chemotherapy is given to kill rapidly dividing cells by attacking DNA and therby impair cell division. In general, three different regimens of chemotherapy are used [10]; CMF combination (cyclophosphamide, metotrexate and fluorouracil), anthracycline chemotherapy and regimens combining taxanes and anthracycline chemotherapy. In Norway, the Norwegian Breast Cancer Group have concluded that the general basis for adjuvant chemotherapy should be anthracycline chemotherapy, usually by FEC (fluorouracil, epirubicin and cyclophosphamide). Anti-angiogenic agents that attacks the formation of new blood vessels into the tumor (i.e. angiogenesis) are being studied for possible improvement of treatment when included in existing regimens. The blood supply will give tumors nutrients and oxygen required to grow beyond a few millimeters in size in addition to anabling metastasis. Due to this, angiogenesis is an established hallmark of cancer [1] and attractive target for cancer treatment. One example is bevacizumab, also known as Avastin®, which blocks the binding of vascular endothelial growth factor (VEGF) to its receptors [20].

Patients diagnosed with primary inoperable tumors are treated with neoadjuvant therapy prior to surgery. The treatment regimens discussed above may then be used pre-surgery to make the tumor operable or to allow for breast conserving surgery. During or after neoadjuvant treatment, the tumor response can be evaluated by physicians. The two most commonly used guidelines for assessing the response are the Response Evaluation Criteria for Solid Tumours (RECIST) and the guidelines from World Health Organization (WHO) [21]. These guidelines are used to classify the response into complete response, partial response progressive disease or stable disease. Studies have shown a association between tumor response and clinical outcome where pathological complete response where a prognostic indicator for overall survival, disease-free survival and relapse-free survival [22].

1.3 The omics of breast cancer

In normal cells, biological processes necessary for cellular function, including DNA repair, cell cycle, differentiation, growth, proliferation, apoptosis, cell migration and cell-to-cell contact, are tightly regulated by complex molecular networks. In cancer, many networks are dysregulated, causing rapid cell proliferation and potentially metastasis. The loss of control is caused by a multistep process where genetic mutations accumulate, predominantly in somatic cells, making cancer an age-related genetic disease [23]. Of all breast cancer cases, approximately 5% are due to inherited mutation in tumor suppressor genes *BRCA1* or *BRCA2*. These mutations will increase the lifetime risk for developing breast and ovarian cancer with over 80% and 40-60%, respectively [24]. Examples of other important inheritable mutations increasing the risk of developing breast cancer are *TP53* and *PTEN*.

Both in normal cells and cancer cells, DNA is transcribed into mRNA transcripts which further can be translated into proteins taking part in molecular pathways and thus controlling the level of metabolites, which will be described in more detail in section 1.3.3. Although additional factors, such as epigenetic alterations, affect and further complicate the flow of this process, the basic principle can be summarized in Figure 1.3.

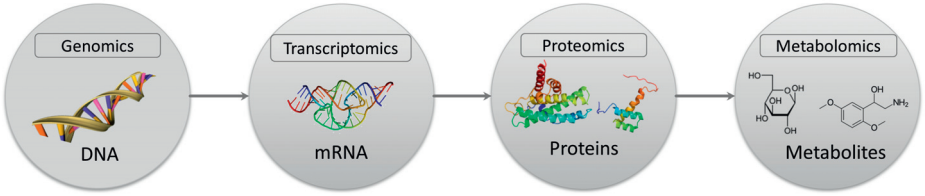

Figure 1.3: Illustration of the omics cascade. The omics flow of information from DNA and genomics to metabolites and metabolomics

1.3.1 Transcriptomics and intrinsic genetic subtypes

The field of transcriptomics studies gene expression trough measuring the transcripts of DNA called mRNA. It has been estimated that between 20 000-25 000 protein coding genes exists within the human DNA [25]. However, which genes are transcribed into protein coding transcripts at a given time is dependent on several factors, e.g. cell type, cell function, epigenetic events and existing mutations.

Depending on the tumor mRNA levels from a set of intrinsic genes with high inter-patient and low intra-patient variation before and after treatment of breast cancer patients, five genetic subtypes have been reported [26, 27]. The intrinsic subtypes, luminal A, luminal B, HER2-enriched, basal-like and normal-like, have characteristic differences in gene expression pattern that correlate with tumor characteristics and clinical outcome [27]. The frequencies of the subtypes varies among ethnicity and age, but in general, luminal A is the most common subtype followed by basal-like, HER2-enriched and luminal B [28].

Both of the luminal subtypes are typically hormonal receptor positive with important differences in the proliferation signature and the rate of relapse-free survival. Luminal A cancers are considered a good prognosis group because of the association with lower expression of proliferating genes and longer relapse-free survival than luminal B cancers. Although the majority of luminal cases are HER2−, approximately 9% and 21% of luminal A and luminal B, respectively are HER2+ [29]. Basal-like and HER2-enriched subtypes have been associated with poorer prognosis and shorter survival times [27]. Most of basal-like cancers are triple negative breast cancers (TNBC), i.e. ER−/PgR−/HER2−, but also here there are variability with 6-29% being ER+ and 9-13% being HER2+ [27]. An additional rare gene expression subtype called claudin-low has been suggested [30], with several similarities to the genetic profile of basal-like, but with lower expression of a set of cell-to-cell adhesion proteins and higher expression of genes linked to immune system response. One of the main characteristics of the HER2-enriched subtype is over-expression of *ERBB2* and a group of adjacent located genes, although this is not the case for all tumors classified within this subtype [28]. The normal-like subtype resembles the gene expression of tissue samples from normal breast cancer samples. A centroid based identifier called PAM50 has been developed where prediction analysis of microarrays (PAM) of 50 genes is used to predict and classify breast cancer into one of the five subtypes [31].

1.3.2 Proteomics and protein expression subtypes

Proteins are the functional product of genes and become the workers of cellular pathways and networks controlling cell function as well as cell malignancy [23]. Genetic alterations could possibly affect the activity, function or abundance of proteins directly. Additionally, protein expression and activity are not solely results of gene expression level (i.e. mRNA level), but a product of several ongoing processes,

e.g. post-transcription modification processes. Studies of proteomic profiles within breast cancer as well as cancer in general may thus further increase the understanding of the complex heterogeneity and pathogenesis [32]. As previously described, the expression of hormone receptors ER and PgR and expression of HER2 are valuable targets for current treatment regimens. Further proteomic characterization may identify new pathological biomarkers and therapeutic targets.

Based on the expression of 171 breast cancer related proteins, six subtypes have been proposed; basal, Her2, luminal A, luminal A/B, reactive I and reactive II [33]. These subtypes were found to overlap tightly with the intrinsic genetic subtypes thus providing information about existing differences at the protein expression level. As the proteins are measured by reverse phase protein array (RPPA), the subtypes referred are to as RPPA subtypes.

1.3.3 Metabolomics and breast tumors metabolism

Downstream genomics, transcriptomics and proteomics is metabolomics, a relatively new field that studies small-molecular compounds called metabolites. These compounds are end products or intermediates of chemical processes needed for cell viability, e.g synthesis of building blocks, energy production and cell signaling. The metabolic profile of a cell, tissue or living organism depends on the preceding 'omcis' levels as well as environmental factors like diet and drugs [34]. Small alterations in gene expression levels or in the activity of enzymes could have large impact on the concentration of metabolites which can be viewed as an amplified output of ongoing cellular activity [35]. Due to the accumulated alterations within the cancer cells that contributes to their characteristic uncontrollable growth, they exhibit important metabolic differences compared to normal cells. When presenting the emerging hallmarks of cancer, Hanahan and Weinberg suggested a crucial event of tumor development to be deregulation of cellular energetics [3]. Altered metabolic activity is thus becoming an established characteristic of malignancy. Further elucidation for better understanding of metabolic reprogramming and changes observed in cancer may contribute to revealing dependencies and therapeutic targets (discussed in more detail in 5.1) [36].

In the following sections, altered glucose, choline and amino acid metabolism in relation to cancer are introduced.

Glucose metabolism

Glucose is the main source of energy in living cells. During glycolysis, a small amount of adenosine triphosphate (ATP), the chemical energy transporter essential for cellular processes, is formed when glucose is converted to pyruvate. If oxygen is present, pyruvate can be oxidized in the tricarboxylic acid (TCA) cycle followed by oxidative phosphorylation to produce ATP. In hypoxic situations, i.e. low oxygen concentrations, pyruvate is used to make lactate yielding only 2 ATP molecules per glucose compared to 36 in aerobic conditions.

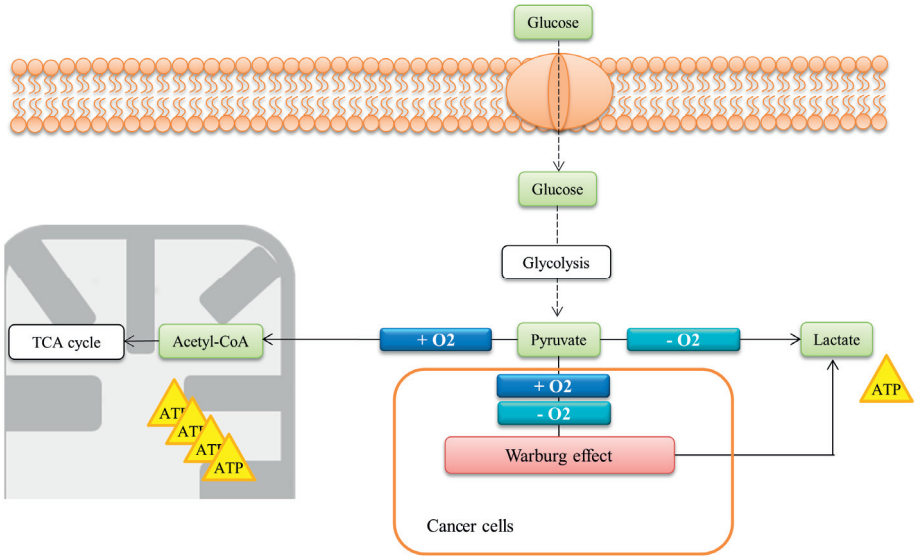

Figure 1.4: Glucose metabolism in normal and cancer cells. Glucose enters the cell and is converted to pyruvate through the process called glycolysis. In normal cells, pyruvate is converted to acetyl-CoA or lactate depending on the level of oxygen present. In cancer cells, most of the pyruvate is converted to lactate, independently of the level of oxygen, an event called the Warburg Effect.

For most cancer cells glucose metabolism is altered and even if oxygen is present, most of the pyruvate is converted to lactate (Figure 1.4). This characteristic, discovered in the 1950's, is referred to as the Warburg effect [37]. In addition, cancer cells inside solid tumors often experience hypoxia due to the low blood supply, causing production of lactate from pyruvate to be the only possibility to make ATP.

The reduced efficacy to generate ATP has been suggested to be an adaption to facilitate the uptake and incorporation of nutrients into biomass needed to produce a new cell [38]. It is also suggested that the production of lactate favors tumor cells, making them more resistant to the immune system and also by generating an acidic microenvironment which is hostile to surrounding normal tissue and promotes metastasis [39]. To compensate for the inefficient ATP production, most tumors have an increased rate of glucose uptake.

Choline metabolism

Choline is an essential organic compound functioning as a precursor for phosphatidylcholine (PtdCho), one of the most abundant phospholipid in eukaryotic cellular membranes [40]. PtdCho is formed de novo from choline by the Kennedy pathway shown in Figure 1.5. Choline is first transported into the cell and phosphorylated to phosphocholine (PCho) by the enzyme choline kinase. PCho is then added a cytidyldiphosphate (CDP) group forming the high-energy donor CDP-Choline. To synthesize PtdCho, a lipid anchor such as diacylglycerol (DAG) is used by the enzyme called DAG-cholinephosphotransferase [40]. The breakdown products of PtdCho are glycerophosphocholine (GPC) and 1-acylglycerophosphocholine.

Tumor cells grow rapidly and therefore require high production of phospholipids like PtdCho. The abnormal high production of PtdCho from choline and choline-containing compounds has therefore been studied for examination of cancer metabolism in several decades [41] and is an emerging metabolic hallmark for tumor progression [42].

Amino acid metabolism

Although over 300 different amino acids exist, only 20 commonly serve as building blocks for proteins in the human body [43]. Amino acids also have roles as regulators or intermediate metabolites for several important metabolic pathways necessary for cellular maintenance and growth. The anabolic processes that are active during cancer development thus rely on altered flow of amino acid compared to normal cells. Although glucose is considered the main energy source in human cells, amino acids such as glutamine can be utilized to produce ATP through refilling of intermediates to the TCA cycle. Glutamine is normally considered a non-essential amino acid, however studies have shown that in rapidly dividing cells, including both normal

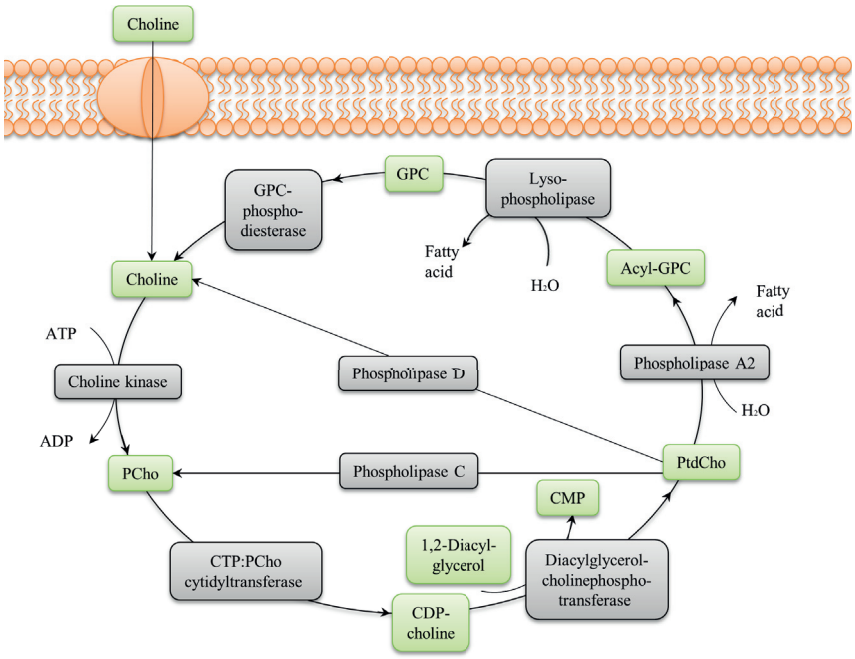

Figure 1.5: Choline metabolism. Choline is transported into the cell and used for synthesis of PtdCho by choline conversion to first PCho followed by CDP-Choline synthesis. PtdCho can further be catabolized directly to choline or PCho, or to GPC through acyl-GPC production. Choline metabolism is frequently observed to be altered in cancers. PCho: phosphocholine, CTP: cytidyltriphosphate, CDP: cytidyldiphosphate, CMP: cytidylmonophosphate, PtdCho: phosphatidylcholine, GPC: glycerophosphocholine.

and cancer cells, it is conditional essential [44]. It is important for the biosynthesis of nucleic acids and can be converted, by glutaminase, to glutamate which further can be used for production of other amino acids or function as a precursor for the important antioxidant glutathione [45]. In addition, glutamate is a precursor for α-ketoglutarate, a TCA intermediate and substrate for dioxygenases (i.e enzymes that modify DNA and proteins) [44].

1.4 Metabolic detection through magnetic resonance spectroscopy (MRS)*

Magnetic resonance spectroscopy (MRS) can be used to identify and quantify metabolites by using the magnetic properties that some atomic nuclei possess. For nuclei with an uneven number of protons and/or neutrons, i.e. spin quantum number $I \neq 1$, the nucleus generates the magnetic momentum (μ) used in MRS given by $\mu = \gamma I$, where γ is the gyromagnetic ratio (unit: MHz/Tesla) dependent on the type of nucleus. Examples of nuclei that all posses this magnetic property and occur naturally in the body are ^{1}H, ^{13}C, ^{23}Na, ^{31}P. If such nuclei are placed in an external static magnetic field ($\mathbf{B}_0$, unit: Tesla) they will orient in $2I+1$ possible spin states. For the highly abundant and most commonly used nucleus in MRS, proton (^{1}H), with $I = 1/2$ and $\gamma = 42.6$ MHz/Tesla, there exists two spin states for the nuclei at equilibrium when placed in a magnetic field; a low energy state where the magnetic momentum aligns with the applied field and a high energy state where the magnetic momentum aligns against the applied magnetic field (Figure 1.6). The energy differences between these two states are proportional to the strength of the magnetic field.

The nuclei will spin around its own axis and around the axis of the magnetic field in an motion called precession. The frequency ω of this motion is given by the Larmor equation: $\omega = \gamma \mathbf{B}_0$

*This section is based on [46] unless otherwise stated

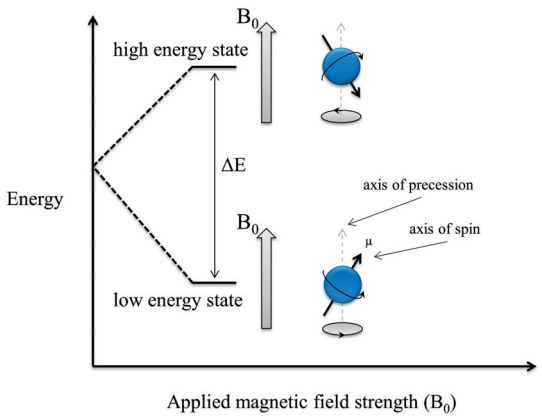

Figure 1.6: The basic principle of magnetic resonance. Atomic nuclei with spin number 1/2 will orient with or against an applied magnetic field ($\mathbf{B}_0$). The nuclei spin around their axis creating a magnetic momentum (μ) that precess about $\mathbf{B}_0$.The anti-parallel spin state is referred to as the high energy state (top) while the parallel spin state has a lower energy state (bottom). With increasing strength of the applied magnetic field, the difference in energy states (ΔE) increases.

In the applied magnetic field $\mathbf{B}_0$, a slight excess of nuclei will align in the low energy state causing an net magnetization pointing along $\mathbf{B}_0$'s direction. It is this magnetization that MR techniques manipulate to get the MR signal. By applying an external radio frequency (RF) pulse equal or close to the nuclei's Larmor frequency, nuclei will excite to the high energy state. When the RF pulse is turned off, the spins returns back to the original low state through longitudinal (T_1) and transverse (T_2) relaxation. At the same time as the relaxation occurs, the nuclei emit energy that can be detected as a signal called free induction decay (FID). A Fourier transformation of the time dependent FID will result in a frequency dependent spectrum known as the MR spectrum. Due to slight differences in their chemical environment caused by metabolites chemical structure and electrons shielding the nuclei from the magnetic field, peaks will appear at different positions in the spectra, known as chemical shifts reported in parts per million (ppm).

1.4.1 MRS acquisition

Due to the large amount of water within biological tissues, water suppression is needed to increase the signal from small metabolites found in much lower con-

centrations. A variety of pulse sequences exist, but the two most common metabolomics experiments are Nuclear Overhauser Effect Spectroscopy (NOESY) and Carr-Purcell-Meiboom-Gill (CPMG). These methods use a pre-saturation of water molecules by exposing the sample to a relatively long, low power RF pulse. CPMG sequences are additionally designed to decrease the signals from macromolecules and lipids that cause broad peaks possibly overlapping with important metabolites. To accomplish this, CPMG experiments take advantage of the short T_2 relaxation large molecules have and filter them out using a long echo-time (TE) prior to the acquisition. More specific, after pre-saturation of the water signal and a 90 °pulse, there is a following repeated loop of 180 °pulses with delay τ between each (Figure 1.7). This loop will refocus and preserve the signals from small molecules with long T_2, consequently reducing signals from macromolecules.

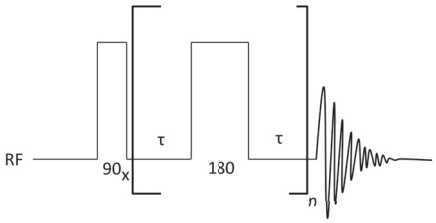

Figure 1.7: Schematic illustration of CPMG pulse sequence. RF: radio frequence, τ: time delay

1.5 High Resolution Magic Angle Spinning MRS

The quality of MR spectra is highly dependent on the molecular orientation and their possibility to reorient. Within semi-solid material (e.g. tissue), molecules are less mobile leading to anisotropic interactions between nuclei, which give rise to broad peaks, possibly concealing relevant spectral information [41]. After its discovery, the use of MRS was thus strictly limited to dissolved or melted solid samples or liquid samples [47]. Within these samples the anisotropic interactions are averaged out by the rapid isotropic movement of molecules resulting in MR spectra with narrow line width. Andrew and Lowe were the first to describe a solution to the problem of semi-solid samples in 1958 [48,49]. By imposing nuclei motion with rapid spinning (4-6kHz) of the sample angled 54.7° (the magic angle) to the static magnetic field $\mathbf{B}_0$ (Figure 1.8), referred to as magic angle spinning (MAS), line broadening is reduced and MR spectra of high resolution are produced.

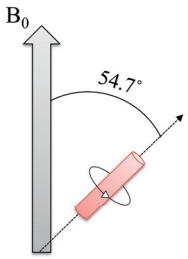

Figure 1.8: Magic angle spinning (MAS). Rapidly spinning the sample at the magic angle of 54.7° to the magnetic field $\mathbf{B}_0$ produces high resolution spectra with line width that resemble spectra obtained from liquid samples.

1.5.1 ^{1}H HR MAS MRS analysis of breast cancer tissue

Ex vivo high resolution magic angle spinning MR spectroscopy (HR MAS MRS) gives qualitative and quantitative metabolic information from biological tissue with minimal sample preparations. It is also a non-destructive technique allowing subsequent analysis, for example histopathological examination or gene expression profiling, of the tissue after MRS [50]. Metabolic profiling alone and in combination with complementary methods is important for assessment of cancer biology, thus making HR MAS MRS an attractive method [41].

HR MAS MRS is widely used to study central metabolic processes related to cancer progression, including glycolysis, choline phospholipid metabolism and amino acid metabolism. Analyzing breast cancer tissue, ^{1}H HR MAS MRS has identified more than 30 metabolites [51]. A representative breast cancer spectra is illustrated in Figure 1.9.

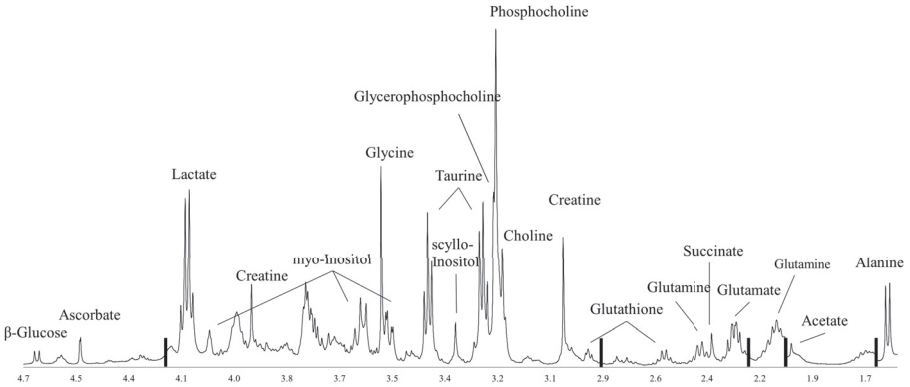

Figure 1.9: A representative ^{1}H HR MAS MRS breast cancer spectra. Black bars represents excluded lipid regions.

To explore metabolic changes in relation to alterations in glycolysis and glucose metabolism, both glucose and lactate are detectable with ^{1}H HR MAS MRS, and can thus be evaluated. A general hypothesis is that decreasing levels of glucose reflects that the tumor has an increasing energy demand while the degree of lactate production might indicate whether the glucose is guided towards TCA cycle or used for aerobic glycolysis. In accordance with a higher energy demand and thereby higher glucose demand in tumors with actively proliferating cells, a previous study reported glucose levels to be negatively correlated to proliferation index (MIB-1) [52]. If glucose is metabolized though aerobic glycolysis, regardless of oxygen availability, lactate will be produced. Lactate has been suggested a key player for cancer development and metastasis [39] and high levels of this metabolite, together with high glycine levels, has been associated with poor-prognosis for patients with ER+ invasive ductal carcinoma [53]. Accumulation of lactate in tissue extracts analyzed by MRS has previously shown to be correlated to metastasis [54, 55]. Furthermore, in a study of patients diagnosed with locally advanced breast cancer, higher lactate levels prior to treatment start was observed for those who did not survive (5 year), supporting it as a poor-prognosis marker [56]. Non-survivors also

had higher levels of choline containing metabolites prior to treatment. These metabolites are associated to the synthesis and degradation of the phospholipid PtdCho, referred to as choline metabolism (see section 1.3.3), often observed to be altered in cancers [42]. With HR MAS MRS, several choline metabolites can be detected, including choline, PCho and GPC. Increased amounts of these metabolites have been detected when comparing breast cancer tissue to non-involved breast tissue, both in surgery-excised tissue [51, 57] and in core needle biopsies from breast cancer patients [58]. The altered choline metabolism is also found in xenograft models, and shown to differ between different breast cancer subtypes [59]. Basal-like tumor xenografts, which have a more aggressive breast cancer phenotype, are characterized with higher GPC concentration realtive to PCho than the less aggressive phenotype of luminal-like xenograft models.

Changes in the levels of several amino acids have also been observed by ^{1}H HR MAS MRS in breast cancer tumors. Higher levels of glycine has been observed in tumors larger than 2 cm compared to smaller tumors [57] and a trend of higher glycine in samples from poor prognosis patients [52]. Additionally, as a response to neoadjuvant chemotherapy, a significant decrease in glycine levels was found in samples from long-term survivors (> 5 years) [56, 60]. Other amino acids that can be elucidated using ^{1}H HR MAS MRS are taurine, which have been linked to lymph node metastasis [57], and glutamine, that were found to be significantly lower in TNBCs compared to triple positive breast cancer [61].

1.5.2 Pre-processing of MRS spectra[†]

The acquired HR MAS MRS spectra are highly complex, typically consisting of thousands of variables. To extract useful information and obtain high quality and comparable spectra eligible for statistical analysis, different pre-processing operations are performed to remove irrelevant sources of variance. These operations may include baseline correction, deletion of irrelevant noise regions, peak alignment, normalization and scaling. Each step is conducted simultaneously on the whole data set to ensure identical protocol for all samples.

Baseline correction is performed to remove unevenness in what should be a flat baseline. Without correction, baseline additives will cause errors when performing statistical tests and during quantification as signal intensities, and thereby metabo-

[†]This section is based on [62, 63] unless otherwise stated

lite concentrations, are influenced and will be incorrect. Different algorithms can be performed on either time domain or frequency domain to correct for uneven baseline caused by noise, macromolecules or alternations in the first points of the FID. One of the most common approaches is estimating a base line which is subtracted from the spectral data. When the optimal baseline is achieved, the next step is often to remove areas with no metabolic information or areas that contain pollutions such as chemicals from sample preparation. This can be followed by peak alignment which has the intention to correct for chemical shift differences between the samples, normally caused by changes in pH, temperature, instrumental factors or molecular interactions. Different approaches can be used, that either align the entire spectra (global alignment) or separate segments (local alignment). Icoshift [64] is one of the approaches recommended for HR MAS MRS data [65]. Here, user defined segments of optional sizes are shifted to optimize their cross correlation to the same segment of a selected reference spectra using Fast Fourier Transformation (FFT). The reference spectra can be a spectrum from the original data set or can be generated by the user (e.g. mean or median spectra of the data set). After alignment, normalization ensures comparable spectra by removing variation in signal intensities caused by sample size or dilution. Area normalization, where each variable of the samples is divided by the sum or average of all its variables, can be considered a standard normalization approach for MRS metabolic data. Examples of other approaches are range normalization and probabilistic quotient normalization (PQN). The latter uses a method where the estimated most probable 'dilution factor' caused by sample size of each spectra is calculated based on comparison to a reference spectrum [66].

The signal intensities of metabolites are proportional to their abundance within the sample. Although fluctuations within metabolites of low concentrations might be of biological importance, their variation might be masked by metabolites of higher concentrations. The pre-processing step of scaling aims to balance the importance of each variable making them more comparable. Scaling methods are thus variable-based, and not sample-based as normalization. Prior to other scaling procedures, mean centering is often applied. Here, each variable within the data set is divided by its own mean resulting in a values that vary around zero. Depending on the nature of the data, following scaling approaches can be autoscaling (dividing each variable on its standard deviation), pareto scaling (dividing each variable on the

square root standard deviation) or variable stability scaling (dividing each variable on its standard deviation and coefficient of variation).

Additional pre-processing operations such as variable selection might also be included. Since decisions on what pre-processing procedures to include will affect the result of multivariate analysis, each step should be carefully evaluated and optimized for the specific data it will be applied to.

1.6 Multivariate analysis

Analyzing data sets with pre-processed spectral information requires statistical methods that handle a high number of variables. Additionally, many of the variables obtained by MR spectroscopy are collinear, ruling out standard statistical methods. Two approaches are used to extract and maximize the information recovery from such data sets; unsupervised and supervised methods. Unsupervised methods are exploratory, with no other information than the spectral data set as input. These methods can be used to visualize the data in a few dimensions to reveal hidden structures or groups within the data set. Supervised methods require a priori knowledge about the objects, referred to as response variable(s), with either categorical or continuous information. The independent variables, i.e. spectral intensities, are then used to build models that can classify or predict the response.

1.6.1 Principal Component Analysis (PCA)

Principal component analysis is an unsupervised multivariate method that aims to reduce noise and emphasize systematic data structures. By taking advantage of the many collinear variables within most multivariate data sets, linear combinations are used to reduce the number of variables into new variables called principal components (PCs). Here, the first PC explains the largest amount of the variance within the data set, while the following and subsequent PCs explains as much of remaining variation as possible. The PCs become axes of a new coordinate system and each sample is given score values to mark their position. Plotting samples in a scores plot defined by the PCs is a good tool for visualizing high dimensional data, find underlying patterns and for identifying outliers. Each PC will have a corresponding loading vector which describes how important each of the original variables have been in construction of the specific PC. Together the score and loading plot will give new information and help in the interpretation of the data set. Figure 1.10 shows one example of a PCA score plot and the corresponding first loading. Here, the samples have been colored according to their PC1 scores (positive or negative). By observing samples distribution in the scores plot combined with the corresponding loading plot, variables important for separating the samples in the new coordinate system (i.e PCs) can be found.

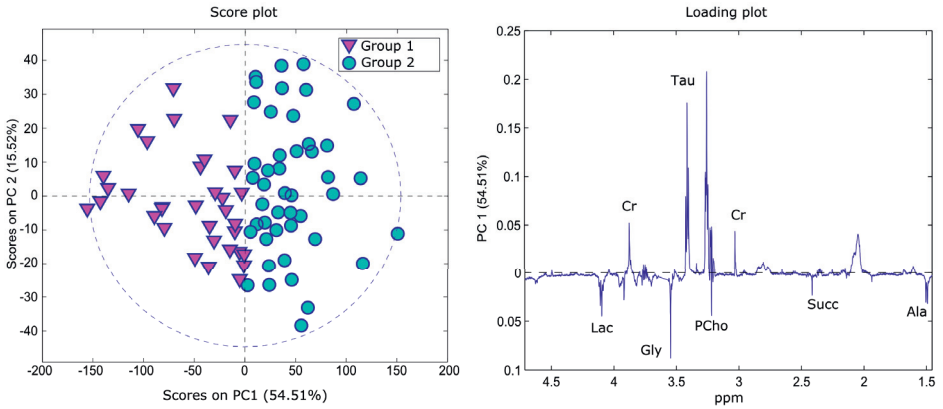

Figure 1.10: Principal component analysis (PCA) for two groups of patients. In the score plot (left), similar samples cluster close to each other. The loading plot (right) shows what variables were important for separating samples on the chosen principal component, here PC 1. Lac: lactate, Cr: creatine, Gly: glycine, Tau: taurine, PCho: phosphocholine, Succ: succinate, Ala: alanine.

1.6.2 Hierarchical Cluster Analysis

Hierarchical cluster analysis is an unsupervised method that can be used to find natural groups of samples within a data set, typically used for genomic and transcriptomic data. Complementary to the score plot from PCA, grouping of samples is visualized in a dendrogram, also known as a hierarchical tree. This tree is built with a bottom-up approach and illustrates the grouping of samples according to their pairwise similarity or dissimilarity. At the initial stage, and bottom of the dendrogram, all objects are considered individual clusters. After calculating similarity measurements between every possible pair of objects, the two closest are joined by a branch at the first level. For the next and following levels the process is repeated until only one cluster remains, as illustrated in Figure 1.11. Clusters more similar to each other will thus be connected by shorter branches than clusters less similar.

Several metrics for calculating the similarity between objects exists. Common approaches include Euclidean distance and correlation distance. The Euclidean distance between two points $A(a, b, c)$ and $W(x, y, z)$ is defined in equation (1)

$$d(A, W) = [(a - x)^2 + (b - y)^2 + (c - z)^2]^{1/2} \quad (1)$$

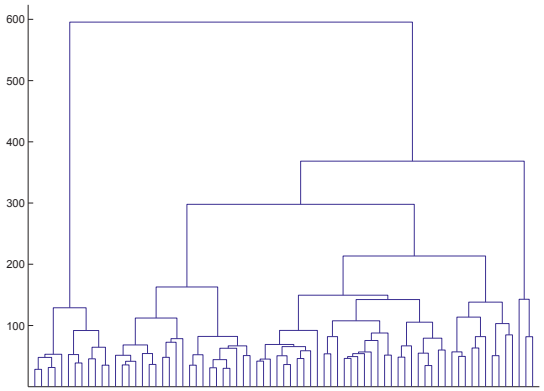

Figure 1.11: Dendrogram obtained by hierarchical cluster analysis.

When two objects are joined into a cluster, their new distance measurements to other clusters are decided by the chosen algorithm, typically single or complete linkage, or Wards method. Single linkage defines the distance as the distance between the two closest objects of the two clusters, while complete linkage does the opposite; the distance is defined as the longest possible distance. Wards method calculates the variance within each cluster and the total variance summing all cluster variances. The two clusters that will cause the smallest change in total variance will be fused into a larger cluster.

The resulting dendrogram can in the final step of cluster analysis be used to divide the original data set into groups by deciding a cutoff level. All objects linked by a branch at the cutoff level will belong to one cluster. An alternative approach is deciding the number of clusters and cutting the dendrogram where this criteria is fulfilled.

1.6.3 Partial Least Squares (PLS)

Similar to PCA, partial least squares aims to find linear relationships within a multivariate data matrix, X, to reduce its complexity. However, PLS uses a supervised approach by including the response variable(s) Y with relevant information, e.g clinical data or class membership, to construct the descriptive model. The method aims to find latent variables (LVs) that explains the variation of the data while maximizing the covariance between the X and Y. More specifically, the LVs will give

information about which variables within X that are most important for separating levels or groups within Y. In cases where Y is a categorical variable, the method is called PLS discriminant analysis (PLS-DA). Figure 1.12 shows a constructed example of PLS-DA discrimination between two groups of samples. The resulting model consists of new score values for each sample, and loading vectors corresponding to each LV, and can be interpreted similar to PCA models.

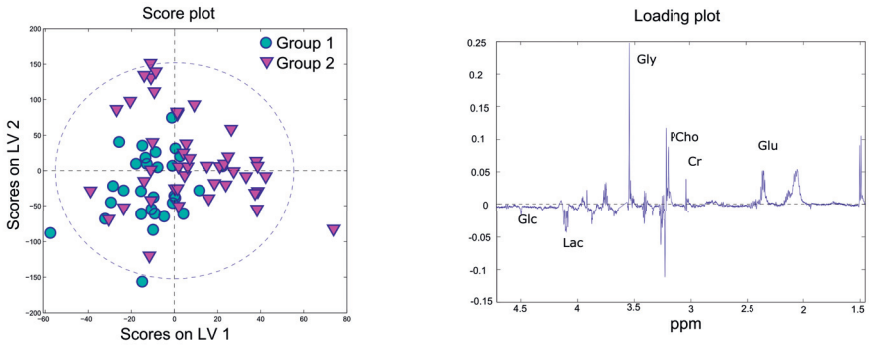

Figure 1.12: Partial least squares discriminant analysis (PLS-DA) example. Similar to PCA, the score plot (left) will cluster similar samples close to each other. The loading plot (right) shows what variables were important for separating samples on the chosen principal component, here PC 1. The corresponding loading plot shows which variables were most important for the PC. Glc: glucose, Lac: lactate, Gly: glycine, PCho: phosphocholine, Glu: glutamate.

1.6.4 Validation of multivariate models

One of the goals when building classification models using methods like PLS-DA is to find variables important for discriminating groups of samples. Additionally, the model could potentially be used for predicting the status of new samples. Prior to such interpretation and classification, proper validation of the model is needed. If it is over-fitted to the data used to build the model, it will not describe the population wide relationships between X and Y. To assess the models robustness and evaluate its performance, common validation approaches include the use of independent data, cross validation and permutation testing. The preferred method for validation is using an independent data set, however this is often not possible due to lack of a validation cohort or a small number of samples. In such cases cross validation can be used. Here, the cohort is divided into training and test sets. The

training set is used to build a model that subsequently is used to classify the objects within the test set. This procedure can be repeated for several training and test sets, measuring the performance (e.g number of correct and incorrect classifications, sensitivity and specificity, respectively) based on the predicted classification for the test sets. The size of the test and training set depends on the cohort. For small sample cohorts (n=20) leave-one-out cross validation can be used, where each sample is left out once. However, this could possible lead to an over-fitted model. For bigger cohorts, the test set can include a specific percentage of samples leaving the remaining samples within the training set. Further extension of cross validation to double cross validation can be used to optimize the model. This approach will have two loops: one outer and one inner loop. The outer loop is identical to the cross validation structure described above. For each round of outer loop validation, there is further an inner loop where the training set is divided into an optimization and second test sets (Figure 1.13). This is repeated for a specific number of times before a new round of the outer loop is repeated. The inner loop is used to decide the optimal number of LVs in PLS.

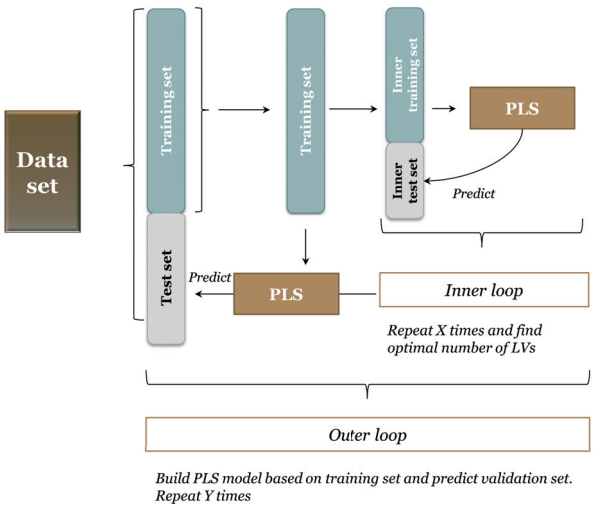

Figure 1.13: An illustration of double cross validation. The data is divided into a training and a test set. In the inner loop, model parameters, here for a partial least squares (PLS) model, are optimized and used for predicting samples in the test set of the outer loop. Single cross validation is performed using only the outer loop.

Permutation testing is a way of testing whether the model achievements are better than random classification. This technique permutes, or shuffles, the response variable Y before building the model. Consequently, the result obtained from this permuted model represents the result that could be obtained by chance. Comparing the real- and permuted models classification results will tell whether the real model can be regarded as significant.

1.7 Linear Mixed Models (LMM)

In the previous sections, methods to analyze different metabolites or complete spectral profiles simultaneously have been described. Another approach is to build separate multilevel statistical models for each individual metabolite. Such is the case with linear mixed-effects models (LMM), which describe relationships between a particular outcome, e.g. a metabolite concentration, and different categorical or continuous factors, e.g. response group or sample tumor cell percentage, respectively. These factors are regarded as fixed, because they can affect the outcome variable but have known, fixed values and therefore one has modeling control over them. Random effects are also incorporated in LMM, thus the name mixed model. These take into account the variation that cannot be controlled for experimentally and arise due to individual patient differences that are unknown, e.g. unrecorded diet and physical fitness level.

LMM can be applied in a variety of settings, most notably to account for intra-subject correlation that occurs when multiple observations or measurements are included for a single patient. This occurs in longitudinal studies, which are designed to follow up subjects and remeasure the same variables repeatedly at different time points. This allows tracking of individual changes in the measured variables with time. In addition, LMM can handle incomplete data, which is statistically challenging and is typical in longitudinal studies since it is difficult to obtain measurements from all patients at every time point [67].

2 Aims

Overall aim

The main aim of the thesis work was to further characterize breast cancer through metabolic profiling using HR MAS MRS.

Specific objectives

- To identify an optimal sample handling protocol for metabolic studies of tumor tissue with respect to freezing delay time and experiment durability.
- To determine naturally occurring metabolic clusters of primary operable breast tumors and further integrate the metabolic characteristics with gene and protein expression data.
- To investigate the metabolic effect of neoadjuvant treatment with respect to treatment response and the effect bevacizumab treatment.

3 Materials and Methods

A summary of materials and methods used for the present thesis is given in Table 3.1

Table 3.1: Materials and methods used in paper I-III

		Paper I	Paper II	Paper III
Materials	Human tissue samples	n = 14	n = 228	n = 270(122 patients)
	Xenograft samples	n = 42		
Methods	Metabolomics	^{1}H HR MAS MRS	^{1}H HR MAS MRS	^{1}H HR MAS MRS
	Proteomics		RPPA	
	Transcriptomics		microarray	microarray
	Other methods	HES Nile Red	HES	HES
Data analysis	Multivariate analysis	PCA	PCA Hierarchical cluster analysis PLS-DA	PCA PLS-DA
	Metabolite level calculation	Integration	Integration	Integration Imputation
	Longitudinal data analysis	LMM		LMM
	Gene and protein expression		SAM, DAVID, GSEA PAM50-subtyping RPPA-subtyping	PAM50-subtyping
	Combing data levels		Integrated pathway analysis	

^{1}H HR MAS MRS: proton high resolution magic angle spinning MR spectroscopy, RPPA: reverse phase protein array, HES: hematoxylin-eosin-safron, PCA: principal component analysis, PLS-DA: partial least square discriminant analysis, LMM: linear mixed model, SAM: significance analysis of microarrays, DAVID: database for annotation, visualization and integrated discovery, GSEA: gene set enrichment analysis

3.1 Patients and xenograft models

3.1.1 Breast cancer xenograft models

The xenograft models MAS98.06 and MAS98.12 used for paper I was established as described in [68] by implanting primary breast tumors specimens from patients into the fat pad of immunodeficient mice. Passages of tumors to new animals were conducted when tumors reached a diameter of 15 mm. Ethical guide lines from European Convention for the Protection of Vertebrates used for Scientific Purposes were followed during the animal work. Gene expression analysis have shown that these pre-clinical models have a luminal-like and basal-like phenotype respectively. Furthermore, these models have been characterized by MRS [59, 69] showing similarities between metabolic profiles of these models and the profiles

from corresponding patient tumors [59]. Xenografts were established and grown at the Oslo University Hospital, Radiumhospitalet, and transported from Oslo to Trondheim prior to HR MAS MRS analysis. The mice were sacrificed by cervical dislocation and tumors (n=6) were harvested immediately. The tumors were split into seven before following the work flow illustrated in Figure 3.1. One sample was analyzed without snap-freezing, while the remaining were exposed to freezing time delays of 0, 15, 30, 60, 90 and 120 minutes.

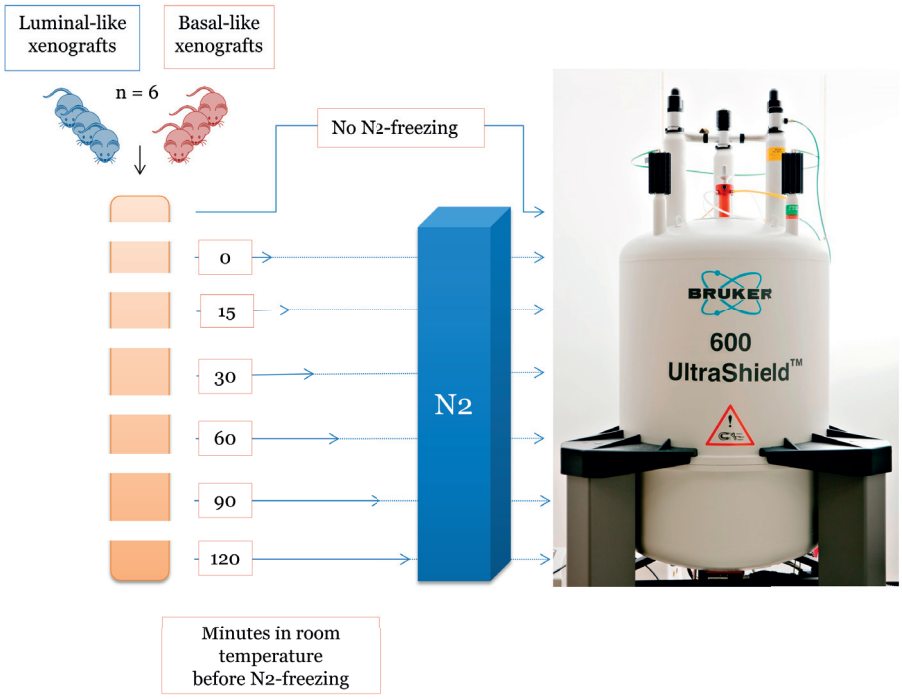

Figure 3.1: Study design for evaluating effect of freezing time delay on tissue samples in paper I.

After HR MAS MRS analysis, samples were immediately frozen and stored (2 years) in liquid nitrogen before sectioning in 4 μl and 10 μl and staining with hematoxylin-eosin-safron (HES) and Nile Red as described in (21), respectively.

3.1.2 Patients cohorts

All three papers included samples from female patients diagnosed with breast cancer.

For paper I, samples (n=14) were collected during surgery at St Olav's Hospital (Trondheim, Norway) and Molde Hospital (Molde, Norway). Written informed consent was obtained from all patients and the study was approved by the Regional Ethics Committee, Central Norway. Immediately after surgical removal the samples were snap-frozen and stored in liquid nitrogen.

For paper II, tumor samples (n=228) obtained from the Oslo2 breast cancer cohort were included. This is a cohort of patients diagnosed with primary operable disease where patient material (clinical data, tumor material, serum) have been collected at several hospitals in south-eastern Norway. Written informed consent was obtained from all patients and the study is approved by the Regional Committee for Medical and Health Research Ethics (REC South East). The samples for paper II were collected in the time period 2006-2009 from patients operated at the Oslo University Hospital (Radium Hospital and Ullevål Hospital, Norway). Tumor material was fresh frozen after surgery and stored at -80 °C. Depending on tumor size, one sample from each tumor was divided in three (Figure 3.2). The two side parts were sectioned for hormone receptor analysis and histological evaluation performed by a pathologist. Sample material from the mid part was used for HR MAS MRS while the tumor remnants were pooled and used for extraction of RNA (n=201) and/or protein (n=217) for analysis of gene and protein expression (RPPA) respectively.

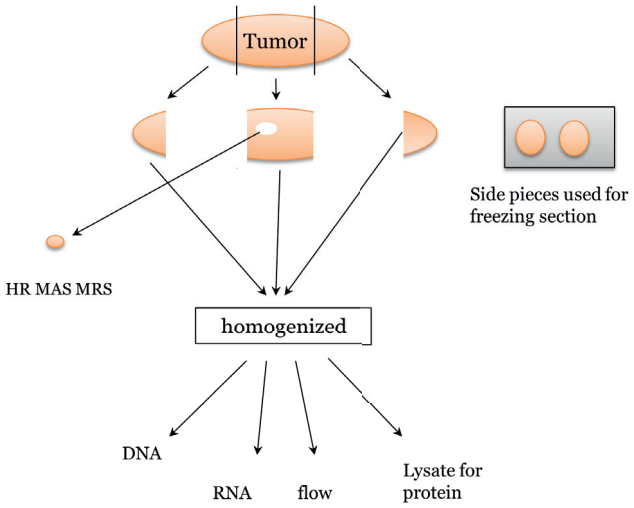

Figure 3.2: Flow chart for division of tumor material in paper II.

For paper III, tumor samples (n=270) obtained from 122 patients (age $\geq$ 18 years) within the Neo-Ava breast cancer cohort (Neoadjuvant Avastin in Breast Cancer) were included. This is a randomized phase 2 trial including patients with large (size $\geq$ 2.5 cm) and HER2− tumors that followed the neoadjuvant treatment regimens described below. Written informed consent was obtained from all patients and the study was approved by Regional Ethics Committee and the Norwegian Medical Agency. Ultrasound guided core needle-biopsies were harvested at treatments start (TP1) and 12 weeks into treatment (TP2) before surgical removal of the tumor 25 weeks after TP1 (TP3) (Figure 3.3). The surgeries were performed at Oslo University Hospital (Radium Hospital and Ullevål Hospital, Norway) and St Olav's Hospital (Trondheim, Norway). Tumor material from TP1 was used for evaluation of hormone receptors status and histopathological diagnosis. For TP1 and TP2, a mid part from a first core-needle biopsy was separated for HR MAS MRS, before pooling the remnants with a second core-needle biopsy for further molecular analysis. For the surgical samples taken at TP3, a similar approach as for tumor preparation in paper II was used (Figure 3.2), where the two side parts were sent for histopathological analysis and a mid part was obtained for HR MAS MRS. The remnants were pooled and used for molecular analysis.

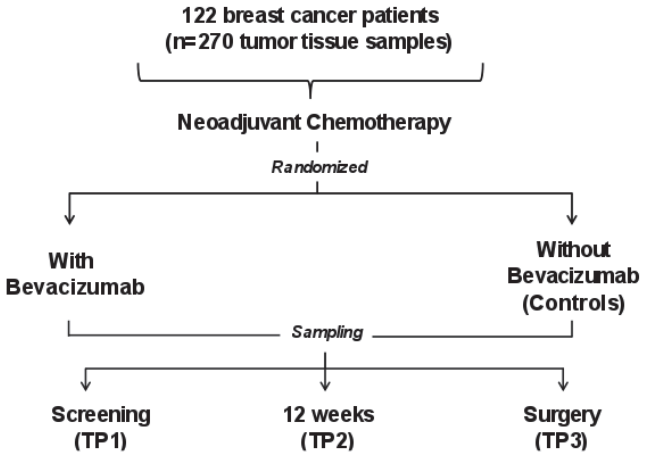

Figure 3.3: Flow chart for randomized neoadjuvant chemotherapy with or without bevacizumab in paper III. Reproduced with permission from Leslie R. Euceda.

3.1.3 Patient treatment protocols and response measurements

In paper III, all patients received neoadjuvant chemotherapy according to Norwegian guidelines and were randomized to additionally receive bevacizumab. The chemotherapy regimen consisted of 12 weeks with anthracyclines treatment (four three-weekly cycles of FEC100; epirubicin 100 mg/m2, 5-fluorouracil 600 mg/m2, cyclophosphamide 600 mg/m2) followed by 12 weeks of taxane-based therapy (four three-weekly cycles of paclitaxel 80 mg/m2 or docetaxel 100 mg/m2). For patients receiving bevacizumab, this was administered in three-weeks cycles (15 mg/kg) during the anthracyclines and docetaxel treatment. Due to toxicity issues, docetaxel treatment was exchanged with paclitaxel for a majority of the patients. For those receiving bevacizumab, the dose was changed to 10 mg/kg every two-weeks.

Tumor size was measured by radiologist at TP1 using MR imaging (MRI), ultrasound and/or mammography and by a pathologist at TP3 when the tumor was surgically removed. To evaluate response of treatment, two characteristics were used; pathological tumor diameter at TP3 and response ratio calculated by pathological tumor diameter at TP3/tumor diameter at TP1. In cases where no MRI was available at TP1, the biggest diameter from ultrasound and/or mammography was used. To prevent the loss of patients experiencing good treatment response, but not qualifying for pathological complete response (pCR) where no invasive cells are detected (in breast nor lymph nodes), a cut-off of tumor diameter < 1 cm was set to classify pathological minimal residual disease (pMRD). Criteria for response classification are summarized in Table 3.2.

Table 3.2: Tumor response classification criteria used in paper III

Pathological response	
Response class	**Tumor size at TP3**
pathological minimal residual diasease (pMRD)	< 1 cm
pathological non-reponder (pNR)	> 1 cm

Response ratio	
Good response (GR)	≤ 0.10
Intermediate response (IR)	$<0.10, 0.90>$
No response (NR)	≥ 0.90

3.2 ^{1}H HR MAS MRS experiments

3.2.1 Sample preparation

For human samples included in paper I, biopsies were kept frozen on an ice block during preparation (Figure 3.4) and cut to fit leak-proof disposable 30 μl inserts

(Bruker, Biospin Corp, USA) containing 3 μl of phosphate buffered saline (PBS) based on D_2O with Trimethylsilyl propionic acid (TSP, 1 mM) and sodium formate (1 mM). The insert were placed in a 4-mm diameter zirconium MAS rotor and samples analyzed immediately.

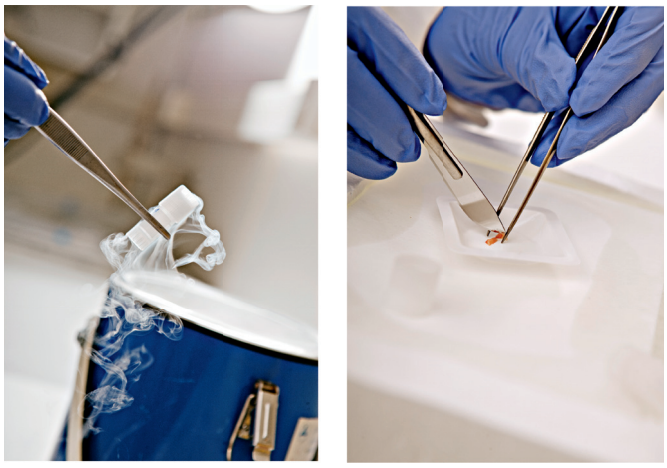

Figure 3.4: Sample preparation before HR MAS MRS experiments. The samples are stored in liquid nitrogen until analysis (left). The samples are kept frozen during preparation and cut to fit inserts MAS rotors prior to analysis. Photo: Geir Mogen/NTNU

For xenograft samples in paper I and human samples in paper II and III, samples were kept frozen on a metal block bathed in liquid nitrogen during preparation and cut to fit leak-proof disposable 30 μl inserts (Bruker, Biospin Corp, USA) containing 3 μl cold sodium formate in D_2O (24.29 mM). The insert were placed in a 4-mm diameter zirconium MAS rotor and samples kept -20°C and for maximum 6-8 hours before the experiments.

3.2.2 Acquisition protocol

Samples were analyzed on a Bruker Avance DRX600 spectrometer (Bruker, Biospin GmbH, Germany) equipt with a ^{1}H/^{13}C MAS probe with gradient. Before acquisition, samples were spun for 5 minutes to allow for temperature acclimation. CPMG experiments (cpmgpr1D, Bruker) were run using acquisition parameters as specified in Table 3.3.

Table 3.3: Acquisition parameters

	Paper I		**Paper II & III**
	Human samples	Xenograft samples	Human samples
Temperature	4°C	5°C	5°C
Spin rate	5 kHz	5 kHz	5 kHz
Relexation delay	4 s	4 s	4 s
Delay(τ)	1 ms	0.3 ms	0.3 ms
Echo time	273.5 ms	78 ms	78 ms
Number of loops	136	126	126
Number of scans	128	64	256

3.3 Spectral pre-processing and analysis

The acquired spectral data was Fourier transformed into 64k real points by multiplying the FID with a 0.30 Hz exponential function. Each spectrum was automatically phase corrected in TopSpin 3.1 (Bruker Biospin). Spectral data was further pre-processed in Matlab R2013b (The Mathworks, Inc., Natick, USA); chemical shifts were referenced to TSP at 0 ppm (human samples, paper I) or formate at 8.46 ppm (xenograft samples, paper I and human samples, paper II and III), additional baseline correction was achieved by subtracting each spectrum with the lowest value, and peak alignment was performed using icoshift [64]. Pre-processed spectral data from human samples were normalized by mean normalization (paper I and II) or PQN (paper III), while spectral data from xenograft samples (paper I) were normalized to sample weights.

3.3.1 Multivariate analysis

PCA and PLS-DA were performed in Matlab using PLS toolbox version 7.5.2 (Eigenvector Research, Wenatchee, USA) on mean centered data performed by subtracting the average spectrum from each spectra. Hierarchical cluster analysis (paper II) was performed on pre-processed spectral data in Matlab using the Statistical toolbox (Matlab R2013b, The Mathworks, Inc., USA). Euclidean distance was set as distance parameter and Ward's method as the clustering distance.

PLS-DA models were validated using double cross validation where each round of the outer loop divided the data set into a training set consisted of 80 % (paper

II) or 90 % (paper III) of the samples and a test set with the remaining samples. In the inner loop, the training set was equally divided into a new test and training set using the same percentages. For each outer loop (repeated in total 20 times) the inner loop were repeated 20 times. The optimal number of LVs were decided based on the inner loop, while classification result (sensitivity, specificity and classification error) were calculated using the performance of the models during the outer loop of the double cross validation. Permutation testing was performed by building models on data where the response variable (Y) had been shuffled (paper II and III). This was repeated 1000 times before comparing the classification result of the permuted model with the original model. P-values ≤ 0.01 (paper II) and ≤ 0.05 (paper III) were considered significant.

3.3.2 Univariate and multilevel analysis

Metabolite identification was based on previously published HR MAS MRS analyses of human breast cancer [51]. Metabolite levels were calculated using integration of peaks (Matlab). Due to overlapping lipid peaks in the 4.1 ppm lactate region for 116 samples in paper III, the levels were imputed. This was performed in R 3.1.1 [70] using the method of multivariate imputation by chained equation (MICE) [71] and was validated using a resampling procedure.

LMM was performed in R 3.1.1 using the 'nlme' package [72].

3.4 Gene and protein experiments

3.4.1 Gene expression and genetic subtypes

In paper II and III, total RNA was isolated using TRIzol®reagent (Invitrogen, Carlsbad, CA, USA). The RNA purity and concentration was determined with a NanoDrop spectrophotometer (Thermo Fisher scientific, Waltham, MA, USA). Gene expression analysis with 100 ng RNA as input for labeling was performed using SurePrint G3 Human GE 8x60K (Agilent Technologies) according to the manufacturer's protocol (One-Color Microarray-Based Gene expression Analysis, Low Input Quick Amp Labeling, v.6.5, May 2010). For paper II, microarray signals were log2-transformed, quantile normalized and hospital adjusted. The gene specific expression was calculated by taking the average of values from probes with identical Entrez ID. For paper III, all values were log2-transformed and quantile

normalized before adjustment for batch effect from array design, centre differences and correlations to RIN value and background signal. For both paper II and III, the PAM50 subtype algorithm [31] was used to classify samples into luminal A, luminal B, HER2-enriched, basal-like or normal-like. The claudin-low subtype was not included within the studies of this thesis and will thus not be further discussed.

3.4.2 Protein expression and proteomic subtypes

In paper II, measurements of protein expression was performed using the high throughput technique reverse phase protein array (RPPA). Here, protein lysates from up to 1000 samples are printed in dilutions on slides followed by hybridization to specific antibodies. This enables direct comparison of the expression of protein between samples. The expression of breast cancer related proteins were detected using 150 primary antibodies for protein extracts of 217 samples in paper II. The samples were diluted in five 2-fold series. Signal intensity was measured using a biotin conjugated secondary antibody and amplified with DakoCytomation-catalyzed system (Dako, Glostrup, Denmark). MicroViegene software (Vigene Inc., Carlise, MA) was used to measure spot signal intensities before protein expression was quantified using a standard curve from the serial dilutions. The expression levels were log2-transformed and normalized by mean centering of the samples for each of the antibodies.

Samples were classified to their RPPA-subtype using consensus clustering with an option of 4 or 5 groups. The best fit was 5 groups; luminal, HER2, basal, reactive I and reactive II as defined in The Cancer Genome Atlas Network data set [33].

3.4.3 Analysis of gene expression data

In paper II, Significance Analysis of Microarrays (SAM) [73] was performed in R 2.15.2 [70] on expression levels of 21851 genes (found based on 42405 mRNA probes) to identify differences between the metabolic clusters. To validate the findings, a total of 100 permutations were performed.

For functional annotation of genes differently expressed between the metabolic clusters in paper II, Database for Annotation, Visualization and Integrated Discovery (DAVID), an online network analysis tool was used [74]. Additionally, enrichment of sets of genes were identified using Gene Set Enrichment Analysis (GSEA) [75].

3.4.4 Integrated pathway analysis

The online available tool 'Integrated pathway analysis' in MetaboAnalyst 3.0 software (`www.metaboanalyst.ca`) [76] was used to combine data of differently expressed genes and metabolites of metabolic clusters in paper II.

4 Summary of papers

4.1 Paper I

Impact of freezing delay time on tissue samples for metabolomic studies

Metabolic profiling of intact tumor tissue by high resolution magic angle spinning MR spectroscopy (HR MAS MRS) provides important biological information possibly useful for clinical diagnosis and development of novel treatment strategies. However, generation of high-quality data requires that sample handling from surgical resection until analysis is performed using systematically validated procedures. In this study, we investigated the effect of post-surgical freezing delay time on global metabolic profiles and stability of individual metabolites in intact tumor tissue.

Tumor tissue samples collected from two patient derived breast cancer xenograft models (n=3 for each model) were divided into pieces that were snap-frozen in liquid nitrogen at 0, 15, 30, 60, 90, and 120 minutes after surgical removal. In addition, one sample was analyzed immediately, representing the metabolic profile of fresh tissue exposed neither to liquid nitrogen nor to room temperature. We also evaluated the metabolic effect of prolonged spinning during the HR MAS experiments in biopsies from breast cancer patients (n=14). All samples were analyzed by ^{1}H HR MAS MRS on a Bruker Avance DRX600 spectrometer, and changes in metabolic profiles were evaluated using multivariate analysis and linear mixed modeling (LMM).

Multivariate analysis showed that the metabolic differences between the two breast cancer models were more prominent than variation caused by freezing delay time. No significant changes in levels of individual metabolites were observed in samples frozen within 30 minutes of resection. After this time point, levels of choline increased whereas ascorbate, creatine and glutathione (GS) levels decreased. Freezing had a significant effect on several metabolites, but is an essential procedure for research and biobank purposes. Furthermore, four metabolites (glucose, glycine, glycerophosphocholine and choline) were affected by prolonged HR MAS experiment time possibly caused by physical release of metabolites caused by spinning or due to structural degradation processes. In conclusion, the MR metabolic profiles of tumor samples are reproducible and robust to variation in post-surgical freezing delay up to 30 minutes.

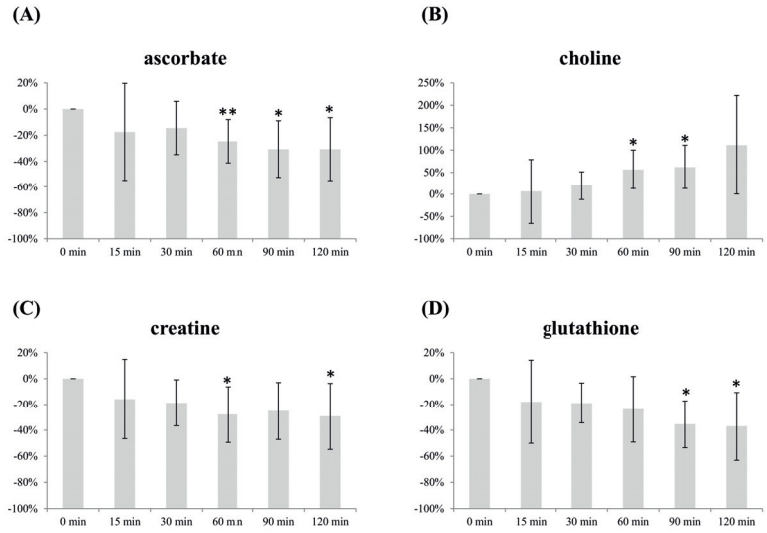

Figure 4.1: Impact of freezing delay time on level of (A) ascorbate, (B) choline, (C) creatine and (D) glutathione. Metabolite integrals from samples subject to 15, 30, 60, 90 and 120 minutes freezing delay time compared with samples frozen immediately (0 minutes). * and ** indicates that the level is significantly different from the sample frozen after 0 minutes (*p $<$0.05, **p $<$0.01).

4.2 Paper II

Metabolic clusters of breast cancer in relation to gene- and protein expression subtypes

The heterogeneous biology of breast cancer leads to high diversity in prognosis and response to treatment, even for patients with similar clinical diagnosis, histology and stage of disease. Identifying mechanisms contributing to this heterogeneity may reveal new cancer targets or clinically relevant subgroups for treatment stratification. In this study metabolite, protein and gene expression data from breast cancer patients were combined to examine the heterogeneity at a molecular level.

The study included primary tumor samples from 228 non-treated breast cancer patients. High resolution magic angle spinning magnetic resonance spectroscopy (HR MAS MRS) was performed to extract the tumors metabolic profiles further used for hierarchical cluster analysis resulting in three significantly different metabolic clusters (Mc1, Mc2 and Mc3). The clusters were further combined with gene and protein expression data.

The result revealed distinct differences in the metabolic profile of the three metabolic clusters. Among the most interesting differences, Mc1 had the highest levels of glycerophosphocholine (GPC) and phosphocholine (PCho), Mc2 had the highest levels of glucose and Mc3 the highest levels of lactate and alanine. Integrated pathway analysis of metabolite and gene expression data uncovered differences in glycolysis/gluconeogenesis and glycerophospholipid metabolism between the clusters. All three clusters had significant differences in the distribution of protein subtypes classified by the expression of breast cancer related proteins. Genes related to collagens and extracellular matrix were downregulated in Mc1 and consequently upregulated in Mc2 and Mc3, underpinning the differences in protein subtypes within the metabolic clusters. Genetic subtypes were evenly distributed among the three metabolic clusters and could therefore contribute to additional explanation of breast cancer heterogeneity.

In conclusion, three naturally occurring metabolic clusters of breast cancer were detected among primary tumors from non-treated breast cancer patients. The clusters expressed differences in breast cancer related protein as well as genes related to extracellular matrix and metabolic pathways known to be aberrant in cancer. Analysis of metabolic activity combined with gene and protein expression provides new information about the heterogeneity of breast tumors and, importantly, the meta-

bolic differences infer that the clusters may be susceptible to different metabolically targeted drugs.

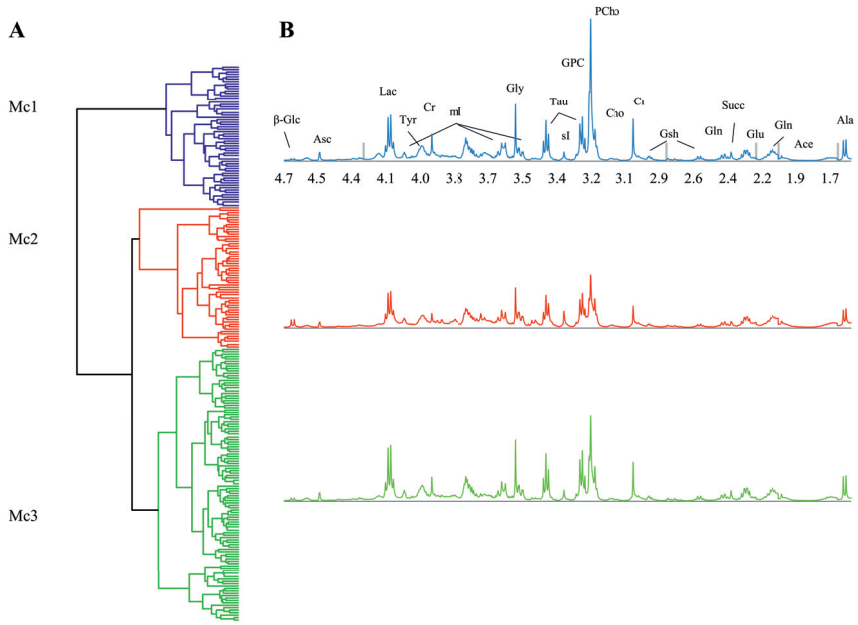

Figure 4.2: Metabolic subtyping of breast cancer tissue samples using HCA. (A) The HRMAS 1H MRS spectra for 228 samples was clustered using Euclidean distance and Wards linkage as similarity measure which separated the samples into three metabolic clusters (Mc); Mc1, Mc2 and Mc3. (B) Mean spectra for the three metabolic clusters. β-Glc: β-glucose, Asc: ascorbate, Lac: lactate, Tyr: tyrosine, Cr: creatine, mI: myoinositol, Gly: glycine, Tau: taurine, sI: scylloinositol, GPC: glycerophosphocholine, PCho: phosphocholine, Cho: choline, Gsh: glutathione, Gln:; glutamine, Succ: succinate, Glu: glutamate, Ace: acetate, Ala: alanine. Grey bars indicate removed spectral regions (containing lipid peaks).

4.3 Paper III

Evaluation of metabolomic changes during neoadjuvant chemotherapy combined with bevacizumab in breast cancer using MR spectroscopy

Metabolomics investigates biochemical processes directly, potentially complementing transcriptomics and proteomics in providing insight into treatment outcome. This study aimed to use magnetic resonance (MR) spectroscopy on breast tumor tissue to explore the effect of neoadjuvant therapy on metabolic profiles, determine metabolic effects of the antiangiogenic drug bevacizumab, and to investigate whether responders could be discriminated from non-responders at the metabolic level.

The metabolic profiles of 122 tumors from breast cancer patients were determined by high resolution magic angle spinning MR spectroscopy (HR MAS MRS). All patients received neoadjuvant chemotherapy, while they were randomized to receive bevacizumab or not. Biopsies were sampled prior, during, and after treatment. Multivariate strategies were used to analyze the metabolic profiles. The levels of 16 metabolites were calculated by peak integration and analyzed by linear mixed models (LMM).

Principal component analysis showed clear metabolic changes as an effect of chemotherapy, pointing to a decline in glucose consumption and a transition to normal breast adipose tissue with treatment progression. Partial least squares-discriminant analysis (PLS-DA) revealed metabolic differences between pathological minimal residual disease (pMRD) patients and pathological non-responders (pNRs) after treatment, but not before or during treatment, with an accuracy of 77 % ($p < 0.001$). Furthermore, metabolic profiles before and after treatment discriminated patients exhibiting a good response ($\geq$ 90 % tumor reduction) from those with no response ($\leq$ 10 % tumor reduction) with a classification accuracy of 76 % ($p=0.001$) and 75 % ($p=0.002$), respectively. Lower glucose and higher lactate was observed in the good response group before treatment, while the opposite was observed after treatment. Bevacizumab-receiving and chemotherapy-only patients could not be discriminated at any time point. LMM revealed significant differences during treatment for 11/16 metabolites, while 8/16 metabolites differed between pMRD and pNRs. A significant interaction between time and bevacizumab for glutathione revealed higher levels of this antioxidant in chemotherapy-only patients than in bevacizumab receivers after treatment.

In conclusion, MR based metabolic profiles reflected changes as an effect of chemotherapy and successfully discriminated pMRD patients from pNRs after treatment, showing potential for assessment of metabolic response to treatment and to improve the understanding of underlying mechanisms affecting pathological response.

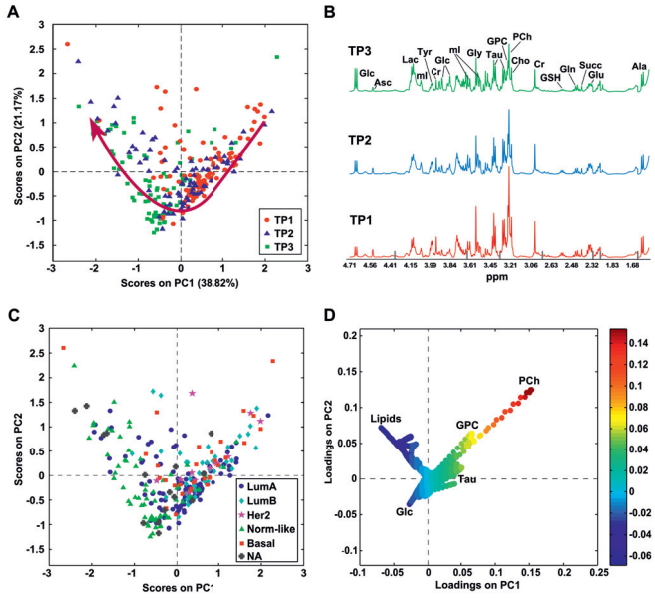

Figure 4.3: PCA score plot, mean spectra from time points and loading plot. (A) The scores plot shows a trend in the direction of the arrow with increasing time point. (B) PQN-normalized mean spectra at each time point. Gray bars indicate removed spectral regions. (C) The normal-like gene expression subtype is most clearly separated from the rest in the scores plot, showing a similar distribution as TP3 in A. (D) The loadings plot indicates higher phosphocholine, glycerophosphocholine, and taurine at TP1 and increasing glucose and lipids with increasing time of treatment and in normal-like samples. Loadings are colored according to LV1. LumA: luminal A, LumB: luminal B, Norm-like: normal-like, NA: not available, Glc: glucose, Asc: ascorbate, Lac: lactate, mI: myo-inositol, Tyr: tyrosine, Cr: creatine, Gly: glycine, Tau: taurine, GPC: glycerophosphocholine, PCh: phosphoscholine, Cho: choline, GSH: glutathione, Gln: glutamine, Succ: succinate, Glu: glutamate, Ala: alanine

5 Discussion

The main objective of this thesis was to characterize the metabolism of breast cancer in untreated and treated patients as well as to evaluate the metabolic effects of sample handling prior to and during HR MAS experiments. Altogether, this work demonstrates the potential of MR metabolomics in complementing gene and protein expression data to provide insight into breast cancer heterogeneity and treatment outcome, at the same time also gaining insight in how to design sample handling for safe and reproducible measurements.

In paper I, the metabolic effects of sample handling, with a focus on freezing time delay and prolonged experiment time, were evaluated. Tumor samples snap-frozen within 30 minutes after excision did not express significant changes in metabolite levels as measured with ^{1}H HR MAS MRS. However, in the time frame of 60-120 minutes, and prolonged experiment time for 90 minutes, several metabolite levels were altered. Optimal sample handling protocols are important when designing and interpreting results from metabolomics studies, such as those conducted in paper II and III. Sample handling regimens in these studies were within the time limits indicated in paper I. In paper II, three naturally occurring metabolic clusters of untreated breast cancer were discovered. These were found to have distinct differences in metabolic profiles and in the distribution of protein subtypes, but no significant association to the distribution of gene expression subtypes. In paper III, the tumor metabolic responses in patients undergoing neoadjuvant chemotherapy with or without bevacizumab were evaluated and related to treatment response. Metabolic effects of the treatment were observed as well as differences in the metabolic profiles of responders compared to non-responders. Furthermore, a metabolic effect possibly linked to bevacizumab treatment was observed.

5.1 Metabolic profiles of breast cancer

Metabolic reprogramming is now widely accepted as an independent hallmark of cancer [3]. Genomic and transcriptomic characterization of breast cancer have been extensively performed in the past few decades, while the metabolic level has been less thoroughly explored. Importantly, cancer cells must convert nutrients to biomass while maintaining energy production, which requires reprogramming of central metabolic processes in the cells. This phenomenon is increasingly recognized

as a potential target for treatment, but also as a source for biomarkers that can be used for prognosis, risk stratification and therapy monitoring. The metabolic pathways of interest in the current thesis are summarized in Figure 5.1.

Metabolic characterization of breast cancer

With its limited need of sample preparation and its high reproducibility, HR MAS MRS can give important metabolic information of cancer samples prior to additional analysis. This can improve current breast cancer characterization and, when combined with data from other molecular levels, solve some of the challenges linked to breast cancer heterogeneity.

A short summary of the main metabolic findings of the current thesis is given in Table 5.1.

Table 5.1: Summary of metabolic findings in paper I-III

Summary of results	**Samples**	**n**	**Sample group**	**↑ Metabolites increased**	**↓ Metabolites decreased**
Paper I	Basal-like and luminal-like xenografts	14	Freezing delay > 30 min	Cho	Asc, Cr
			Freezing delay > 60 min		GS
	Human samples, primary operable tumors	6	Exp. time > 90 min	Glc, Gly, Cho	GPC
Paper II	Primary operable tumors	228	Mc1	GPC, PCho	mI, Glc, Glu, Ace
			Mc2	Glc, Ace	Lac, Asc, Tyr, Gly, GPC, PCho, Ala
			Mc3	Lac, Gly, Tau, Ala	Glc
Paper III	Primary inoperable tumors, HER2−	122	Neoadjuvant Chemotherapy	Glc, Lac, Gln	Cho, PCho, GPC, Tyr, Cr
			pMRD compared to pNR	Glc, Lac	Cho, PCho, GPC, GSH, Succ, Tyr, Cr
			GR compared to NR	Glc,	Lac, Cho, PCho, GPC, GSH, Succ, Tau, Tyr, Cr
			Bevacizumab		GSH

Cho: choline, Asc: ascorbate, Cr: creatine, GS: glutathione (total), Glc: glucose, Gly: glycine, Cho: choline, GPC: glycerophosphocholine, PCho:phosphocholine, mI: myoinositol, Glu: glutamate, Ace: acetate, Lac: lactate, Tyr: tyrosine, Ala: alanine, Tau: taurine, pMRD: pathological minimal residual disease, pNR: pathological non-responder, GSH: glutathione (reduced), GR: good response, NR: no response, Succ: succinate.

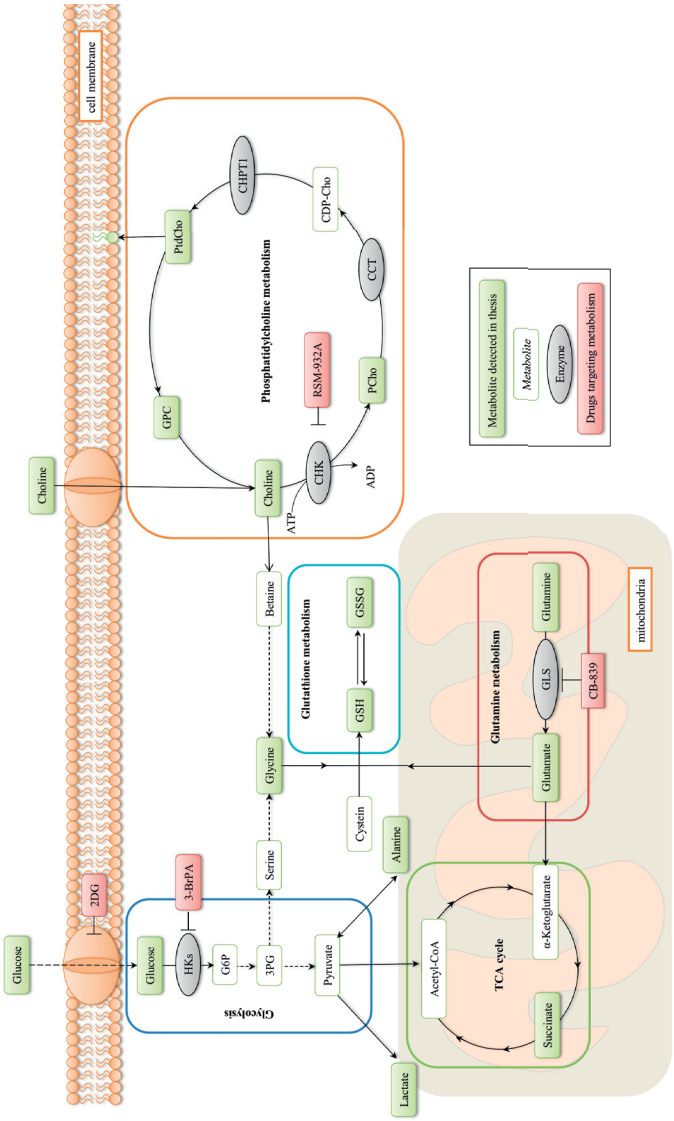

Figure 5.1: An overview of the most relevant metabolites discussed in this thesis. 2DG:2-deoxy-D-glucose, HKs: hexokinases, G6P: glucose 6-phosphate, 3PG:3-Phosphoglyceric acid, GSH; reduced glutathione, GSSG: oxidized glutathione, GLS: glutaminase, CHK: choline kinase, PCho: phosphocholine, CCT: cytidylyltransferase, CHPT1: choline phosphotransferase 1, PtdCho: phosphatidylcholine, GPC: glycerophosphocholine

Glucose metabolism

Cancer cells divide and grow uncontrollably with high demand for energy and molecular building blocks. Although energy production through mitochondrial oxidative phosphorylation is much more efficient, most cancer cells tend to convert glucose to lactate regardless of oxygen availability, the phenomenon known as the Warburg effect. Consequently, an increased glycolytic rate has been observed as a characteristic of many tumors [77]. This is frequently utilized in tumor detection through positron emission tomography (PET) [78] where the glucose analog fludeoxyglucose is injected into cancer patients and used to detect tumors with high glucose uptake. Among genetic subtypes, luminal-like xenograft tumors express a higher glycolytic rate compared to the more aggressive and fast growing tumors of basal-like xenografts [69]. Further exploration of luminal A tumors from patients has revealed three subgroups within this subtype, with one exhibiting higher energy consumption [50]. Glucose metabolism does not necessarily behave similarly within each genetic subtype, but could possibly contribute to important characteristics of the heterogeneity within breast cancer metabolism.

Among the three metabolic clusters described in paper II, Mc2 was characterized by high levels of glucose indicative of lower glycolytic rate, while Mc3 had evidence of higher Warburg effect with low levels of glucose and higher levels of lactate and alanine. The genetic subgroups were evenly distributed among these clusters, underpinning that metabolic differences may add information on breast cancer heterogeneity. Due to its low glucose levels combined with other findings that will be discussed later, Mc2 was suggested to be a group with less aggressive tumors compared to Mc1. Lactate has been linked to tumor aggressiveness and metastasis and has been suggested as a key player in cancer metabolism [39, 79]. Expressing the highest lactate level among the three clusters, Mc3 exhibited metabolic features associated with aggressiveness. For ER+ breast cancer patients, higher levels of lactate and glycine have been found to be associated with lower survival rates [53]. The distribution of ER+ patients among the metabolic clusters were found to be equal, and therefore not the reason for higher lactate in Mc3. No differences in gene expression among the clusters could explain these metabolic differences in glucose metabolism, however, significant differences in the distribution of protein expression subtypes were discovered among the clusters. For Mc2, where high levels of glucose imply a low proliferative rate, 44 % belonged to RPPA subtype reactive-I,

known to have features related to stromal activity; this was in accordance with gene expression findings for this cluster and would be of interest to investigate further.

Although metabolic prediction of treatment response prior to onset of neoadjuvant treatment in breast cancer patients currently has not been achieved [56, 60], increase in glucose levels during treatment for responders (paper III) and for 5 year survivors have been observed [60]. For paper III, the main criteria for evaluation of treatment was tumor size reduction. Pathological responders' metabolic profile after treatment (TP3) showed higher lactate in addition to higher glucose compared to pathological non-responders (pNR). While high glucose could be explained by a lower energy demand in accordance with tumor reduction, the high level of lactate was more unexpected. For many of the samples (116 of 270) lactate levels were imputed due to overlapping lipid residuals, however, this calculation was validated using a resampling procedure and is unlikely to have caused the observed increased lactate levels. This finding could support the suggested dual metabolic effect of cancer cells, where glucose consumption decreases due to a non-glycolytic phenotype caused by lactic acidosis [80], or simply by morphological changes in the cancer tissue, limiting cell lactate secretion and removal.

When assessing tumor response using the defined response ratio, patients classified with good response showed a more prominent metabolic shift from lower glucose and higher lactate prior to treatment towards higher glucose and lower lactate after treatment compared to patients with no response. This indicated that tumors with high Warburg effect were targeted more effectively by the current chemotherapy treatment. Due to the exclusion of the high number of patients with intermediate response in this comparison (69 of 122 patients), the model was limited by a lower sample size therefore not valid for prediction, but the glycolytic response of good responders showed similarities to those observed for long-term survivors of locally advanced breast cancer [60]. When intermediate response patients were included, however, increasing lactate correlating with clinically better response ratio was observed, similar to the finding for pathological minimal residual disease. Whether this increase in lactate is a predictor of poorer outcome for patients in paper III regardless of good pathological response still needs to be elucidated. If so, previous findings showed that 5 year survival, but not clinical response to treatment, is predicted from metabolic profiles measured prior to treatment with lower lactate levels in 5 year survivors [56].

Choline metabolism

Suggested as an emerging hallmark of cancer, abnormal choline metabolism has been associated with proliferation, tumor progression and oncogenic signaling through the production and degradation of the phospholipid phosphatidylcholine (PtdCho) [42]. This phospholipid is an essential constituent of cellular membranes and consequently needed during cancer cell proliferation and tumor growth. Normal proliferating mammary cells do not show the same characteristics [81], linking this feature to malignancy. The three key intermediates of PtdCho metabolism, choline, phosphocholine (PCho), and glycerophosphocholine (GPC) or tCho when summed together, are detectable using ^{1}H HR MAS MRS and are found to be altered in several types of cancer. In breast cancer tissue, these choline containing metabolites have been found to be expressed at higher levels than in normal or adjacent breast tissue [52, 57, 82]. These findings can be correlated with detected upregulation of expression and activity of specific enzymes in breast cancer, presented in a recent review of choline metabolism in malignant transformation by Glunde et al [42]. More specifically, several choline metabolism enzymes such as choline kinase α (CHKA) and PtdCho-specific phospholipase D (PLD) are found to be overexpressed in cancer and are associated with altered choline metabolism. The distinct differences in choline metabolite profiles observed in luminal-like and basal-like xenografts have also been found to correlate with gene expression differences [59, 83] further supporting the need to combine data levels for better breast cancer stratification.

The results of paper I, where the effect of freezing time delay on cancer metabolites was studied, showed that choline significantly increased in the time interval of 30-60 minutes at room temperature. For GPC and PCho no significant effect was observed, however, a trend towards increased levels was observed. Although proper sample handling whereby samples are stored in liquid nitrogen within 30 minutes from collection should both be possible and standard for metabolic studies, it is important to consider this effect while planning and controlling the study design. Limited time at room temperature will improve the sample quality and enable valid interpretation of findings related to choline metabolism.

Of the three metabolic clusters obtained in paper II, Mc1 was found to have significantly higher levels of PCho and GPC. Differences in PCho/GPC ratio is a common metabolic characteristic distinguishing luminal-like and basal-like xenograft tumors [69], and high PCho has been suggested as a biomarker of breast cancer [84]. While 5 year survivors of locally advanced breast cancer were found to have higher

levels of tCho compared to non-survivors, their lactate levels were lower [56]. Combined with findings related to glucose metabolism in addition to its gene expression profile, we hypothesize that patients classified into Mc1 have the worst prognosis of the three clusters. This hypothesis will be tested once long-term follow up data is available.

Differences in the gene expression level of choline metabolism related enzymes have been observed when exploring differences between basal-like and luminal-like xenograft model [59]. These findings could possibly explain the higher GPC concentration relative to PCho observed in basal-like xenograft tumors, which is found to be a more aggressive phenotype. This suggests that the differences in metabolic profiles together with gene expression data could improve characterization of breast cancer heterogeneity. Several genes linked to choline metabolism were found to be down-regulated in the Mc1-tumors compared to the two other clusters. Although none of these genes code for enzymes directly linked to PCho or GPC formation, they are involved in PtdCho metabolism. The high tCho observed in Mc1 has been detected in other breast cancer cohorts *in vivo* and its reduction has been used as a marker for response to neoadjuvant therapy measured by *in vivo* MRS [77, 85, 86]. This reduction was in accordance with the findings of paper III, where a general trend was decreased levels of choline, PCho, and GPC with treatment time. Additionally, levels of choline and PCho were found to be lower in patients with pathological minimal residual disease compared to non-responders at the end of treatment. Patients with good or poor prognosis according to TNM classification system, however, did not show the same difference in tCho levels [52], in agreement with the metabolic response seen in 5 year survivors [60].

Amino acid metabolism

A number of amino acids are found to be elevated in cancers [41]. Following abnormal cell growth there is an increased requirement for energy and building blocks to support the synthesis of proteins and other important molecular components; amino acid metabolism can help cancer cells fulfill this need [87]. When glucose supply is limited or directed towards lactate production, cancer cells can use some amino acids to refuel the TCA cycle. Glutamine metabolism, where glutamine can be converted to glutamate, is one possibility to refuel α-ketoglutarate into the TCA cycle. The conversion from glutamine to glutamate is catalyzed by glutaminase (GLS), an enzyme that has been found to be overexpressed in several cancer types

and cancer cell lines [88]. When comparing Mc1 to the two remaining clusters (paper II) significant lower levels of both *GLS* and glutamate in Mc1 tumors were observed, while no differences in glutamine levels could be detected between the clusters. This could indicate more glutamate being guided into other pathways, or simply that glutamine metabolism is less active within these tumors. The latter is also hypothesized to be a general effect of chemotherapy for patients in paper III, which was attributed to increased glutamine levels from TP2 to TP3, independent of response to treatment.

Elevated levels of glycine has repeatedly been linked to tumor aggressiveness and poor prognosis [52, 53, 57, 89], however, to find its role in breast cancer, this has not been fully elucidated. Glycine can be synthesized from different routes including intermediates from the glycolysis pathway and from choline degradation. It can be used for production of DNA and RNA building blocks as well as the important antioxidant, glutathione [90]. In paper II, Mc2 patients exhibited lower levels of glycine than Mc3 patients. Combined with high levels of glucose within Mc2 tumors, this was found to be in accordance to the assumption that Mc2 is associated with better prognosis than the two other clusters. Mc3 on the other hand, expressed higher levels of both glycine and lactate, which for ER+ patients were found to be related to poor prognosis [53]. Higher expression of genes involved in choline metabolism, previously suggested to be linked to increased glycine levels [59], could explain this glycine profile of Mc3. There was no evidence of glycine predicting pathological treatment response (paper III), however, when comparing patients with good and no response according to response ratio, a trend of higher glycine was observed for non-responders at the end of treatment. This finding was not further evaluated in paper III, but underpins the need to evaluate glycine when clinical survival data becomes available for this cohort.

Glycine, together with glutamate and cysteine, can be directed towards synthesis of glutathione, whose modulation has been described as a double-edged sword [91]. While important for protection against cancer development by reducing reactive oxygen species (ROS) and maintaining redox homeostasis, high glutathione levels have been linked to malignancy in cancer development. It has been hypothesised that high levels of glutathione could contribute to treatment resistance by reducing the effectiveness of drugs intended to damage cancer cells [91]. Additionally, cancer cells with lower levels of glutathione are found to be more sensitive to radiation therapy, therefore glutathione is important to consider when designing the opti-

mal treatment regimen. Furthermore, in a chemo-resistant breast cancer cell line, decreased glutathione levels were suggested to be an essential event in treatment-induced reduction of their resistant properties [92]. Importantly, glutathione levels are dependent on sample handling and should only be interpreted in studies were the samples were frozen within 60 minutes from collection (paper I). After this time point, its levels were found to be significantly decreased, possibly a result of oxidative stress within the tumors. Decreased glutathione levels were also observed as a possible effect of bevacizumab observed at the end of treatment (paper III). Based on previous findings, this could indicate that these tumors are less likely to continue to avoid apoptosis and more likely to be sensitive to chemotherapy. Low levels of glutathione could indicate that Mc2 patients are more sensitive to chemotherapy than Mc3, which had the highest glutathione levels of those two groups (paper II).

Metabolism and tumor microenvironment

Emerging evidence suggests that cancer cell progression and metastasis is dependent on the tumor microenvironment [93]. Cancer cells and their surrounding stroma, including blood vessels, cancer-associated fibroblasts, immune cells, fat, extracellular matrix (ECM) and extracellular molecules, will together affect the tumor microenvironment with cellular interactions and molecular crosstalk. Although not malignant themselves, stromal cells within the tumor microenvironment can contribute to the malignant phenotype of cancer cells, for example through production of growth factors and cytokines [94]. Metabolic profiling and combination of data from several omics levels therefore have the potential to unveil biomarkers within tumor microenvironment for metastatic disease and new metabolic targets for treatment [95].

The metabolic clusters of paper II exhibited gene expression differences linked to changes in stromal activity. More specifically, Mc2 and Mc3 had significantly up-regulated genes compared to Mc1. Gene annotation and enrichment tools showed that a significant number of these genes were linked to alternations in the ECM, cell adhesion, and basement membrane. Interestingly, when compared to Mc1, both of these clusters were also found to have higher amounts of the protein expression-defined subtypes, reactive I and reactive II. Since the two 'reactive' subtypes are thought to be produced by stromal/microenvironmental elements [96], this finding is in accordance with the gene expression characteristics, suggesting a correlation between metabolic phenotype and stromal activity. The tumor microenvironment is important for tumor progression, metastasis and redox status. Thus, these charac-

teristics might be a result of the cancer cells promoting changes in the extracellular conditions needed for growth [97].

Targeting dependencies in cancer metabolism

All cancer cells exhibit altered metabolism to facilitate the energy demand and synthesis of biomass needed for rapid proliferation. Distinct differences between the three metabolic clusters in paper II were identified. This is interesting, as therapeutic agents that target metabolic dependencies are considered to be a promising anti-cancer strategy. One of the biggest obstacles for the success of this approach is the similarity between cancer cells and normal rapid proliferating cells [95]. This is also an existing well-known challenge in more traditional cancer therapies, resulting in multiple and undesired side effects. An additional obstacle for successful outcome when targeting metabolic dependencies is the redundant nature of metabolic pathways. Alternative routes for the same metabolic end product might exist, impairing the effect of targeted drugs [95]. Despite these issues, several drugs that target metabolic pathways have shown promising results leading to clinical trials [98]. In fact, some of the conventional drugs against cancer are inhibitors of metabolic enzymes, including 5-fluourouracil and methotrexate [97]. After finding evidence of asparagine supply dependency in the acute lymphocytic leukemia (ALL) cancer cells, these patients now benefit from L-asparaginase treatment [99], showing the importance of metabolic characterization in cancer. Metformin, a drug initially intended to lower blood glucose levels for type 2 diabetics, has shown anti-neoplastic effects and has been tested in clinical trials for several cancer types [100], including breast cancer, where the drug was linked with decreased proliferation [101]. Metformin has been observed to reprogram tumor cell metabolism, making chemoresistant breast cancer cells more similar to their chemosensitive counterparts [92], were metformin not only altered the metabolism of glucose, but was also suggested to reprogram glutathione metabolism. Since the sensitivity to radiation and chemotherapy has been found to be associated with glutathione levels in cells and neoplastic tissues, respectively [91], this link should further be investigated. Metformin, or other drugs that alter glutathione metabolism, could potentially be used when targeting tumors found to have high glutathione levels like those observed for the metabolic cluster Mc3.

Mc3 had evidence of high aerobic glycolytic activity, observed as low glucose levels combined with high levels of lactate, a characteristic that is being targeted

using different approaches [102]. Direct inhibition of glucose metabolism using the glucose analogue 2-deoxy-D-glucose (2DG) has been extensively studied in cancer cells, especially in combination with other treatments [103, 104]. Although preclinical toxicity issues have been a concern regarding this drug, it has been reported as well tolerated by patients [105]. By binding to the glucose transporters, 2DG inhibits glucose uptake and thereby all downstream pathways that rely on glucose to contribute with intermediates in both glycolysis and mitochondrial oxidative phosphorylation. Other possible glycolytic targets includes the hexokinases (HKs) where the use of 3-bromopyruvate (3-BrPA) have been found to induce autophagy in breast cancer cell lines [106, 107].

Altered choline metabolism is considered an attractive cancer therapy target and was found to be one of the main characteristics of Mc1. One of the key enzymes in altered choline metabolism is CHKA [108], the first enzyme in the choline pathway. Inhibition of this enzyme (RSM-932A) induced antiproliferative effects, which were detected both in cancer cell lines and xenograft models of human tumors [109]. These promising results combined with low toxicity profiles have led to the drug being tested in phase I clinical trials [109]. One of the benefits of targeting choline metabolism is the possibility of detecting and monitoring treatment response by observing the tCho signal using *in vivo* MRSI [86]. *Ex vivo* monitoring, using HR MAS MRS of fine needle biopsies, could also be valuable tool. Using this approach, a transient increase in choline containing metabolites has been found to be an early marker for docetaxel sensitivity in a BRAC1-mutated mice model [110]. For treatment strategies targeting choline metabolism directly, several metabolic enzymes with altered expression and activity could potentially be used such as choline transporter-like protein 1 (CLT1) and CTP:phosphocholine cytidylyltransferase (CCT) [42].

Targeting amino acid metabolism has been suggested as a promising strategy in cancer therapy [111]. Glutamine, with its potential of providing both carbon and nitrogen to cellular building blocks, is considered to be essential in rapidly dividing cells [44]. However, with the possibility of de novo synthesis of glutamine together with a potential supply of glutamine from other glutamine producing cells [112], information about the variety of and degree of glutamine reprogramming among cancer subtypes is still lacking. If better characterized, prediction of which tumors are more likely to benefit from glutamine targeted treatment could be promising [44]. Glutaminase has been found to be upregulated in several types of cancer [113]

making it a promising target. The glutaminase inhibitor CB-839 is currently being investigated in phase I trials [114] and could potentially be used for tumors found to be glutamine dependent. Among the genetic subtypes of breast cancer, basal-like epithelial cells were found to be more dependent on glutamine supply compared to luminal-like [112]. Targeted investigation into both gene and protein expression differences related to glutamine metabolism could possibly clarify these metabolic differences and predict which are more likely to benefit from targeted treatment. For the metabolic clusters in paper II, Mc1 is reprogrammed in such a way that the glutamate produced is more rapidly guided towards production of proliferative building blocks, or simply that glutamine supply of Mc2 and Mc3 tumors is higher, and converted to glutamate more rapidly due to higher availability of the GLS enzyme.

5.2 Methodological considerations

In a research setting, the study design and choice of methods, both at the experimental stage and during data analysis, is important as it can influence the results. In the following sections, methods used within the current thesis are discussed.

Patients and tumor tissue samples

In this work, both breast cancer xenograft tissue and patient tissue were analyzed. Samples from the patient-derived xenograft models, MAS98.08 and MAS98.12, were used to study the metabolic effects of prolonged time at room temperature prior to freezing (freezing time delay) (paper I) [68]. These models were established by implementing bulk tumor tissue, harvested from breast cancer patients, directly into the mammary fat pad of immunodeficient mice. By using direct grafting of tumor tissue, in contrast to injection of cell lines or using genetically engineered mice, more of the human tumor characteristics are captured. Additionally, injection into the mammary fat pad provides a tumor microenvironment that is more similar to the tumors original surrounding compared subcutaneous injection. Although a tumor model will never be able to capture all properties and aspects of the human cancer, it was considered to be good model system for the methodological purpose of paper I - detecting metabolites affected by sample handling differences. Performing a similar study using patient material would also be valuable, it could however, be influenced to a higher degree by tumor heterogeneity. The models used have been characterized both at the genetic [68] and metabolic [69] level showing small inter- and intra-tumor variability. Metabolic effects detected in paper I should thus be representative for the ongoing degradation processes in human tumor tissue caused by freezing time delay.

Tumor tissue from breast cancer patients can be harvested through needle biopsies or during surgery. From the moment blood supply is cut, the tumor is prone to degradation processes. To minimize metabolic alterations, as well as ischemic influence on other cellular processes, samples for HR MAS MRS analysis should be snap-frozen in liquid nitrogen as soon as possible [115]. Although the snap-freezing might have metabolic consequences [116], as observed in paper I, the alternative approach of analyzing samples directly after harvesting is often inconvenient. The human samples utilized in paper I and II were obtained from untreated patients during final surgery, while samples in paper III were collected prior to, during and

after neoadjuvant treatment of HER2 negative (HER2−) breast cancer patients. After surgical removal, samples in paper I were immediately ($\backsim$ 5 min) snap-frozen and stored for a maximum of 3 years in liquid nitrogen until HR MAS MRS analysis. Surgical samples in paper II and III were evaluated by a pathologist within 30-60 minutes prior to storage in -80°C, and stored for a maximum of 5 or 3 years, respectively. The samples were transferred to storage in liquid nitrogen minimum 6 months prior to analysis. The metabolic effect of long-term storage prior to HR MAS analysis was found to be insignificant for prostate tissue stored for 3 years at -80°C [117]. In a more recent study however, significant changes in both breast cancer tissue and adjacent healthy tissue were reported after 12 months of storage [118]. Choline increased significantly for both groups while levels of PCho decreased significantly in 'healthy' samples. Despite these findings, metabolic differences between neoplastic and healthy tissue were considered sufficient for discrimination. The metabolic changes thought to be related to storage could, however, be influenced by degradation processes caused by the repeated freezing and thawing (to 5°C inside HR MAS MRS magnet) needed to reanalyze the same sample after prolonged storage.

Tumor size for treatment response assessment

In paper III, exploring the association between metabolic profile and treatment response was a major objective. The RECIST criteria are commonly used to assess treatment response in solid tumors [119]. However, due to the lack of MRI measurements for some patients before treatment, which in addition to computed tomography (CT) is a recommended method in the RECIST guidelines, we chose to look into alternative measures of treatment response. Pathological complete response, where a total eradication of the invasive cancer cells in the breast and lymph nodes are achieved, would have been a good option for defining responders and non-responders in this cohort, especially since pathological complete response is known to be a prognostic factor after neoadjuvant chemotherapy [24]. However, pathological complete response was only achieved for 20 of 122 patients in our study. If this criterion was to be used for response assessments, valuable information from the cases where the tumors had shrunk significantly with treatment, but not fulfilling pathological complete response criteria, would be lost. Tumor size reduction as a measure of treatment response may have limitations for the evaluation of drugs that do not cause tumor shrinkage [120], which is the case for some antiangiogenetic drugs like

bevacizumab [121]. However, since the main purpose of neoadjuvant chemotherapy is to make the tumor operable, pathological minimal residual disease (pathological tumor size < 1 cm) was considered a good choice for classifying responders. An additional response assessment measure was also defined, which described tumor reduction from treatment onset until final surgery.

Metabolomics analysis

Magnetic resonance spectroscopy (MRS), can be considered one of the two main approaches employed for metabolic profiling together with mass spectrometry (MS) [34]. Although neither of these methods can independently identify and quantify the entire metabolome (i.e all metabolites present within the cell/tissue/organ etc), they give high quality data, which is valuable for metabolomics studies. MS methods have high sensitivity, but require more sample preparation, thus reducing its reproducibility. More specifically, prior to analysis, tissue samples have to be extracted, introducing analytical steps that might lead to loss of metabolic information. In contrast, HR MAS MRS is a non-destructive technique requiring minimal sample preparation resulting in data with high specificity and reproducibility. The main disadvantage is its relatively low sensitivity (micromolar range compared to picomolar range for some MS based methods), however, in breast cancer tissue, more than 30 metabolites involved in important cancer related pathways have been detected [51] and distinctive differences have been characterized between normal adjacent tissue and cancer tissue (reviewed in [41]).

As described, sufficient tumor material for the HR MAS MRS analysis in paper II and III were separated from the main sample prior to other molecular analyzes. HR MAS is non-destructive and allows for further subsequent analysis, and previous studies report high RNA integrity after HR MAS MRS [122]. However, this opportunity was not utilized in the current thesis due to the study design involving collection of a high number of samples which were analyzed using several molecular platforms. Furthermore, performing HR MAS MRS studies prior to the remaining methods would be time consuming and lead to logistical challenges due to geographical distances between the collaborating laboratories in this work. Depending on the original tumor size and degree of intratumoral heterogeneity, it could be questioned whether the analyzed part of the tumor is representative of the tumor as a whole. However, as extraction of DNA, RNA and proteins (if applicable) for

the combined molecular analysis were performed in closely adjacent material, we consider the metabolic profiles to be representative.

Metabolic quantification

Due to the anatomy of the female breast, tumor biopsies obtained from breast cancer patients might contain fractions of adipose tissue. The aliphatic side chains of fatty acids within this tissue can give rise to large and broad peaks in MR spectra, potentially overlapping with and influencing signals from important small metabolites. To limit this effect, HR MAS MRS acquisition within the current thesis was performed using a CPMG sequence. As previously described, this takes advantage of the short T_2 relaxation of larger molecules, like fatty acids, and selectively suppresses their signal, consequently enhancing signals from small metabolites. Because of small differences in T_2 relaxation, absolute quantification would be unreliable without proper and time-consuming T_2 measurements. However, the signal intensities and therefore the metabolite levels, are still comparable between the spectra obtained from the samples. Thus, spectral integration of metabolite regions were used to obtain the levels of metabolites identified in the spectra. Overlapping metabolites can cause inaccuracy in these measurements, but integrals were still considered sufficient when used in combination with multivariate approaches within the exploratory studies of this thesis. An alternative approach that could be used to quantify metabolites is manual peak fitting. Manual peak fitting would better correct for overlapping metabolites than integration, however it would be prone to subjective judgment and for big sample cohorts it is extremely time consuming. Automatic peak fitting in tools such as LCModel [123] have been used to quantify metabolites in brain [124] and prostate tissue [125]. In spite of efforts to develop the same automatic method for breast tissue in this thesis, problems caused by the broad lipids peaks has limited its success so far.

An additional alternative to absolute quantification is the use of metabolic ratios rather than concentrations, typically ratios given relative to creatine levels [110, 126, 127]. However, since we observed a significant decrease in creatine levels with freezing time delay (paper I), such ratios should only be used if samples were frozen within 30 minutes after collection. Other ratios could also give valuable information, e.g. GPC/PCho or glucose/lactate, but would not carry information if both metabolites in the ratio increase or decrease simultaneously.

Pre-processing and multivariate analysis

Prior to quantification and multivariate analysis, appropriate pre-processing methods are important to obtain valid and interpretable results. In this thesis, established pre-processing protocols were applied to all data. Baseline correction and alignment of peaks was visually evaluated before performing normalization, which was done to minimize the effect from variations in sample size. The choice of normalization method can largely affect the result and should be carefully chosen. In paper I and II, spectral data obtained from breast cancer patients were normalized to equate areas under the curves after excluding lipid regions. As previously discussed, spectra obtained from patient samples can be largely influenced by fatty acids found in adipose tissue surrounding the tumor. In contrast, tumor tissue from xenografts are found to be more homogenous, with lipid droplets distributed inside the tumor. Lipid regions in spectra from xenografts (paper I) were thus not excluded, but included for statistical analysis. The spectra were normalized to sample weight to account for differences in sample size. In paper III, probabilistic quotient normalization (PQN) [66] was applied. Here, the most probable sample dilution or amount of sample is calculated. As this method is more robust to variance in individual metabolites, it was chosen in paper III because many pre-surgery samples were contaminated with the local anesthetic lidocaine. Although these regions later were removed from the spectra, PQN is more robust for analysis of spectra containing significant amounts of unwanted metabolites.

Absolute quantification enables direct comparisons of metabolic concentrations between studies, but there are also important benefits using multivariate approaches, where the entire spectral data are analyzed as a whole. From complex metabolic data, such statistical methods can be used to extract differences in metabolic profiles and patterns of several metabolites simultaneously, rather than single metabolites. Although these approaches are not quantitative, they are valuable for interpretation as well as validation of complex data. In the current thesis, multivariate methods were used to identify differences in metabolic features between groups of patients. PCA was used for exploratory purposes to look for the main differences within each study sample cohort and to detect outliers. For paper II, unsupervised hierarchical cluster analysis grouped breast cancer tumors into three metabolic clusters, before PLS-DA was performed to evaluate the robustness of these groups. In paper III, PLS-DA models were used to identify metabolic differences between different

groups of patients, e.g. responders versus non-responders. To ensure the quality of the metabolic clusters in paper II and the PLS-DA models built in paper III, proper validation was essential. The optimal choice for validation would always be to use independent test sets, for many studies, however, including the ones in the current thesis, sample size was a limiting factor.

Double cross validation was considered to be the best alternative to independent test sets for validation of multivariate models, thereby also finding the optimal number of LVs. Here, the models were built using a subset of the samples, 80 % and 90 % for paper II and paper III, respectively, while the remaining were used to test each model's performance. Based on the performance of each model (i.e. classification results) and whether it performed better than random classification obtained by permutation tests, each model's metabolic interpretation was evaluated. Still, regardless of each model's performance, it is important to keep in mind that the model built cannot be any better than the cohort used to build it, meaning that cohorts that do not represent the real variability within a population may produce over-optimistic results.

To further investigate how generic findings are, i.e. the metabolic clusters defined in paper II, comparison with data from similar cohorts should be performed. However, we were not able to identify any published cohort with similar patient characteristics (primary operable tumor) where both metabolic and transcriptomic data were made public. There are still relatively few public metabolomics data bases compared to transcriptomic and proteomic data bases and no general standard for how to report metabolite values. In addition, journals do not require submission of metabolic data to the same extent [128]. An obstacle and possible reason for the establishment of metabolic data bases is the high variety of data structure. Differences in metabolic methods, raw data, choice of pre-processing approaches and quantification make it hard to find ways to design a user friendly data base.

Combining omics

Metabolomics has proven to be an important tool for the identification of new biomarkers for targeted treatment, treatment evaluation and prediction of cancer survival [129–132]. Previous studies have also shown the potential and benefit of combining different omics approaches (e.g. transcriptomics and metabolomics) for better molecular characterization and stratification of breast cancer [50, 133, 134]. Breast cancer molecular profiling using combined omics data may thus provide mul-

tiple targets at different molecular levels and possibly improve breast cancer subtyping. Targeting metabolic reprogramming is considered a promising approach for cancer therapy, and in combination with genetic characteristics could lead to more effective treatments [95].

In this work, specifically paper II, combined analysis of transcriptomic, proteomic and metabolic data was performed, employing a similar approach to the discovery of genetic subgroups of breast cancer [26]. Breast tumors were classified into three metabolic clusters by hierarchical clustering. Although both types of data are multivariate, their information structure is different. Each data point from gene expression microarrays represents measurements from a single probe, while when pre-processed spectra are input, multiple variables together make up the signal from one metabolite. When applied to gene expression data, two dimensional clustering is frequently performed (i.e. both samples and probes are set to be clustered), resulting in groups of probes as well as samples. This is a helpful tool for identifying probes with similar expression profiles within a highly complex data set. Due to the well-known collinearity of MR spectra, two dimensional clustering of spectral data would not have the same utility. Despite these differences, the one dimensional clustering approach, as performed in paper II, will help to reduce data complexity and identify metabolic patterns within the data cohort. Samples clustered together have important similarities with each other and dissimilarities with samples clustered further apart. Established in an unsupervised manner, they thus reflect the metabolic variety within the data set used for analysis. A similar approach has previously been used to define metabolic clusters within the genetic subtype luminal A [50]. With a higher number of samples and a more heterogeneous sample cohort in paper II, the statistical power is improved from the previously defined metabolic clusters. The metabolic clusters were combined with available gene expression data for evaluation of transcriptomic differences using available tools (SAM, DAVID, GSEA) and with protein expression subgroups (RPPA-subtype). Furthermore, significantly different expressed genes and metabolites were combined to look for possible biological connections between the two omic levels using online available integrated analysis. The aim of using this approach was to better understand the underlying mechanisms for the metabolic phenotype as well as its link to clinical parameters. The findings emphasizes that the metabolic properties of tumors is a result of a complex network of pathways that cannot solely be explained by gene and protein expression levels.

6 Conclusion and future perspectives

In this thesis, MR metabolic profiling of tumor tissue from breast cancer patients was used to assess metabolic heterogeneity of primary operable tumors and metabolic response to neoadjuvant chemotherapy within primary inoperable tumors. Furthermore, optimal sample handling for metabolomic studies was evaluated using tissue samples from xenograft models, as well as breast cancer patients.

The metabolic profile of tumor samples were found to be robust to freezing delay times of up to 30 minutes prior to sample storage in liquid nitrogen. Longer freezing delay times were found to significantly affect the levels of choline, creatine and important antioxidants. As MR metabolomics is a widely used approach in translational research where metabolic profiles can be linked to other disease parameters and, ultimately, patient outcome, consistent sample collection and preparation is crucial for valid interpretation of the resulting data. Paper I elucidated the importance of minimizing both time prior to storage and experimental duration.

In paper II, three novel metabolic clusters of breast cancer were identified and found to have differences in metabolic pathways known to be aberrant in cancer. Furthermore, the metabolic clusters were found to express differences in breast cancer related proteins as well as genes related to the extracellular matrix. Interestingly, genetic subtypes were evenly distributed among the three metabolic clusters, thus metabolomics contribute with additional information beyond the intrinsic gene sets for understanding breast cancer heterogeneity. Based on previous metabolic findings, one of the clusters was expected to have a worse prognosis. 5-year survival data will, when available, be used to evaluate the prognostic potential of the clusters. In addition, available data from other platforms including DNA methylation, copy number aberrations and expression of miRNA could potentially lead to deeper understanding of the mechanisms for the metabolic reprogramming taking place in the individual clusters.

In paper III, changes in the metabolic profiles as an effect of chemotherapy were detected. In addition, successful discrimination of responders and non-responders after treatment was obtained. Together, this shows potential for MR metabolomics in providing insight into metabolic response to treatment, and to increase the understanding of the underlying mechanisms affecting pathological response. Furthermore, tumors obtained from patients receiving the antiangiogenic drug bevacizumab were found to have alterations in glutathione metabolism, a characteristic

that should be further investigated. In accordance with previous findings, metabolic prediction of response prior to treatment start was not possible. The metabolic data should thus be combined with survival data when available. This could further be used to obtain the prognostic value of metabolic profiles prior to, during and after neoadjuvant chemotherapy.

Altogether, the findings of this thesis have clarified the metabolic consequences of sample handling procedures, and contributed to further improvement of characterization of breast cancer metabolism. As the metabolites may serve as phenotypic markers resulting from both genome and proteome alterations, MR metabolomics can potentially be used to provide important predictive and prognostic information. Future studies combining metabolic profiles with data from other platforms could potentially lead to an improvement in patient stratification and treatment strategies targeting metabolic pathways.

References

[1] D. Hanahan and R. Weinberg, "The hallmarks of cancer," *Cell*, vol. 100, no. 1, pp. 57–70, 2000.

[2] J. Ferlay, I. Soerjomataram, R. Dikshit, S. Eser, C. Mathers, M. Rebelo, D. Parkin, D. Forman, and F. Bray, "Cancer incidence and mortality worldwide: sources, methods and major patterns in GLOBOCAN 2012," *Int J Cancer*, no. 5, pp. E359–86, 2014.

[3] D. Hanahan and R. Weinberg, "Hallmarks of cancer: the next generation," *Cell*, vol. 144, no. 5, pp. 646–74, 2011.

[4] J. Ferlay, I. Soerjomataram, R. Dikshit, S. Eser, C. Mathers, M. Rebelo, D. Parkin, D. Forman, and F. Bray, "Cancer incidence and mortality worldwide: sources, methods and major patterns in GLOBOCAN 2012," *Int J Cancer*, vol. 136, no. 5, pp. E359–86, 2015.

[5] Cancer Registry of Norway, "Cancer in norway 2013 - cancer incidence, mortality, survival and prevalence in norway," tech. rep., 2015.

[6] T. Key, P. Verkasalo, and E. Banks, "Epidemiology of breast cancer," *Lancet Oncol*, vol. 2, no. 3, pp. 133–40, 2001.

[7] K. McPherson, C. Steel, and J. Dixon, "Breast cancer-epidemiology, risk factors, and genetics," *Br Med J*, vol. 321, no. 7261, p. 624, 2000.

[8] H. Weedon-Fekjær, P. Romundstad, and L. Vatten, "Modern mammography screening and breast cancer mortality: population study," *BMJ*, vol. 348, p. g3701, 2014.

[9] G. Lahat, D. Lev, F. Gerstenhaber, J. Madewell, H. Le-Petross, and R. Pollock, "Sarcomas of the breast," *Expert Rev Anticancer Ther*, vol. 12, no. 8, pp. 1045–51, 2012.

[10] Norsk Bryst Cancer Gruppe (NBCG), "Nasjonalt handlingsprogram med retningslinjer for diagnostikk, behandling og oppfølging av pasienter med brystkreft," *Helsedirektoratet (Norway)*, vol. 6, 2015.

[11] F. Tavassoli and P. Devilee, *WHO Classification of Tumours. Pathology and genetics of tumours of the breast and female genital organs*, vol. 4. IARC, Lyon 2003.

[12] D. Arps, P. Healy, L. Zhao, C. Kleer, and J. Pang, "Invasive ductal carcinoma with lobular features: a comparison study to invasive ductal and invasive lobular carcinomas of the breast," *Breast Cancer Res Treat*, vol. 138, no. 3, pp. 719–26, 2013.

[13] E. Rakha, J. Reis-Filho, F. Baehner, D. Dabbs, T. Decker, V. Eusebi, S. Fox, S. Ichihara, J. Jacquemier, S. Lakhani, J. Palacios, A. Richardson, S. Schnitt, F. Schmitt, P. Tan, G. Tse, S. Badve, and I. Ellis, "Breast cancer prognostic classification in the molecular era: the role of histological grade," *Breast Cancer Res*, vol. 12, no. 4, p. 207, 2010.

[14] L. Bernstein and M. Press, "Does estrogen receptor expression in normal breast tissue predict breast cancer risk?," *J Nat l Cancer Inst*, vol. 90, no. 1, pp. 5–7, 1998.

[15] M. Weigel and M. Dowsett, "Current and emerging biomarkers in breast cancer: prognosis and prediction," *Endocr Relat Cancer*, vol. 17, no. 4, pp. R245–R262, 2010.

[16] L. Dunnwald, M. Rossing, and C. Li, "Hormone receptor status, tumor characteristics, and prognosis: a prospective cohort of breast cancer patients," *Breast Cancer Res*, vol. 9, no. 1, p. R6, 2007.

[17] M. Engstrøm, S. Opdahl, A. Hagen, P. Romundstad, L. Akslen, O. Haugen, L. Vatten, and A. Bofin, "Molecular subtypes, histopathological grade and survival in a historic cohort of breast cancer patients," *Breast Cancer Res Treat*, vol. 140, no. 3, pp. 463–73, 2013.

[18] W. Wang, Y. Lei, J. Mei, and C. Wang, "Recent progress in HER2 associated breast cancer," *Asian Pac J Cancer Prev*, vol. 16, no. 7, pp. 2591–600, 2015.

[19] M. Figueroa-Magalhães, D. Jelovac, R. Connolly, and A. Wolff, "Treatment of HER2-positive breast cancer," *Breast*, vol. 23, no. 2, pp. 128–36, 2014.

[20] N. Ferrara, K. Hillan, H.-P. Gerber, and W. Novotny, "Discovery and development of bevacizumab, an anti-VEGF antibody for treating cancer," *Nature Rev Drug Discov*, vol. 3, no. 5, pp. 391–400, 2004.

[21] M. Lobbes, R. Prevos, and M. Smidt, "Response monitoring of breast cancer patients receiving neoadjuvant chemotherapy using breast MRI - a review of current knowledge," *J Cancer Ther Res*, vol. 1, no. 1, p. 34, 2012.

[22] X. Kong, M. Moran, N. Zhang, B. Haffty, and Q. Yang, "Meta-analysis confirms achieving pathological complete response after neoadjuvant chemotherapy predicts favourable prognosis for breast cancer patients," *Eur J Cancer*, vol. 47, no. 14, pp. 2084–90, 2011.

[23] D. Snustad and M. Simmons, *Principles of genetics (5th Edition)*. Wiley New Jersey, 2010.

[24] M.-C. King, J. Marks, and J. Mandell, "Breast and ovarian cancer risks due to inherited mutations in *BRCA1* and *BRCA2*," *Science*, vol. 302, no. 5645, pp. 643–6, 2003.

[25] International Human Genome Sequencing Consortium, "Finishing the euchromatic sequence of the human genome," *Nature*, vol. 431, no. 7011, pp. 931–45, 2004.

[26] C. Perou, T. Sørlie, M. Eisen, M. van de Rijn, S. Jeffrey, C. Rees, J. Pollack, D. Ross, H. Johnsen, and L. Akslen, "Molecular portraits of human breast tumours," *Nature*, vol. 406, no. 6797, pp. 747–52, 2000.

[27] T. Sørlie, C. Perou, R. Tibshirani, T. Aas, S. Geisler, H. Johnsen, T. Hastie, M. Eisen, M. van de Rijn, and S. Jeffrey, "Gene expression patterns of breast carcinomas distinguish tumor subclasses with clinical implications," *Proc Natl Acad Sci U S A*, vol. 98, no. 19, pp. 10869–74, 2001.

[28] C. Perou and A.-L. Børresen-Dale, "Systems biology and genomics of breast cancer," *Cold Spring Harb Perspect Biol*, vol. 3, no. 2, p. a003293, 2011.

[29] A. Prat and C. M. Perou, "Deconstructing the molecular portraits of breast cancer," *Mol Oncol*, vol. 5, no. 1, pp. 5–23, 2011.

[30] J. Herschkowitz, K. Simin, V. Weigman, I. Mikaelian, J. Usary, Z. Hu, K. Rasmussen, L. Jones, S. Assefnia, and S. Chandrasekharan, "Identification of conserved gene expression features between murine mammary carcinoma models and human breast tumors," *Genome Biol*, vol. 8, no. 5, p. R76, 2007.

[31] J. Parker, M. Mullins, M. Cheang, S. Leung, D. Voduc, T. Vickery, S. Davies, C. Fauron, X. He, and Z. Hu, "Supervised risk predictor of breast cancer based on intrinsic subtypes," *J Clin Oncol*, vol. 27, no. 8, pp. 1160–7, 2009.

[32] R. Sallam, "Proteomics in cancer biomarkers discovery: Challenges and applications," *Dis Markers*, vol. 2015, 2015.

[33] T. C. G. A. Network, "Comprehensive molecular portraits of human breast tumours," *Nature*, vol. 490, no. 7418, pp. 61–70, 2012.

[34] J. T. Bjerrum, "Metabonomics: Analytical techniques and associated chemometrics at a glance," in *Metabonomics: Methods and Protocols* (J. T. Bjerrum, ed.), pp. 1–14, Humana Press, 2015.

[35] C. Denkert, E. Bucher, M. Hilvo, R. Salek, M. Oresic, J. Griffin, S. Brockmoller, F. Klauschen, S. Loibl, and D. Barupal, "Metabolomics of human breast cancer: new approaches for tumor typing and biomarker discovery," *Genome Med*, vol. 4, no. 4, p. 37, 2012.

[36] A. Schulze and A. Harris, "How cancer metabolism is tuned for proliferation and vulnerable to disruption," *Nature*, vol. 491, no. 7424, pp. 364–73, 2012.

[37] O. Warburg, "On the origin of cancer cells," *Science*, vol. 123, no. 3191, pp. 309–14, 1956.

[38] M. Vander Heiden, L. Cantley, and C. Thompson, "Understanding the Warburg effect: the metabolic requirements of cell proliferation," *Science*, vol. 324, no. 5930, pp. 1029–33, 2009.

[39] F. Hirschhaeuser, U. Sattler, and W. Mueller-Klieser, "Lactate: a metabolic key player in cancer," *Cancer Res*, vol. 71, no. 22, pp. 6921–5, 2011.

[40] F. Gibellini and T. Smith, "The Kennedy pathway-de novo synthesis of phosphatidylethanolamine and phosphatidylcholine," *IUBMB Life*, vol. 62, no. 6, pp. 414–28, 2010.

[41] S. Moestue, B. Sitter, T. Bathen, M.-B. Tessem, and I. Gribbestad, "HR MAS MR spectroscopy in metabolic characterization of cancer," *Curr Top Med Chem*, vol. 11, no. 1, pp. 2–26, 2011.

[42] K. Glunde, Z. Bhujwalla, and S. Ronen, "Choline metabolism in malignant transformation," *Nat Rev Cancer*, vol. 11, no. 12, pp. 835–48, 2011.

[43] P. Champe, R. Harvey, and D. Ferrier, *Biochemistry*. Lippincott Williams & Wilkins, 3 ed., 2005.

[44] C. Hensley, A. Wasti, and R. DeBerardinis, "Glutamine and cancer: cell biology, physiology, and clinical opportunities," *J Clin Invest*, vol. 123, no. 9, p. 3678, 2013.

[45] W. Lu, H. Pelicano, and P. Huang, "Cancer metabolism: is glutamine sweeter than glucose?," *Cancer Cell*, vol. 18, no. 3, pp. 199–200, 2010.

[46] P. Rinck, "Magnetic resonance in medicine: the basic textbook of the european magnetic resonance forum," *Clin Radiol*, vol. 49, no. 11, p. 842, 1994.

[47] J. Hennel and J. Klinowski, *Magic-angle spinning: a historical perspective*, pp. 1–14. Springer, 2005.

[48] E. Andrew, A. Bradbury, and R. Eades, "Nuclear magnetic resonance spectra from a crystal rotated at high speed," *Nature*, vol. 182, no. 4650, p. 1659, 1958.

[49] I. Lowe, "Free induction decays of rotating solids," *Physical Review Letters*, vol. 2, no. 7, pp. 285–7, 1959.

[50] E. Borgan, B. Sitter, O. Lingjærde, H. Johnsen, S. Lundgren, T. Bathen, T. Sørlie, A.-L. Børresen-Dale, and I. Gribbestad, "Merging transcriptomics and metabolomics-advances in breast cancer profiling," *BMC Cancer*, vol. 10, no. 1, p. 628, 2010.

[51] B. Sitter, U. Sonnewald, M. Spraul, H. Fjøsne, and I. Gribbestad, "High-resolution magic angle spinning MRS of breast cancer tissue," *NMR Biomed*, vol. 15, no. 5, pp. 327–37, 2002.

[52] B. Sitter, T. Bathen, T. Singstad, H. Fjøsne, S. Lundgren, J. Halgunset, and I. Gribbestad, "Quantification of metabolites in breast cancer patients with different clinical prognosis using HR MAS MR spectroscopy," *NMR Biomed*, vol. 23, no. 4, pp. 424–31, 2010.

[53] G. Giskeødegård, S. Lundgren, B. Sitter, H. Fjøsne, G. Postma, L. Buydens, I. Gribbestad, and T. Bathen, "Lactate and glycine–potential MR biomarkers of prognosis in estrogen receptor-positive breast cancers," *NMR Biomed*, vol. 25, no. 11, pp. 1271–9, 2012.

[54] U. Sharma, A. Mehta, V. Seenu, and N. Jagannathan, "Biochemical characterization of metastatic lymph nodes of breast cancer patients by in vitro ^{1}H magnetic resonance spectroscopy: a pilot study," *Magn Reson Imaging*, vol. 22, no. 5, pp. 697–706, 2004.

[55] V. Seenu, M. Kumar, U. Sharma, S. Gupta, S. Mehta, and N. Jagannathan, "Potential of magnetic resonance spectroscopy to detect metastasis in axillary lymph nodes in breast cancer," *Magn Reson Imaging*, vol. 23, no. 10, pp. 1005–10, 2005.

[56] M. Cao, B. Sitter, T. Bathen, A. Bofin, P. Lønning, S. Lundgren, and I. Gribbestad, "Predicting long-term survival and treatment response in breast cancer patients receiving neoadjuvant chemotherapy by MR metabolic profiling," *NMR Biomed*, vol. 25, no. 2, pp. 369–78, 2012.

[57] B. Sitter, S. Lundgren, T. Bathen, J. Halgunset, H. Fjøsne, and I. Gribbestad, "Comparison of HR MAS MR spectroscopic profiles of breast cancer tissue with clinical parameters," *NMR Biomed*, vol. 19, no. 1, pp. 30–40, 2006.

[58] M. Li, Y. Song, N. Cho, J. Chang, H. Koo, A. Yi, H. Kim, S. Park, and W. Moon, "An HR-MAS MR metabolomics study on breast tissues obtained with core needle biopsy," *PloS one*, vol. 6, no. 10, p. e25563, 2011.

[59] S. Moestue, E. Borgan, E. Huuse, E. Lindholm, B. Sitter, A.-L. Børresen-Dale, O. Engebraaten, G. Mælandsmo, and I. Gribbestad, "Distinct choline metabolic profiles are associated with differences in gene expression for basal-like and luminal-like breast cancer xenograft models," *BMC Cancer*, vol. 10, no. 1, p. 433, 2010.

[60] M. Cao, G. Giskeødegård, T. Bathen, B. Sitter, A. Bofin, P. Lønning, S. Lundgren, and I. Gribbestad, "Prognostic value of metabolic response in breast cancer patients receiving neoadjuvant chemotherapy," *BMC Cancer*, vol. 12, no. 1, pp. 12–39, 2012.

[61] M. Cao, S. Lamichhane, S. Lundgren, A. Bofin, H. Fjøsne, G. Giskeødegård, and T. Bathen, "Metabolic characterization of triple negative breast cancer," *BMC Cancer*, vol. 14, no. 1, p. 941, 2014.

[62] L. Euceda, G. Giskeødegård, and T. Bathen, "Preprocessing of NMR metabolomics data," *Scand J Clin Lab Invest*, vol. 75, no. 3, pp. 193–203, 2015.

[63] R. Vettukattil, "Preprocessing of raw metabonomic data," in *Metabonomics: Methods and Protocols* (J. T. Bjerrum, ed.), vol. 1277 of *Methods in Molecular Biology*, pp. 123–36, Springer New York, 2015.

[64] F. Savorani, G. Tomasi, and S. Engelsen, "icoshift: A versatile tool for the rapid alignment of 1D NMR spectra," *J Magn Reson*, vol. 202, no. 2, pp. 190–202, 2010.

[65] G. Giskeødegård, T. Bloemberg, G. Postma, B. Sitter, M.-B. Tessem, I. Gribbestad, T. Bathen, and L. Buydens, "Alignment of high resolution magic angle spinning magnetic resonance spectra using warping methods," *Anal Chim Acta*, vol. 683, no. 1, pp. 1–11, 2010.

[66] F. Dieterle, A. Ross, G. Schlotterbeck, and H. Senn, "Probabilistic quotient normalization as robust method to account for dilution of complex biological mixtures. application in ^{1}H NMR metabonomics," *Anal Chem*, vol. 78, no. 13, pp. 4281–90, 2006.

[67] J. Ibrahim and G. Molenberghs, "Missing data methods in longitudinal studies: a review," *Test*, vol. 18, no. 1, pp. 1–43, 2009.

[68] A. Bergamaschi, G. Hjortland, T. Triulzi, T. Sørlie, H. Johnsen, A. Ree, H. Russnes, S. Tronnes, G. Mælandsmo, and Ø. Fodstad, "Molecular profiling and characterization of luminal-like and basal-like *in vivo* breast cancer xenograft models," *Mol Oncol*, vol. 3, no. 5, pp. 469–82, 2009.

[69] M. Grinde, S. Moestue, E. Borgan, Ø. Risa, O. Engebraaten, and I. Gribbestad, "^{13}C high-resolution-magic angle spinning MRS reveals differences in glucose metabolism between two breast cancer xenograft models with different gene expression patterns," *NMR Biomed*, vol. 24, no. 10, pp. 1243–52, 2011.

[70] R Core Team, *R: A Language and Environment for Statistical Computing*. R Foundation for Statistical Computing, Vienna, Austria, 2014.

[71] S. Buuren and K. Groothuis-Oudshoorn, "mice: Multivariate imputation by chained equations in R," *J Stat Softw*, vol. 45, no. 3, 2011.

[72] J. Pinheiro, D. Bates, S. DebRoy, and D. Sarkar, "nmle: Linear and nonlinear mixed effects models. R package version 3.1-117." URL: http://CRAN.R-project.org/package=nlme, 2014.

[73] V. Tusher, R. Tibshirani, and G. Chu, "Significance analysis of microarrays applied to the ionizing radiation response," *Proc Natl Acad Sci U S A*, vol. 98, no. 9, pp. 5116–21, 2001.

[74] W. Huang da, B. Sherman, and R. Lempicki, "Systematic and integrative analysis of large gene lists using DAVID bioinformatics resources," *Nat Protoc*, vol. 4, no. 1, pp. 44–57, 2008.

[75] A. Subramanian, P. Tamayo, V. Mootha, S. Mukherjee, B. Ebert, M. Gillette, A. Paulovich, S. Pomeroy, T. Golub, and E. Lander, "Gene set enrichment analysis: a knowledge-based approach for interpreting genome-wide expression profiles," *Proc Natl Acad Sci U S A*, vol. 102, no. 43, pp. 15545–50, 2005.

[76] J. Xia, R. Mandal, I. Sinelnikov, D. Broadhurst, and D. Wishart, "Metaboanalyst 2.0–a comprehensive server for metabolomic data analysis," *Nucleic Acids Res*, vol. 40, no. Web Server issue, pp. W127–33, 2012.

[77] R. Gillies and D. Morse, "In vivo magnetic resonance spectroscopy in cancer," *Annu Rev Biomed Eng*, vol. 7, pp. 287–326, 2005.

[78] D. Mankoff, J. Eary, J. Link, M. Muzi, J. Rajendran, A. Spence, and K. Krohn, "Tumor-specific positron emission tomography imaging in patients:[^{18}F] fluorodeoxyglucose and beyond," *Clin Cancer Res*, vol. 13, no. 12, pp. 3460–9, 2007.

[79] S. Walenta, T. Schroeder, and W. Mueller-Klieser, "Lactate in solid malignant tumors: potential basis of a metabolic classification in clinical oncology," *Curr Med Chem*, vol. 11, no. 16, pp. 2195–204, 2004.

[80] J. Xie, H. Wu, C. Dai, Q. Pan, Z. Ding, D. Hu, B. Ji, Y. Luo, and X. Hu, "Beyond Warburg effect-dual metabolic nature of cancer cells," *Sci Rep*, vol. 4, 2014.

[81] E. Aboagye and Z. Bhujwalla, "Malignant transformation alters membrane choline phospholipid metabolism of human mammary epithelial cells," *Cancer Res*, vol. 59, no. 1, pp. 80–4, 1999.

[82] R. Katz-Brull, D. Seger, D. Rivenson-Segal, E. Rushkin, and H. Degani, "Metabolic markers of breast cancer enhanced choline metabolism and reduced choline-ether-phospholipid synthesis," *Cancer Res*, vol. 62, no. 7, pp. 1966–70, 2002.

[83] M. Grinde, N. Skrbo, S. Moestue, E. Rødland, E. Borgan, A. Kristian, B. Sitter, T. Bathen, A.-L. Børresen-Dale, G. Mælandsmo, O. Engebraaten, T. Sørlie, E. Marangoni, and I. Gribbestad, "Interplay of choline metabolites and genes in patient-derived breast cancer xenografts," *Breast Cancer Res*, 2014.

[84] G. Eliyahu, T. Kreizman, and H. Degani, "Phosphocholine as a biomarker of breast cancer: molecular and biochemical studies," *Int J Cancer*, vol. 120, no. 8, pp. 1721–30, 2007.

[85] N. Jagannathan, M. Kumar, V. Seenu, O. Coshic, S. Dwivedi, P. Julka, A. Srivastava, and G. Rath, "Evaluation of total choline from in-vivo volume localized proton MR spectroscopy

and its response to neoadjuvant chemotherapy in locally advanced breast cancer," *Br J Cancer*, vol. 84, no. 8, p. 1016, 2001.

[86] H.-M. Baek, J.-H. Chen, K. Nie, H. Yu, S. Bahri, R. Mehta, O. Nalcioglu, and M.-Y. Su, "Predicting pathologic response to neoadjuvant chemotherapy in breast cancer by using MR imaging and quantitative ^{1}H MR spectroscopy," *Radiology*, vol. 251, no. 3, pp. 653–62, 2009.

[87] J. Locasale, "Serine, glycine and one-carbon units: cancer metabolism in full circle," *Nat Rev Cancer*, vol. 13, no. 8, pp. 572–83, 2013.

[88] R. J. DeBerardinis and T. Cheng, "Q's next: the diverse functions of glutamine in metabolism, cell biology and cancer," *Oncogene*, vol. 29, no. 3, pp. 313–24, 2010.

[89] M. Jain, R. Nilsson, S. Sharma, N. Madhusudhan, T. Kitami, A. Souza, R. Kafri, M. Kirschner, C. Clish, and V. Mootha, "Metabolite profiling identifies a key role for glycine in rapid cancer cell proliferation," *Science*, vol. 336, no. 6084, pp. 1040–4, 2012.

[90] I. Amelio, F. Cutruzzola, A. Antonov, M. Agostini, and G. Melino, "Serine and glycine metabolism in cancer," *Trends Biochemi Sci*, vol. 39, no. 4, pp. 191–8, 2014.

[91] N. Traverso, R. Ricciarelli, M. Nitti, B. Marengo, A. Furfaro, M. Pronzato, U. Marinari, and C. Domenicotti, "Role of glutathione in cancer progression and chemoresistance," *Oxid Med Cell Longev*, vol. 2013, 2013.

[92] M. Cioce, M. Valerio, L. Casadei, C. Pulito, A. Sacconi, F. Mori, F. Biagioni, C. Manetti, P. Muti, and S. Strano, "Metformin-induced metabolic reprogramming of chemoresistant ALDH^{bright} breast cancer cells," *Oncotarget*, vol. 5, no. 12, p. 4129, 2014.

[93] D. Quail and J. Joyce, "Microenvironmental regulation of tumor progression and metastasis," *Nat Med*, vol. 19, no. 11, pp. 1423–37, 2013.

[94] H. Li, X. Fan, and J. Houghton, "Tumor microenvironment: the role of the tumor stroma in cancer," *J Cell Biochem*, vol. 101, no. 4, pp. 805–15, 2007.

[95] M. Vander Heiden, "Targeting cancer metabolism: a therapeutic window opens," *Nat Rev Drug Discov*, vol. 10, no. 9, pp. 671–84, 2011.

[96] Y. Chae and A. Gonzalez-Angulo, "Implications of functional proteomics in breast cancer," *Oncologist*, vol. 19, no. 4, pp. 328–35, 2014.

[97] P. Ghaffari, A. Mardinoglu, and J. Nielsen, "Cancer metabolism: a modeling perspective," *Front Physiol*, vol. 6, 2015.

[98] L. Galluzzi, O. Kepp, M. Vander Heiden, and G. Kroemer, "Metabolic targets for cancer therapy," *Nat Rev Drug Discov*, vol. 12, no. 11, pp. 829–46, 2013.

[99] R. Pieters, S. Hunger, J. Boos, C. Rizzari, L. Silverman, A. Baruchel, N. Goekbuget, M. Schrappe, and C. Pui, "L-asparaginase treatment in acute lymphoblastic leukemia," *Cancer*, vol. 117, no. 2, pp. 238–49, 2011.

[100] D. Tennant, R. Durán, and E. Gottlieb, "Targeting metabolic transformation for cancer therapy," *Nat Rev Cancer*, vol. 10, no. 4, pp. 267–77, 2010.

[101] S. Hadad, P. Coates, L. Jordan, R. Dowling, M. Chang, S. Done, C. Purdie, P. Goodwin, V. Stambolic, and S. Moulder-Thompson, "Evidence for biological effects of metformin in operable breast cancer: biomarker analysis in a pre-operative window of opportunity randomized trial," *Breast Cancer Res Treat*, vol. 150, no. 1, pp. 149–55, 2015.

[102] S. Elf and J. Chen, "Targeting glucose metabolism in patients with cancer," *Cancer*, vol. 120, no. 6, pp. 774–80, 2014.

[103] J. Islamian, F. Aghaee, A. Farajollahi, B. Baradaran, and M. Fazel, "Combined treatment with 2-Deoxy-D-glucose and doxorubicin enhances the in vitro efficiency of breast cancer radiotherapy," *Asian Pac J Cancer Prev*, vol. 16, no. 18, pp. 8431–8, 2014.

[104] S. Ma, R. Jia, D. Li, and B. Shen, "Targeting cellular metabolism chemosensitizes the doxorubicin-resistant human breast adenocarcinoma cells," *Biomed Res Int*, vol. 2015, 2015.

[105] D. Zhang, J. Li, F. Wang, J. Hu, S. Wang, and Y. Sun, "2-Deoxy-D-glucose targeting of glucose metabolism in cancer cells as a potential therapy," *Cancer Lett*, vol. 355, no. 2, pp. 176–83, 2014.

[106] Z. Liu, Y.-Y. Zhang, Q.-W. Zhang, S.-R. Zhao, C.-Z. Wu, X. Cheng, C.-C. Jiang, Z.-W. Jiang, and H. Liu, "3-bromopyruvate induces apoptosis in breast cancer cells by downregulating Mcl-1 through the PI3K/Akt signaling pathway," *Anticancer Drugs*, vol. 25, no. 4, pp. 447–55, 2014.

[107] Q. Zhang, Y. Zhang, P. Zhang, Z. Chao, F. Xia, C. Jiang, X. Zhang, Z. Jiang, and H. Liu, "Hexokinase II inhibitor, 3-BrPA induced autophagy by stimulating ROS formation in human breast cancer cells," *Genes Cancer*, vol. 5, no. 3-4, p. 100, 2014.

[108] K. Glunde, L. Jiang, S. Moestue, and I. Gribbestad, "MRS and MRSI guidance in molecular medicine: Targeting and monitoring of choline and glucose metabolism in cancer," *NMR Biomed*, vol. 24, no. 6, pp. 673–90, 2011.

[109] J. Lacal and J. Campos, "Preclinical characterization of RSM-932A, a novel anticancer drug targeting the human choline kinase alpha, an enzyme involved in increased lipid metabolism of cancer cells," *Mol Cancer Ther*, vol. 14, no. 1, pp. 31–9, 2015.

[110] J. van Asten, R. Vettukattil, T. Buckle, S. Rottenberg, F. van Leeuwen, T. Bathen, and A. Heerschap, "Increased levels of choline metabolites are an early marker of docetaxel treatment response in BRCA1-mutated mouse mammary tumors: an assessment by *ex vivo* proton magnetic resonance spectroscopy," *J Transl Med*, vol. 13, no. 1, p. 114, 2015.

[111] E. Ananieva, "Targeting amino acid metabolism in cancer growth and anti-tumor immune response," *World J Biol Chem*, vol. 6, no. 4, p. 281, 2015.

[112] H.-N. Kung, J. Marks, and J.-T. Chi, "Glutamine synthetase is a genetic determinant of cell type-specific glutamine independence in breast epithelia," *PLoS Genet*, vol. 7, no. 8, p. e1002229, 2011.

[113] W. Katt and R. Cerione, "Glutaminase regulation in cancer cells: a druggable chain of events," *Drug Discov Today*, vol. 19, no. 4, pp. 450–7, 2014.

[114] B. Ratnikov, Y. Jeon, J. Smith, and Z. Ronai, "Right on TARGET: glutamine metabolism in cancer," *Oncoscience*, vol. 2, no. 8, p. 681, 2015.

[115] G. Giskeødegård, M. Cao, and T. Bathen, "High-resolution magic-angle-spinning NMR spectroscopy of intact tissue," in *Metabonomics: Methods and Protocols* (J. T. Bjerrum, ed.), vol. 1277 of *Methods in Molecular Biology*, pp. 37–50, Springer New York, 2015.

[116] C.-L. Wu, J. Taylor, W. He, A. Zepeda, E. Halpern, A. Bielecki, R. Gonzalez, and L. Cheng, "Proton high-resolution magic angle spinning NMR analysis of fresh and previously frozen tissue of human prostate," *Magn Reson Med*, vol. 50, no. 6, pp. 1307–11, 2003.

[117] K. Jordan, W. He, E. Halpern, C.-L. Wu, and L. Cheng, "Evaluation of tissue metabolites with high resolution magic angle spinning MR spectroscopy human prostate samples after three-year storage at -80°C," *Biomark Insights*, vol. 2, p. 147, 2007.

[118] V. Righi, L. Schenetti, A. Maiorana, E. Libertini, S. Bettelli, L. Bonetti, and A. Mucci, "Assessment of freezing effects and diagnostic potential of biobank healthy and neoplastic breast tissues through HR-MAS NMR spectroscopy," *Metabolomics*, vol. 11, no. 2, pp. 487–98, 2015.

[119] E. Eisenhauer, P. Therasse, J. Bogaerts, L. Schwartz, D. Sargent, R. Ford, J. Dancey, S. Arbuck, S. Gwyther, and M. Mooney, "New response evaluation criteria in solid tumours: revised RECIST guideline (version 1.1)," *Eur J Cancer*, vol. 45, no. 2, pp. 228–47, 2009.

[120] K. Brindle, S. Bohndiek, F. Gallagher, and M. Kettunen, "Tumor imaging using hyperpolarized ^{13}C magnetic resonance spectroscopy," *Magnetic Resonance in Medicine*, vol. 66, no. 2, pp. 505–19, 2011.

[121] P. Boonsirikamchai, M. Asran, D. Maru, J.-N. Vauthey, H. Kaur, S. Kopetz, and E. Loyer, "CT findings of response and recurrence, independent of change in tumor size, in colorectal liver metastasis treated with bevacizumab," *Am J Roentgenol*, vol. 197, no. 6, pp. W1060–6, 2011.

[122] H. Bertilsson, M.-B. Tessem, A. Flatberg, T. Viset, I. Gribbestad, A. Angelsen, and J. Halgunset, "Changes in gene transcription underlying the aberrant citrate and choline metabolism in human prostate cancer samples," *Clinical Cancer Research*, vol. 18, no. 12, pp. 3261–9, 2012.

[123] S. W. Provencher, "Estimation of metabolite concentrations from localized in vivo proton NMR spectra," *Magn Reson Med*, vol. 30, no. 6, pp. 672–9, 1993.

[124] K. Opstad, A. Wright, B. Bell, J. Griffiths, and F. Howe, "Correlations between in vivo ^{1}H MRS and ex vivo ^{1}H HRMAS metabolite measurements in adult human gliomas," *J Magn Reson Imaging*, vol. 31, no. 2, pp. 289–97, 2010.

[125] G. Giskeødegård, H. Bertilsson, K. Selnæs, A. Wright, T. Bathen, T. Viset, J. Halgunset, A. Angelsen, I. Gribbestad, and M.-B. Tessem, "Spermine and citrate as metabolic biomarkers for assessing prostate cancer aggressiveness," *PloS one*, vol. 8, no. 4, p. e62375, 2013.

[126] J. Choi, H.-M. Baek, S. Kim, M. Kim, J. Youk, H. Moon, E.-K. Kim, K. Han, D.-H. Kim, and S. Kim, "HR-MAS MR spectroscopy of breast cancer tissue obtained with core needle biopsy: Correlation with prognostic factors," *PloS one*, vol. 7, no. 12, p. e51712, 2012.

[127] J. Choi, H.-M. Baek, S. Kim, M. Kim, J. Youk, H. Moon, E.-K. Kim, and Y. Nam, "Magnetic resonance metabolic profiling of breast cancer tissue obtained with core needle biopsy for predicting pathologic response to neoadjuvant chemotherapy," *PloS one*, 2013.

[128] A. Carroll, P. Zhang, L. Whitehead, S. Kaines, G. Tcherkez, and M. Badger, "Phenometer: a metabolome database search tool using statistical similarity matching of metabolic phenotypes for high-confidence detection of functional links," *Front Bioeng Biotechnol*, vol. 3, 2015.

[129] A. Nordström and R. Lewensohn, "Metabolomics: moving to the clinic," *J Neuroimmune Pharmacol*, vol. 5, no. 1, pp. 4–17, 2010.

[130] T. Bathen, B. Geurts, B. Sitter, H. Fjøsne, S. Lundgren, L. Buydens, I. Gribbestad, G. Postma, and G. Giskeødegård, "Feasibility of MR metabolomics for immediate analysis of resection margins during breast cancer surgery," *PLoS One*, vol. 8, no. 4, p. e61578, 2013.

[131] W. Claudino, P. Goncalves, A. di Leo, P. Philip, and F. Sarkar, "Metabolomics in cancer: a bench-to-bedside intersection," *Critl Rev Oncol Hematol*, vol. 84, no. 1, pp. 1–7, 2012.

[132] O. Aboud and R. Weiss, "New opportunities from the cancer metabolome," *Clin Chem*, vol. 59, no. 1, pp. 138–46, 2013.

[133] M. Cuperlovic-Culf, I. Chute, A. Culf, M. Touaibia, A. Ghosh, S. Griffiths, D. Tulpan, S. Léger, A. Belkaid, and M. Surette, "^{1}H NMR metabolomics combined with gene expression analysis for the determination of major metabolic differences between subtypes of breast cell lines," *Chem Sci*, vol. 2, no. 11, pp. 2263–70, 2011.

[134] U. Martinez-Outschoorn, M. Prisco, A. Ertel, A. Tsirigos, Z. Lin, S. Pavlides, C. Wang, N. Flomenberg, E. Knudsen, and A. Howell, "Ketones and lactate increase cancer cell "stemness," driving recurrence, metastasis and poor clinical outcome in breast cancer: achieving personalized medicine via Metabolo-Genomics," *Cell Cycle*, vol. 10, no. 8, pp. 1271–86, 2011.

Paper I

frontiers in Oncology

ORIGINAL RESEARCH
published: 28 January 2016
doi: 10.3389/fonc.2016.00017

Impact of Freezing Delay Time on Tissue Samples for Metabolomic Studies

Tonje H. Haukaas[1,2†], Siver A. Moestue[1,3†], Riyas Vettukattil[1], Beathe Sitter[4], Santosh Lamichhane[1,5], Remedios Segura[6], Guro F. Giskeødegård[1,3] and Tone F. Bathen[1,2]*

[1] Department of Circulation and Medical Imaging, Norwegian University of Science and Technology, Trondheim, Norway, [2] Faculty of Medicine, K. G. Jebsen Center for Breast Cancer Research, Institute of Clinical Medicine, University of Oslo, Oslo, Norway, [3] St. Olavs Hospital, Trondheim University Hospital, Trondheim, Norway, [4] Department of Health Science, Faculty of Health and Social Science, Sør-Trøndelag University College, Trondheim, Norway, [5] Department of Food Science, Faculty of Science and Technology, Aarhus University, Årslev, Denmark, [6] Metabolomic and Molecular Image Laboratory, Health Research Institute INCLIVA, Valencia, Spain

Introduction: Metabolic profiling of intact tumor tissue by high-resolution magic angle spinning (HR MAS) MR spectroscopy (MRS) provides important biological information possibly useful for clinical diagnosis and development of novel treatment strategies. However, generation of high-quality data requires that sample handling from surgical resection until analysis is performed using systematically validated procedures. In this study, we investigated the effect of postsurgical freezing delay time on global metabolic profiles and stability of individual metabolites in intact tumor tissue.

Materials and methods: Tumor tissue samples collected from two patient-derived breast cancer xenograft models (n = 3 for each model) were divided into pieces that were snap-frozen in liquid nitrogen at 0, 15, 30, 60, 90, and 120 min after surgical removal. In addition, one sample was analyzed immediately, representing the metabolic profile of fresh tissue exposed neither to liquid nitrogen nor to room temperature. We also evaluated the metabolic effect of prolonged spinning during the HR MAS experiments in biopsies from breast cancer patients (n = 14). All samples were analyzed by proton HR MAS MRS on a Bruker Avance DRX600 spectrometer, and changes in metabolic profiles were evaluated using multivariate analysis and linear mixed modeling.

Results: Multivariate analysis showed that the metabolic differences between the two breast cancer models were more prominent than variation caused by freezing delay time. No significant changes in levels of individual metabolites were observed in samples frozen within 30 min of resection. After this time point, levels of choline increased, whereas ascorbate, creatine, and glutathione (GS) levels decreased. Freezing had a significant effect on several metabolites but is an essential procedure for research and biobank purposes. Furthermore, four metabolites (glucose, glycine, glycerophosphocholine, and choline) were affected by prolonged HR MAS experiment time possibly caused by physical release of metabolites caused by spinning or due to structural degradation processes.

Conclusion: The MR metabolic profiles of tumor samples are reproducible and robust to variation in postsurgical freezing delay up to 30 min.

Keywords: cancer, freezing time delay, HR MAS, metabolic profile, MR spectroscopy, metabolomics, snap-freezing, degradation

OPEN ACCESS

Edited by:
Franca Podo,
Istituto Superiore di Sanità, Italy

Reviewed by:
Egidio Iorio,
Istituto Superiore di Sanità, Italy
Claudio Luchinat,
University of Florence, Italy

***Correspondence:**
Tone F. Bathen
tone.f.bathen@ntnu.no

†Shared first authorship; Tonje H. Haukaas and Siver A. Moestue contributed equally to this work.

Specialty section:
This article was submitted to Cancer Imaging and Diagnosis, a section of the journal Frontiers in Oncology

Received: *18 November 2015*
Accepted: *16 January 2016*
Published: *28 January 2016*

Citation:
Haukaas TH, Moestue SA, Vettukattil R, Sitter B, Lamichhane S, Segura R, Giskeødegård GF and Bathen TF (2016) Impact of Freezing Delay Time on Tissue Samples for Metabolomic Studies. Front. Oncol. 6:17. doi: 10.3389/fonc.2016.00017

INTRODUCTION

The field of metabolomics has the potential to fill important gaps within the knowledge of cancer biology (1). Within this field, molecular pathways and interactions are studied through the expression of small molecular compounds called metabolites. These compounds are intermediates or end products of ongoing biochemical processes, and the overall metabolic profile represents a unique fingerprint of the cellular state at a specific time point. Metabolites constitute the final level in the -omics cascade, downstream to genomics, transcriptomics, and proteomics, reflecting the combined effect of all the upstream molecular levels (2). However, the metabolic snapshot obtained from a tumor tissue specimen depends on additional factors, such as the tumor microenvironment and the polyclonality frequently observed in cancer, which introduces additional complexity for the interpretation of the metabolic information. Nevertheless, metabolic profiling of intact fresh frozen tissue is gaining popularity in clinical research, as it potentially can identify novel prognostic or predictive metabolic biomarkers or explore the abnormal biochemical activity aiming to identify novel therapeutic approaches.

Metabolomic studies using high-resolution magic angle spinning MR spectroscopy (HR MAS MRS) enables investigation of tumor tissue with minimal sample preparation, thus limiting loss of information through tissue extraction and maintaining high reproducibility (3). HR MAS MRS is also a non-destructive technique (4) shown to retain histopathological characteristics (5) and high RNA quality (6) of analyzed tissue. This technology has been used to discriminate between tumor and normal tissues in several cancers (7), but is increasingly used to explore the role of metabolomics in patient stratification for personalized oncology (8–10). In these studies, biobanks have been established after collecting tumor tissue from large patient cohorts and the association between metabolic characteristics and disease outcome has been investigated. The quality of data from such studies requires a high degree of analytical accuracy and precision, as well as highly standardized and validated protocols for sample collection, storage, and handling prior to analysis.

One of the critical points during sample collection, especially in a clinical setting, is the time period from blood supply cutoff during surgical resection until the sample is frozen for storage (freezing delay time). This interval may vary depending on the difficulty of the surgical procedure and the required tissue processing procedures, while cellular enzymatic and chemical reactions will take place and potentially cause alterations in the tissue metabolomic profile. Therefore, it is important to assess the susceptibility of these profiles to systematic variability resulting from sample handling and analysis. The main objective of this study was to investigate the metabolic effects of freezing delay time, aiming to validate the sample collection protocols normally used in biobanking for MR metabolomics studies. To minimize the impact of inter- and intratumor variability, tumor tissue was obtained from two well-characterized breast cancer xenograft models (11, 12). Furthermore, we describe the metabolic effects of snap-freezing tumor samples and the degradation pattern caused by prolonged HR MAS MRS acquisitions using human breast cancer samples. Finally, sample collection and handling procedures that ensure optimal data quality in metabolomic studies of cancer tissue are suggested.

MATERIALS AND METHODS

Tissue Samples

Animal Model

The two orthotopic xenograft models MAS98.12 and MAS98.06 were established by direct transplantation of biopsy tissue from primary mammary carcinomas in immunodeficient SCID mice and thereafter passaged as previously described (11). These models have been characterized by unsupervised hierarchical clustering of intrinsic genes (13, 14) to represent basal-like (poor prognosis) and luminal-like (better prognosis) breast cancer phenotype respectively (11), and they also have distinct metabolic profiles (12, 15). Mice carrying xenograft tumors [basal-like ($n = 3$) and luminal-like ($n = 3$)] were sacrificed by cervical dislocation and tumor tissue was harvested and snap-frozen in liquid nitrogen according to the protocol below. All procedures and experiments involving animals were approved by the National Animal Research Authority and carried out according to the European Convention for the Protection of Vertebrates used for Scientific Purposes.

Patient Material

Breast cancer tissue samples from 14 female patients undergoing surgery at St. Olav's Hospital (Trondheim, Norway) and Molde Hospital (Molde, Norway) were included in the study. Patients were chosen without any other prior clinical information. The biopsies were snap-frozen immediately after excision during the surgical procedure and further stored in liquid nitrogen until subsequent analyses. All patients have signed a written informed consent, and the study was approved by the Regional Ethics Committee, Central Norway.

Experimental Design and HR MAS MRS Experiments

Effect of Freezing Delay Time

One tumor from each mouse was divided into pieces and left at room temperature for 0, 15, 30, 60, 90, and 120 min, prior to snap-freezing in liquid nitrogen. This procedure covers both realistic and extreme freezing time delays, which could occur in tissue harvesting procedures during breast cancer surgery. In addition, one sample was analyzed immediately after excision representing the metabolic profile of the tumor tissue without exposure to liquid nitrogen or freezing. The total number of samples analyzed for this study was 42.

Before HR MAS MRS experiments, 3 μL cold sodium formate in D_2O (24.29 mM) was added to a leak-proof disposable 30-μL insert (Bruker, Biospin GmbH, Germany) as a shimming reference. Tissue samples were cut to fit the insert (mean sample weight 9.8 mg) on a dedicated work station designed to keep the samples frozen (16) during preparation. The insert containing the frozen sample was placed in a 4-mm diameter zirconium rotor (Bruker, Biospin GmbH, Germany) and kept at −20°C for 6–8 h before the experiments to minimize degradation.

HR MAS MRS experiments were performed on a Bruker Avance DRX600 spectrometer (Bruker, Biospin GmbH, Germany) equipped with a $^{1}H/^{13}C$ MAS probe with gradient aligned with the magic angle (Bruker, Biospin GmbH, Germany). Samples were spun at 5000 Hz and experiments run at 5°C. The samples were allowed 5 min temperature acclimatization before shimming and spectral acquisition.

Spin-echo spectra were recorded using a Carr–Purcell–Meiboom–Gill (cpmg) pulse sequence (cpmgpr1D; Bruker, L4 = 126). T_2 filtering was obtained using a delay of 0.6 ms between each 180° pulse to suppress macromolecules and lipid signals and enhance signal from small molecules. This resulted in a total echo time (TE) of 77 ms. The total number of scans (NS) were 64 over a spectral width of 20 ppm (−5 to 15 ppm) with an acquisition time of 3.07 s.

Degradation during Prolonged HR MAS MRS Analysis

Frozen human breast cancer tissue samples were cut to fit a leak-proof 30-μL disposable insert (mean sample weight: 8.8 mg) added 3 μL of phosphate-buffered saline (PBS) based on D_2O with trimethylsilyl propionate (TSP, 1 mM) and sodium formate (1 mM). The insert was placed in a 4-mm diameter zirconium rotor (Bruker, Biospin GmbH, Germany). Spin-echo experiments (cpmgpr1D; Bruker, L4 = 136) were run with 2 ms delay between 180° pulses, TE of 273.5 ms, spectral width of 20 ppm (−5 to 15 ppm) and NS of 256 scans (17). To evaluate the effect of prolonged HR MAS MRS experimental time, data acquisition was repeated after 1.5 h. The sample was kept spinning (5000 Hz) within the magnet at 5°C in this time interval.

Data Preprocessing and Statistical Analysis

The FIDs were multiplied by a 0.30 Hz exponential function and Fourier transformed into 64k real points. Phase correction was performed automatically for each spectrum using TopSpin 3.1 (Bruker). Further preprocessing of the HR MAS spectra was performed in Matlab R2013b (The Mathworks, Inc., USA). Due to unavailability of a stable internal reference, human spectra were referenced to the TSP peak (0 ppm) while xenograft spectra were referenced to formate (8.46 ppm). Baseline correction was achieved by setting the minimum value of each spectrum to 0 and subtracting the lowest value. Peak alignment was performed using icoshift (18). The spectral region of interest in the human samples (2.89–4.73 ppm), which excludes the main lipid peaks, was normalized to equal total mean area, while the total spectral region (0.62–4.70 ppm) was normalized to sample weight in the xenograft spectra. In human tissue, lipid signals mainly originate from adipose tissue, and the lipid peaks may be very dominant in samples with low tumor content. Thus, the normalization accounts for differences in sample size and tumor cell content, the latter not necessary in xenograft samples with homogenous distribution of cancer cells.

To find underlying structure and main differences in the dataset, the unsupervised multivariate method principal component analysis (PCA) was used. PCA is a powerful method to decrease the complexity of collinear multivariate data, such as MR spectra, into a few principal components (PCs). PCA was performed (using PLS_Toolbox 7.5.2, Matlab, Eigenvector Research, Inc., Wenatchee, WA, USA) on xenograft spectra and human breast cancer spectra to explore the metabolic variation within samples exposed to increasing delays in postsurgical freezing and prolonged experiment time respectively.

For both cohorts, metabolite assignment was based on previous published data from HR MAS MRS analyses of breast tumors (19). Furthermore, metabolite levels were determined by integrating fixed spectral regions (performed in Matlab R2013b) corresponding to the metabolites of interest and used for univariate analysis. For metabolites with baseline strongly affected by closely resonating lipids, a linear baseline ranging from the first to the last point of the integral area was used.

Linear mixed models (LMM), an extension of linear regression, can be used to model data where several measurements from the same object are available. LMM accounts for both fixed and random effects in the modeling of the metabolite levels. Fixed effects are those that are of particular interest, e.g., effect of freezing delay time, while random effects are often not of interest but cannot be adjusted for prior to the modeling, e.g., effects originating from between subjects variation. In the current study, freezing delay time as well as type of xenograft model (basal-like or luminal-like) were set as fixed effects (continuous and categorical variable respectively), while xenograft subject was set as an random effect (without interaction term). The modeling was performed in R (20) using the "nlme" package (21).

Paired *t*-test was used to find time points were the metabolic levels had changed compared to baseline and to evaluate the effect of snap-freezing. Wilcoxon signed-rank test were performed to test the effect of prolonged experiment time on metabolite levels in human tumor tissue.

To adjust for the multiple metabolites tested, calculated *p* values were corrected for using The Benjamini Hochberg false discovery rate (FDR) in Matlab R2013b (The Mathworks, Inc., USA), and the differences were considered statistically significant for adjusted *p*-values ≤ 0.05.

Histopathology and Nile Red Staining

Histopathological analysis was performed in order to evaluate the presence of viable tumor tissue and mobile lipid droplets in each individual xenograft sample. After HR MAS MRS analysis, samples were immediately frozen in liquid nitrogen. About 4 and 10 μm frozen sections were stained with hematoxylin–eosin–saffron (HES) and Nile Red as described in Ref. (22), respectively.

RESULTS

Effect of Freezing Delay Time in Xenograft Tumor Tissue

To examine the metabolic effect of delayed freezing, samples from the same xenograft tumor were left in room temperature for 0, 15, 30, 60, 90, and 120 min prior to freezing. A PCA score plot of the spectra from all 42 samples revealed a clear separation of

basal-like and luminal-like xenograft model samples (**Figure 1A**). The variability between samples was predominantly attributed to the lipid content (PC1), whereas the levels of taurine, glycerophosphocholine, and phosphocholine (PC2) contributed to discrimination between the two xenograft models (**Figure 1B**).

A trajectory PCA score plot suggests that freezing delay time had no systematic effect on metabolic profiles (**Figure 1C**).

The Impact of Freezing Delay Time on Individual Metabolites in Xenograft Samples

The LMM result for glucose was excluded due to non-normally distributed residuals. The percentage change in levels of 15 metabolites measured by HR MAS MRS in samples subject to increasing delays before freezing ($n = 36$) are shown in **Table 1**. After adjusting p-values for multiple testing, LMM revealed that three metabolites were significantly affected by type of xenograft model (basal-like and luminal-like) and four metabolites were significantly affected by delayed freezing (**Table 2**).

Figure 2 illustrates the change in average level of ascorbate, choline, creatine, and glutathione (GS) with increasing freezing delay time. The levels of ascorbate, creatine, and GS decreased with time. Both ascorbate and creatine levels decreased with approximately 30% within the 120 min time frame, while levels of GS were approximately 40% lower. The choline levels increased with time, reaching a level approximately 110% higher than baseline at freezing delay time of 120 min.

Ascorbate, choline, and creatine levels were significantly different from baseline sample (frozen immediately) after 60 min freezing delay time while the same was observed for GS levels after 90 min (**Figure 2**).

Metabolic Effect of Freezing

Immediately snap-frozen samples (0 min, $n = 6$) were compared to samples analyzed directly after excision (not frozen, 0 min, $n = 6$). A clear effect of freezing compared to unfrozen tissue was seen for 12 of 16 metabolites (**Figure 3**). Increased levels were observed for all of these metabolites after snap-freezing.

Histopathology

Visual inspection of HES-stained sections of xenograft samples analyzed by HR MAS MRS confirmed that the samples predominantly consisted of viable tumor tissue without significant necrosis or fibrosis. No adipose tissue or normal mammary gland tissue was observed. Due to the observed heterogeneity in lipid content of samples obtained from the same xenograft, we examined whether the lipids detected were located in adipose cells lining the tumor or in lipid droplets within the tumor. Visual inspection of the Nile Red stained histological sections showed good correlation between lipid signal intensity in spectral data and the amount of lipid detected by Nile Red staining (Figures S1 and S2 in Supplementary Material). The lipids were also observed to be located inside tumors and were therefore considered to represent mobile lipids in the cancer cells and not adipose tissue adjacent to the tumors. No systematic difference in lipid content

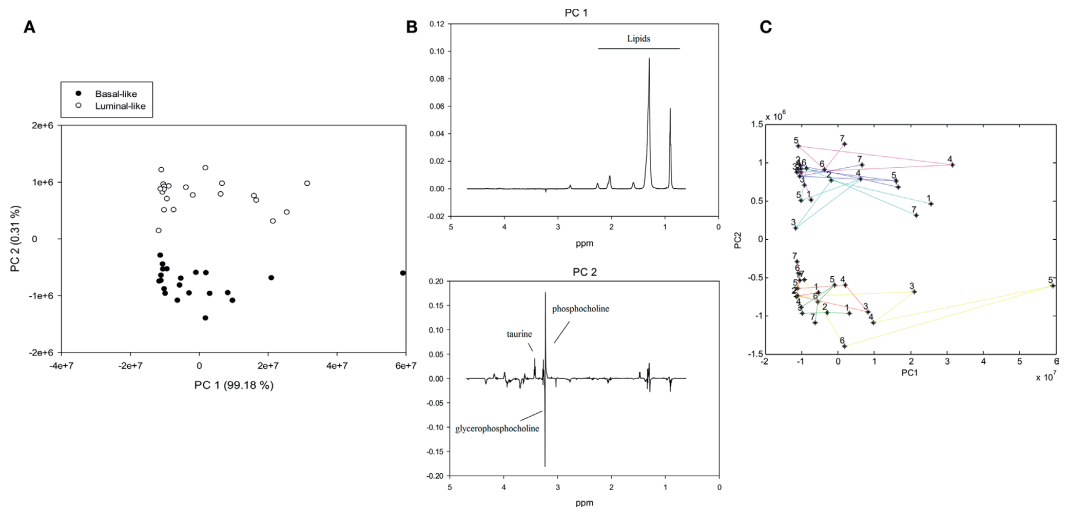

FIGURE 1 | PCA of MR spectra from xenografts tumors exposed to variable freezing delay time, (A) score plot with samples colored by xenograft type, (B) loading plots for PC1 (identifying lipid content as the most significant contributor to variability) and PC2 (identifying the metabolic difference between xenograft models as the second most significant contributor to variability), (C) PCA trajectory score plot. Samples from the same animal are connected with colored lines and numbered according to freezing delay time: (1) not frozen, (2) 0 min, (3) 15 min, (4) 30 min, (5) 60 min, (6) 90 min, and (7) 120 min.

TABLE 1 | Metabolic effect of freezing delay time.

Metabolite	ppm	15 min	30 min	60 min	90 min	120 min
Glucose	4.65	22 ± 107%	−8 ± 19%	31 ± 41%	6 ± 50%	26 ± 71%
Ascorbate	4.53	−18 ± 37%	−15 ± 20%	−25 ± 17%	−31 ± 22%	−31 ± 24%
Lactate	4.13	4 ± 44%	10 ± 24%	12 ± 29%	16 ± 27%	19 ± 45%
Tyrosine	3.99	−8 ± 32%	−10 ± 21%	−13 ± 19%	−15 ± 22%	−17 ± 29%
Glycine	3.55	−7 ± 45%	−4 ± 22%	−5 ± 25%	1 ± 45%	6 ± 62%
Myoinositol	3.53	12 ± 49%	11 ± 19%	26 ± 28%	26 ± 27%	43 ± 64%
Taurine	3.42	−7 ± 38%	−7 ± 15%	−8 ± 16%	−8 ± 20%	−4 ± 31%
Glycerophosphocholine	3.23	−9 ± 22%	−10 ± 18%	−3 ± 25%	0 ± 34%	28 ± 40%
Phosphocholine	3.22	−19 ± 24%	−7 ± 16%	1 ± 32%	7 ± 25%	34 ± 63%
Choline	3.21	6 ± 72%	20 ± 31%	56 ± 44%	62 ± 49%	111 ± 111%
Creatine	3.03	−16 ± 31%	−19 ± 18%	−28 ± 22%	−25 ± 22%	−29 ± 26%
Glutathione (GS)	2.55	−18 ± 32%	−19 ± 15%	−24 ± 25%	−35 ± 18%	−37 ± 26%
Succinate	2.41	−5 ± 35%	−13 ± 22%	−2 ± 33%	−13 ± 29%	−15 ± 38%
Glutamine	2.44	5 ± 49%	−1 ± 40%	28 ± 55%	−1 ± 22%	7 ± 54%
Glutamate	2.37	−10 ± 35%	−11 ± 17%	−20 ± 17%	−16 ± 25%	−14 ± 37%
Alanine	1.49	−7 ± 42%	9 ± 40%	2 ± 42%	17 ± 72%	23 ± 108%

Percentage (average ± SD) increase or decrease of metabolite level in samples exposed to freezing delay time compared to samples frozen immediately after tumor collection.

TABLE 2 | LMM-results reporting the effect of xenograft model and freezing delay time on levels of 15 metabolites.

Metabolite	Xenograft model			Freezing time delay		
	Adj. *p*-value	Est. effect	SD	Adj. *p*-value	Est. effect	SD
Ascorbate	0.628	1.6	2.2	**0.037***	−1.2	0.4
Lactate	0.849	−2.5	12.2	0.281	4.5	3.0
Tyrosine	0.059	128.3	33.4	0.343	−7.1	5.6
Glycine	0.649	−9.4	16.9	0.838	1.2	2.8
Myoinositol	0.373	−4.8	3.9	0.072	2.7	1.1
Taurine	**0.025***	240.9	37.9	0.838	−2.2	7.0
Glycerophosphocholine	**0.017***	−477.3	56.6	0.255	23.9	14.6
Phosphocholine	**0.040***	470.3	94.3	0.255	22.7	13.8
Choline	0.068	43.5	12.5	**0.002****	16.2	3.7
Creatine	0.059	−41.6	10.3	**0.037***	−8.4	3.0
Glutathione (GS)	0.649	−4.1	7.3	**0.005****	−6.0	1.6
Succinate	0.112	8.7	3.1	0.301	−1.0	0.7
Glutamine	0.194	12.3	6.2	0.838	0.3	0.9
Glutamate	0.322	−20.9	14.4	0.348	−3.7	3.1
Alanine	0.194	17.1	8.4	0.838	0.4	1.6

*The estimated effect (Est. effect) reports each fixed factors (i.e., xenograft model or freezing time delay) influence on metabolite levels. Adjusted p-values in bold indicates that the level is significantly different from the sample frozen after 0 min (*adjusted $p < 0.05$, **adjusted $p < 0.01$).*

due to delayed freezing time was observed. While Figure S1 in Supplementary Material shows a pattern of decreasing Nile Red signal with increased delay before freezing, Figure S2 in Supplementary Material shows an example where the same pattern was not observed.

Degradation during Prolonged HR MAS Analysis

Repeated HR MAS MRS analysis of 14 human breast cancer samples was performed with 1.5 h interval to observe the metabolic effect of prolonged time in the magnet. The levels of glucose, glycine, glycerophosphocholine, and choline were found to significantly change from the first to the second acquisition (**Table 3**). While glucose, glycine, and choline increased, levels of glycerophosphocholine decreased with prolonged experiment time. A PCA score plot of all spectra showed that the metabolic variation between samples was higher than variation in spectra obtained from the same sample (Figure S3 in Supplementary Material).

DISCUSSION

In this study, we evaluated the metabolic effect of freezing delay time, snap-freezing in liquid nitrogen and prolonged experimental time using HR MAS MRS. The results show that levels of HR MAS MRS visible metabolites in breast tumors are not subject to significant degradation if snap-frozen within 30 min after surgical excision.

Principal component analysis showed that differences in lipid content explained most of the variance between the samples from the two different breast cancer xenograft models. This was

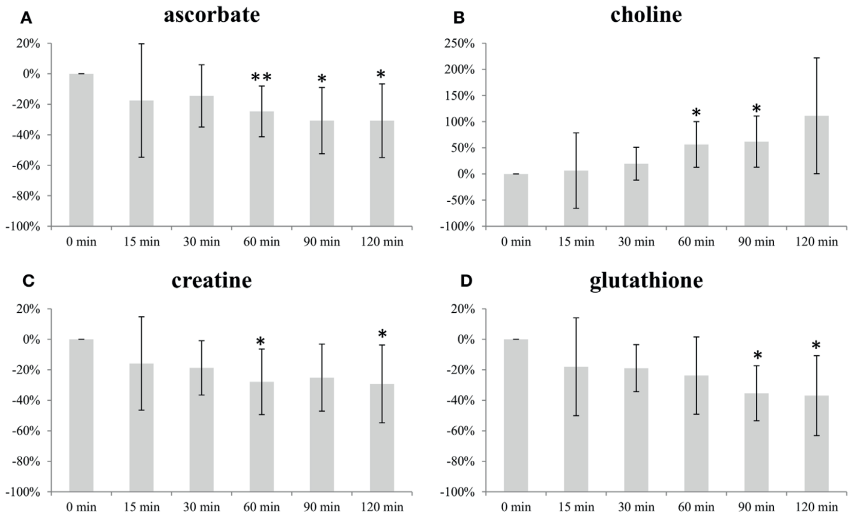

FIGURE 2 | Impact of freezing delay time on level of (A) ascorbate, (B) choline, (C) creatine, and (D) glutathione. Metabolite integrals from samples subject to 15, 30, 60, 90, and 120 min freezing delay time compared with samples frozen immediately (0 min). * and ** indicates that the level is significantly different from the sample frozen after 0 min (*$p < 0.05$, **$p < 0.01$).

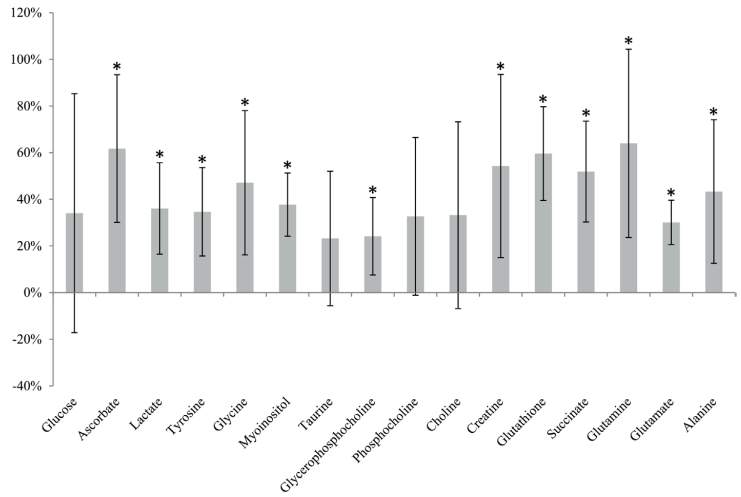

FIGURE 3 | Metabolic effect of snap-freezing. Percentage change in metabolite levels measured in frozen samples relative to samples not frozen prior to HR MAS MRS analysis. * indicates that the level is significantly different from the sample not frozen (*adjusted $p < 0.05$).

further examined by histopathological staining of frozen sections with Nile Red, which showed no correlation between lipid content and freezing delay time. Hence, the variability explained by lipid content most likely reflects tumor heterogeneity rather than the sample handling conditions. Furthermore, PCA clearly discriminated between samples from the two xenograft models (i.e., basal-like or luminal-like breast cancer subtype). Basal-like xenografts had higher levels of glycerophosphocholine, while

TABLE 3 | Metabolic effect of prolonged experiment time.

Metabolite	ppm	1.5 h	Adj. *p*-value
Glucose	4.65	21 ± 20%	**0.006****
Ascorbate	4.53	−4 ± 6%	0.078
Lactate	4.15	0 ± 7%	0.903
Tyrosine	3.98	3 ± 6%	0.08
Glycine	3.56	8 ± 7%	**0.006****
Myoinositol	3.54	7 ± 11%	0.08
Taurine	3.42	0 ± 5%	0.903
Glycerophosphocholine	3.23	−15 ± 12%	**0.001****
Phosphocholine	3.22	−4 ± 6%	0.08
Choline	3.21	11 ± 13%	**0.011***
Creatine	3.03	0 ± 6%	0.903

*Percentages (average ± SD) were calculated relative to the metabolite levels (integrals) from the initial experiment. Adjusted p-values in bold indicates that the level is significantly different from the sample frozen after 0 min (*adjusted $p < 0.05$, **adjusted $p < 0.01$).*

luminal-like xenografts had higher levels of phosphocholine and taurine, in accordance with previously published data from these xenograft models (15). The same metabolic differences between the xenograft models were observed in LMM.

Discrimination between the two xenograft models based on overall metabolic profile did not depend on freezing delay time. Furthermore, no significant changes in individual metabolite levels were observed at 30 min past tumor excision. At 60 min, levels of three metabolites had significantly changed from baseline measurements. Thus, samples should be frozen within 30 min of resection, which in general should be sufficient when obtaining tissue biopsies during surgical procedures. Ascorbate, choline, creatine, and GS were the only metabolites exhibiting significant changes within the time frame (0–120 min) used in the current study. For the majority of metabolites, no systematic dependency on freezing time delay was observed, suggesting that intratumor heterogeneity is the predominant source of variability.

Ascorbate, also known as vitamin C, and GS are important antioxidants in animal cells that, together with other antioxidants, are responsible for eliminating reactive oxygen species (ROS) from oxidative stress (23, 24). As a consequence of high ROS levels in cancer cells, GS levels are often elevated compared to normal tissue (25). GS has also been reported to be increased in estrogen receptor (ER) negative tumors compared to ER-positive (26). ROS levels can increase as a consequence of ischemia, potentially leading to oxidative damage. It is therefore plausible that the decreased levels of GS and ascorbate reflect oxidative stressed caused by prolonged ischemia. Ascorbate levels obtained from samples frozen 60, 90, and 120 min after excision were significantly lower than the levels from samples frozen immediately. The same was observed for GS levels at 90 and 120 min of freezing delay. Consequently, biological interpretation of the levels of these antioxidants should only be considered if the experimental design of the study includes a controlled freezing delay time of <30 min.

The levels of choline increased with increasing freezing delay time. Although not significant, a similar trend was observed for the choline-containing metabolites phosphocholine and glycerophosphocholine, suggesting that ischemia affects choline metabolism. Studying the effect of hypoxia in human MDA-MB-231 breast cancer cell and tumors, Jiang et al. detected higher concentrations of total choline-containing metabolites (tCho; composed of phosphocholine, glycerophosphocholine, and free choline), mainly contributed by phosphocholine, in hypoxic regions (27). Altered choline metabolism is considered an emerging hallmark in malignant transformation (28). A major component of mammalian cell membranes, phosphatidylcholine (PtdCho), is synthesized from choline, thus making choline and choline-containing intermediates essential for the increased proliferation observed in tumor cells. Several *ex vivo* breast cancer studies using HR MAS MRS have detected increased concentrations of choline, phosphocholine, and glycerophosphocholine in tumor tissue compared to non-involved breast tissue (19, 29, 30). Differences in tCho have been found to have predictive value for the 5-year survival of breast cancer patients receiving neoadjuvant chemotherapy (31) and higher choline concentrations have been found in core needle biopsies from patients that are ER- and/or PgR-negative compared to ER- and/or PgR-positive patients (10). Delays in freezing time up to 30 min had no significant impact on choline levels. While choline levels at 60 and 90 min delay were significantly increased, this was not observed at 120 min ($p = 0.065$), probably due to variability within these last measurements. However, because of the biological relevance of choline metabolism in cancer, this trend of increasing levels with freezing delay time emphasize the importance of reporting and controlling sample handling to limit possible effects.

Levels of creatine significantly decreased as a result of prolonged time before freezing, where 60 min was found to be the first time point significantly different from samples frozen directly after exiting. Creatine is involved in energy storage through formation of phosphocreatine and thus functions as a carrier of energy within cells. Decreasing levels of creatine (or phosphocreatine) could be suggestive of energy depletion caused by ischemia. Several studies use creatine for calculation of metabolic ratios to allow for comparable quantities between samples (10, 32–34) and in studies of breast cancer tissue, higher level of this metabolite have been correlated to ER-positive (35) and PgR-positive tumors (15). As the tendency of decreasing levels is seen from the initial time point, it is important to keep the time before freezing minimal to allow the usage of ratios involving creatine.

Rapid metabolic phenotyping in operating theaters of unfrozen tissue has been proposed to facilitate real-time diagnostics and further aid decision making during surgery (36). To evaluate the metabolic effect of snap-freezing, tumor tissue was analyzed by HR MAS MRS without any exposure to liquid nitrogen and compared to tissue from the same xenografts that were immediately frozen after excision. Freezing was found to significantly increase the level of 12 metabolites. In previous studies, the freezing of rat kidney and liver tissue has reportedly led to increased amounts of amino acids (37, 38) and decreased contents of choline, glycerophosphocholine, glucose, myoinositol, trimethylamine N-oxide (TMAO), and taurine (38) using HR MAS MRS. The increased levels of multiple metabolites observed in the current study might be caused by intracellular lysis releasing metabolites. Metabolites bound to cellular molecules or compartments are more restricted and thus less MR-visible. If these metabolites are released as a consequence of freezing, HR MAS MRS will detect higher levels

than in unfrozen tissue as found here. The findings underpin that studies of fresh and frozen tissue are not directly comparable. Although the effect of freezing was significant for the majority of metabolites, we believe that analyzing fresh tissue samples is neither feasible nor optimal in the current clinical and research setting. Care must therefore be taken not to compare metabolic information obtained in unfrozen samples with data from frozen biobank tissue.

We also examined the effect on the metabolic profile of prolonged HR MAS MRS analysis. After the first acquisition, the sample was kept spinning inside the magnet and reanalyzed after 1.5 h. The level of four metabolites was found to differ significantly from the initial acquisition. Glucose, glycine, and choline were found to increase with time, while glycerophosphocholine decreased. Similar effects on glycine, choline, and glycerophosphocholine levels have been observed in lung cancer tissue (39) and in brain tumor tissue (40) supporting the current findings. As Rocha et al. describe, the changes might be caused by spinning effects causing release of bound metabolites or due to ongoing metabolic activity (39). Importantly, these metabolic effects should be considered for quantitative two-dimensional HR MAS MRS studies where long acquisition time is required.

In conclusion, this study confirms that HR MAS MRS metabolic profiles are robust to metabolic changes due to delayed freezing within a timeframe of 30 min. This allows biological interpretation of metabolic profiles, including metabolites involved in protection against ROS formation/oxidative stress, such as GS and ascorbate, as well as evaluation of the levels of creatine and choline-containing metabolites. Within the 30 min freezing delay time window, the effect of structural or biochemical degradation on metabolic profiles is insignificant. A clear effect of freezing was observed for most of the detected metabolites. However, this step in sample handling is considered essential for biobanking and research purposes. The study also identified moderate metabolic consequences of prolonged HR MAS experiment time, and thus, the protocol should be designed to keep experiment time to a minimum.

AUTHOR CONTRIBUTIONS

Author contributions included: study design (TH, SM, BS, and TB), data acquisition (SM, TH, and SL), data analysis (TH, SM, RV, SL, and RS), data interpretation (TH, SM, GG, and TB), and drafting the manuscript (TH, SM, and TB). All authors contributed in revising the manuscript.

ACKNOWLEDGMENTS

The HR MAS MRS analysis was performed at the MR Core Facility, Norwegian University of Science and Technology (NTNU). MR core facility is funded by the Faculty of Medicine at NTNU and Central Norway Regional Health Authority. The staining of histology sections was provided by the *Cellular and Molecular Imaging* Core Facility (CMIC), NTNU. *CMIC* is funded by the Faculty of Medicine at NTNU and Central Norway Regional Health Authority.

FUNDING

This work was funded by K.G. Jebsen Center for Breast Cancer Research, Norwegian Cancer Society grant 2209215-2011, The Research Council of Norway grant number FRIMED-221879 and 239940/F20, the Financial Statement Grants SAF2011-23029 and SAF2014-52875R from Ministerio de Economía y Competitividad of Spain, the Liaison Committee between the Central Norway Regional Health Authority (RHA), the Norwegian University of Science and Technology grant number 46056655, and INCLIVA Foundation with funding for scholarship stay in prestigious center 2013.

SUPPLEMENTARY MATERIAL

The Supplementary Material for this article can be found online at http://journal.frontiersin.org/article/10.3389/fonc.2016.00017

REFERENCES

1. Patel S, Ahmed S. Emerging field of metabolomics: big promise for cancer biomarker identification and drug discovery. *J Pharm Biomed Anal* (2015) **107**:63–74. doi:10.1016/j.jpba.2014.12.020
2. Zhang A-H, Sun H, Qiu S, Wang X. Metabolomics in noninvasive breast cancer. *Clin Chim Acta* (2013) **424**:3–7. doi:10.1016/j.cca.2013.05.003
3. Pan Z, Raftery D. Comparing and combining NMR spectroscopy and mass spectrometry in metabolomics. *Anal Bioanal Chem* (2007) **387**(2):525–7. doi:10.1007/s00216-006-0687-8
4. Bathen TF, Sitter B, Sjøbakk TE, Tessem M-B, Gribbestad IS. Magnetic resonance metabolomics of intact tissue: a biotechnological tool in cancer diagnostics and treatment evaluation. *Cancer Res* (2010) **70**(17):6692–6. doi:10.1158/0008-5472.CAN-10-0437
5. Bathen T, Geurts B, Sitter B, Fjøsne H, Lundgren S, Buydens L, et al. Feasibility of MR metabolomics for immediate analysis of resection margins during breast cancer surgery. *PLoS One* (2013) **8**(4):e61578. doi:10.1371/journal.pone.0061578
6. Bertilsson H, Tessem M-B, Flatberg A, Viset T, Gribbestad I, Angelsen A, et al. Changes in gene transcription underlying the aberrant citrate and choline metabolism in human prostate cancer samples. *Clin Cancer Res* (2012) **18**(12):3261–9. doi:10.1158/1078-0432.CCR-11-2929
7. Moestue S, Sitter B, Bathen T, Tessem M-B, Gribbestad I. HR MAS MR spectroscopy in metabolic characterization of cancer. *Curr Top Med Chem* (2011) **11**(1):2–26. doi:10.2174/156802611793611869
8. Giskeødegard GF, Bertilsson H, Selnæs KM, Wright AJ, Bathen TF, Viset T, et al. Spermine and citrate as metabolic biomarkers for assessing prostate cancer aggressiveness. *PLoS One* (2013) **8**(4):e62375. doi:10.1371/journal.pone.0062375
9. Giskeødegård G, Lundgren S, Sitter B, Fjøsne HE, Postma G, Buydens L, et al. Lactate and glycine – potential MR biomarkers of prognosis in estrogen receptor-positive breast cancers. *NMR Biomed* (2012) **25**(11):1271–9. doi:10.1002/nbm.2798
10. Choi J, Baek H-M, Kim S, Kim M, Youk J, Moon H, et al. HR-MAS MR spectroscopy of breast cancer tissue obtained with core needle biopsy: correlation with prognostic factors. *PLoS One* (2012) **7**(12):e51712. doi:10.1371/journal.pone.0051712
11. Bergamaschi A, Hjortland G, Triulzi T, Sørlie T, Johnsen H, Ree A, et al. Molecular profiling and characterization of luminal-like and basal-like *in vivo* breast cancer xenograft models. *Mol Oncol* (2009) **3**(5):469–82. doi:10.1016/j.molonc.2009.07.003
12. Grinde MT, Moestue SA, Borgan E, Risa Ø, Engebraaten O, Gribbestad IS. 13C High-resolution-magic angle spinning MRS reveals differences in glucose metabolism between two breast cancer xenograft models with different gene

expression patterns. *NMR Biomed* (2011) **24**(10):1243–52. doi:10.1002/nbm.1683
13. Sørlie T, Perou C, Tibshirani R, Aas T, Geisler S, Johnsen H, et al. Gene expression patterns of breast carcinomas distinguish tumor subclasses with clinical implications. *Proc Natl Acad Sci U S A* (2001) **98**(19):10869–74. doi:10.1073/pnas.191367098
14. Sørlie T, Tibshirani R, Parker J, Hastie T, Marron J, Nobel A, et al. Repeated observation of breast tumor subtypes in independent gene expression data sets. *Proc Natl Acad Sci U S A* (2003) **100**(14):8418–23. doi:10.1073/pnas.0932692100
15. Moestue S, Borgan E, Huuse E, Lindholm E, Sitter B, Børresen-Dale A-L, et al. Distinct choline metabolic profiles are associated with differences in gene expression for basal-like and luminal-like breast cancer xenograft models. *BMC Cancer* (2010) **10**(1):433. doi:10.1186/1471-2407-10-433
16. Giskeødegård G, Cao M, Bathen T. High-resolution magic-angle-spinning NMR spectroscopy of intact tissue. In: Bjerrum, Jacob T, editor. *Metabonomics: Methods and Protocols*. New York: Springer (2015). p. 37–50.
17. Cao M, Lamichhane S, Lundgren S, Bofin A, Fjøsne H, Giskeødegård G, et al. Metabolic characterization of triple negative breast cancer. *BMC Cancer* (2014) **14**(1):941. doi:10.1186/1471-2407-14-941
18. Savorani F, Tomasi G, Engelsen S. icoshift: a versatile tool for the rapid alignment of 1D NMR spectra. *J Magn Reson* (2010) **202**(2):190–202. doi:10.1016/j.jmr.2009.11.012
19. Sitter B, Sonnewald U, Spraul M, Fjösne H, Gribbestad I. High-resolution magic angle spinning MRS of breast cancer tissue. *NMR Biomed* (2002) **15**(5):327–37. doi:10.1002/nbm.775
20. R Core Team. *R: A Language and Environment for Statistical Computing*. Vienna: R Foundation for Statistical Computing (2012).
21. Pinheiro J, Bates D, DebRoy S, Sarkar D, R Core Team. *nlme: Linear and Nonlinear Mixed Effects Models*. R Package Version 3.1-117 (2014). Available from: http://CRAN.R-project.org/package=nlme
22. Opstad KS, Bell BA, Griffiths JR, Howe FA. An investigation of human brain tumour lipids by high-resolution magic angle spinning 1H MRS and histological analysis. *NMR Biomed* (2008) **21**(7):677–85. doi:10.1002/nbm.1239
23. Gorrini C, Harris IS, Mak TW. Modulation of oxidative stress as an anticancer strategy. *Nat Rev Drug Discov* (2013) **12**(12):931–47. doi:10.1038/nrd4002
24. Bánhegyi G, Braun L, Csala M, Puskás F, Mandl J. Ascorbate metabolism and its regulation in animals. *Free Radic Biol Med* (1997) **23**(5):793–803. doi:10.1016/S0891-5849(97)00062-2
25. Gamcsik MP, Kasibhatla MS, Teeter SD, Colvin OM. Glutathione levels in human tumors. *Biomarkers* (2012) **17**(8):671–91. doi:10.3109/1354750X.2012.715672
26. Tang X, Lin C-C, Spasojevic I, Iversen ES, Chi J-T, Marks JR. A joint analysis of metabolomics and genetics of breast cancer. *Breast Cancer Res* (2014) **16**(4):415. doi:10.1186/s13058-014-0415-9
27. Jiang L, Greenwood TR, Artemov D, Raman V, Winnard PT, Heeren RM, et al. Localized hypoxia results in spatially heterogeneous metabolic signatures in breast tumor models. *Neoplasia* (2012) **14**(8):732–41. doi:10.1593/neo.12858
28. Glunde K, Bhujwalla Z, Ronen S. Choline metabolism in malignant transformation. *Nat Rev Cancer* (2011) **11**(12):835–48. doi:10.1038/nrc3162
29. Sitter B, Lundgren S, Bathen T, Halgunset J, Fjosne H, Gribbestad I. Comparison of HR MAS MR spectroscopic profiles of breast cancer tissue with clinical parameters. *NMR Biomed* (2006) **19**(1):30–40. doi:10.1002/nbm.992
30. Gribbestad IS, Sitter B, Lundgren S, Krane J, Axelson D. Metabolite composition in breast tumors examined by proton nuclear magnetic resonance spectroscopy. *Anticancer Res* (1998) **19**(3A):1737–46.
31. Cao M, Sitter B, Bathen T, Bofin A, Lønning P, Lundgren S, et al. Predicting long-term survival and treatment response in breast cancer patients receiving neoadjuvant chemotherapy by MR metabolic profiling. *NMR Biomed* (2012) **25**(2):369–78. doi:10.1002/nbm.1762
32. Choi JS, Baek H-M, Kim S, Kim MJ, Youk JH, Moon HJ, et al. Magnetic resonance metabolic profiling of breast cancer tissue obtained with core needle biopsy for predicting pathologic response to neoadjuvant chemotherapy. *PLoS One* (2013) **8**(12):e83866. doi:10.1371/journal.pone.0083866
33. van Asten JJ, Vettukattil R, Buckle T, Rottenberg S, van Leeuwen F, Bathen TF, et al. Increased levels of choline metabolites are an early marker of docetaxel treatment response in BRCA1-mutated mouse mammary tumors: an assessment by ex vivo proton magnetic resonance spectroscopy. *J Transl Med* (2015) **13**(1):114. doi:10.1186/s12967-015-0458-4
34. Vettukattil R. Preprocessing of raw metabonomic data. *Methods Mol Biol* (2015) **1277**:123–36. doi:10.1007/978-1-4939-2377-9_10
35. Giskeødegård G, Grinde M, Sitter B, Axelson D, Lundgren S, Fjøsne H, et al. Multivariate modeling and prediction of breast cancer prognostic factors using MR metabolomics. *J Proteome Res* (2010) **9**(2):972–9. doi:10.1021/pr9008783
36. Kinross JM, Holmes E, Darzi AW, Nicholson JK. Metabolic phenotyping for monitoring surgical patients. *Lancet* (2011) **377**(9780):1817–9. doi:10.1016/S0140-6736(11)60171-2
37. Middleton DA, Bradley DP, Connor SC, Mullins PG, Reid DG. The effect of sample freezing on proton magic-angle spinning NMR spectra of biological tissue. *Magn Reson Med* (1998) **40**(1):166–9. doi:10.1002/mrm.1910400122
38. Waters N, Garrod S, Farrant R, Haselden J, Connor S, Connelly J, et al. High-resolution magic angle spinning 1 H NMR spectroscopy of intact liver and kidney: optimization of sample preparation procedures and biochemical stability of tissue during spectral acquisition. *Anal Biochem* (2000) **282**(1):16–23. doi:10.1006/abio.2000.4574
39. Rocha CM, Barros AS, Gil AM, Goodfellow BJ, Humpfer E, Spraul M, et al. Metabolic profiling of human lung cancer tissue by 1H high resolution magic angle spinning (HRMAS) NMR spectroscopy. *J Proteome Res* (2009) **9**(1):319–32. doi:10.1021/pr9006574
40. Opstad KS, Bell BA, Griffiths JR, Howe FA. An assessment of the effects of sample ischaemia and spinning time on the metabolic profile of brain tumour biopsy specimens as determined by high-resolution magic angle spinning 1H NMR. *NMR Biomed* (2008) **21**(10):1138–47. doi:10.1002/nbm.1296

Conflict of Interest Statement: The authors declare that the research was conducted in the absence of any commercial or financial relationships that could be construed as a potential conflict of interest.

Supplementary figures

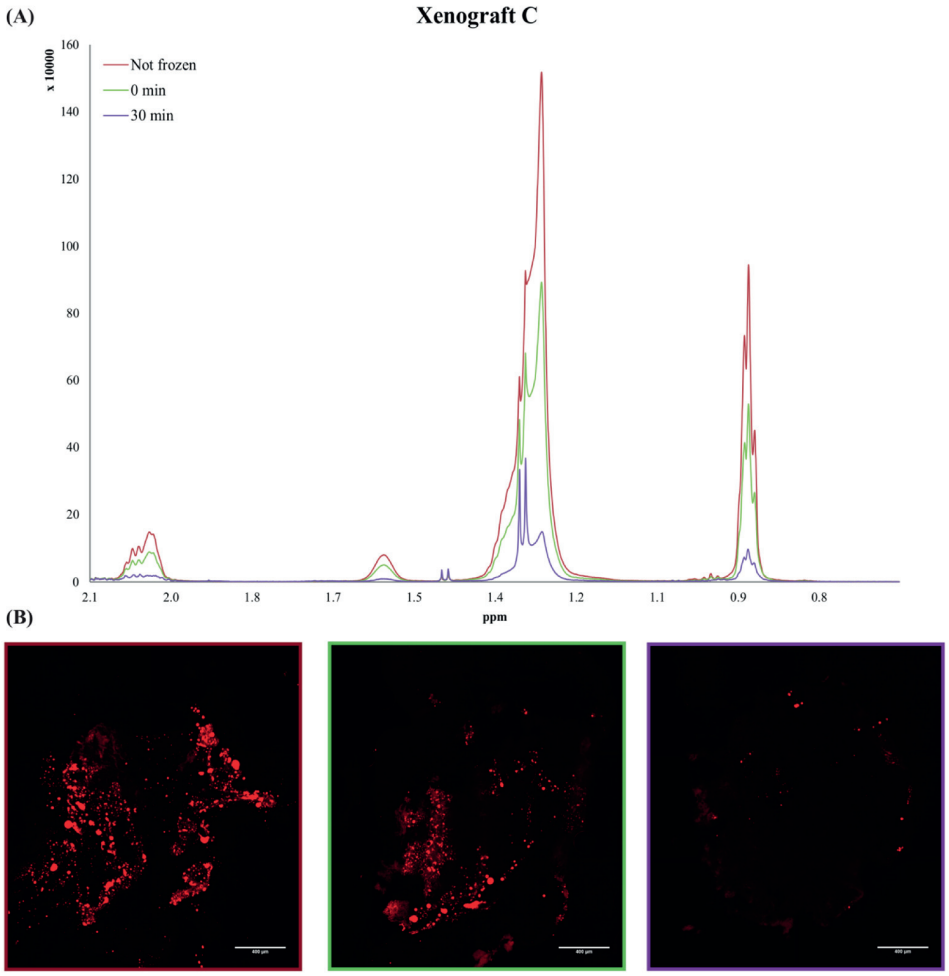

Supplementary Figure 1: Example lipid heterogeneity within samples from the same tumor **(A)** Xenograft HR MAS spectra (2.1 - 0.8 ppm) from sample not frozen and samples with freezing time delay of 0 and 30 minutes **(B)** The samples corresponding Nile Red fluorescent-stained images showing lipid droplets within the tumor samples.

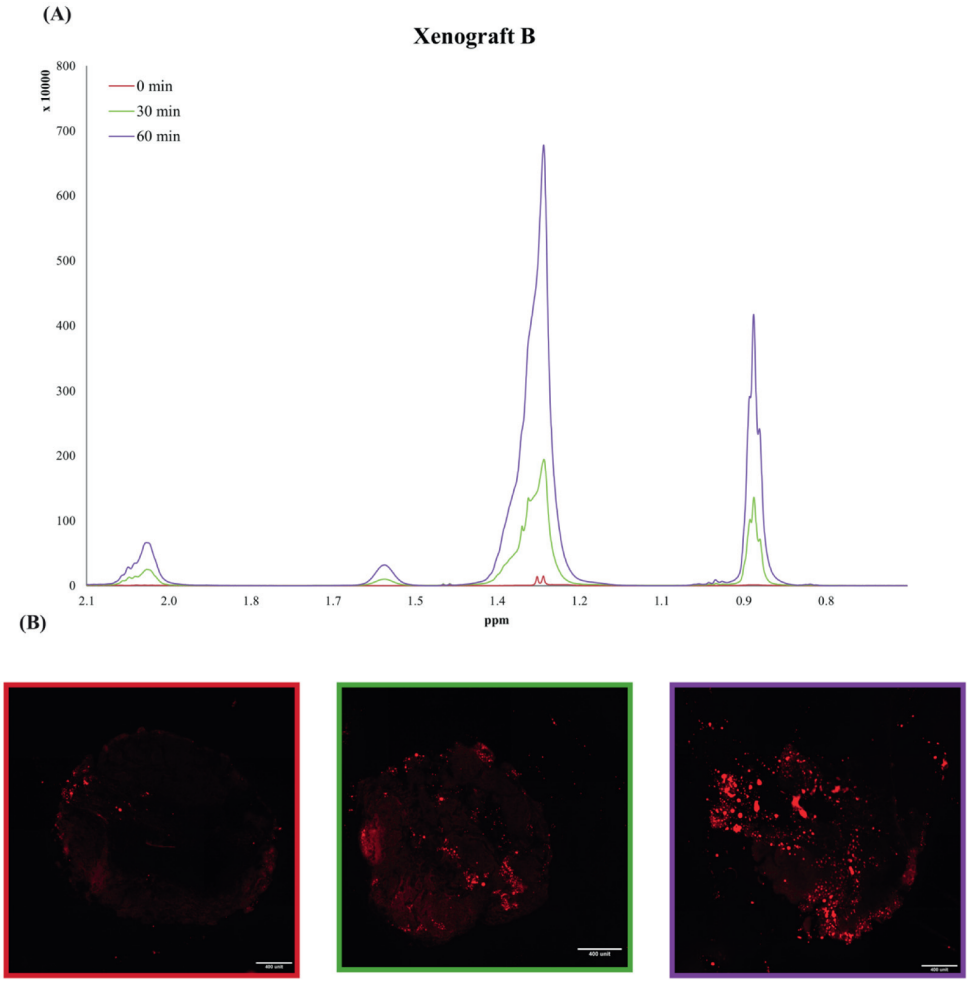

Supplementary Figure 2: Example lipid heterogeneity within samples from the same tumor **(A)** Xenograft HR MAS spectra (2.1 - 0.8 ppm) from freezing time delay of 0, 30 and 60 minutes **(B)** The samples corresponding Nile Red fluorescent-stained images showing lipid droplets within the tumor samples.

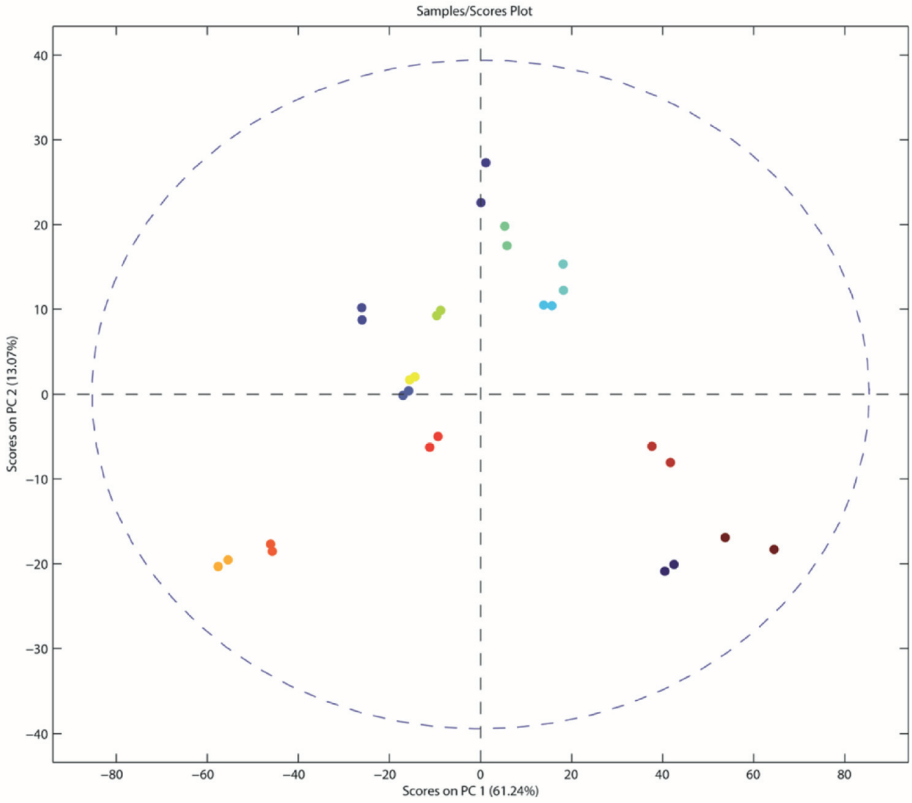

Supplementary Figure 3: PCA score plot for samples analyzed with 1.5 hour time interval. Spectra acquired from the same sample are colored accordingly.

Paper II

Metabolic clusters of breast cancer in relation to gene- and protein expression subtypes

Authors and affiliations:

Tonje H. Haukaas[1,2] , Leslie R. Euceda[1], Guro F. Giskeødegård[1,3], Santosh Lamichhane[1,4], Marit Krohn[2,5], Sandra Jernström[2,5], Miriam R. Aure[2,5], Ole C. Lingjærde[2,6,7], Ellen Schlichting[8], Øystein Garred[9], Eldri U. Due[2,5], The Oslo Breast Cancer Consortium (OSBREAC)[*], Gordon B. Mills[10], Kristine K. Sahlberg[2,11], Anne-Lise Børresen-Dale[2,5], Tone F. Bathen[1,2]

[1]Department of Circulation and Medical Imaging, Norwegian University of Science and Technology (NTNU), Trondheim, Norway. [2]K.G. Jebsen Center for Breast Cancer Research, Institute of Clinical Medicine, Faculty of Medicine, University of Oslo, Oslo, Norway. [3]St. Olavs Hospital, Trondheim University Hospital, Trondheim, Norway. [4]Department of Food Science, Aarhus University, Faculty of Science and Technology, Årslev, Denmark. [5]Department of Cancer Genetics, Institute for Cancer Research Oslo University Hospital, The Norwegian Radium Hospital, Oslo, Norway. [6]Department of Computer Science, University of Oslo, Oslo, Norway.[7]Centre for Cancer Biomedicine, University of Oslo, Oslo, Norway. [8]Section for Breast and Endocrine Surgery, Oslo University Hospital, Ullevål, Oslo, Norway.[9]Department of Pathology, Oslo University Hospital, Oslo, Norway. [10]Department of Systems Biology, The University of Texas M.D. Anderson Cancer Center, Houston, TX, USA.[11]Department of Research, Vestre Viken, Drammen, Norway.

[*]List of participants and their affiliations in Additional file 1.

Corresponding authors: Tone F. Bathen, Department of Circulation and Medical Imaging - MR Center, Norwegian University of Science and Technology (NTNU), Postboks 8905, Medisinsk Teknisk Forskningssenter, 7491 Trondheim, Norway; Phone: +47 73598888, Fax: +47 73598613, E.mail: tone.f.bathen@ntnu.no. Anne-Lise Børresen-Dale, Department of Cancer Genetics, Institute for Cancer Research, Rikshospitalet-Radiumhospitalet Medical Centre, Montebello, 0310 Oslo, Norway; Phone: +47 22781333, Fax: +47 22781395, E-mail: a.l.borresen-dale@medisin.uio.no

Email: Tonje H. Haukaas tonje.h.haukaas@ntnu.no – Leslie R. Euceda leslie.e.wood@ntnu.no – Guro F. Giskeødegård guro.giskeodegard@ntnu.no – Santosh Lamichhane santosh.lamichhane@food.au.dk – Marit Krohn Marit.Krohn@rr-research.no – Sandra Jernström Sandra.Nyberg@rr-research.no – Miriam R. Aure Miriam.Ragle.Aure@rr-research.no – Ole C. Lingjærde ole@ifi.uio.no – Ellen Schlichting ELSCHL@ous-hf.no – Øystein Garred UXYSGA@ous-hf.no – Eldri U. Due Eldri.Undlien.Due@rr-research.no – Gordon B. Mills gmills@mdanderson.org – Kristine K. Sahlberg kristine.sahlberg@vestreviken.no – Anne -Lise Børresen-Dale a.l.borresen-dale@medisin.uio.no – Tone F. Bathen tone.f.bathen@ntnu.no

Abstract

Background: The heterogeneous biology of breast cancer leads to high diversity in prognosis and response to treatment, even for patients with similar clinical diagnosis, histology and stage of disease. Identifying mechanisms contributing to this heterogeneity may reveal new cancer targets or clinically relevant subgroups for treatment stratification. In this study we have merged metabolite, protein and gene expression data from breast cancer patients to examine the heterogeneity at a molecular level.

Methods: The study included primary tumor samples from 228 non-treated breast cancer patients. High resolution magic angle spinning magnetic resonance spectroscopy (HR MAS MRS) was performed to extract the tumors metabolic profiles further used for hierarchical cluster analysis resulting in three significantly different metabolic clusters (Mc1, Mc2 and Mc3). The clusters were further combined with gene and protein expression data.

Results: Our result revealed distinct differences in the metabolic profile of the three metabolic clusters. Among the most interesting differences, Mc1 had the highest levels of glycerophosphocholine (GPC) and phosphocholine (PCho), Mc2 had the highest levels of glucose and Mc3 the highest levels of lactate and alanine. Integrated pathway analysis of metabolite and gene expression data uncovered differences in glycolysis/gluconeogenesis and glycerophospholipid metabolism between the clusters. All three clusters had significant differences in the distribution of protein subtypes classified by the expression of breast cancer related proteins. Genes related to collagens and extracellular matrix were downregulated in Mc1 and consequently upregulated in Mc2 and Mc3, underpinning the differences in protein subtypes within the metabolic clusters. Genetic subtypes were evenly distributed among the three metabolic clusters and could therefore contribute to additional explanation of breast cancer heterogeneity.

Conclusions: Three naturally occurring metabolic clusters of breast cancer were detected among primary tumors from non-treated breast cancer patients. The clusters expressed differences in breast cancer related protein as well as genes related to extracellular matrix and metabolic pathways known to be aberrant in cancer. Analyses of metabolic activity combined with gene and protein expression provides new

information about the heterogeneity of breast tumors and, importantly, the metabolic differences infer that the clusters may be susceptible to different metabolically targeted drugs.

Key Words: Metabolomics, HR MAS MRS, breast cancer subgroups, metabolic cluster, extracellular matrix

Background

Breast cancer accounts for 25% of newly diagnosed cancers and 15% of cancer deaths among women worldwide [1]. It is a heterogeneous disease [2] with high diversity in prognosis and response to treatment. Identification of underlying mechanisms contributing to this heterogeneity may reveal new cancer targets and clinically relevant subgroups and has thus been the focus of many recent studies [3-5].

Searching for genetic features causing the variation in breast cancers, Perou et al. used gene expression analyses followed by hierarchical clustering and defined naturally occurring molecular subtypes [4, 6]. These subtypes are named basal-like, luminal A, luminal B, Erb-B2+ (Her2 enriched), and normal-like, and are found to be associated with tumor characteristics and clinical outcome; patients with basal-like tumors having the shortest and luminal A the longest relapse-free survival [6]. A centroid based method called prediction analysis of microarrays 50 (PAM50), which uses the expression of 50 genes to classify breast cancer into these five intrinsic subtypes was later established and is now broadly implemented [7].

Proteins are the ultimate cellular effectors of pathways and networks within cells, tissues and organisms. Although protein levels are dependent on mRNA expression, not all mRNA will be translated into protein and further protein levels are also influenced by protein stability. In a study by Myhre et al. only 22 of 52 quantified breast cancer related proteins were found to correlate with mRNA expression levels [8] and similar low levels of correlation have been seen in large scale studies [9, 10]. Protein expression subtypes of breast cancer could give further understanding of underlying mechanisms causing heterogeneity [11]. Based on the expression of 171 breast cancer- associated proteins detected by reverse phase protein array (RPPA), six breast cancer subtypes, called RPPA-subtypes, have been defined [5]. Four of these subgroups were in high accordance with the gene expression profiles of the PAM50 subtypes and named accordingly; Basal, Her2, Luminal A and Luminal A/B. In addition, two new subgroups were defined; reactive I and reactive II, based on expression of proteins possibly produced by the surrounding microenvironment.

The chemical processes controlled by proteins involve metabolites as intermediates or end- products. In metabolomics, metabolite levels are measured to gather the final downstream information of ongoing cellular processes. Which processes are active at a specific time point, is strongly influenced by environmental factors like diet and drugs as well as disease state. Well-established metabolic differences have been observed when comparing cancer cells to normal cells. Cancer cell energy production frequently depends on increased glycolysis and production of lactate from glucose regardless of access to oxygen, in contrast to normal cells which produce pyruvate and lactate in aerobic conditions [12]. Also, to produce macromolecules/biomass, mitochondrial metabolism is reprogrammed [13]. Altered metabolism has therefore been included as one of the emerging hallmarks of cancer [14]. In breast cancer, metabolic differences between cancer tissue and normal adjacent tissue have been studied by the magnetic resonance spectroscopy (MRS) method high resolution magic angle spinning (HRMAS) MRS [15]. Using this technique, metabolic profiles and biomarkers predicting long-term survival for locally advanced breast cancer [16], node involvement of patients with infiltrating ductal carcinoma [17] and 5-year survival for ER positive patients [18] have been identified.

Merging transcriptomics and metabolomics led to the discovery of three luminal A subgroups with distinct metabolic profiles and significant differences within gene set expression in a study by Borgan et al. [19]. The aim of the current study was to establish clusters of breast cancer based on the metabolic expression using an approach similar to Borgan et al., but in a larger cohort of patients including all PAM50 subgroups. This approach reveals the main metabolic differences between untreated breast tumors. In addition, the combination of the metabolic clusters with transcriptomics and protein expression data provide an opportunity for information gain from each -omics technology, giving further characterization of the defined metabolic clusters.

Methods

Patients and tissue samples

Primary breast carcinoma samples from 228 patients at the Oslo University Hospital (Radium Hospital and Ullevål Hospital) were collected in the time period 2006 – 2009 as part of the Oslo2 study. The study is approved by the Norwegian Regional Committee for Medical Research Ethics (Biobank approval 1.2006.1607), and all patients have given written consent for the use of material for research purposes. The samples were fresh frozen after surgery and stored at -80˚C. The tumors were divided into smaller pieces depending on their size and one of them was selected for this study. The samples were cut into three sections where the edges of the two outer pieces were used for histological evaluation and an adequate part of the mid pieces were used for HR MAS MRS experiments to obtain metabolic profiles. The remnants of all three pieces were pooled and cut into smaller pieces with scalpel, and depending on the size of the tumor divided into fractions used for extraction of DNA, RNA and protein. Due to high lipid content, HR MAS MRS was performed on a second piece from the same tumor for 13 of the samples. A total of 228 samples were analyzed by MR spectroscopy, of which 201 and 217 were analyzed for gene expression by arrays and protein expression using RPPA, respectively, leaving a total of 191 samples analyzed by all three methods. Patient and tumor characteristics are shown in Table 1.

HR MAS MRS Spectra

HR MAS MRS spectra were acquired from tissue samples (mean sample weight: 7.3 mg) on a Bruker Avance III 600MHz/54 mm US (Bruker, Biospin GmbH, Germany) equipped with a 1H/13C MAS probe with gradient aligned with the magic angle (Bruker, Biospin GmbH, Germany). Spin-echo spectra were recorded using a Carr-Purcell-Meiboom-Gill (cpmg) pulse sequence (cpmgpr1d; Bruker). For experimental details and information about data processing, see Additional file 1.

43 samples were excluded from the original sample cohort of 271 samples due to large lipid content. The spectral region between 1.40 and 4.70 ppm was chosen for further analysis excluding lipid peaks at 4.36-4.27, 2.88-2.70, 2.30-2.20, 2.09-1.93 and 1.67-1.50 ppm. After removal of the lipid residuals, the spectra

were mean normalized to account for differences in tumor cell percentage and sample weight, as it can be assumed that most of the lipid signals from breast samples do not originate from cancer cells.

Protein experiments and protein expression subtyping

Protein levels were determined using Reverse Phase Protein Array (RPPA), a platform were single protein levels can be measured across a series of samples simultaneously [20]. 150 primary antibodies were used to detect breast cancer related proteins (Additional file 2, Add. Table 1). For analytical details, see Additional file 1.

The samples underwent consensus clustering with an option for 4 or 5 groups. The best fit on consensus clustering identified 5 groups, luminal, HER2, basal and reactive I and II subsets as defined in The Cancer Genome Atlas Network data set [5].

mRNA expression profiling and gene expression subtyping

Total RNA was isolated with TRIzol (Invitrogen, Carlsbad, CA, USA). Expression of mRNA was measured using SurePrint G3 Human GE 8x60K (Aglient Technologies) according to the manufactory's protocol (One-Color Microarray-Based Gene expression Analysis, Low Input Quick Amp Labeling, v.6.5, May 2010) and 100 ng RNA was used as input for labeling. Arrays were log2-transformed, quantile normalized and hospital adjusted [21]. Values corresponding to probes with identical Entrez ID were averaged to form a single expression value per gene.

The PAM50 subtype algorithm [7] was used to assign a subtype label to each sample as previously described [22].

Statistical analysis

Subgrouping with cluster analysis of metabolic data

Hierarchical cluster analysis (HCA) was performed with Euclidean distance as the distance parameter and Ward's method (furthest inner square distance) as the clustering distance (Statistical toolbox, Matlab

R2013b, The Mathworks, Inc., USA) on the preprocessed metabolic spectra. Similar spectra based on the distance measures cluster together. The dendrogram was cut to give three clusters. To evaluate the robustness of the three HCA clusters, Partial Least Square Discriminant analysis (PLS-DA) model, using the cluster group for classification was carried out and classification accuracy was evaluated. For details, see Additional file 1.

Analysis of metabolic profiles

Metabolite assignments were performed based on literature values [23] and metabolite levels were calculated as the integral of fixed regions corresponding to the metabolite of interest. Kruskal-Wallis test was performed to compare metabolite levels between clusters. Calculated p values were corrected for multiple testing by The Benjamini Hochberg false discovery rate (FDR) in Matlab, and the differences were considered statistically significant for adjusted $p \leq 0.05$.

Analysis of subtype and clinical distributions

Differences in the distributions of RPPA and PAM50 subtype as well as that of other clinical characteristics of the tumors between the different metabolic clusters were tested for significance using Fisher's Exact Test for Count Data (R 2.15.2). Calculated p values were corrected for multiple testing by The Benjamini Hochberg FDR, and the differences were considered statistically significant for adjusted $p < 0.05$.

Analysis of gene expression data

Significance Analysis of Microarrays (SAM) was used to identify differentially expressed gene between the metabolic clusters [24]. SAM analysis was performed using 21851 genes from 42405 mRNA probes. The expression analysis was performed in R 2.15.2 [25] with the cluster group as the dependent variable and a total of 100 permutations. T-statistics/Wilcoxon statistics were calculated using multiclass comparisons and two-class unpaired tests while comparing two clusters. The differences were considered statistically significant for adjusted $p < 0.01$.

DAVID, an online network analysis tool [26], was used to search for biological functions within gene sets. DAVID was performed on the gene list over for each of the class comparisons produced by SAM. Official gene symbol was selected as gene identifier. The Functional Annotation Clustering report of this software reports similar annotations together, where the member of a cluster have similar biological meaning due to sharing of similar gene members.

Gene Set Enrichment Analysis (GSEA) was used to identifying sets of genes that were enriched in the metabolic clusters [27, 28]. During each cluster comparison genes were ranked depending on calculated absolute signal to noise-ratio (eq.1), where μ and σ are the mean and standard deviation, respectively.

$$abs\left(\frac{\mu_A - \mu_B}{\sigma_A + \sigma_B}\right) \qquad \text{(eq. 1)}$$

High absolute signal to noise -ratio will represent genes that are more likely to be "class markers" in the comparison because of high difference in expression.

The gene set C5 (Gene Ontology (GO) gene sets) available from the Molecular Signatures Database (MSigDB) [29] from The Broad Institute was chosen for evaluation of enrichment. 1004 (of 1454) gene sets from this data base passed the filtering of lacking any gene from the expression data followed by minimum and maximum size of 15 and 500 genes, respectively. For each comparison, 1000 permutations on phenotypes were performed and FDR cutoff was set to 25% (recommended in the manual).

Integrated Pathway Analysis

To combine transcriptomics and metabolic data the 'Integrated pathway analysis' tool in MetaboAnalyst 3.0 software was used [30]. Genes with adjusted $p < 0.05$ from SAM analysis and metabolites differently expressed between the clusters were used as input. Pathways with p values ≤ 0.05 were interpreted as significant.

Results

Three main metabolic clusters of breast cancer

From the spectral data of 228 breast tumors, hierarchical clustering gave a dendrogram divided in three metabolic clusters (Mc) (Figure 1A) Mc1, Mc2 and Mc3. The mean spectra of the clusters are illustrated in Figure 1B.

Prediction of the metabolic clusters by PLS-DA resulted in a model with two valid latent variables LVs (Figure 2A). The clusters Mc1 and Mc2 were well separated in the score plot of LV1 and LV2, while most Mc3 samples had low values of LV2. Classification accuracy was found to be 91.1%, 88.7% and 69.9%, respectively, for the three clusters. Permutation testing showed that all three clusters had significantly different metabolic profiles ($p < 0.001$). The regression vectors for each of the clusters (Figure 2B) indicate each metabolite's influence on the cluster prediction. The regression vector for Mc1 showed that high levels of glycerophosphocholine (GPC) and phosphocholine (PCho) and low levels of lactate (Lac), taurine (Tau) and alanine (Ala) were important for the class prediction result. For Mc2, high levels of β-glucose (β-Glc) were important as well as low levels of Lac, creatine (Cr), glycine (Gly), Tau, GPC, PCho and Ala. Mc3 had a regression profile with low β-Glc, GPC and PCh levels, and high Lac, Gly, Tau, Cr and Ala levels. Univariate comparison of metabolite levels between the three clusters revealed that 15 out of 18 metabolites analyzed were found to be significantly different (adjusted $p < 0.05$) between at least two of the clusters (Table 2). Combination of metabolic cluster labels and heatmap of metabolite fold change further illustrate this (Figure 3).

Clinical parameters (tumor size, histology, grade, node status, hormone receptor status) were analyzed for differences in distribution among the metabolic clusters. Only histology was found to be significantly different between the clusters (adjusted $p = 0.0144$), where 11 of 21 lobular tumors and all ductal carcinoma in situ (DCIS) ($n = 4$) were classified as Mc2 (Table 1).

Protein expression subtype (RPPA) distribution differs between the three metabolic clusters

The metabolic clusters were investigated for differences in distribution of PAM50- and RPPA subtypes. While PAM50 subtypes did not show increased frequency of occurrence in any of the metabolic clusters, (Figure 3C, adjusted $p = 0.138$), RPPA distribution was significantly different (Figure 3D, adjusted $p = 1.43E-04$) with only 9% of the RPPA reactive I and II samples being classified as Mc1, and 44% of Mc2 samples subtyped as reactive I. The complete distribution of PAM50- and RPPA subtypes is listed in Table 3.

SAM reveals only one metabolic cluster to have differences in gene expression

SAM was performed to identify expression differences between the metabolic clusters. Of the 21851 genes, multiclass SAM showed that 696 were differently expressed between the metabolic clusters with adjusted $p < 0.01$ (Figure 3E, Additional file 2, Add. Table 2). Further investigation through two-class SAM revealed that Mc2 and Mc3 did not have significant differences in mRNA expression, while they had 413 and 617 genes upregulated, respectively, compared to Mc1 (Additional file 2, Add. Table 3 and 4, respectively). Out of these, 277 genes were found in both comparisons and upregulated compared to Mc1. DAVID software was used to investigate the biological interactions between genes that were found to be significantly differentially expressed between the metabolic clusters.

A total of 404 of the 413 significant genes from SAM between Mc1 and Mc2 were identified by DAVID. Functional Annotation Clustering resulted in 117 clusters (Top 10 in Additional file 2, Add. Table 5), where the clusters with the highest enrichment scores were linked to signaling, extracellular region and cell adhesion.

A total of 653 of the 671 significant genes from SAM between Mc1 and Mc3 were identified by DAVID. Functional Annotation Clustering resulted in 236 clusters (Top 10 in Additional file 2, Add. Table 6), where the clusters with the highest enrichment scores were linked to extracellular matrix (ECM), cell adhesion and basement membrane.

Enrichment analysis shows gene expression differences to be related to extracellular matrix (ECM) activity

Since Mc1 was found to have a gene expression pattern different from both Mc2 and Mc3 and these two clusters lacked statistically significant gene expression differences, Mc1 was compared to Mc2 and Mc3 combined in GSEA. This resulted in 146 of the gene ontology gene sets altered in Mc1 compared to Mc2 and Mc3 (Additional file 2, Add. Table 7). Gene sets with the highest significance were classified with functions within collagen, ECM and integrin binding. None of the gene ontology sets were significantly different when comparing Mc2 to Mc1 combined with Mc3, but 44 gene sets were significantly enriched when comparing Mc2 to Mc1 alone, with gene ontology terms relevant to ECM dominating the result (Additional file 2, Add. Table 8). 11 gene sets were significantly altered between Mc3 and Mc1 combined with Mc2 (Additional file 2, Add. Table 9) and also here ECM related findings were reported. 114 gene sets were significantly different between Mc1 and Mc3, while none were significant between Mc2 and Mc3 (results not shown).

Joint analysis of gene and metabolite expression shows differences in metabolic pathways

Integrated Pathway Analysis resulted in 12 significantly different metabolic pathways (p value < 0.05) between Mc1 and Mc2 (Additional file 2, Add. Table 10). The most significant pathway was 'Tyrosine metabolism' with 8 hits of genes and metabolites, but also 'D-Glutamine and D-glutamate metabolism', 'Glycolysis / Gluconeogenesis' (Figure 4A) and 'Glycerophospholipid metabolism' (Figure 4B) were among the significant pathways. Integrated Pathway Analysis resulted in 4 significantly different metabolic pathways (p value < 0.05) between Mc1 and Mc3 (Additional file 2, Add. Table 11). The most significant pathway was 'Glycerophospholipid metabolism' with 9 hits, succeeded by 'D-Glutamine and D-glutamate metabolism'.

Discussion

In the present work, metabolite, protein and gene expression data from 228 breast tumors were combined to search for new insight into the heterogeneity of breast cancer. MR metabolite data was used to derive naturally occurring metabolic clusters, which were further combined with data from the proteomics and transcriptomics levels. We identified three significantly different metabolic clusters, Mc1, Mc2, and Mc3, with significant differences in gene expression and protein expression profiles, but not within PAM50 subgroups. The metabolic clusters could therefore contribute with additional information beyond the intrinsic gene sets for understanding breast cancer heterogeneity.

Of the three metabolic clusters, Mc1 was on a separate branch in the dendrogram indicating that the metabolic profile of this cluster was the most different. This cluster is defined by significantly higher levels of GPC and PCho, two choline-containing metabolites involved in the synthesis and degradation of phosphatidylcholine (PtdCho), a major component of cell membranes [31]. Altered choline metabolism has been considered an emerging hallmark for malignant transformations, and has been detected in several cancer types including breast cancer [32]. PCho in particular has been suggested a biomarker of breast cancer [33]. Both GPC and PCho are confirmed elevated in tumor tissue compared to adjacent non-involved tissue from breast cancer patients [17] and a higher GPC/PCho-ratio has been reported in ER negative tumors [34, 35]. The latter was also observed for our cohort (results not shown), however, there was no significant difference in ER status between the three metabolic clusters. Thus, the high level of GPC and PCho is not resulting from differences in the distribution of estrogen receptor (ER) status. Interestingly, integrated pathway analysis showed that 'Glycerophospholipid metabolism' was the most significant pathway, when comparing Mc1 to Mc2. This metabolic pathway had eight hits including the metabolites GPC and PCho and genes *LCAT, LPCAT2, PPAP2A, PPAP2B, PLD1* and *AGPAT4*. Downregulation of the expression of these genes in Mc1 indicate a less active degradation of PtdCho causing an accumulation of GPC and PCho, thus explaining the higher levels of GPC and PCho in Mc1. Furthermore, *LPCAT2* is involved in the reaction where the GPC precursor (acyl-GPC) is converted into

PtdCho. Lower expression of this gene may explain why the GPC precursor is directed to the production of GPC instead of PtdCho. The same hits were obtained when Mc1 was compared to Mc3. In addition, *PLA2G5*, one of the enzymes degrading PtdCho to acyl-GPC, is downregulated in Mc1 compared to Mc3, further supporting that Mc1 has an altered PtdCho metabolism.

For Mc1 compared to Mc2 through integrated pathway analysis, 'D-glutamine and D-glutamate metabolism' has only two hits, but comes out as significant because of the small number of genes and metabolites within this pathway. Interestingly, the gene *GLS* which catalyzes the conversion of glutamine to glutamate is downregulated in Mc1, the cluster with lowest levels of glutamate. Glutamine metabolism is considered a therapeutic target as some cancer cells exhibit high uptake and addiction to this nonessential amino acid [36]. Since there were no differences in glutamine levels of Mc1 and Mc2, less glutamate in Mc1 could indicate that more glutamine is directed towards other metabolic pathways necessary for proliferation, glutathione needed for reducing power or further that glutamate is rapidly metabolized in cells through the TCA cycle or other mechanisms.

The distribution of protein subtypes (RPPA) was significantly different between the metabolic clusters, whereas no significant differences in the distribution of PAM50 subtypes were found. Thus, the metabolic difference between Mc1, Mc2 and Mc3 is not a result of intrinsic subtypes and might therefore contain additional information for understanding breast cancer heterogeneity. Among the tumors clustered in Mc1, 12% were classified as RPPA-reactive (either I or II) while 49% were classified as RPPA-luminal. The reactive RPPA subtypes have a characteristic protein expression pattern probably produced by the microenvironment [5], indicating less microenvironmental activity within Mc1. Mc1 also had downregulation of several genes involved in processes within the ECM of the stroma compared to both Mc2 and Mc3. As ECM changes can drive cancer behavior [37], these genetic differences between Mc1 and Mc2 might be of prognostic relevance. In fact, differences in expression of ECM-related genes have been used to stratify breast carcinomas into four groups, where the subgroup ECM1 have the worst prognosis [38]. ECM-classification was not performed on this cohort. However, 34 of 43 genes that

clustered with a tendency of being downregulated in ECM1 and ECM2 were also found to be downregulated in Mc1. In addition, only 5 of 46 genes reported to be downregulated in ECM2 compared to ECM1 were downregulated in Mc1 (results extracted from SAM analyses, Additional file 2, Add. Table 5-6). These results support the contention that Mc1 tumors have an ECM signature similar to the reported ECM2 tumors. ECM2 did not show significant difference in disease outcome compared to ECM3 and ECM4, but had better prognosis than ECM1 tumors [38].

Mc2 has a metabolic profile with significant higher glucose level and at the same time lower levels of most of the other metabolites compared to one or both of the remaining clusters. High glucose level could reflect lower glucose consumption, inferring a lower demand for energy within these tumors. 'Glycolysis / Gluconeogenesis' came out as a significant pathway when Mc1 was compared to Mc2 during integrated pathway analysis with two metabolite hits and five gene hits. For the most significant metabolite, glucose, the levels are higher in Mc2 compared to Mc1. Glucose is the main source of energy for mammalian cells, either through aerobic glycolysis (production of lactate even in the presence of oxygen) or tricarboxylic acid (TCA) cycle and oxidative phosphorylation. For normal proliferating cells and cancer cells, which both have an increased energy demand, a glycolytic switch is often observed (higher glycolytic rate) [12]. The increased glycolysis is followed by fermentation of the pyruvate to lactate (Warburg effect), in contrast to the conversion of acetyl CoA through the TCA cycle that occurs in normal non-proliferating cells. Increased glucose consumption is commonly used in tumor detection using a glucose analogue and positron emission tomography (PET) [39] and has shown to correlate with poor prognosis and tumor aggressiveness [12]. However, not all breast cancers are detected by PET. Here we expect lower sensitivity in detection of Mc2 tumors due to the possible difference in glycolytic rate. None of the genes with hits in 'Glycolysis / Gluconeogenesis' for the comparison of Mc1 and Mc2 could directly explain the high glucose levels of Mc2 tumors, but altered expression of the genes indicate pyruvate being guided towards the TCA cycle rather than lactate production. Two of the alternative fates of pyruvate showed significantly higher levels (alanine) or levels approaching significance (lactate, adjusted $p = 0.056$),

supporting a higher glycolytic rate in Mc1 and that the pyruvate produced is not directed to metabolism in the TCA cycle. The significantly lower acetate levels in Mc1compared to Mc2 could be linked to *ALDH1A3* and *ALDH2* downregulation, since the enzymatic product of these genes catalyzes the reversible reaction where acetaldehyde is converted to acetate.

Both DAVID and GSEA showed that many of the genes found to be downregulated in Mc1 and consequently upregulated in Mc2 were related to ECM activity. Mc2 had the highest percentage of RPPA-reactive I with 44% of Mc2 tumors classified as this protein subtype, also related to stromal changes. Together with the metabolic finding, this implies that Mc2 tumors have cancer cells with low proliferating rate and at the same time ongoing changes within the ECM of the stroma. Mc2 tumors also had a higher frequency of lobular and ductal carcinoma in situ, indicating metabolic differences between histological subtypes of breast cancer which should be further investigated.

Mc3 has the highest lactate levels of all three clusters and higher glycine level than Mc2. These metabolites have been related to poor prognosis in ER positive patients [18] and higher levels of glycine is also associated with poor prognosis in a study irrespective of ER status [40]. Although the ER-positive patients are equally distributed among our reported metabolic clusters, Mc3 expressed higher levels of both of these metabolites compared to Mc2. Moestue et al. detected differences in the expression of genes involved in choline degradation that could explain higher glycine concentrations in the poor-prognosis basal-like breast cancer xenograft model compared to luminal-like [41]. Five of the genes described by Moestue et al. were significantly upregulated in Mc3 compared to Mc1; *AGPAT4, PPAP2B, PPAP2A, LCAT* and *PLD1*. Of these, *LCAT* and *PLD1* are directly involved in choline metabolism. *LCAT* catalyze the conversion of PtdCho to acyl-GPC while *PLD1* catalyzes the conversion of PtdCho to choline. Higher GPC levels, but no difference in choline levels in Mc3 compared to Mc1 indicates that a higher amount of GPC is converted to choline in Mc3, and further contributing to higher glycine levels through choline degradation.

Mc3 share similarities with a previously reported metabolic subgroup of luminal A tumors with significantly lower levels of glucose, higher levels of alanine and nearly significantly higher lactate levels [19]. In Mc3 we also see a significant higher level of lactate. Since one of the main sources of alanine is pyruvate, which also is the source for lactate, it appears that Mc3 is a cluster with a switch in glycolytic activity.

The majority of Mc3 tumors were classified as RPPA-luminal, similar to Mc1. In contrast to Mc1, Mc3 had a higher percentage of RPPA–reactive II tumors, probably linked to changes in stromal content. Also gene expression wise this was observed by significantly different gene expressions linked to ECM activity and the gene expression profile of Mc3 was found similar to the previously reported ECM3 or ECM4 subtypes [38].

In this study, information flow between the transcriptomics, proteomics and metabolomics levels is illustrated; at the transcriptomics level only one of the metabolic clusters shows difference in gene expression compared to the two others, while at the proteomics level there is difference between all three clusters. Combining these findings, Mc1 is expected to have the worst prognosis due to the distinct gene expression profile and the alterations in both glycerophospholipid metabolism and evidence of increased glycolytic rate. However, this has to be validated when 5-years follow-up of this cohort is available. The main metabolic characteristics, especially of Mc1 and Mc3, have been proposed as treatment targets that could improve the therapeutic effect [42]. Cancer therapy targeting choline kinase alpha (CHK-α), the enzyme responsible for PCho production from choline, cause tumor growth arrest and apoptosis in preclinical models [43], while treatment targeting glycolytic enzymes in combination with chemotherapy has been shown to re-sensitize cancer cells that had become resistant to treatment [42]. Metabolic classification as illustrated here could therefore be relevant for developing a more targeted treatment plan. Importantly, the prognostic value of the clusters should be evaluated once 5-year follow-up is available.

Conclusion

We have here identified three metabolic clusters of breast cancer, also characterized with differences at the proteomic and transcriptomic level. The metabolic clusters are not reflecting the intrinsic genetic subtypes and may give important additional information for understanding breast cancer heterogeneity. Gene enrichment analysis revealed diverse ECM characteristics among these clusters in accordance with RPPA-subtyping. The approach of combining information from several -omics levels in the same tumor shows promise in improving the understanding of breast cancer heterogeneity potentially leading to more patient specific treatment.

Abbreviations

Ala: alanine; Cr: creatine; DCIS: ductal carcinoma in situ; ER: Estrogen receptor; ECM: extracellular matrix; FDR: False discovery rate; GSEA: Gene Set Enrichment Analysis; GPC: glycerophosphocholine; Gly: glycine; HCA: Hierarchical cluster analysis; HR MAS MRS: High resolution magic angle spinning magnetic resonance spectroscopy; Lac: lactate; MRS: Magnetic resonance spectroscopy; Mc: Metabolic cluster; MSigDB: Molecular Signatures Database; PLS-DA: Partial Least Square Discriminant analysis; PtdCho: phosphatidylcholine (PtdCho); PCho: phosphocholine; PET: positron emission tomography; PAM50: prediction analysis of microarrays 50; RPPA: reverse phase protein array; SAM: Significance Analysis of Microarrays; Tau: taurine; TCA: tricarboxylic acid; β-Glc: β-glucose.

Competing interests

The authors disclose no potential competing interest.

Authors' contributions

THH, LRE, GFG, OLC, ES, ØG, OSBREAC, KKS, ALBD and TFB participated in the design of the study. KKS, ALDB and TFB conceived the study. THH, LRE, GFG, KKS, ALDB and TFB interpreted the data. SL and THH performed the HR MAS MRS acquisition. THH performed statistical analysis and

drafted the manuscript. MK, SJ, MRA, OCL, ES, ØG, EUD, OSBREAC, GBM, KKS, ALDB and TFB participated in acquisition of the data. All authors have read and helped to revise the manuscript. The final manuscript is approved by all the authors.

Acknowledgements

The HR MAS MRS analysis was performed at the MR Core Facility, Norwegian University of Science and Technology (NTNU). MR core facility is funded by the Faculty of Medicine at NTNU and Central Norway Regional Health Authority

This work was supported by:

(1) K. G. Jebsen Center for Breast Cancer Research. The funders had no role in study design, data collection and analysis, decision to publish, or preparation of the manuscript.
(2) Cancer Society of Norway
(3) South-Eastern Norway Regional Health Authority (Project no 2011042, OSBREAC: Towards personalized therapy for breast cancer)
(4) The Research Council of Norway, Imaging the breast cancer metabolome, Project no 221879
(5) Liaison Committee between the Central Norway Regional Health Authority and NTNU Project no 46056615
(6) NCI grants P01CA0099031 and P30 CA016672 to GBM

References

1. Ferlay J, Soerjomataram I, Ervik M, Dikshit R, Eser S, Mathers C, et al. GLOBOCAN 2012 v1.0, Cancer Incidence and Mortality Worldwide: IARC CancerBase No. 11. 2013. http://globocan.iarc.fr. Accessed:04/01 2015.
2. Polyak K. Heterogeneity in breast cancer. J Clin Invest. 2011;121(10):3786-8.
3. Wang Y K and Crampin E J. Biclustering reveals breast cancer tumour subgroups with common clinical features and improves prediction of disease recurrence. BMC genomics. 2013;14(1):102.
4. Perou C M, Sørlie T, Eisen M B, van de Rijn M, Jeffrey S S, Rees C A, et al. Molecular portraits of human breast tumours. Nature. 2000;406(6797):747-52.
5. The Cancer Genome Atlas Network. Comprehensive molecular portraits of human breast tumours. Nature. 2012;490(7418):61-70.
6. Sørlie T, Perou C M, Tibshirani R, Aas T, Geisler S, Johnsen H, et al. Gene expression patterns of breast carcinomas distinguish tumor subclasses with clinical implications. Proc Natl Acad of Sci U S A. 2001;98(19):10869-74.
7. Parker J S, Mullins M, Cheang M C, Leung S, Voduc D, Vickery T, et al. Supervised risk predictor of breast cancer based on intrinsic subtypes. J Clin Oncol. 2009;27(8):1160-7.
8. Myhre S, Lingjærde O-C, Hennessy B T, Aure M R, Carey M S, Alsner J, et al. Influence of DNA copy number and mRNA levels on the expression of breast cancer related proteins. Mol Oncol. 2013;7(3):704-18.
9. Akbani R, Ng P K S, Werner H M, Shahmoradgoli M, Zhang F, Ju Z, et al. A pan-cancer proteomic perspective on The Cancer Genome Atlas. Nat Commun. 2014;5.
10. Zhang B, Wang J, Wang X, Zhu J, Liu Q, Shi Z, et al. Proteogenomic characterization of human colon and rectal cancer. Nature. 2014;513(7518):382-7.
11. Hennessy B T, Lu Y, Gonzalez-Angulo A M, Carey M S, Myhre S, Ju Z, et al. A technical assessment of the utility of reverse phase protein arrays for the study of the functional proteome in non-microdissected human breast cancers. Clin Proteomics. 2010;6(4):129-51.
12. Gatenby R A and Gillies R J. Why do cancers have high aerobic glycolysis? Nat Rev Cancer. 2004;4(11):891-9.
13. Ward P S and Thompson C B. Metabolic reprogramming: a cancer hallmark even warburg did not anticipate. Cancer cell. 2012;21(3):297-308.
14. Hanahan D and Weinberg R A. Hallmarks of cancer: the next generation. Cell. 2011;144(5):646-74.
15. Bathen T F, Geurts B, Sitter B, Fjøsne H E, Lundgren S, Buydens L M, et al. Feasibility of MR metabolomics for immediate analysis of resection margins during breast cancer surgery. PLoS One. 2013;8(4):e61578.
16. Cao M D, Sitter B, Bathen T F, Bofin A, Lønning P E, Lundgren S, et al. Predicting long-term survival and treatment response in breast cancer patients receiving neoadjuvant chemotherapy by MR metabolic profiling. NMR Biomed. 2012;25(2):369-78.
17. Sitter B, Lundgren S, Bathen T F, Halgunset J, Fjosne H E, and Gribbestad I S. Comparison of HR MAS MR spectroscopic profiles of breast cancer tissue with clinical parameters. NMR Biomed. 2006;19(1):30-40.
18. Giskeødegård G F, Lundgren S, Sitter B, Fjøsne H E, Postma G, Buydens L, et al. Lactate and glycine—potential MR biomarkers of prognosis in estrogen receptor-positive breast cancers. NMR Biomed. 2012;25(11):1271-9.
19. Borgan E, Sitter B, Lingjærde O C, Johnsen H, Lundgren S, Bathen T F, et al. Merging transcriptomics and metabolomics-advances in breast cancer profiling. BMC Cancer. 2010;10(1):628.

20. Tibes R, Qiu Y, Lu Y, Hennessy B, Andreeff M, Mills G B, et al. Reverse phase protein array: validation of a novel proteomic technology and utility for analysis of primary leukemia specimens and hematopoietic stem cells. Mol Cancer Ther. 2006;5(10):2512-21.
21. Aure M R, Jernström S, Krohn M, Vollan H K M, Due E U, Rødland E, et al. Integrated analysis reveals microRNA networks coordinately expressed with key proteins in breast cancer. Genome Med. 2015;7(1).
22. Nilsen G, Vollan H K M, Pladsen A V, Borgan Ø, Liestøl K, Vitelli V, et al., Dissecting genome aberration patterns in tumors, Submitted 2015.
23. Sitter B, Sonnewald U, Spraul M, Fjösne H E, and Gribbestad I S. High-resolution magic angle spinning MRS of breast cancer tissue. NMR Biomed. 2002;15(5):327-37.
24. Tusher V G, Tibshirani R, and Chu G. Significance analysis of microarrays applied to the ionizing radiation response. Proc Natl Acad Sci U S A. 2001;98(9):5116-21.
25. R Core Team. R: A language and environment for statistical computing. 2012. http://www.R-project.org.
26. Da Wei Huang B T S and Lempicki R A. Systematic and integrative analysis of large gene lists using DAVID bioinformatics resources. Nat Protoc. 2008;4(1):44-57.
27. Subramanian A, Tamayo P, Mootha V K, Mukherjee S, Ebert B L, Gillette M A, et al. Gene set enrichment analysis: a knowledge-based approach for interpreting genome-wide expression profiles. Proc Natl Acad Sci U S A. 2005;102(43):15545-50.
28. Mootha V K, Lindgren C M, Eriksson K-F, Subramanian A, Sihag S, Lehar J, et al. PGC-1α-responsive genes involved in oxidative phosphorylation are coordinately downregulated in human diabetes. Nat Genet. 2003;34(3):267-73.
29. Liberzon A, Subramanian A, Pinchback R, Thorvaldsdóttir H, Tamayo P, and Mesirov J P. Molecular signatures database (MSigDB) 3.0. Bioinformatics 2011. http://www.broadinstitute.org/gsea/msigdb/index.jsp. Accessed:08/10 14.
30. Xia J, Mandal R, Sinelnikov I V, Broadhurst D, and Wishart D S. MetaboAnalyst 2.0--a comprehensive server for metabolomic data analysis. Nucleic Acids Res. 2012;40(Web Server issue):W127-33.
31. Gibellini F and Smith T K. The Kennedy pathway--de novo synthesis of phosphatidylethanolamine and phosphatidylcholine. IUBMB Life. 2010;62(6):414-28.
32. Glunde K, Bhujwalla Z M, and Ronen S M. Choline metabolism in malignant transformation. Nat Rev Cancer. 2011;11(12):835-48.
33. Eliyahu G, Kreizman T, and Degani H. Phosphocholine as a biomarker of breast cancer: molecular and biochemical studies. Int J Cancer. 2007;120(8):1721-30.
34. Grinde M T, Skrbo N, Moestue S A, Rødland E A, Borgan E, Kristian A, et al. Interplay of choline metabolites and genes in patient-derived breast cancer xenografts. Breast Cancer Res. 2014.
35. Giskeødegård G F, Grinde M T, Sitter B, Axelson D E, Lundgren S, Fjøsne H E, et al. Multivariate modeling and prediction of breast cancer prognostic factors using MR metabolomics. J Proteome Res. 2010;9(2):972-79.
36. Wise D R and Thompson C B. Glutamine addiction: a new therapeutic target in cancer. Trends Biochem Sci. 2010;35(8):427-33.
37. Tlsty T D and Hein P W. Know thy neighbor: stromal cells can contribute oncogenic signals. Curr Opin Genet Dev. 2001;11(1):54-9.
38. Bergamaschi A, Tagliabue E, Sørlie T, Naume B, Triulzi T, Orlandi R, et al. Extracellular matrix signature identifies breast cancer subgroups with different clinical outcome. J Pathol. 2008;214(3):357-67.
39. Mankoff D A, Eary J F, Link J M, Muzi M, Rajendran J G, Spence A M, et al. Tumor-specific positron emission tomography imaging in patients:[18F] fluorodeoxyglucose and beyond. Clin Cancer Res. 2007;13(12):3460-9.

40. Sitter B, Bathen T F, Singstad T E, Fjøsne H E, Lundgren S, Halgunset J, et al. Quantification of metabolites in breast cancer patients with different clinical prognosis using HR MAS MR spectroscopy. NMR Biomed. 2010;23(4):424-31.
41. Moestue S A, Borgan E, Huuse E M, Lindholm E M, Sitter B, Børresen-Dale A-L, et al. Distinct choline metabolic profiles are associated with differences in gene expression for basal-like and luminal-like breast cancer xenograft models. BMC Cancer. 2010;10(1):433.
42. Zhao Y, Butler E, and Tan M. Targeting cellular metabolism to improve cancer therapeutics. Cell Death Dis. 2013;4(3):e532.
43. Glunde K, Jiang L, Moestue S A, and Gribbestad I S. MRS and MRSI guidance in molecular medicine: targeting and monitoring of choline and glucose metabolism in cancer. NMR Biomed. 2011;24(6):673-90.

Tables

Table 1. Patient and tumor characteristics

	Total	Mc1	Mc2	Mc3
Number of patients	228	58	58	112
Age (years)				
Mean (range)	55.5 (31.8 – 81.1)	58.0 (33.2 - 80.8)	58.6 (40.9 - 81.1)	52.7 (31.8 - 73.9)
Clinical classification				
Histology				
Ductal	186	52	37	97
Lobular	21	4	11	6
Medullary	0	0	0	0
Ductal carsinoma in situ (DCIS)	4	0	4	0
Metaplastic	1	0	1	0
Mucinous	4	0	2	2
Tubular	4	1	1	2
Mixed	2	1	0	1
Papillary	0	0	0	0
NA	6	0	2	4
Primary tumor				
Tx or *NA*	9	1	3	5
T0	0	0	0	0
pTis	4	0	4	0
T1	113	31	28	54
T2	93	24	21	48
T3	9	2	2	5
T4	0	0	0	0
Grade				
I	31	8	10	13
II	93	20	24	49
III	97	30	21	46
NA	7	0	3	4
Node status				
N0	133	34	36	63
N1(mi)	8	3	3	2
N1	59	17	13	29
N2	14	2	3	9
N3	8	2	1	5
NA	6	0	2	4
Receptor status				
HER2+	26	7	7	12
HER2-	192	51	45	96
ER+	178	49	42	87
ER-	40	9	10	21
PR+	155	39	36	80
PR-	63	19	16	28
NA	10	0	6	4

NA: not available

Table 2. Metabolite levels for the metabolic clusters

Metabolite name	Mc1 (n=58)		Mc2 (n=58)		Mc3 (n=112)		Adjusted *P* value	Significant between
	Mean	SE	Mean	SE	Mean	SE		
Beta-D-Glucose	**30.0**	27.7	**71.7**	55.2	**32.3**	16.3	3.62E-09	Mc2 vs rest
Ascorbate	**40.0**	17.1	**28.8**	8.6	**38.3**	13.6	1.02E-05	Mc2 vs rest
Lactate	**259.5**	73.0	**229.4**	57.6	**303.6**	76.7	4.98E-09	Mc3 vs rest
L-Tyrosine	**407.5**	56.5	**352.8**	82.6	**405.9**	62.4	1.22E-04	Mc2 vs rest
Glycine	**187.0**	80.8	**152.3**	41.9	**195.7**	68.8	1.04E-04	Mc2 vs Mc3
Myoinositol	**163.7**	47.0	**217.7**	53.5	**196.1**	54.3	9.44E-07	all
Taurine	**332.2**	122.7	**330.2**	84.0	**369.3**	99.3	0.017	Mc1 vs Mc3
Scylloinositol	**55.0**	16.2	**94.7**	186.5	**62.5**	32.1	0.138	NS
Glycerophosphocholine	**210.0**	91.6	**107.9**	33.6	**151.2**	48.4	4.44E-12	all
Phosphocholine	**552.0**	131.1	**216.8**	66.8	**327.2**	69.9	9.59E-33	all
Choline	**135.2**	44.6	**120.3**	37.7	**132.9**	42.2	0.128	NS
Creatine	**149.9**	64.2	**93.2**	33.7	**136.0**	52.1	1.41E-09	Mc2 vs rest
Glutathione	**57.5**	13.8	**50.9**	13.9	**58.1**	14.5	0.011	Mc2 vs Mc3
Glutamine	**134.4**	41.3	**134.3**	30.2	**145.4**	43.6	0.223	NS
Succinate	**58.0**	15.7	**53.6**	10.6	**62.2**	15.7	0.003	Mc2 vs Mc3
Glutamate	**237.9**	61.3	**266.2**	63.3	**277.5**	61.2	1.95E-04	Mc1 vs rest
Acetate	**32.7**	9.0	**48.4**	17.2	**40.3**	13.1	7.89E-08	all
Alanine	**82.6**	36.6	**66.0**	24.9	**95.1**	33.8	6.56E-07	all

The values are calculated by integrated peak areas from normalized spectra to equal total areas. Kruskal- Wallis test was performed to compare metabolite levels between clusters and *P* values were adjusted for multiple testing by The Benjamini Hochberg false discovery rate.
NS: not significant (adjusted $p > 0.05$)

Table 3: Distribution of PAM50 and RPPA subtype among the metabolic clusters. Values in brackets are each subtype's percentage distribution within the metabolic clusters.

		Metabolic cluster		
PAM50 subtype	**Total**	**Mc1**	**Mc2**	**Mc3**
Luminal A	85	19 (35)	18 (43)	48 (46)
Luminal B	56	23 (42)	5 (12)	28 (27)
Basal	24	6 (11)	5 (12)	13 (13)
Her2-enriched	22	5 (9)	7 (17)	10 (10)
Normal-like	14	2 (4)	7 (17)	5 (5)
NA	*27*	*4*	*15*	*8*
Total	201	55	42	104
RPPA subtype				
Reactive I	43	4 (7)	24 (44)	15 (14)
Reactive II	36	3 (5)	8 (15)	25 (23)
Basal	47	16 (29)	8 (15)	23 (21)
Her2	18	5 (9)	4 (7)	9 (8)
Luminal	73	27 (49)	11 (20)	35 (33)
NA	*11*	*3*	*3*	*5*
Total	217	55	55	107

NA: not available

Figure legends

Figure 1: Metabolic subtyping of breast cancer tissue samples using HCA. **(A)** The HRMAS 1H MRS spectra for 228 samples was clustered using Euclidean distance and Wards linkage as similarity measure which separated the samples into three metabolic clusters (Mc); Mc1, Mc2 and Mc3. **(B)** Mean spectra for the three metabolic clusters. β-Glc; β-glucose, Asc; ascorbate, Lac; lactate, Tyr; tyrosine, Cr; creatine, mI; myoinositol, Gly; glycine, Tau; taurine, sI; scylloinositol, GPC; glycerophosphocholine, PCho; phosphocholine, Cho; choline, Gsh; glutathione, Gln; glutamine, Succ; succinate, Glu; glutamate, Ace; acetate, Ala; alanine. Grey bars indicate removed spectral regions (containing lipid peaks).

Figure 2: Results from PLS-DA of metabolic clusters. **(A)** Score plot of the two first latent variables explaining 42.2% of the X-variance and 28.2% of the Y-variance; **(B)** Regression vectors for the three metabolic clusters (Mc)

Figure 3: Main differences between metabolic subtypes (A) Metabolic cluster label from hierarchical clustering with Euclidean distance and Wards linkage of HR MAS MR spectra of samples. The samples clustered in three groups called Mc1, Mc2 and Mc3. **(B)** Fold change in expression levels of (1) scylloinositol, (2) GPC, (3) PCho, (4) creatine, (5) ascorbate, (6) taurine, (7) GSH, (8) tyrosine, (9) lactate, (10) glutamate, (11) succinate, (12) glutamine, (13) glycine, (14) alanine, (15) choline, (16) myoinositol, (17) acetate, (18) glucose. Blue regions in the heat map represent decreased levels while red levels represent increased metabolite levels. **(C)** PAM50-subtypes **(D)** RPPA-subtype **(E)** Gene expression levels (quantile normalized, log 2 transformed) for the 277 overlapping significant genes (SAM, adjusted $p < 0.01$) between Mc1 and Mc3. The genes have been clustered.

Figure 4: Illustration of metabolic pathways reported to have altered gene and metabolite expression by Integrated Pathway Analysis (MetaboAnalyst) (A) Result within 'Glycolysis/Glutaminolysis' genes and metabolites differently expressed in metabolic cluster (Mc) Mc2 compared to Mc1. Adapted from KEGG ID: hsa00010. LDHB: lactate dehydrogenase B;

ADH1A/ADH1B/ADH1C: Alcohol dehydrogenase 1A/ 1B/ 1C; ALDH1A3: Aldehyde dehydrogenase 1 family member A3; ALDH2: Aldehyde dehydrogenase 2 family; ACSS1: Acetate CoA ligase; TCA cycle: trucarboxylic acid cycle.

(B) Result within 'Glycerophospholipid metabolism' of genes and metabolites differently expressed in Mc1 compared to Mc2. Adapted from KEGG ID: hsa00564. CHKA: Choline kinase alpha; PCYT1A: Phosphate cytidyltransferase 1; CEPT1: Choline/ethanolamine phosphotransferase 1; PLA2G5: phospholipase A2; LCAT: Lecithin-cholesterol acyltransferase; LPCAT2: Lysophosphatidyl-choline acyltransferase; PC-PLD: Phospholipase D; Lyso-PLA1: Lysophospholipase I; GPC-PDE: Glycerophos-phocholine phosphodiesterase; PLC: Phospholipase C; PLD1: Phospholipidase D1; PPAP2A, PPAP2B: phosphatidate phosphatase LPIN; AGPAT4: 1-acylglycerol-3-phosphate O-acyltransferase.

Figure 1

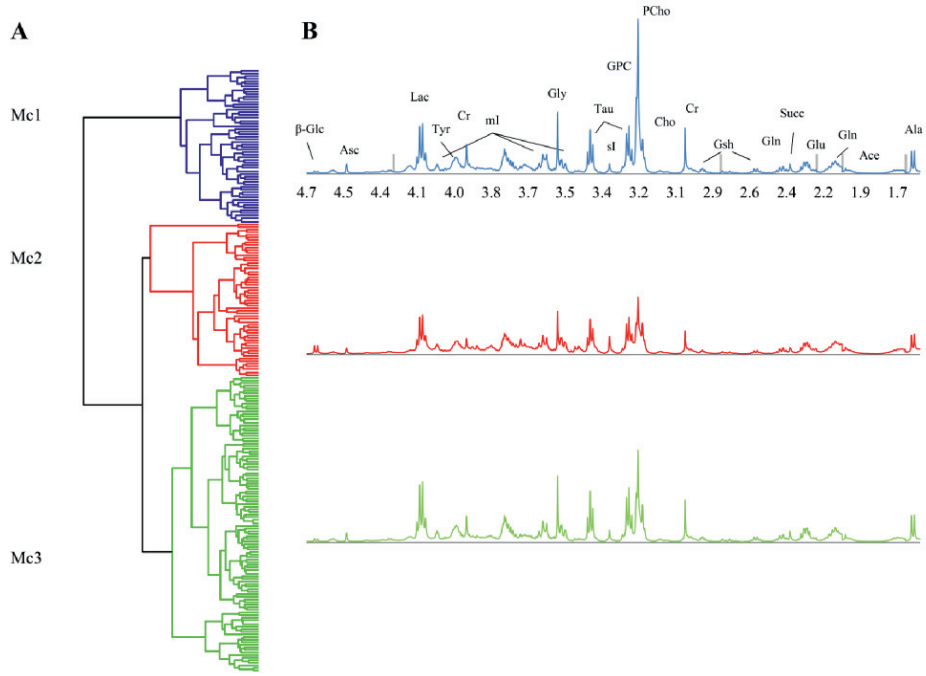
A
B
Mc1
Mc2
Mc3
β-Glc
Asc
Lac
Tyr
Cr
mI
Gly
Tau
sI
GPC
PCho
Cho
Cr
Gsh
Gln
Succ
Glu
Gln
Ace
Ala
4.7 4.5 4.4 4.1 4.0 3.8 3.7 3.5 3.4 3.2 3.1 2.9 2.6 2.4 2.2 1.9 1.7

Figure 2

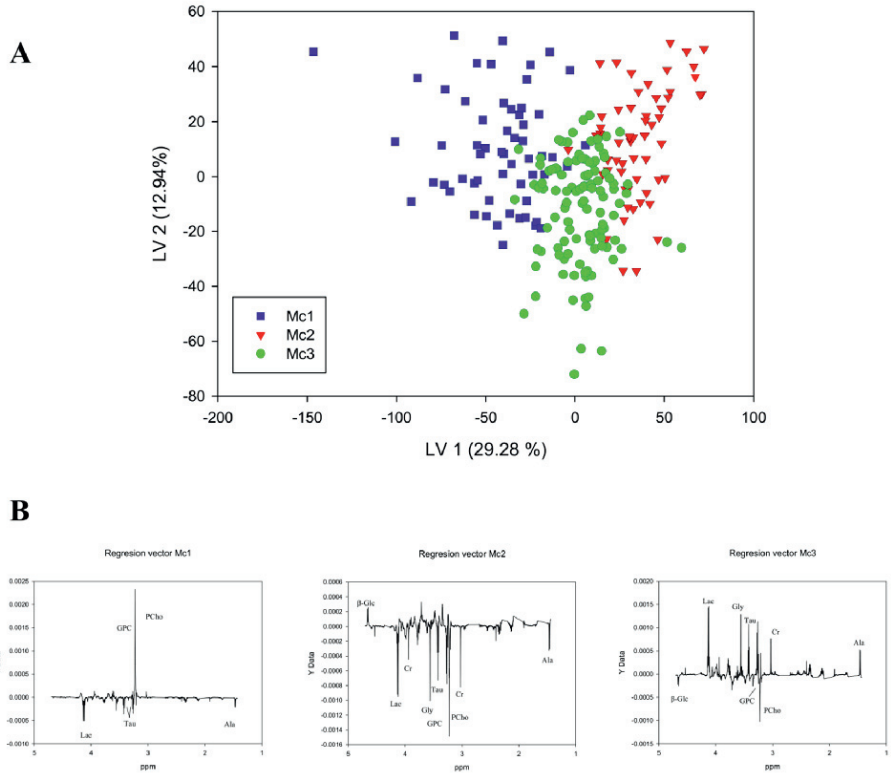
A
LV 2 (12.94%)
LV 1 (29.28 %)
Mc1
Mc2
Mc3
B
Regresion vector Mc1
Regresion vector Mc2
Regresion vector Mc3
Y Data
ppm
Lac
Tau
Ala
GPC
PCho
β-Glc
Cr
Gly

Figure 3

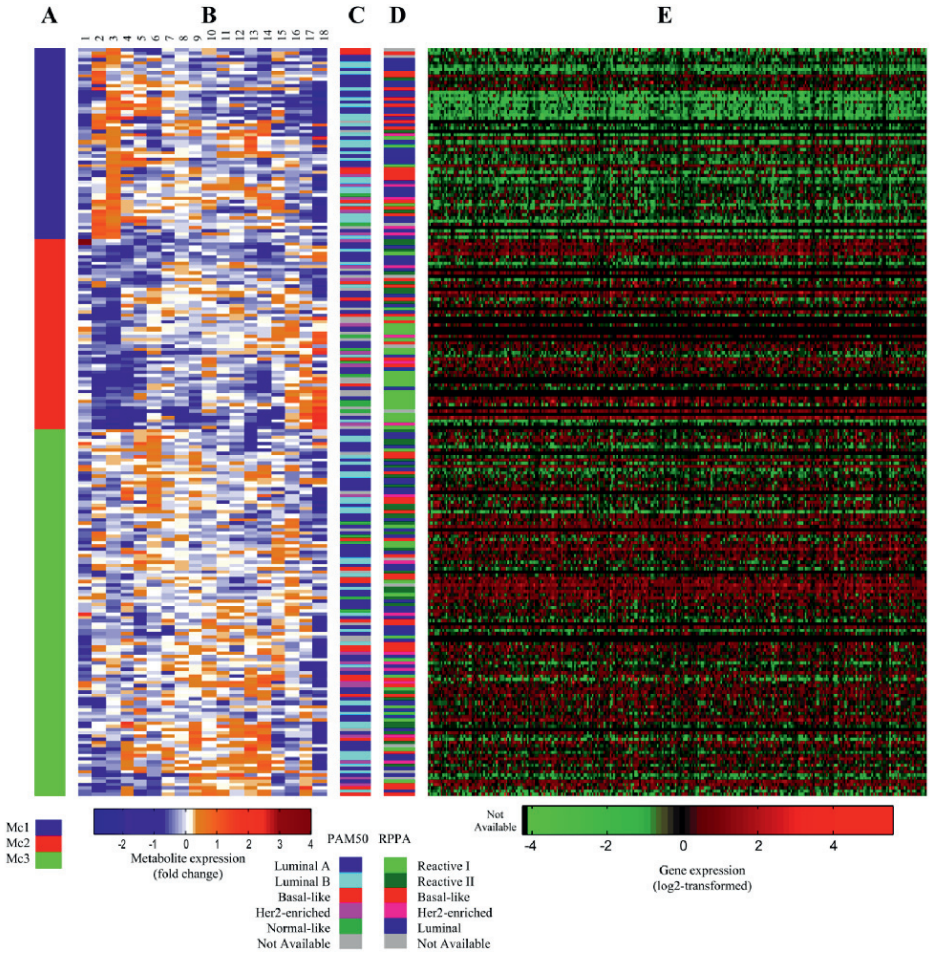
A
B
C
D
E
1 2 3 4 5 6 7 8 9 10 11 12 13 14 15 16 17 18
Mc1
Mc2
Mc3
-2 -1 0 1 2 3 4
Metabolite expression
(fold change)
PAM50
Luminal A
Luminal B
Basal-like
Her2-enriched
Normal-like
Not Available
RPPA
Reactive I
Reactive II
Basal-like
Her2-enriched
Luminal
Not Available
Not Available
-4 -2 0 2 4
Gene expression
(log2-transformed)

Figure 4

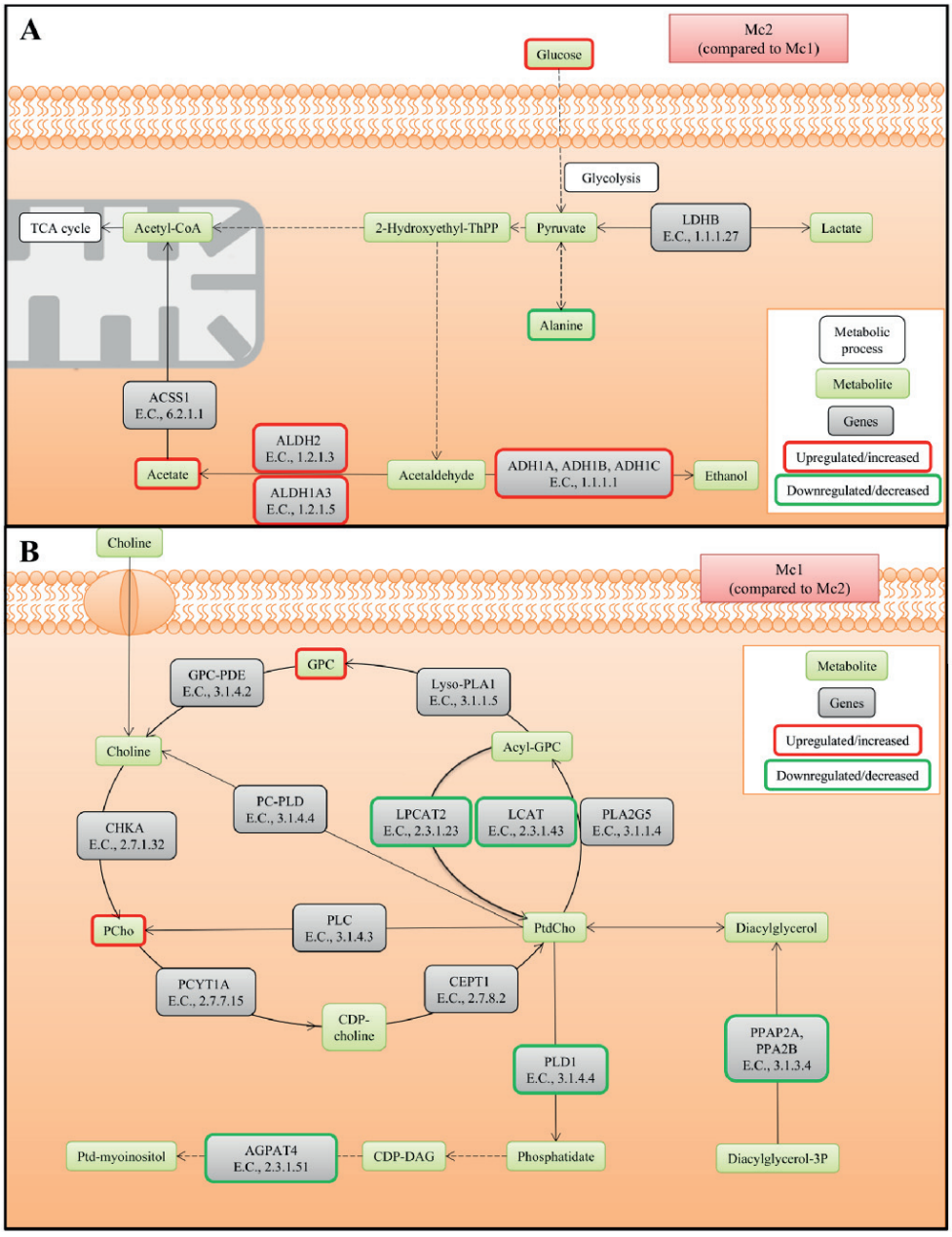
A
Mc2
(compared to Mc1)
Glucose
Glycolysis
TCA cycle
Acetyl-CoA
2-Hydroxyethyl-ThPP
Pyruvate
LDHB
E.C., 1.1.1.27
Lactate
Alanine
ACSS1
E.C., 6.2.1.1
ALDH2
E.C., 1.2.1.3
ALDH1A3
E.C., 1.2.1.5
Acetate
Acetaldehyde
ADH1A, ADH1B, ADH1C
E.C., 1.1.1.1
Ethanol
Metabolic process
Metabolite
Genes
Upregulated/increased
Downregulated/decreased
B
Choline
Mc1
(compared to Mc2)
GPC
GPC-PDE
E.C., 3.1.4.2
Lyso-PLA1
E.C., 3.1.1.5
Acyl-GPC
Choline
PC-PLD
E.C., 3.1.4.4
LPCAT2
E.C., 2.3.1.23
LCAT
E.C., 2.3.1.43
PLA2G5
E.C., 3.1.1.4
CHKA
E.C., 2.7.1.32
PCho
PLC
E.C., 3.1.4.3
PtdCho
Diacylglycerol
PCYT1A
E.C., 2.7.7.15
CDP-
choline
CEPT1
E.C., 2.7.8.2
PPAP2A,
PPA2B
E.C., 3.1.3.4
PLD1
E.C., 3.1.4.4
Ptd-myoinositol
AGPAT4
E.C., 2.3.1.51
CDP-DAG
Phosphatidate
Diacylglycerol-3P
Metabolite
Genes
Upregulated/increased
Downregulated/decreased

Additional Information to:

Metabolic clusters of breast cancer in relation to gene- and protein expression subtypes

Tonje H. Haukaas , Leslie R. Euceda, Guro F. Giskeødegård, Santosh Lamichhane, Marit Krohn, Sandra Jernström, Miriam R. Aure, Ole C. Lingjærde, Ellen Schlichting, Øystein Garred, Eldri U. Due, The Oslo Breast Cancer Consortium (OSBREAC), Gordon B. Mills, Kristine K. Sahlberg, Anne-Lise Børresen-Dale, Tone F. Bathen

Additional Authors

The Oslo Breast Cancer Research Consortium (OSBREAC)

Vessela N Kristensen[1,2,3], Torill Sauer[4,5], Elin Borgen[6], Olav Engebråten[7,8,9], Øystein Fodstad[7,9], Rolf Kåresen[9,10], Bjørn Naume[2,8], Gunhild Mari Mælandsmo[2,7,11], Hege G Russnes[1,2,12], Therese Sørlie[1,2], Helle Kristine Skjerven[13], Britt Fritzman[14]

[1]Department of Cancer Genetics, Institute for Cancer Research, Oslo University Hospital, Oslo, Norway. [2]K.G. Jebsen Centre for Breast Cancer Research, Institute for Clinical Medicine, University of Oslo, Oslo, Norway. [3]Department of Clinical Molecular Biology and Laboratory Science (EpiGen), Division of Medicine, Akershus University Hospital, Lørenskog, Norway. [4]Department of Pathology, Akershus University Hospital, Lørenskog, Norway. [5]Institute of Clinical Medicine, Faculty of Medicine, University of Oslo, Oslo, Norway. [6]Department of Pathology, Division of Diagnostics and Intervention, Oslo University Hospital, Oslo, Norway. [7]Department of Tumor Biology, Institute for Cancer Research, Oslo University Hospital, Oslo, Norway.[8]Department of Oncology, Division of Surgery and Cancer and Transplantation Medicine, Oslo University Hospital, Oslo, Norway.[9]Institute of Clinical Medicine,

Faculty of Medicine, University of Oslo, Oslo, Norway. [10]Department of Breast- and Endocrine Surgery, Division of Surgery, Cancer and Transplantation, Oslo University Hospital, Oslo, Norway.[11]Department of Pharmacy, Faculty of Health Sciences, University of Tromsø, Tromsø, Norway. [12]Department of Pathology, Oslo University Hospital, Oslo, Norway.[13]Breast and Endocrine Surgery, Department of Breast and Endocrine Surgery, Vestre Viken Hospital, Drammen, Norway.[14]Østfold Hospital, Østfold, Norway

Email: Vessela N Kristensen v.n.kristensen@medisin.uio.no – Torill Sauer Torill.sauer@medisin.uio.no – Elin Borgen ebg@ous-hf.no – Olav Engebråten Olav.engebraten@medisin.uio.no – Øystein Fodstad Oystein.Fodstad@rr-research.no – Rolf Kåresen rolf.karesen@medisin.uio.no – Bjørn Naume bjorn.naume@medisin.uio.no – Gunhild Mari Mælandsmo Gunhild.Mari.Malandsmo@rr-research.no – Hege G Russnes Hege.russnes@rr-research.no – Therese Sørlie therese.sorlie@rr-research.no – Helle Kristine Skjerven Helle.skjerven@vestreviken.no – Britt Fritzman Britt.Fritzman@so-hf.no

Additional Methods

HR MAS MRS acquisition and data processing. Before HR MAS MRS experiments, 3 µL cold sodium formate in D2O (24.29mM) was added to a leak-proof disposable 30µL insert (Bruker, Biospin GmbH, Germany) as a chemical shift reference. Tissue samples were cut to fit the insert on a dedicated work station designed to keep the samples frozen [1]. The insert containing the frozen sample was placed in a 4-mm diameter zirconium rotor (Bruker, Biospin GmbH, Germany) and kept at -20 ˚C for maximum 8 hours before the experiments. Samples were spun at 5000 Hz and experiments run at 5 ˚C. The samples were allowed 5 minutes temperature acclimatization before shimming and spectral acquisition. Spin-echo spectra were recorded using a Carr-Purcell-Meiboom-Gill (cpmg) pulse sequence (cpmgpr1d; Bruker) with 4s water suppression prior to a 90° excitation pulse. T2 filtering was obtained using a delay of 0.6 ms between each 180˚ pulse to suppress macromolecules and lipid signals and enhance signal from small molecules. This resulted in an effective TE of 77 ms. A total of 256 scans over a spectral region of 12 kHz was collected into 72k complex data points with an acquisition time of 3.07 s. The FIDs were multiplied by a 0.30 Hz exponential weighting function and Fourier transformed into 64k real points. Phase

correction was performed automatically for each spectrum using TopSpin 3.1 (Bruker). Further preprocessing of the HR MAS spectra were performed in Matlab R2013b (The Mathworks, Inc., USA). Chemical shifts were referenced to the creatine peak at 3.92 ppm. Baseline correction was performed using asymmetric least squares [2] with parameters λ = 1e7 and p = 0.0001, and baseline offset was adjusted by setting the minimum value of each spectrum to zero by subtracting the lowest value. Peak alignment was performed using icoshift [3].

Reverse Phase Protein Array (RPPA). Tumor tissue was lysed by homogenization in lysis buffer containing proteinase inhibitors and phosphatase inhibitors. The tumor lysates were diluted in 1.33 mg/ml concentration as assessed by bicinchonic acid assay (BCA) and boiled in 1% SDS and 2-mercaptoethanol. Supernatants were manually diluted in five serial 2-fold dilutions with lysis buffer. The samples were spotted onto and immobilized on nitrocellulose-coated FAST slides. The slides were probed with 151 primary antibodies (Supplementary Table 1) in appropriate dilutions. The signal intensity was captured by a biotin conjugated secondary antibody and was amplified by Dako Cytomation-catalysed system (Dako, Glostrup, Denmark). Slides were scanned, analyzed and quantitated using MicroVigene software (VigeneTech Inc., Carlise, MA, USA) to generate spot signal intensities. These were then processed by the R package SuperCurve /version 1.01. The protein concentrations were derived from the supercurve for each sample by curve fitting, log2-transformed, and the relative concentrations were normalized by median centering of the samples for each of the antibodies [4].

Statistical analysis. PLS-DA was performed on mean centered spectra using double cross validation [5]. The model was built on randomly chosen training samples (80 % of the spectra) and used to predict the class of the remaining independent test samples (20 % of the spectra). This was repeated 20 times before average classification results were calculated. To validate that the result is not achieved simply by random predictions, permutation testing was performed. Here Y-data (class labels for the samples) are permutated to resemble random classification. For each permutation 20 random training and test sets are chosen as described for the PLS-DA model. This was repeated 1000 times before the error distribution was

compared with the classification error for the original data. P values ≤ 0.01 were considered significant. PCA and PLS-DA were performed in Matlab using PLS_Toolbox 7.5.2 (Eigenvector Research, Inc., Wenatchee, USA).

Additional References

1. Giskeødegård, G.F., M.D. Cao, and T.F. Bathen, *High-Resolution Magic-Angle-Spinning NMR Spectroscopy of Intact Tissue*, in *Metabonomics: Methods and Protocols*, J.T. Bjerrum, Editor 2015, Springer New York. p. 37-50.
2. Eilers, P.H., *Parametric time warping.* Anal Chem, 2004. **76**(2): p. 404-411.
3. Savorani, F., G. Tomasi, and S.B. Engelsen, *icoshift: A versatile tool for the rapid alignment of 1D NMR spectra.* J Magn Reson, 2010. **202**(2): p. 190-202.
4. Aure, M.R., et al., *Integrated analysis reveals microRNA networks coordinately expressed with key proteins in breast cancer.* Genome Med, 2015. **7**(1).
5. Smilde, A.K., et al., *Data processing in metabolomics*, in *Metabolomics in practice: successful strategies to generate and analyze metabolic data*, M. Lämmerhofer and W. Weckwerth, Editors. 2013, John Wiley & Sons.

Additional Table Legends:

Add. Table 1: Antibodies used for reverse phase protein array (RPPA)

Add. Table 2: Significantly different expressed genes between the three metabolic clusters

Add. Table 3: Significantly different expressed genes between the metabolic clusters Mc1 and Mc2

Add. Table 4: Significantly different expressed genes between the metabolic clusters Mc1 and Mc3

Add. Table 5: Statistically over-represented annotation terms, according to DAVID, of differently expressed genes between metabolic cluster Mc1 and Mc2

Add. Table 6: Statistically over-represented annotation terms, according to DAVID, of differently expressed genes between metabolic cluster Mc1 and Mc3

Add. Table 7: Gene set enrichment analysis (GSEA) result for Gene Ontology (GO) gene sets. Metabolic cluster Mc1 was compared with Mc2 and Mc3.

Add. Table 8: Gene set enrichment analysis (GSEA) result for Gene Ontology (GO) gene sets. Metabolic cluster Mc1 was compared with Mc2.

Add. Table 9: Gene set enrichment analysis (GSEA) result for Gene Ontology (GO) gene sets. Metabolic cluster Mc3 was compared with Mc1 and Mc2.

Add. Table 10: Integrated pathway analysis result from comparison of the metabolic clusters Mc1 compared to Mc2

Add. Table 11: Integrated pathway analysis result from comparison of the metabolic clusters Mc1 compared to Mc3

Add. Table 1: Antibodies used for reverse phase protein array (RPPA)

RPPA Antibody	Company	Catalog #	Dilution used	Validation status	Species
14-3-3_epsilon	Santa Cruz	sc-2395	250	C- use with caution	Mouse
4E-BP1	CST	9452	100	V - validated	Rabbit
4E-BP1_pS65	CST	9456	250	V - validated	Rabbit
53BP1	CST	4937	400	C- use with caution	Rabbit
A-Raf_pS299	CST	4431	100	NA	Rabbit
ACC_pS79	CST	3661	200	V - validated	Rabbit
ACC1	Epitomics	1768-1	300	C- use with caution	Rabbit
AIB1	BD	611105	100	V - validated	Mouse
Akt	CST	9272	250	V - validated	Rabbit
Akt_pS473	CST	9271	100	V - validated	Rabbit
Akt_pT308	CST	9275	50	V - validated	Rabbit
alpha-Catenin	Calbiochem	CA1030	750	V - validated	Mouse
AMPK_alpha	CST	2532	200	C- use with caution	Rabbit
AMPK_pT172	CST	2535	100	V - validated	Rabbit
Annexin_I	Invitrogen	71-3400	90000	V - validated	Rabbit
AR	Epitomics	1852-1	50	V - validated	Rabbit
B-Raf	Santa Cruz	sc-5284	500	NA	Mouse
Bak	Epitomics	1542-1	50	C- use with caution	Rabbit
Bax	CST	2772	300	V - validated	Rabbit
Bcl-2	Dako	M0887	50	V - validated	Mouse
Bcl-X	Epitomics	1018-1	100	C- use with caution	Rabbit
Bcl-xL	CST	2762	50	V - validated	Rabbit
Beclin	Santa Cruz	sc-10086	200	V - validated	Goat
beta-Catenin	CST	9562	800	V - validated	Rabbit
Bid	Epitomics	1008-1	50	C- use with caution	Rabbit
Bim	Epitomics	1036-1	50	V - validated	Rabbit
c-Jun_pS73	CST	9164	50	C- use with caution	Rabbit
c-Kit	Epitomics	1522	50	V - validated	Rabbit
c-Met	CST	3127	500	C- use with caution	Mouse
c-Met_pY1235	CST	3129	500	C- use with caution	Rabbit
c-Myc	CST	9402	200	C- use with caution	Rabbit
C-Raf	Millipore	05-739	1000	V - validated	Rabbit
C-Raf_pS338	CST	9427	300	C- use with caution	Rabbit
Caspase-3_active	Epitomics	1476-1	200	C- use with caution	Rabbit
Caspase-7_cleavedD198	CST	9491	50	C- use with caution	Rabbit
Caspase-8	CST	9746	250	C- use with caution	Mouse
Caspase-9_cleavedD330	CST	9501	250	C- use with caution	Rabbit
Caveolin-1	CST	3238	500	V - validated	Rabbit
CD31	Dako	M0823	50	V - validated	Mouse
CDK1	CST	9112	250	V - validated	Rabbit
Chk1	CST	2345	100	C- use with caution	Rabbit
Chk1_pS345	CST	2348	50	C- use with caution	Rabbit
Chk2	CST	3440	300	C- use with caution	Mouse
Chk2_pT68	CST	2197	150	C- use with caution	Rabbit
cIAP	Millipore	07-759	250	V - validated	Rabbit
Claudin-7	Novus	NB100-91714	1000	V - validated	Rabbit
Collagen_VI	Santa Cruz	sc-20649	250	V - validated	Rabbit
COX-2	Epitomics	2169-1	150	C- use with caution	Rabbit
Cyclin_B1	Epitomics	1495-1	500	V - validated	Rabbit
Cyclin_D1	Santa Cruz	sc-718	150	V - validated	Rabbit
Cyclin_E1	Santa Cruz	sc-247	150	V - validated	Mouse
DJ-1	Abcam	ab76008	10000	C- use with caution	Rabbit
Dvl3	CST	3218	1000	V - validated	Rabbit
E-Cadherin	CST	4065	750	V - validated	Rabbit
eEF2	CST	2332	100	V - validated	Rabbit
eEF2K	CST	3692	250	V - validated	Rabbit
EGFR	Santa Cruz	sc-03	350	C- use with caution	Rabbit
EGFR_pY1068	CST	2234	50	V - validated	Rabbit
EGFR_pY1173	Epitomics	1124	50	C- use with caution	Rabbit
EGFR_pY992	CST	2235	50	V - validated	Rabbit
eIF4E	CST	9742	250	V - validated	Rabbit
ER-alpha	Lab Vision	RM-9101-S	200	V - validated	Rabbit
ER-alpha_pS118	Epitomics	1091-1	150	V - validated	Rabbit
ERCC1	Lab Vision	MS-671-PO	100	C- use with caution	Mouse
FAK	Epitomics	1700-1	75	C- use with caution	Rabbit
Fibronectin	Epitomics	1574-1	5000	C- use with caution	Rabbit
FOXO3a	CST	9467	50	C- use with caution	Rabbit
FOXO3a_pS318_S321	CST	9465	75	C- use with caution	Rabbit
GAB2	CST	3239	250	V - validated	Rabbit
GATA3	BD	558686	100	V - validated	Mouse
GSK3_pS9	CST	9336	250	V - validated	Rabbit
GSK3-alpha-beta	Santa Cruz	sc-7291	2000	V - validated	Mouse
GSK3-alpha-beta_pS21_S9	CST	9331	250	V - validated	Rabbit
HER2	Lab Vision	MS-325-P1	250	V - validated	Mouse
HER2_pY1248	R&D	AF1768	350	NA	Rabbit

RPPA Antibody	Company	Catalog #	Dilution used	Validation status	Species
HER3	Santa Cruz	sc-285	250	V - validated	Rabbit
HER3_pY1298	CST	4791	250	C- use with caution	Rabbit
IGF-1R-beta	CST	3027	250	C- use with caution	Rabbit
IGFBP2	CST	3922	50	V - validated	Rabbit
INPP4B	Santa Cruz	sc-12318	250	C- use with caution	Goat
IRS1	Millipore	06-248	2000	V - validated	Rabbit
JNK2	CST	4672	50	C- use with caution	Rabbit
K-Ras	Santa Cruz	sc-30	75	C- use with caution	Mouse
MAPK_pT202_Y204	CST	4377	100	V - validated	Rabbit
MEK1	Epitomics	1235-1	5000	V - validated	Rabbit
MEK1_pS217_S221	CST	9121	500	V - validated	Rabbit
MIG-6	Sigma	WH0054206M1	100	V - validated	Mouse
Mre11	CST	4847	250	C- use with caution	Rabbit
MSH2	CST	2850	50	C- use with caution	Mouse
MSH6	SDI	2203.00.02	1000	C- use with caution	Rabbit
N-Cadherin	CST	4061	50	V - validated	Rabbit
NF-kB-p65_pS536	CST	3033	100	C- use with caution	Rabbit
NF2	SDI	2271.00.02	500	C- use with caution	Rabbit
Notch1	CST	3268	50	V - validated	Rabbit
Notch3	Santa Cruz	sc-5593	600	C- use with caution	Rabbit
P-Cadherin	CST	2130	50	C- use with caution	Rabbit
p21	Santa Cruz	sc-397	100	C- use with caution	Rabbit
p27	Epitomics	1591-1	50	V - validated	Rabbit
p27_pT157	R&D	AF1555	500	C- use with caution	Rabbit
p27_pT198	Abcam	ab64949	75	V - validated	Rabbit
p38_MAPK	CST	9212	100	C- use with caution	Rabbit
p38_pT180_Y182	CST	9211	50	V - validated	Rabbit
p53	CST	9282	2500	V - validated	Rabbit
p70S6K	Epitomics	1494-1	750	V - validated	Rabbit
p70S6K_pT389	CST	9205	50	V - validated	Rabbit
p90RSK_pT359_S363	CST	9344	50	C- use with caution	Rabbit
PARP_cleaved	CST	9546	50	C- use with caution	Mouse
Paxillin	Epitomics	1500-1	500	V - validated	Rabbit
PCNA	Abcam	ab29	500	V - validated	Mouse
PDK1_pS241	CST	3061	500	V - validated	Rabbit
PI3K-p110-alpha	CST	4255	150	C- use with caution	Rabbit
PI3K-p85	Millipore	06-195	10000	V - validated	Rabbit
PKC-alpha	Millipore	05-154	1000	V - validated	Mouse
PKC-alpha_pS657	Millipore	06-822	750	V - validated	Rabbit
PR	Epitomics	1483-1	200	V - validated	Rabbit
PRAS40_pT246	Biosource	441100G	1000	V - validated	Rabbit
PTCH	SDI	2113.00.02	1000	C- use with caution	Rabbit
PTEN	CST	9552	750	V - validated	Rabbit
Rab11	CST	3539	250	V - validated	Rabbit
Rab25	Covance	Custom	2500	C- use with caution	Rabbit
Rad50	Millipore	05-525	100	C- use with caution	Mouse
Rad51	Chem Biotech	na 71	125	C- use with caution	Mouse
Rb	CST	9309	200	V - validated	Mouse
Rb_pS807_S811	CST	9308	250	V - validated	Rabbit
S6_pS235_S236	CST	2211	3000	V - validated	Rabbit
S6_pS240_S244	CST	2215	2000	V - validated	Rabbit
Shc_pY317	CST	2431	50	NA	Rabbit
Smac	CST	2954	250	V - validated	Mouse
Smad1	Epitomics	1649-1	250	V - validated	Rabbit
Smad3	Epitomics	1735-1	750	V - validated	Rabbit
Smad4	Santa Cruz	sc-7866	50	V - validated	Mouse
Snail	CST	3895	100	C- use with caution	Mouse
Src	Millipore	05-184	200	V - validated	Mouse
Src_pY416	CST	2101	125	C- use with caution	Rabbit
Src_pY527	CST	2105	250	V - validated	Rabbit
STAT3_pY705	CST	9131	50	V - validated	Rabbit
STAT5-alpha	Epitomics	1289-1	250	V - validated	Rabbit
Stathmin	Epitomics	1972-1	150	V - validated	Rabbit
Syk	Santa Cruz	sc-1240	250	V - validated	Mouse
Tau	Millipore	05-348	100	C- use with caution	Mouse
TAZ_pS89	Santa Cruz	sc-17610	75	C- use with caution	Rabbit
Tuberin	Epitomics	1613-1	500	C- use with caution	Rabbit
VASP	CST	3112	50	C- use with caution	Rabbit
VEGFR2	CST	2479	5000	V - validated	Rabbit
XIAP	CST	2042	50	C- use with caution	Rabbit
XRCC1	CST	2735	50	C- use with caution	Rabbit
YAP	Santa Cruz	sc-15407	300	V - validated	Rabbit
YAP_pS127	CST	4911	350	C- use with caution	Rabbit
YB-1	SDI	1725.00.02	200	V - validated	Rabbit
YB-1_pS102	CST	2900	150	V - validated	Rabbit

Add. Table 2: Significantly different expressed genes between the three metabolic clusters

Gene ID	Gene Name	Score (d)	Numerator (r)	Denominator (s+s0)	contrast 1	contrast 2	contrast 3	adjusted *P* value (%)	Direction
CALD1	2825	0.8	0.138	0.173	-3.427	1.454	1.225	0	Up
TAGLN	18949	0.774	0.168	0.218	-3.239	1.689	1.031	0	Up
FERMT2	6321	0.772	0.1	0.13	-3.384	1.624	1.134	0	Up
NNMT	13555	0.764	0.163	0.214	-3.207	0.811	1.369	0	Up
CTGF	4323	0.749	0.168	0.224	-3.148	1.414	1.094	0	Up
GPX8	7474	0.74	0.138	0.186	-3.146	0.877	1.309	0	Up
MRC2	12641	0.74	0.146	0.198	-3.081	0.466	1.441	0	Up
RUNX2	17000	0.739	0.086	0.116	-2.988	-0.457	1.765	0	Up
CLMP	3830	0.737	0.136	0.184	-3.137	0.946	1.277	0	Up
DPYSL3	5150	0.737	0.16	0.217	-3.108	1.192	1.162	0	Up
GEM	7035	0.735	0.146	0.199	-3.047	1.907	0.841	0	Up
COL18A1	3970	0.729	0.128	0.175	-3.082	0.576	1.397	0	Up
TSHZ3	20086	0.715	0.118	0.165	-3.019	0.472	1.406	0	Up
NEXN	13395	0.712	0.098	0.137	-3.114	1.352	1.101	0	Up
PTRF	15990	0.712	0.078	0.109	-3.201	1.178	1.217	0	Up
MSRB3	12776	0.705	0.141	0.2	-2.98	1.426	1	0	Up
CYR61	4528	0.701	0.164	0.234	-2.891	1.727	0.831	0	Up
PLS3	15215	0.7	0.136	0.195	-2.866	1.989	0.712	0	Up
ACTA2	202	0.699	0.163	0.233	-2.862	1.832	0.774	0	Up
TIMP2	19344	0.698	0.141	0.202	-2.948	0.796	1.238	0	Up
SRPX2	18547	0.698	0.142	0.203	-2.897	0.414	1.365	0	Up
GFPT2	7054	0.697	0.123	0.177	-2.877	0.188	1.446	0	Up
CNN2	3901	0.691	0.141	0.204	-2.92	1.308	1.016	0	Up
TCF4	19112	0.689	0.108	0.157	-2.975	1.219	1.081	0	Up
VCAN	20645	0.686	0.157	0.229	-2.846	0.518	1.296	0	Up
TGFB1I1	19244	0.684	0.104	0.152	-2.958	1.35	1.019	0	Up
FAP	6172	0.684	0.161	0.236	-2.795	0.311	1.353	0	Up
LMOD1	9739	0.68	0.075	0.111	-3	1.753	0.879	0	Up
FBLN2	6199	0.678	0.163	0.241	-2.843	1.027	1.089	0	Up
LOXL2	11683	0.677	0.138	0.204	-2.746	0.096	1.413	0	Up
LIMS2	9684	0.676	0.093	0.138	-2.851	1.956	0.718	0	Up
COL3A1	3983	0.675	0.18	0.266	-2.742	0.3	1.329	0	Up
S100A10	17025	0.674	0.117	0.173	-2.872	1.458	0.93	0	Up
DACT3	4555	0.674	0.139	0.206	-2.852	1.184	1.03	0	Up
GSN	7558	0.673	0.104	0.155	-2.808	1.934	0.704	0	Up
NID1	13456	0.672	0.129	0.192	-2.847	0.754	1.201	0	Up
ANGPTL2	633	0.671	0.134	0.199	-2.799	0.461	1.294	0	Up
SLIT3	18036	0.666	0.142	0.213	-2.8	0.736	1.183	0	Up
PDLIM4	14775	0.666	0.087	0.13	-2.831	1.921	0.721	0	Up
ISM1	8696	0.666	0.152	0.228	-2.763	1.56	0.831	0	Up
FSTL1	6776	0.662	0.143	0.217	-2.789	0.862	1.127	0	Up
SNAI2	18133	0.662	0.096	0.145	-2.879	0.945	1.141	0	Up
MIR100HG	12463	0.661	0.13	0.197	-2.804	1.207	0.995	0	Up
PDGFRB	14755	0.66	0.115	0.174	-2.782	0.46	1.285	0	Up
MRVI1	12739	0.659	0.114	0.173	-2.806	1.449	0.899	0	Up
LOX	11680	0.658	0.141	0.214	-2.678	0.176	1.345	0	Up
PLK3	15203	0.656	0.085	0.129	-2.877	1.408	0.952	0	Up
TPM4	19855	0.656	0.101	0.153	-2.787	0.43	1.301	0	Up
SPARC	18362	0.652	0.155	0.238	-2.665	0.3	1.288	0	Up
C5orf62	2509	0.648	0.12	0.185	-2.742	1.445	0.867	0	Up
PODN	15296	0.648	0.099	0.153	-2.807	1.128	1.029	0	Up
SKAP2	17634	0.648	0.095	0.147	-2.714	1.876	0.677	0	Up
RARRES2	16240	0.646	0.152	0.236	-2.698	1.339	0.886	0	Up
GLT8D2	7182	0.646	0.079	0.123	-2.809	0.442	1.307	0	Up
SHOX2	17566	0.644	0.092	0.143	-2.807	0.931	1.109	0	Up
EMILIN1	5520	0.644	0.108	0.168	-2.719	0.45	1.256	0	Up
PODNL1	15297	0.644	0.098	0.152	-2.79	1.059	1.048	0	Up
MGC24103	12397	0.643	0.142	0.22	-2.654	0.376	1.252	0	Up
EGR1	5396	0.64	0.177	0.276	-2.557	1.817	0.618	0	Up
ANXA1	754	0.639	0.129	0.203	-2.627	1.735	0.688	0	Up
TMEM200A	19554	0.638	0.086	0.135	-2.793	0.878	1.123	0	Up
MXRA5	12901	0.637	0.092	0.145	-2.737	0.52	1.237	0	Up
DKK3	4932	0.636	0.1	0.158	-2.746	1.188	0.972	0	Up
SERPINF1	17400	0.635	0.129	0.203	-2.692	1.101	0.979	0	Up
PDLIM7	14777	0.635	0.092	0.145	-2.763	1.15	0.997	0	Up
GPR124	7367	0.635	0.104	0.163	-2.735	0.947	1.064	0	Up
RNF144A	16653	0.634	0.089	0.14	-2.705	0.352	1.288	0	Up
PRKCDBP	15652	0.631	0.11	0.175	-2.701	1.204	0.942	0	Up
COL5A1	3991	0.63	0.102	0.162	-2.595	0.076	1.342	0	Up
CNN1	3900	0.629	0.185	0.295	-2.424	2.015	0.468	0	Up
VIM	20673	0.629	0.099	0.157	-2.711	0.82	1.102	0	Up
ZEB1	21166	0.628	0.107	0.171	-2.675	0.629	1.161	0	Up
HTRA3	8272	0.628	0.119	0.189	-2.43	-0.352	1.427	0	Up
IGFBP3	8405	0.628	0.115	0.184	-2.676	0.879	1.06	0	Up
POSTN	15383	0.627	0.179	0.285	-2.532	0.246	1.239	0	Up
ITPRIP	8761	0.627	0.094	0.151	-2.719	0.975	1.044	0	Up
NDN	13282	0.626	0.111	0.177	-2.63	1.566	0.759	0	Up
MYL9	12956	0.624	0.125	0.201	-2.618	1.423	0.81	0	Up
NOX4	13603	0.624	0.093	0.149	-2.514	-0.195	1.408	0	Up
COL1A2	3973	0.623	0.17	0.273	-2.522	0.25	1.233	0	Up
HTRA1	8270	0.623	0.156	0.251	-2.577	0.524	1.151	0	Up
SCG5	17165	0.623	0.11	0.177	-2.643	0.597	1.157	0	Up
PALLD	14490	0.623	0.078	0.126	-2.732	0.661	1.178	0	Up
COL5A2	3992	0.621	0.167	0.269	-2.453	-0.024	1.307	0	Up
LTBP2	11867	0.621	0.093	0.15	-2.691	1.199	0.939	0	Up
DSE	5180	0.62	0.088	0.142	-2.657	0.425	1.234	0	Up
DZIP1L	5277	0.618	0.071	0.115	-2.708	0.406	1.268	0	Up
FEZ1	6326	0.618	0.075	0.121	-2.688	1.629	0.764	0	Up
ARHGAP28	926	0.616	0.082	0.133	-2.665	0.486	1.213	0	Up
TUBB6	20251	0.615	0.122	0.198	-2.613	0.979	0.986	0	Up
TRPC1	20038	0.613	0.09	0.147	-2.659	0.822	1.074	0	Up
SERPING1	17402	0.611	0.08	0.131	-2.669	1.367	0.859	0	Up
C1S	2133	0.611	0.118	0.193	-2.595	1.088	0.933	0	Up
THY1	19311	0.61	0.121	0.198	-2.477	0.081	1.277	0	Up
CHADL	3589	0.609	0.127	0.209	2.555	-1.338	-0.811	0	Up
RHOJ	16542	0.609	0.092	0.152	-2.578	1.622	0.709	0	Up
FOXO1	6712	0.609	0.077	0.127	-2.47	2.137	0.443	0	Up
TNS1	19782	0.609	0.074	0.122	-2.69	1.263	0.912	0	Up
DACT1	4553	0.608	0.126	0.208	-2.559	0.64	1.095	0	Up
GAS1	6942	0.608	0.13	0.215	-2.554	1.265	0.84	0	Up
AEBP1	364	0.608	0.154	0.254	-2.502	0.431	1.149	0	Up
DCN	4634	0.606	0.157	0.26	-2.53	0.849	0.995	0	Up
TNFAIP6	19715	0.606	0.13	0.214	-2.484	0.235	1.219	0	Up
GADD45B	6883	0.605	0.099	0.163	-2.597	1.238	0.873	0	Up
AKAP12	465	0.605	0.104	0.172	-2.435	1.928	0.509	0	Up

Gene ID	Gene Name	Score (d)	Numerator (r)	Denominator (s+s0)	contrast 1	contrast 2	contrast 3	adjusted *P* value (%)	Direction
LAMA4	9489	0.605	0.078	0.129	-2.628	0.497	1.189	0	Up
PRICKLE1	15627	0.604	0.137	0.226	-2.538	1.167	0.871	0	Up
MYLK	12958	0.604	0.138	0.229	-2.473	1.599	0.662	0	Up
PCSK5	14697	0.604	0.054	0.089	-2.788	0.801	1.151	0	Up
COL1A1	3972	0.604	0.165	0.273	-2.415	0.113	1.231	0	Up
TPM2	19853	0.602	0.109	0.181	-2.573	0.928	0.986	0	Up
EGR2	5397	0.602	0.127	0.21	-2.449	1.711	0.604	0	Up
BGN	1500	0.601	0.103	0.172	-2.562	0.633	1.099	0	Up
FBN1	6202	0.601	0.108	0.179	-2.44	0.01	1.286	0	Up
BHLHE41	1507	0.6	0.133	0.222	-2.455	1.614	0.647	0	Up
CDH11	3348	0.6	0.089	0.148	-2.533	0.262	1.234	0	Up
UHMK1	20465	0.599	0.061	0.102	2.512	-2.131	-0.468	0	Up
INHBA	8573	0.599	0.148	0.246	-2.303	-0.261	1.324	0	Up
CFH	3562	0.598	0.101	0.17	-2.565	1.098	0.913	0	Up
FIBIN	6389	0.598	0.12	0.2	-2.536	0.914	0.972	0	Up
GRASP	7484	0.597	0.094	0.157	-2.527	1.556	0.708	0	Up
KCNMB4	8924	0.597	0.122	0.205	-2.496	0.478	1.127	0	Up
ANTXR1	750	0.597	0.108	0.181	-2.537	0.663	1.074	0	Up
ISLR	8694	0.596	0.133	0.223	-2.506	0.765	1.016	0	Up
SRPX	18546	0.596	0.123	0.206	-2.52	0.847	0.991	0	Up
MMP19	12536	0.594	0.062	0.104	-2.687	0.932	1.045	0	Up
SEMA5A	17317	0.593	0.115	0.194	-2.511	1.193	0.846	0	Up
PPIC	15449	0.593	0.098	0.166	-2.527	0.556	1.112	0	Up
C1R	2131	0.592	0.114	0.192	-2.516	1.092	0.89	0	Up
PRRX1	15774	0.592	0.121	0.204	-2.445	0.285	1.178	0	Up
ARL4C	996	0.592	0.106	0.179	-2.462	1.594	0.658	0	Up
RPRD2	16856	0.591	0.05	0.085	2.704	-1.656	-0.761	0	Up
DLC1	4936	0.59	0.059	0.1	-2.664	1.387	0.849	0	Up
MMP2	12537	0.589	0.126	0.213	-2.49	0.915	0.947	0	Up
THBS2	19280	0.588	0.146	0.248	-2.399	0.274	1.158	0	Up
NAP1L3	13066	0.588	0.074	0.127	-2.447	1.901	0.526	0	Up
FBLN5	6200	0.586	0.12	0.205	-2.45	1.386	0.736	0	Up
PPAPDC3	15424	0.586	0.06	0.102	-2.609	0.418	1.211	0	Up
CCDC8	3099	0.585	0.114	0.194	-2.387	1.693	0.579	0	Up
TEAD1	19159	0.585	0.072	0.123	-2.294	-0.496	1.414	0	Up
PDGFRA	14754	0.582	0.128	0.219	-2.453	0.919	0.926	0	Up
MEG3	12275	0.581	0.083	0.143	-2.516	0.611	1.084	0	Up
COL6A3	3996	0.581	0.103	0.178	-2.283	-0.253	1.31	0	Up
RBMS1	16338	0.581	0.088	0.152	-2.516	0.868	0.98	0	Up
CXorf57	4437	0.58	0.09	0.154	-1.891	2.587	-0.045	0	Up
SFRP2	17448	0.58	0.164	0.283	-2.412	0.85	0.932	0	Up
MARVELD1	12120	0.58	0.103	0.179	-2.362	0.038	1.234	0	Up
EMP1	5529	0.579	0.105	0.182	-2.25	2.007	0.379	0	Up
CYS1	4529	0.578	0.118	0.204	-2.414	0.447	1.096	0	Up
LHFP	9642	0.577	0.112	0.194	-2.431	1.293	0.764	0	Up
ADAMTS6	284	0.577	0.055	0.095	-2.571	0.27	1.251	0	Up
MMP14	12532	0.577	0.125	0.216	-2.36	0.218	1.16	0	Up
PTPN21	15959	0.576	0.098	0.171	-2.366	1.706	0.562	0	Up
PDLIM3	14774	0.576	0.103	0.179	-2.317	1.817	0.492	0	Up
EHD2	5403	0.575	0.087	0.151	-2.486	1.178	0.839	0	Up
PRKD1	15660	0.575	0.073	0.127	-2.467	1.61	0.655	0	Up
RPUSD1	16914	0.575	0.065	0.113	2.397	-1.956	-0.478	0	Up
CAV2	2944	0.575	0.064	0.111	-2.24	2.289	0.26	0	Up
SPON1	18456	0.574	0.165	0.287	-2.382	0.714	0.971	0	Up
MXRA8	12903	0.574	0.121	0.211	-2.402	0.517	1.061	0	Up
APCDD1	809	0.573	0.125	0.218	-2.314	1.67	0.549	0	Up
CYTH3	4535	0.572	0.098	0.171	-2.45	1.117	0.845	0	Up
COL6A1	3994	0.572	0.13	0.228	-2.271	-0.048	1.22	0	Up
EVC2	5727	0.571	0.045	0.078	-2.686	0.6	1.178	0	Up
FN1	6649	0.571	0.157	0.276	-2.064	-0.558	1.317	0	Up
C9orf125	2684	0.571	0.081	0.143	-2.449	1.422	0.721	0	Up
AGPAT4	404	0.57	0.065	0.113	-2.542	0.752	1.04	0	Up
FGF1	6341	0.568	0.043	0.075	-2.691	0.561	1.196	0	Up
PROS1	15712	0.568	0.071	0.125	-2.481	1.387	0.752	0	Up
RGS2	16502	0.568	0.136	0.24	-2.071	2.112	0.242	0	Up
MGC4294	12410	0.567	0.101	0.179	-2.14	-0.485	1.327	0	Up
MDFIC	12218	0.567	0.071	0.124	-2.492	0.635	1.062	0	Up
sep.11	17342	0.566	0.09	0.159	-2.443	0.794	0.971	0	Up
CCDC80	3100	0.566	0.114	0.201	-2.394	1.102	0.821	0	Up
EFHA2	5366	0.565	0.071	0.126	-2.496	0.891	0.96	0	Up
PSMD4	15868	0.565	0.051	0.09	2.515	-1.752	-0.623	0	Up
C1orf15-NBL1	2163	0.564	0.115	0.205	-2.375	0.605	1.011	0	Up
COL6A2	3995	0.562	0.118	0.21	-2.373	0.745	0.954	0	Up
PLXDC1	15224	0.561	0.066	0.118	-2.454	0.392	1.14	0	Up
LUM	11879	0.56	0.155	0.276	-2.294	0.379	1.06	0	Up
ADAM12	247	0.56	0.072	0.128	-2.384	0.16	1.196	0	Up
SVEP1	18824	0.56	0.066	0.118	-2.433	1.539	0.665	0	Up
FOXF2	6694	0.559	0.059	0.105	-2.446	1.638	0.632	0	Up
LCAT	9536	0.558	0.069	0.124	-2.469	0.878	0.951	0	Up
SERPINH1	17403	0.558	0.113	0.203	-2.207	-0.128	1.219	0	Up
LAYN	9528	0.557	0.084	0.151	-2.322	1.628	0.57	0	Up
RFX8	16471	0.556	0.065	0.117	-2.298	-0.177	1.287	0	Up
CD200	3228	0.556	0.067	0.12	-2.42	1.464	0.689	0	Up
DNAJB5	5018	0.555	0.065	0.116	-2.473	0.775	0.995	0	Up
SLC2A3	17831	0.555	0.045	0.08	-2.562	0.361	1.209	0	Up
PDPN	14781	0.555	0.107	0.193	-2.356	0.772	0.934	0	Up
HSPB2	8233	0.554	0.123	0.222	-2.212	1.686	0.489	0	Up
NID2	13457	0.552	0.063	0.114	-2.25	-0.303	1.312	0	Up
ZFP36	21191	0.552	0.107	0.193	-2.298	1.412	0.645	0	Up
SGCD	17470	0.552	0.082	0.148	-2.314	0.16	1.159	0	Up
DAB2	4549	0.551	0.082	0.149	-2.393	0.966	0.875	0	Up
VEGFC	20657	0.551	0.078	0.142	-2.337	1.517	0.624	0	Up
FOSB	6676	0.55	0.182	0.331	-2.048	1.891	0.319	0	Up
TBX15	19068	0.55	0.052	0.094	-2.512	0.635	1.072	0	Up
SSPN	18583	0.55	0.1	0.182	-2.333	1.175	0.759	0	Up
PMEPA1	15241	0.549	0.103	0.188	-2.303	0.393	1.059	0	Up
PDGFRL	14756	0.549	0.145	0.264	-2.281	0.61	0.96	0	Up
CAV1	2943	0.549	0.11	0.2	-2.093	1.944	0.322	0	Up
SH3PXD2A	17528	0.548	0.085	0.154	-2.374	0.876	0.901	0	Up
HIF1A	7874	0.548	0.083	0.151	-2.362	0.583	1.014	0	Up
C12orf34	1798	0.547	0.097	0.178	2.336	-1.068	-0.804	0	Up
SLC2A14	17829	0.547	0.08	0.147	-2.358	0.54	1.029	0	Up
VGLL3	20667	0.547	0.05	0.092	-2.484	0.462	1.127	0	Up
CTSK	4353	0.546	0.133	0.243	-2.288	0.767	0.901	0	Up
TWIST2	20278	0.546	0.113	0.207	-2.304	1.061	0.79	0	Up
PRRX2	15775	0.546	0.102	0.186	-2.319	0.667	0.957	0	Up

Gene ID	Gene Name	Score (d)	Numerator (r)	Denominator (s+s0)	contrast 1	contrast 2	contrast 3	adjusted *P* value (%)	Direction
COPZ2	4039	0.545	0.108	0.198	-2.267	0.319	1.07	0	Up
C10orf10	1681	0.545	0.121	0.222	-2.207	1.553	0.54	0	Up
C14orf37	1892	0.545	0.076	0.139	-2.359	0.505	1.044	0	Up
CLIP3	3821	0.545	0.067	0.123	-2.407	0.697	0.991	0	Up
HABP4	7685	0.545	0.073	0.133	-2.355	1.36	0.696	0	Up
IKBIP	8438	0.545	0.05	0.092	-2.273	-0.35	1.343	0	Up
C11orf96	1787	0.544	0.106	0.196	-2.288	1.218	0.718	0	Up
CACNA2D1	2793	0.543	0.051	0.094	-2.438	0.311	1.164	0	Up
KIAA1462	9087	0.542	0.085	0.156	-2.328	0.584	0.995	0	Up
DDR2	4674	0.542	0.076	0.14	-2.366	0.907	0.885	0	Up
PCOLCE	14687	0.542	0.1	0.185	-2.276	0.409	1.038	0	Up
SFXN4	17466	0.541	0.056	0.104	2.418	-1.324	-0.744	0	Up
MARCKS	12111	0.54	0.082	0.152	-2.315	0.463	1.037	0	Up
PVRL3	16018	0.54	0.062	0.114	-2.355	0.292	1.128	0	Up
MAP4K4	12065	0.54	0.058	0.108	-2.425	0.771	0.971	0	Up
SLC12A4	17666	0.538	0.06	0.112	-2.34	1.55	0.612	0	Up
CMTM3	3874	0.538	0.089	0.166	-2.3	1.17	0.744	0	Up
BNC2	1562	0.538	0.071	0.132	-2.327	0.388	1.074	0	Up
GRP	7537	0.537	0.177	0.329	-2.214	1.026	0.756	0	Up
PPFIBP1	15442	0.537	0.065	0.122	-2.329	0.302	1.109	0	Up
KLF12	9198	0.537	0.069	0.128	-2.308	1.462	0.63	0	Up
C7orf10	2582	0.537	0.077	0.144	-2.289	0.325	1.079	0	Up
MYO1B	12972	0.536	0.062	0.116	-2.35	1.394	0.68	0	Up
ADCK3	304	0.536	0.052	0.097	2.436	-1.237	-0.788	0	Up
CELF2	3478	0.536	0.069	0.129	-2.316	1.397	0.661	0	Up
SOBP	18276	0.536	0.054	0.1	-2.419	1.244	0.777	0	Up
PLXDC2	15225	0.536	0.09	0.169	-2.183	-0.003	1.156	0	Up
PXDN	16027	0.535	0.116	0.217	-2.2	0.255	1.061	0	Up
ARAP3	887	0.535	0.077	0.144	-2.252	1.526	0.575	0	Up
LIMS1	9683	0.534	0.06	0.112	-2.361	0.434	1.073	0	Up
CFHR3	3565	0.534	0.086	0.162	-2.291	1.115	0.762	0	Up
RAB23	16092	0.534	0.086	0.161	-2.26	0.36	1.05	0	Up
FOS	6675	0.534	0.162	0.303	-1.938	1.941	0.241	0	Up
MT1M	12797	0.533	0.143	0.268	-2.222	0.953	0.79	0	Up
LRP1	11735	0.533	0.051	0.096	-2.424	0.588	1.045	0	Up
MFAP5	12348	0.533	0.127	0.238	-2.155	0.142	1.082	0	Up
ETV1	5718	0.532	0.05	0.094	-2.436	0.683	1.012	0	Up
PSMB4	15847	0.532	0.054	0.101	2.241	-1.867	-0.431	0	Up
COL16A1	3968	0.532	0.076	0.143	-2.318	0.886	0.868	0	Up
CSRP1	4276	0.532	0.059	0.11	-2.094	2.087	0.264	0	Up
COL8A2	4002	0.531	0.121	0.227	-2.158	0.151	1.081	0	Up
FOXQ1	6719	0.531	0.146	0.275	-2.197	1.097	0.719	0	Up
PPAPDC1A	15421	0.53	0.149	0.281	-2.113	0.084	1.083	0	Up
KIRREL	9182	0.53	0.072	0.135	-2.318	0.694	0.945	0	Up
ARSI	1056	0.53	0.066	0.124	-2.294	0.316	1.086	0	Up
SPON2	18457	0.529	0.065	0.124	-2.343	0.789	0.92	0	Up
PRKCA	15649	0.528	0.1	0.189	-2.103	1.697	0.427	0	Up
RASD1	16251	0.528	0.155	0.293	-1.846	2.036	0.154	0	Up
SCAMP3	17128	0.528	0.055	0.104	2.362	-1.284	-0.731	0	Up
SCARNA17	17147	0.527	0.107	0.202	-2.2	1.27	0.651	0	Up
PPP1R16A	15494	0.527	0.074	0.141	2.214	-1.543	-0.548	0	Up
CLDN11	3758	0.527	0.131	0.25	-1.985	1.833	0.31	0	Up
NIT1	13476	0.526	0.055	0.104	2.313	-1.522	-0.609	0	Up
MT1X	12798	0.526	0.113	0.214	-2.199	1.189	0.683	0	Up
ARRDC3	1046	0.525	0.082	0.157	-2.113	1.74	0.415	0	Up
ADAMTS5	283	0.525	0.11	0.21	-2.22	0.803	0.85	0	Up
KLF2	9204	0.525	0.093	0.178	-2.208	1.295	0.645	0	Up
COL12A1	3964	0.524	0.141	0.269	-2.073	-0.001	1.097	0	Up
GXYLT2	7646	0.524	0.137	0.261	-2.165	0.458	0.96	0	Up
FNDC4	6658	0.524	0.072	0.137	-2.131	1.763	0.415	0	Up
MB21D2	12148	0.524	0.067	0.127	-1.767	2.352	-0.016	0	Up
SLFN11	18026	0.523	0.084	0.161	-2.253	0.756	0.886	0	Up
FNDC1	6655	0.523	0.119	0.229	-2.19	0.613	0.911	0	Up
JDP2	8787	0.523	0.077	0.148	-2.265	0.668	0.928	0	Up
DOCK11	5084	0.522	0.076	0.146	-2.169	1.591	0.504	0	Up
AIM1	446	0.522	0.116	0.223	-1.118	2.569	-0.446	0	Up
H19	7663	0.522	0.125	0.24	-2.038	1.676	0.401	0	Up
YY1AP1	21044	0.521	0.055	0.105	2.35	-1.031	-0.826	0	Up
C1QTNF5	2125	0.521	0.099	0.19	-2.218	0.848	0.831	0	Up
FLNA	6617	0.521	0.062	0.12	-2.278	1.329	0.668	0	Up
LRIG3	11730	0.521	0.094	0.181	-2.196	1.235	0.662	0	Up
TMEM45A	19610	0.521	0.131	0.252	-2.17	0.607	0.902	0	Up
UACA	20323	0.521	0.069	0.132	-2.282	0.674	0.935	0	Up
FMO2	6639	0.52	0.174	0.335	-1.91	1.835	0.269	0	Up
LPCAT2	11695	0.52	0.054	0.103	-2.32	1.347	0.683	0	Up
DPYSL2	5149	0.519	0.083	0.16	-1.976	1.941	0.261	0	Up
KDELC2	8968	0.519	0.062	0.119	-2.261	0.313	1.069	0	Up
ARHGAP39	934	0.519	0.072	0.139	2.265	-0.722	-0.906	0	Up
SGK1	17475	0.519	0.091	0.176	-2.109	1.583	0.476	0	Up
SGIP1	17474	0.518	0.072	0.14	-2.098	-0.165	1.176	0	Up
CLEC11A	3782	0.517	0.105	0.203	-2.141	0.274	1.022	0	Up
CES1	3545	0.517	0.084	0.163	-2.226	0.948	0.794	0	Up
CFI	3568	0.517	0.086	0.166	-2.074	1.691	0.414	0	Up
KLF7	9209	0.517	0.07	0.136	-2.263	0.805	0.872	0	Up
PHLDB1	14949	0.517	0.059	0.115	-2.243	0.226	1.095	0	Up
ACTN1	214	0.517	0.087	0.168	-2.22	0.9	0.81	0	Up
SFRP4	17449	0.516	0.129	0.25	-2.024	1.62	0.416	0	Up
NHS	13452	0.516	0.049	0.095	-2.341	1.263	0.728	0	Up
RECK	16395	0.515	0.065	0.125	-2.265	0.575	0.965	0	Up
GGT5	7072	0.515	0.089	0.172	-2.187	1.182	0.679	0	Up
LRCH2	11717	0.515	0.046	0.09	-2.366	1.213	0.762	0	Up
PRDM1	15591	0.515	0.084	0.164	-2.11	0.025	1.105	0	Up
HOXA11-AS1	8086	0.514	0.094	0.183	-2.138	0.234	1.036	0	Up
HEG1	7809	0.514	0.081	0.158	-2.174	1.341	0.608	0	Up
RUNX1T1	16999	0.514	0.1	0.194	-2.159	1.201	0.657	0	Up
BACH2	1366	0.514	0.043	0.084	-2.236	1.853	0.434	0	Up
LSP1	11857	0.513	0.07	0.136	-2.238	1.085	0.745	0	Up
LAMB1	9491	0.513	0.04	0.078	-2.429	0.696	1.003	0	Up
F2RL1	5787	0.512	0.078	0.153	-2.033	1.769	0.361	0	Up
TSPO2	20120	0.512	0.058	0.114	-2.115	-0.194	1.197	0	Up
ZFHX4	21181	0.512	0.093	0.181	-2.184	0.936	0.777	0	Up
WDR86	20856	0.511	0.136	0.266	-2.115	1.108	0.671	0	Up
PKD2	15071	0.51	0.071	0.139	-2.186	1.324	0.621	0	Up
HOXA3	8089	0.51	0.106	0.207	-2.022	1.616	0.416	0	Up
LOC645676	11405	0.51	0.054	0.107	2.295	-1.013	-0.805	0	Up
MALL	12005	0.51	0.13	0.256	-1.653	2.146	0.008	0	Up

Gene ID	Gene Name	Score (d)	Numerator (r)	Denominator (s+s0)	contrast 1	contrast 2	contrast 3	adjusted *P* value (%)	Direction
FAM89A	6139	0.51	0.086	0.169	-1.907	1.935	0.227	0	Up
HIC1	7872	0.509	0.072	0.142	-2.15	1.438	0.556	0	Up
FAS	6180	0.508	0.057	0.113	-2.239	1.303	0.658	0	Up
NCRNA00241	13204	0.508	0.078	0.153	-2.195	0.619	0.911	0	Up
FAM43A	6040	0.508	0.076	0.15	-2.146	1.388	0.574	0	Up
ASPN	1122	0.508	0.184	0.362	-1.976	-0.027	1.056	0	Up
DIO1	4878	0.507	0.109	0.215	2.139	-0.895	-0.77	0	Up
TGFBR2	19249	0.507	0.08	0.157	-1.869	1.999	0.181	0	Up
HMCN1	8005	0.507	0.107	0.21	-2.079	0.199	1.019	0	Up
COL10A1	3961	0.506	0.174	0.344	-1.768	-0.595	1.175	0	Up
C21orf34	2296	0.506	0.051	0.101	-2.296	1.042	0.793	0	Up
KRTCAP3	9459	0.505	0.097	0.193	2.046	-1.518	-0.469	0.214	Up
ITGA11	8711	0.505	0.127	0.252	-1.952	-0.188	1.108	0.214	Up
ADAMTS14	273	0.505	0.123	0.244	-2.013	0.011	1.06	0.214	Up
NEFH	13351	0.505	0.107	0.212	-2.131	0.642	0.868	0.214	Up
DST	5189	0.505	0.094	0.187	-2.075	1.433	0.519	0.214	Up
SH3PXD2B	17529	0.504	0.083	0.165	-2.17	0.72	0.856	0.214	Up
E4F1	5287	0.504	0.059	0.117	2.201	-1.336	-0.624	0.214	Up
ETS2	5717	0.504	0.067	0.133	-1.812	2.119	0.103	0.214	Up
SCHIP1	17177	0.503	0.1	0.198	-2.109	1.188	0.635	0.214	Up
OLFML2B	13917	0.503	0.084	0.168	-2.129	0.366	0.978	0.214	Up
DZIP1	5276	0.503	0.07	0.14	-2.187	1.045	0.734	0.214	Up
CCDC3	3053	0.502	0.106	0.21	-1.973	1.637	0.382	0.214	Up
MPZL2	12634	0.502	0.102	0.204	-1.668	2.126	0.024	0.214	Up
ZNHIT2	21794	0.502	0.052	0.104	2.229	-1.334	-0.64	0.214	Up
CNRIP1	3925	0.502	0.045	0.089	-2.294	1.295	0.69	0.214	Up
JAG1	8774	0.502	0.074	0.147	-2.181	0.773	0.841	0.214	Up
ZC3H12B	21103	0.502	0.04	0.079	-2.311	1.478	0.625	0.214	Up
SPARCL1	18363	0.501	0.129	0.257	-2.023	1.38	0.513	0.214	Up
SSC5D	18577	0.501	0.117	0.234	-2.083	0.45	0.92	0.214	Up
PRKD3	15662	0.501	0.077	0.154	-2.025	1.639	0.409	0.214	Up
PTPRD	15972	0.5	0.103	0.206	-2.049	0.169	1.016	0.214	Up
CD99	3298	0.499	0.053	0.107	-2.227	0.464	0.99	0.214	Up
SPRY2	18483	0.499	0.1	0.2	-1.991	1.565	0.421	0.214	Up
LOC100130876	10110	0.499	0.104	0.208	-2.107	0.64	0.856	0.214	Up
TMPRSS6	19690	0.499	0.084	0.167	2.025	-1.564	-0.439	0.214	Up
GREM1	7492	0.499	0.097	0.195	-2.072	0.272	0.986	0.214	Up
COL15A1	3967	0.498	0.082	0.164	-2.13	1.106	0.679	0.214	Up
C17orf51	2000	0.498	0.078	0.157	-2.155	0.808	0.813	0.214	Up
GNG11	7241	0.498	0.093	0.187	-2.058	1.374	0.534	0.214	Up
TMEM2	19552	0.498	0.056	0.113	-2.029	-0.29	1.19	0.214	Up
ID3	8312	0.498	0.068	0.136	-2.137	1.303	0.604	0.214	Up
ARHGEF40	965	0.498	0.074	0.149	-2.163	0.749	0.841	0.214	Up
FAM20B	6010	0.497	0.057	0.114	2.072	-1.685	-0.415	0.214	Up
JAZF1	8786	0.497	0.06	0.12	-2.191	1.12	0.706	0.214	Up
ZNF469	21487	0.497	0.116	0.234	-2.061	0.414	0.923	0.214	Up
RBMS3	16340	0.496	0.042	0.085	-2.304	0.586	0.982	0.214	Up
PYCR2	16036	0.496	0.048	0.097	2.105	-1.751	-0.406	0.214	Up
BEND6	1483	0.496	0.04	0.08	-2.314	0.465	1.036	0.214	Up
PYCRL	16037	0.496	0.056	0.113	2.215	-1.015	-0.762	0.214	Up
TARS2	18972	0.495	0.04	0.08	2.228	-1.64	-0.516	0.214	Up
MOXD1	12603	0.495	0.106	0.215	-1.923	1.652	0.35	0.214	Up
GLIPR2	7156	0.495	0.089	0.18	-2.109	0.61	0.869	0.214	Up
ECM2	5316	0.495	0.056	0.113	-2.201	0.536	0.947	0.214	Up
ACSL4	189	0.495	0.053	0.108	-2.204	0.469	0.976	0.214	Up
RAB7L1	16138	0.494	0.078	0.158	-2.118	0.488	0.923	0.214	Up
FXYD6	6823	0.494	0.078	0.157	-1.718	2.082	0.068	0.214	Up
C1orf182	2177	0.494	0.061	0.124	1.707	-2.192	-0.018	0.214	Up
WTIP	20938	0.494	0.083	0.168	-2	1.557	0.429	0.214	Up
ITGB1	8727	0.493	0.059	0.12	-2.162	1.215	0.653	0.214	Up
FZD7	6836	0.493	0.101	0.205	-2.04	1.276	0.563	0.214	Up
ANKRD35	695	0.493	0.123	0.25	-1.977	1.412	0.475	0.214	Up
ZEB2	21168	0.492	0.063	0.127	-2.173	0.831	0.814	0.214	Up
LRRC32	11774	0.492	0.089	0.182	-2.102	0.885	0.754	0.214	Up
ANTXR2	751	0.492	0.048	0.098	-2.177	1.441	0.569	0.214	Up
HEYL	7849	0.492	0.086	0.175	-2.057	0.262	0.982	0.214	Up
LEPRE1	9607	0.491	0.048	0.097	-2.104	-0.098	1.152	0.214	Up
VCL	20646	0.491	0.065	0.132	-1.865	1.938	0.204	0.214	Up
PELI2	14817	0.491	0.081	0.164	-2.107	1.02	0.702	0.214	Up
DUSP1	5217	0.491	0.104	0.211	-2.007	1.361	0.511	0.214	Up
SALL4	17067	0.491	0.115	0.235	-1.935	-0.073	1.053	0.214	Up
CPXM1	4137	0.49	0.085	0.174	-2.034	1.348	0.532	0.363	Up
ACVR2A	234	0.49	0.049	0.1	-2.227	0.932	0.801	0.363	Up
EDN1	5334	0.49	0.112	0.228	-1.874	1.673	0.316	0.363	Up
CTSB	4346	0.489	0.076	0.156	-1.904	-0.331	1.141	0.363	Up
C9orf53	2729	0.489	0.121	0.246	-2.048	0.664	0.815	0.363	Up
ATF3	1147	0.489	0.087	0.177	-2.092	0.844	0.766	0.363	Up
FGF7	6360	0.489	0.062	0.127	-2.143	1.087	0.694	0.363	Up
NTM	13753	0.488	0.057	0.118	-1.978	-0.28	1.159	0.363	Up
LOC100129940	9999	0.488	0.067	0.138	-2.059	0.13	1.036	0.363	Up
CD36	3255	0.488	0.167	0.342	-1.492	2.094	-0.057	0.363	Up
RASA3	16246	0.488	0.069	0.141	-2.125	0.627	0.871	0.363	Up
SNRNP35	18218	0.488	0.048	0.097	2.04	-1.786	-0.358	0.363	Up
MME	12524	0.488	0.086	0.176	-1.901	1.697	0.32	0.363	Up
NXN	13843	0.488	0.061	0.125	-2.14	0.506	0.927	0.363	Up
WNT2	20911	0.487	0.075	0.153	-2.019	0.063	1.042	0.363	Up
ITGA1	8709	0.487	0.064	0.132	-2.058	0.1	1.048	0.363	Up
MAP1B	12033	0.487	0.066	0.136	-2.113	1.14	0.657	0.363	Up
PEX5L	14845	0.487	0.07	0.144	2.116	-0.653	-0.855	0.363	Up
COL5A3	3993	0.486	0.092	0.188	-1.893	-0.24	1.098	0.363	Up
SULF1	18774	0.486	0.118	0.244	-1.76	-0.501	1.133	0.363	Up
FAT1	6188	0.485	0.103	0.212	-2	1.267	0.546	0.363	Up
SPOCK1	18453	0.485	0.121	0.25	-1.847	-0.26	1.082	0.363	Up
JAM3	8784	0.485	0.06	0.124	-2.144	0.937	0.756	0.363	Up
FST	6775	0.484	0.135	0.279	-1.957	0.183	0.961	0.363	Up
SPRY1	18482	0.484	0.086	0.179	-2.009	1.332	0.524	0.363	Up
LIMS3L	9686	0.484	0.067	0.139	-2.102	1.076	0.677	0.363	Up
ZNF300P1	21390	0.484	0.088	0.182	-2.031	1.203	0.589	0.363	Up
RNF175	16670	0.484	0.046	0.096	-2.089	1.629	0.447	0.363	Up
USP21	20558	0.484	0.048	0.099	2.18	-1.18	-0.676	0.363	Up
PRDM6	15602	0.484	0.061	0.125	-2.016	-0.048	1.085	0.363	Up
SELENBP1	17293	0.484	0.122	0.253	2.019	-0.891	-0.708	0.363	Up
DPT	5137	0.483	0.133	0.276	-2.003	0.554	0.835	0.363	Up
PID1	14982	0.483	0.093	0.192	-1.816	1.768	0.247	0.363	Up
MAGEL2	11991	0.482	0.07	0.146	-2.078	1.118	0.647	0.363	Up
FAM195A	5990	0.482	0.056	0.117	2.066	-1.453	-0.506	0.363	Up

Gene ID	Gene Name	Score (d)	Numerator (r)	Denominator (s+s0)	contrast 1	contrast 2	contrast 3	adjusted *P.* value (%)	Direction
AOC3	770	0.482	0.109	0.227	-1.872	1.592	0.347	0.363	Up
LAMA1	9486	0.482	0.056	0.117	-2.147	0.846	0.794	0.363	Up
C5orf13	2477	0.482	0.065	0.135	-2.099	0.52	0.9	0.363	Up
KANK2	8818	0.481	0.067	0.14	-2.068	1.216	0.602	0.363	Up
AKAP13	466	0.481	0.049	0.101	-2.176	1.061	0.722	0.363	Up
TNFRSF10D	19723	0.481	0.075	0.155	-1.726	1.967	0.119	0.363	Up
PTGIR	15922	0.48	0.063	0.131	-2.096	0.495	0.909	0.363	Up
TSHZ2	20085	0.48	0.074	0.155	-1.944	1.556	0.4	0.363	Up
MAMDC2	12007	0.48	0.062	0.13	-2.112	0.75	0.814	0.363	Up
FABP4	5804	0.479	0.125	0.261	-1.372	2.169	-0.15	0.363	Up
WISP1	20897	0.479	0.055	0.114	-2.067	0.131	1.04	0.363	Up
SWAP70	18829	0.479	0.054	0.112	-1.574	2.249	-0.076	0.363	Up
ABCA6	42	0.479	0.091	0.19	-2.03	0.988	0.675	0.363	Up
ADAMTS1	269	0.479	0.101	0.211	-1.933	1.413	0.452	0.363	Up
VSNL1	20740	0.479	0.108	0.226	-1.956	1.289	0.514	0.363	Up
LOC541471	11281	0.478	0.083	0.174	-1.619	-0.816	1.186	0.363	Up
KRT17	9319	0.478	0.228	0.477	-1.774	1.583	0.299	0.363	Up
DAP3	4567	0.478	0.049	0.104	2.162	-0.88	-0.788	0.363	Up
CR2	4142	0.477	0.098	0.206	-0.932	2.384	-0.47	0.363	Up
D4S234E	4545	0.477	0.091	0.19	-1.441	2.165	-0.112	0.363	Up
PECAM1	14810	0.477	0.067	0.14	-1.884	1.721	0.301	0.363	Up
KRT16P2	9318	0.477	0.217	0.455	-1.729	1.671	0.24	0.363	Up
STARD8	18661	0.477	0.051	0.106	-2.149	0.913	0.768	0.363	Up
ADIPOR1	333	0.477	0.054	0.114	2.04	-1.473	-0.484	0.363	Up
JAM2	8783	0.477	0.069	0.144	-2.007	1.357	0.513	0.363	Up
MRPL9	12705	0.477	0.047	0.098	2.174	-0.737	-0.852	0.363	Up
COMP	4020	0.476	0.153	0.32	-1.894	0.096	0.963	0.363	Up
MT1E	12791	0.476	0.107	0.224	-2.006	0.751	0.758	0.363	Up
PARVA	14557	0.476	0.06	0.126	-2.073	1.185	0.618	0.363	Up
ST6GAL2	18617	0.476	0.083	0.174	-1.883	-0.183	1.069	0.363	Up
FAM20A	6009	0.476	0.073	0.154	-2.062	0.778	0.776	0.363	Up
C12orf70	1830	0.475	0.072	0.152	-1.987	0.129	0.999	0.363	Up
ROR1	16743	0.475	0.055	0.117	-2.118	0.753	0.816	0.363	Up
MXRA7	12902	0.475	0.058	0.121	-2.109	0.818	0.785	0.363	Up
FAT4	6191	0.475	0.037	0.077	-2.236	1.206	0.695	0.363	Up
RND3	16628	0.475	0.114	0.241	-1.494	2.053	-0.039	0.363	Up
ITGAV	8725	0.474	0.072	0.153	-2.036	1.075	0.643	0.381	Up
C20orf103	2234	0.474	0.129	0.272	-1.975	0.716	0.755	0.381	Up
RUSC1	17002	0.474	0.051	0.107	2.111	-1.161	-0.647	0.381	Up
ITGA5	8716	0.474	0.075	0.159	-2.012	0.343	0.926	0.381	Up
EIF5A2	5468	0.474	0.049	0.104	-2.097	0.29	0.992	0.381	Up
AKR1B15	488	0.473	0.118	0.249	-0.978	2.321	-0.42	0.381	Up
CADM3	2813	0.473	0.058	0.123	-1.255	2.373	-0.295	0.381	Up
IGFBP7	8409	0.473	0.082	0.175	-2.007	1.06	0.633	0.381	Up
MAGIX	11996	0.472	0.04	0.084	2.193	-1.162	-0.69	0.381	Up
MT1L	12796	0.472	0.096	0.203	-1.999	0.869	0.706	0.381	Up
CCL14	3132	0.472	0.142	0.3	-1.391	2.087	-0.107	0.381	Up
FAM7A1	6115	0.472	0.046	0.097	-1.947	-0.324	1.161	0.381	Up
TROVE2	20036	0.472	0.045	0.095	2.149	-1.092	-0.696	0.381	Up
PDE2A	14730	0.472	0.088	0.187	-1.685	1.88	0.132	0.381	Up
CLIP4	3822	0.472	0.07	0.149	-2.041	0.972	0.687	0.381	Up
SPHK2	18419	0.472	0.039	0.083	2.207	-0.97	-0.775	0.381	Up
MMP23B	12540	0.471	0.092	0.196	-1.875	1.504	0.384	0.381	Up
CLDN5	3774	0.471	0.107	0.227	-1.721	1.767	0.196	0.381	Up
PRNP	15688	0.471	0.095	0.202	-1.986	1.004	0.645	0.381	Up
C20orf194	2258	0.471	0.054	0.115	-2.101	0.661	0.844	0.381	Up
ARHGAP20	918	0.471	0.054	0.116	-2.073	1.16	0.628	0.381	Up
F2R	5786	0.47	0.057	0.121	-2.089	0.772	0.793	0.381	Up
KRT14	9315	0.47	0.235	0.5	-1.738	1.571	0.285	0.381	Up
USP13	20548	0.47	0.062	0.131	2.06	-0.998	-0.686	0.381	Up
ANXA3	761	0.47	0.143	0.304	-1.289	2.143	-0.184	0.381	Up
NPR2	13642	0.47	0.071	0.151	-2.039	0.762	0.77	0.381	Up
LMCD1	9727	0.47	0.087	0.184	-1.93	0.111	0.976	0.381	Up
CECR5-AS1	3467	0.47	0.071	0.151	2.015	-1.095	-0.624	0.381	Up
KLF6	9208	0.469	0.05	0.107	-2.062	1.318	0.558	0.381	Up
LOC150622	10676	0.469	0.06	0.127	-1.046	2.42	-0.424	0.381	Up
HOXA4	8090	0.469	0.057	0.12	-2.024	1.326	0.535	0.381	Up
ITGBL1	8739	0.469	0.117	0.249	-1.903	0.166	0.939	0.381	Up
EFNB2	5378	0.469	0.078	0.167	-2.007	0.989	0.662	0.381	Up
ZFPM2	21206	0.469	0.07	0.15	-2.031	0.922	0.702	0.381	Up
ECI1	5313	0.469	0.072	0.153	2	-1.158	-0.59	0.381	Up
C1orf27	2201	0.469	0.056	0.119	2.055	-1.168	-0.615	0.381	Up
CXCL12	4398	0.468	0.072	0.155	-2.013	0.996	0.662	0.381	Up
VPS72	20728	0.468	0.048	0.103	2.096	-1.14	-0.648	0.381	Up
KIAA0408	9027	0.468	0.053	0.113	-2.003	1.442	0.477	0.381	Up
F3	5790	0.468	0.119	0.254	-1.895	1.258	0.494	0.381	Up
ZNF646	21624	0.467	0.026	0.055	2.23	-1.886	-0.418	0.381	Up
IGF2	8396	0.467	0.066	0.141	-1.99	1.25	0.548	0.381	Up
PEAK1	14806	0.467	0.053	0.114	-2.078	1.01	0.691	0.381	Up
ADH1C	324	0.466	0.153	0.328	-1.265	2.126	-0.19	0.381	Up
C6orf145	2533	0.466	0.075	0.16	-1.789	1.716	0.253	0.381	Up
PTGFRN	15921	0.466	0.07	0.149	-1.983	0.298	0.928	0.381	Up
KIF26A	9151	0.466	0.054	0.116	-1.609	2.095	0.005	0.381	Up
KCTD12	8949	0.465	0.074	0.158	-1.984	1.108	0.602	0.381	Up
ADD3	321	0.465	0.104	0.223	-1.869	1.372	0.434	0.381	Up
TSNAX	20094	0.465	0.047	0.102	2.014	-1.467	-0.472	0.381	Up
SPSB1	18490	0.464	0.067	0.144	-2.018	0.604	0.823	0.381	Up
TMEM43	19608	0.464	0.05	0.108	-2.088	0.698	0.822	0.381	Up
MFAP4	12347	0.463	0.163	0.353	-1.788	1.434	0.366	0.381	Up
GLIS1	7157	0.463	0.075	0.161	-1.827	-0.228	1.058	0.381	Up
SYNPO	18864	0.463	0.054	0.117	-2.022	1.226	0.574	0.381	Up
KIAA0907	9049	0.463	0.044	0.096	2.062	-1.337	-0.551	0.381	Up
CERCAM	3536	0.463	0.061	0.131	-1.812	-0.37	1.108	0.381	Up
NKD2	13486	0.462	0.068	0.147	-1.985	0.383	0.895	0.381	Up
ETHE1	5713	0.462	0.056	0.121	-1.899	1.594	0.36	0.381	Up
WISP2	20898	0.462	0.171	0.37	-1.833	0.124	0.919	0.381	Up
SPHK1	18418	0.462	0.067	0.146	-2.008	0.83	0.727	0.381	Up
EFEMP2	5364	0.461	0.073	0.159	-1.928	0.157	0.956	0.381	Up
PTGIS	15923	0.46	0.1	0.218	-1.716	1.675	0.231	0.381	Up
PTN	15939	0.46	0.155	0.337	-1.607	1.752	0.142	0.381	Up
LYSMD1	11921	0.46	0.063	0.136	1.893	-1.495	-0.398	0.381	Up
SCN3B	17192	0.46	0.082	0.178	-1.935	1.129	0.567	0.554	Up
TCEAL7	19092	0.459	0.063	0.137	-1.701	1.857	0.15	0.554	Up
SPIRE1	18445	0.459	0.051	0.112	0.952	-2.427	0.477	0.554	Up
RAB3A	16113	0.459	0.071	0.154	1.638	-1.89	-0.103	0.554	Up
NSUN7	13736	0.458	0.093	0.203	0.986	1.524	-1.137	0.554	Up

Gene ID	Gene Name	Score (d)	Numerator (r)	Denominator (s+s0)	contrast 1	contrast 2	contrast 3	adjusted *P* value (%)	Direction
SLC26A10	17801	0.458	0.063	0.138	-1.88	-0.082	1.027	0.554	Up
LOC100132891	10294	0.458	0.028	0.062	-2.262	0.461	1.01	0.554	Up
PLSCR4	15219	0.458	0.074	0.162	-1.763	1.67	0.258	0.554	Up
TNFRSF18	19731	0.457	0.09	0.197	1.589	-1.863	-0.088	0.554	Up
C6orf174	2545	0.457	0.06	0.131	-2.006	0.912	0.692	0.554	Up
SYNDIG1	18851	0.457	0.13	0.284	-1.833	0.125	0.919	0.554	Up
RECQL	16396	0.457	0.03	0.066	-2.213	0.379	1.017	0.554	Up
CDKN1C	3411	0.457	0.09	0.197	-1.81	1.47	0.364	0.554	Up
PANX2	14505	0.457	0.033	0.073	2.067	-1.614	-0.441	0.554	Up
ITGB3	8732	0.456	0.093	0.204	-1.918	0.441	0.836	0.554	Up
MYO1D	12974	0.456	0.053	0.115	-2.029	0.566	0.844	0.554	Up
C14orf21	1886	0.456	0.037	0.08	2.086	-1.389	-0.542	0.554	Up
CRISPLD2	4183	0.456	0.065	0.142	-1.985	0.885	0.692	0.554	Up
ADAMTS12	271	0.456	0.045	0.098	-1.858	-0.354	1.126	0.554	Up
OTUD7B	14397	0.455	0.055	0.12	1.922	-1.438	-0.436	0.554	Up
CDO1	3421	0.455	0.108	0.238	-1.553	1.845	0.076	0.554	Up
GOLGA7B	7287	0.454	0.064	0.141	-1.822	-0.206	1.047	0.554	Up
MITF	12471	0.454	0.053	0.116	-1.98	0.257	0.943	0.554	Up
AASS	27	0.454	0.057	0.126	-1.935	1.331	0.486	0.554	Up
AKR1C1	489	0.454	0.094	0.208	-1.291	2.1	-0.165	0.554	Up
CD248	3237	0.454	0.066	0.146	-1.969	0.542	0.822	0.554	Up
TP53I3	19830	0.454	0.067	0.147	-1.786	1.625	0.288	0.554	Up
RCAN2	16364	0.454	0.054	0.119	-1.922	1.422	0.442	0.554	Up
POTEF	15389	0.454	0.056	0.123	-1.98	1.149	0.583	0.554	Up
LRRN4CL	11831	0.454	0.072	0.158	-1.84	1.462	0.383	0.554	Up
WNK2	20903	0.453	0.063	0.138	1.97	-1.002	-0.637	0.554	Up
TMEM204	19560	0.453	0.072	0.158	-1.955	0.687	0.756	0.554	Up
LDB2	9574	0.453	0.051	0.113	-2.021	0.94	0.689	0.554	Up
GLIS2	7158	0.453	0.086	0.19	-1.872	0.189	0.914	0.554	Up
TSPAN18	20105	0.453	0.063	0.139	-1.977	0.821	0.714	0.554	Up
HHIPL1	7863	0.452	0.061	0.135	-1.923	0.173	0.947	0.554	Up
EDIL3	5333	0.452	0.118	0.26	-1.388	-0.93	1.109	0.554	Up
CPZ	4139	0.452	0.076	0.168	-1.913	1.108	0.564	0.554	Up
MAP4K5	12066	0.452	0.046	0.101	-2.052	0.801	0.762	0.554	Up
GNMT	7258	0.451	0.065	0.143	0.974	1.572	-1.15	0.554	Up
XG	20957	0.451	0.063	0.139	-1.949	0.372	0.88	0.554	Up
CASKIN1	2915	0.451	0.055	0.123	1.856	-1.544	-0.358	0.554	Up
KLK8	9270	0.451	0.219	0.486	-1.237	2.011	-0.158	0.554	Up
MIPOL1	12462	0.451	0.065	0.144	1.62	-1.873	-0.1	0.554	Up
TMEM109	19451	0.451	0.062	0.137	-1.307	2.171	-0.185	0.554	Up
PCSK7	14699	0.451	0.036	0.081	-2.068	1.339	0.553	0.554	Up
LOXL1	11682	0.451	0.104	0.23	-1.849	0.221	0.889	0.554	Up
COL8A1	4001	0.451	0.129	0.286	-1.749	-0.104	0.967	0.554	Up
PLAC9	15124	0.451	0.071	0.157	-1.908	1.171	0.536	0.554	Up
SNORA16B	18173	0.451	0.053	0.118	1.842	-1.598	-0.329	0.554	Up
C11orf93	1784	0.451	0.043	0.095	-1.68	1.994	0.083	0.554	Up
ZFAND5	21174	0.45	0.046	0.102	-2	0.282	0.944	0.554	Up
BAIAP3	1384	0.45	0.117	0.259	1.841	-1.129	-0.518	0.554	Up
MAP7D3	12072	0.45	0.041	0.091	-2.038	1.241	0.576	0.554	Up
SLC36A1	17880	0.45	0.062	0.139	-1.853	-0.056	1.002	0.554	Up
EMX2OS	5538	0.449	0.079	0.175	-1.915	0.943	0.632	0.554	Up
TBCE	19050	0.449	0.053	0.119	1.83	-1.6	-0.322	0.554	Up
JUN	8810	0.449	0.095	0.211	-1.756	1.479	0.331	0.554	Up
HOXA7	8093	0.449	0.126	0.28	-1.782	1.304	0.416	0.554	Up
PPP1R15A	15492	0.449	0.053	0.118	-1.748	1.754	0.216	0.554	Up
CAPN5	2876	0.449	0.078	0.174	-1.92	0.838	0.677	0.554	Up
ZFP36L1	21192	0.449	0.072	0.16	-1.854	1.333	0.442	0.554	Up
CYHR1	4466	0.449	0.051	0.114	1.947	-1.283	-0.511	0.554	Up
RCBTB2	16367	0.449	0.052	0.115	-1.85	1.566	0.346	0.554	Up
C12orf75	1834	0.449	0.086	0.191	-1.906	0.846	0.666	0.554	Up
CCDC82	3102	0.448	0.074	0.164	-1.905	1.064	0.578	0.554	Up
FKBP9	6419	0.448	0.033	0.073	-2.108	0.293	0.997	0.554	Up
PBX1	14585	0.448	0.059	0.131	1.97	-0.753	-0.738	0.554	Up
DECR2	4722	0.448	0.054	0.12	1.975	-1.013	-0.635	0.554	Up
PRELP	15614	0.447	0.025	0.056	-2.113	1.819	0.383	0.554	Up
GPC6	7333	0.447	0.076	0.17	-1.877	0.255	0.89	0.554	Up
IGFBP6	8408	0.446	0.083	0.186	-1.831	1.279	0.452	0.554	Up
SLIT2	18035	0.446	0.067	0.15	-1.936	0.741	0.725	0.554	Up
PGM5	14896	0.446	0.053	0.118	-1.756	1.713	0.237	0.554	Up
B4GALT3	1352	0.446	0.061	0.138	1.951	-0.744	-0.731	0.554	Up
KRT5	9347	0.446	0.197	0.443	-1.688	1.418	0.32	0.833	Up
MGC50722	12415	0.446	0.067	0.151	1.851	-1.328	-0.443	0.833	Up
SGMS2	17483	0.446	0.057	0.128	-1.931	0.317	0.893	0.833	Up
ALDH1A3	513	0.446	0.106	0.238	-1.403	1.93	-0.038	0.833	Up
CSRP2	4277	0.445	0.084	0.189	-1.865	1.097	0.543	0.833	Up
FHAD1	6379	0.445	0.03	0.068	-1.986	1.746	0.345	0.833	Up
CTHRC1	4325	0.445	0.117	0.263	-1.833	0.339	0.832	0.833	Up
AKR1B1	486	0.445	0.072	0.161	-1.585	1.825	0.101	0.833	Up
TMEM119	19459	0.445	0.099	0.222	-1.809	1.245	0.454	0.833	Up
SLC26A3	17804	0.445	0.085	0.191	-0.704	2.258	-0.539	0.833	Up
ALDH1L2	516	0.444	0.073	0.164	-1.814	-0.007	0.962	0.833	Up
CXCL2	4403	0.444	0.138	0.311	-1.695	1.452	0.31	0.833	Up
CYP2U1	4503	0.444	0.054	0.122	-1.943	1.103	0.582	0.833	Up
SETDB1	17425	0.444	0.038	0.084	1.952	-1.542	-0.41	0.833	Up
MEIS2	12286	0.444	0.065	0.145	-1.92	0.477	0.823	0.833	Up
FMOD	6645	0.444	0.111	0.249	-1.825	1.081	0.529	0.833	Up
ARPC2	1032	0.444	0.046	0.104	-2.006	0.815	0.732	0.833	Up
EXOC8	5753	0.443	0.039	0.088	1.967	-1.42	-0.467	0.833	Up
STX6	18750	0.443	0.048	0.108	1.957	-1.178	-0.559	0.833	Up
CNIH3	3895	0.443	0.079	0.177	-1.887	0.514	0.79	0.833	Up
PEX19	14840	0.443	0.057	0.128	1.952	-0.757	-0.727	0.833	Up
NVL	13837	0.443	0.069	0.156	1.896	-1.021	-0.59	0.833	Up
SOD3	18286	0.442	0.127	0.288	-1.163	2.05	-0.213	0.833	Up
C22orf13	2313	0.442	0.039	0.087	2.015	-0.313	-0.94	0.833	Up
CNTNAP3	3940	0.442	0.082	0.185	-1.775	1.382	0.381	0.833	Up
CLDN8	3777	0.441	0.091	0.207	-1.216	2.066	-0.191	0.833	Up
NR2F1	13676	0.441	0.137	0.312	-1.587	1.625	0.183	0.833	Up
FBXO28	6241	0.441	0.054	0.121	1.95	-0.932	-0.655	0.833	Up
ENPP2	5562	0.441	0.077	0.174	-1.544	1.817	0.083	0.833	Up
RPS6KA3	16898	0.441	0.058	0.133	-1.833	1.4	0.404	0.833	Up
PLD1	15152	0.441	0.048	0.109	-1.976	0.907	0.679	0.833	Up
HSPG2	8245	0.44	0.046	0.104	-1.943	0.23	0.935	0.833	Up
GJB2	7120	0.44	0.145	0.329	-1.722	-0.017	0.918	0.833	Up
L3MBTL3	9473	0.44	0.048	0.109	-1.689	1.802	0.165	0.833	Up
MRAS	12639	0.44	0.087	0.197	-1.737	1.43	0.341	0.833	Up
APOD	846	0.44	0.181	0.413	-0.431	2.145	-0.638	0.833	Up

Gene ID	Gene Name	Score (d)	Numerator (r)	Denominator (s+s0)	contrast 1	contrast 2	contrast 3	adjusted *P* value (%)	Direction
COG2	3953	0.44	0.052	0.118	1.933	-1.077	-0.587	0.833	Up
LHFPL2	9644	0.439	0.062	0.142	-1.913	0.864	0.663	0.833	Up
LY96	11899	0.439	0.072	0.163	-1.879	0.966	0.603	0.833	Up
OSGIN2	14363	0.439	0.047	0.107	1.98	-0.668	-0.777	0.833	Up
CDKL5	3408	0.439	0.065	0.147	-1.889	1.03	0.583	0.833	Up
ADPRH	346	0.439	0.058	0.132	-1.915	0.998	0.61	0.833	Up
PYGO2	16044	0.439	0.034	0.077	2.074	-1.06	-0.669	0.833	Up
sep.10	17341	0.439	0.065	0.148	-1.728	1.562	0.283	0.833	Up
EGFL6	5387	0.438	0.125	0.286	-1.821	0.771	0.652	0.833	Up
IQCJ-SCHIP1	8647	0.438	0.066	0.15	-1.768	1.46	0.345	0.833	Up
SPATS2L	18389	0.438	0.07	0.16	-1.831	0.155	0.905	0.833	Up
VEGFB	20656	0.438	0.047	0.108	-1.944	1.105	0.582	0.833	Up
P2RY1	14425	0.438	0.049	0.112	-1.938	1.069	0.593	0.833	Up
SV2B	18822	0.438	0.08	0.183	-1.558	1.754	0.116	0.833	Up
SLAMF9	17652	0.437	0.061	0.141	-1.708	-0.325	1.034	0.833	Up
COL14A1	3966	0.437	0.098	0.224	-1.731	1.363	0.365	0.833	Up
PLEKHH2	15184	0.437	0.051	0.116	-1.949	0.764	0.722	0.833	Up
KLHL12	9226	0.437	0.037	0.085	1.923	-1.508	-0.408	0.833	Up
NPC2	13617	0.437	0.061	0.14	-1.795	1.411	0.379	0.833	Up
COL4A2	3985	0.437	0.073	0.167	-1.874	0.556	0.766	0.833	Up
EBF1	5293	0.436	0.048	0.111	-1.899	1.248	0.501	0.833	Up
LGALS1	9618	0.436	0.075	0.172	-1.858	0.448	0.802	0.833	Up
TWIST1	20277	0.436	0.057	0.13	-1.866	1.211	0.498	0.833	Up
S1PR1	17046	0.436	0.071	0.162	-1.557	1.776	0.106	0.833	Up
DNA2	4986	0.436	0.046	0.105	1.965	-0.862	-0.691	0.833	Up
STK17B	18691	0.435	0.058	0.134	-1.864	1.181	0.509	0.833	Up
KLK4	9266	0.435	0.056	0.128	-1.917	0.611	0.767	0.833	Up
MMP7	12547	0.435	0.195	0.449	-1.766	0.914	0.564	0.833	Up
PKIA	15079	0.435	0.091	0.209	-1.341	1.934	-0.072	0.833	Up
SEMA4G	17316	0.435	0.033	0.077	2.063	-0.581	-0.856	0.833	Up
HYMAI	8289	0.435	0.071	0.162	-1.867	0.904	0.622	0.833	Up
FAM189B	5978	0.435	0.046	0.106	1.867	-1.396	-0.423	0.833	Up
FAM203A	6007	0.435	0.065	0.148	1.889	-0.765	-0.69	0.833	Up
CDH13	3350	0.435	0.067	0.154	-1.837	0.217	0.883	0.833	Up
SDHC	17243	0.435	0.047	0.108	1.931	-1.097	-0.578	0.833	Up
LOC728875	11559	0.435	0.082	0.189	-1.842	0.476	0.782	0.833	Up
GRID1	7502	0.435	0.023	0.053	-2.136	1.658	0.46	0.833	Up
FAM69A	6085	0.435	0.045	0.103	-1.921	0.236	0.921	0.833	Up
PDE1B	14728	0.434	0.042	0.097	-1.888	1.408	0.43	0.833	Up
PRR19	15746	0.434	0.056	0.129	1.816	-1.363	-0.41	0.833	Up
LIX1L	9715	0.434	0.04	0.092	-1.81	1.646	0.293	0.833	Up
PALMD	14494	0.434	0.073	0.167	-1.452	1.873	0.011	0.833	Up
DNM1P46	5067	0.434	0.053	0.123	-1.674	1.698	0.2	0.833	Up
LOC100131826	10220	0.433	0.048	0.11	-1.923	0.379	0.864	0.833	Up
C13orf33	1846	0.433	0.093	0.215	-1.768	1.197	0.451	0.833	Up
GABARAPL1	6854	0.433	0.055	0.126	-1.913	0.79	0.693	0.833	Up
ARFGAP2	897	0.433	0.035	0.081	2.026	-0.482	-0.877	0.833	Up
S1PR2	17047	0.433	0.054	0.125	-1.83	1.321	0.434	0.833	Up
ACTBL2	204	0.433	0.069	0.159	-1.801	1.24	0.452	0.833	Up
ANKH	647	0.432	0.069	0.16	-1.863	0.825	0.652	0.833	Up
EPB41L2	5587	0.432	0.058	0.133	-1.884	0.975	0.602	0.833	Up
A2M	5	0.432	0.084	0.195	-1.821	0.959	0.576	0.833	Up
TPST1	19874	0.432	0.067	0.155	-1.803	0.118	0.906	0.833	Up
SYPL2	18871	0.432	0.04	0.092	-1.744	1.747	0.217	0.833	Up
PCDH18	14608	0.432	0.052	0.12	-1.919	0.661	0.748	0.833	Up
MRPL21	12671	0.432	0.06	0.139	1.864	-0.363	-0.839	0.833	Up
LATS2	9526	0.432	0.043	0.1	-1.922	1.192	0.535	0.833	Up
FAM101B	5825	0.432	0.074	0.171	-1.836	0.417	0.803	0.833	Up
CSDC2	4233	0.432	0.042	0.097	-1.895	1.334	0.463	0.833	Up
HAX1	7724	0.431	0.045	0.105	1.949	-0.804	-0.706	0.833	Up
COL7A1	4000	0.431	0.093	0.216	-1.755	0.111	0.883	0.833	Up

Add. Table 3: GigniBcantly diBeZent exUessed genes between the metabHic clusteZs L c3 and L c0

Gene ID	Gene Name	Score (d)	Numerator (r)	Denominator (s+s0)	Fold Change	adjusted *P* value (%)	Direction
CAL	DI 28	8301D	15 03	153DD	715 88	1	4 U
pTG2	38038	- 5 30	15NN2	153N	715D82	1	4 U
G9 6 p0	3DF2-	- 5ND8	15F3F	1530F	715 D-	1	4 U
E6 CTR	3N - .	- 5ND0	353 3	1501D	715 8NF	1	4 U
TL MP 3	. D2.	- 5NF8	15 FD	153 . F	715 - -	1	4 U
pP TXL -	3- DD8	- 5D- 8	1588.	1533N	715F- 0	1	4 U
ACY0	82. D	- 5I28	15N00	153D-	7152 - D	1	4 U
SOHZ8D	- - 2D	- 5FDD	15F28	1532F	7350182	1	4 U
I AYL E0	F203	- 5F- 8	158NN	1530D	715 8N	1	4 U
6 SE6 0	010	- 5F23	353 28	1500-	715F2N	1	4 U
CGR	D88N	- 58N8	15FD-	153- D	7152FN	1	4 U
SVYF3	- 80N	- 58N-	3503	1502	715 83	1	4 U
TXL G0	. FN-	- 58- -	15F1-	1522	7158883	1	4 U
S6 TP 3	0N08	- 580N	15DN2	153D2	715 - 0	1	4 U
Ko To A- 3	381D	- 5813	15N83	153N	715 2.	1	4 U
ACY3	82. F	- 5 F3	353 83	1508N	7150	1	4 U
S6 r 0	0. - -	- 5 2.	15 - F	153	71 5F80	1	4 U
I MOMB	FD80	- 5 28	1588	1533N	7158. 3	1	4 U
XGL 3	NF. F	- 5	15 23	1503 0	7158 38	1	4 U
SRR3	2. 11	- 52N0	3508 0	150NF	7150F-	1	4 U
SECI	- 202	- 52F0	15 F2	1503	715 N-	1	4 U
SP 011	200N	- 5283	15 3D	153 . F	7152N0	1	4 U
I L M0	FF2.	- 5212	3501 8	150N	715F1D	1	4 U
STP R33	2D8N	- 50. -	15 1-	1503 3	715F33	1	4 U
RAOR	322. 8	- 508	1588F	1523	7152N-	1	4 U
EC1 K3X8	3. 0- -	- 500F	15F13	153- 0	715 FD	1	4 U
pYMG3	38D80	- 5000	15- 22	1512	7152 30	1	4 U
6 9 6 p30	- F8	- 500	15F. D	153F8	7158N0	1	4 U
L GYK2	30DDF	- 501N	15N0F	153. F	715 82	1	4 U
TEKp0	33NFD	- 53. 8	1582 2	1530D	7152FD	1	4 U
S 31HZ81	3FN8	- 5NF	15DNN	153NN	715 N8	1	4 U
SSP SN	21. .	- 5N8	15D-	153DD	715F3D	1	4 U
CY6 Gp	D- N-	- 5F8	158N	153- 3	715 38	1	4 U
1 Af 3	F20F	- 538N	15- FN	1532	715D	1	4 U
Yo MI	3F8- 0	- 583	158N-	153- 3	715 10	1	4 U
L VT9	30. 8N	- 53- F	15NN8	1530	7158 32	1	4 U
SGYp3	- 0DF	- 53-	15- 1N	151. .	715N82	1	4 U
6 YYP S2	31- F	- 530	1588	1528	715FN2	1	4 U
pEpR03	38. 8.	- 532	15F- -	1538F	715F0.	1	4 U
SP 2F	2088	- 512	3503 8	150NN	7158. 3	1	4 U
YCG0	3F810	- 5I. D	15 8	1502 0	715 28	1	4 U
L Yr X8	30D2.	- 5I. D	15FN2	153FD	715 . 0	1	4 U
6 RO6 3	D8-	- 5I. -	15N0N	1510	715 1D	1	4 U
RP R	320N0	- 5I. 2	15F. 3	153F.	715 . .	1	4 U
I OVP F	FN02	- 5IF.	1588	1528	7352 13	1	4 U
S. HZ8308	0FN-	- 5IF-	1582	1530-	715 1.	1	4 U
G3116 31	3DI08	- 5IF-	15F. 8	153D8	715 D8	1	4 U
AEG0	8D8D	- 5IF	15 D8	1533D	715 8	1	4 U
AL p3	880.	- 5180	15DD0	153DN	715F- 2	1	4 U
S8HZ8F0	081.	- 5I- .	15DD3	153DN	715 D2	1	4 U
I MGK	FFDF	- 5I- D	3508 2	1523	7158 1F	1	4 U
pT9 2	38012	- 5I- -	15- . .	1502	7150 80	1	4 U
pEYI	38. . 1	- 512N	15- 03	153 1-	7152 1.	1	4 U
L XY311o C	30- F2	- 512-	15D2.	153N2	7152 1F	1	4 U
P pVGT2	8381	- 510.	1 5NN	1503.	715 3-	1	4 U
ESI -	3. 330	- 5108	15F1F	1538	7152 8	1	4 U
S6 r 3	0. - 2	- 510	15D8D	153NN	7158.	1	4 U
STL p	2N21	- 510	15D13	153D-	7153 - F	1	4 U
P TS 3	- . 2F	- 513.	1582	153NN	7152 0-	1	4 U
Y6 GP 3	3F083	- 513.	353 NN	150D8	715 D0	1	4 U
P 9 9 2	- . 20	- 5138	158D8	153- 0	715 2-	1	4 U
SRR0	2. 13	25 . 8	15N1.	1510	715 - N	1	4 U
I MG	FFD8	25 . -	3508	150N0	715F3N	1	4 U
Gr Ap3	3NN0-	25 .	15- 3N	1518	7152F	1	4 U
CpON	D- D-	25 ND	15F. D	153D8	7150D8	1	4 U
R6 p3T2	321FF	25 N-	15 . F	1530-	715N1-	1	4 U
P 6 SE2	- 888	25 F.	15DN	153. D	715 3D	1	4 U
Y6 YYAG0	3F0- 1	25 8N	15 13	1500N	7152DF	1	4 U
6 pSP P3	NI.	25 - D	15N8.	1501D	715F- D	1	4 U
pP TXL 2	3- DD-	25 - F	15FND	153D-	7153D8N	1	4 U
L K03P 0	303- N	25 2D	15- D2	1510	735- N8	1	4 U
pMP R	380. F	25 0-	1588 0	153- 3	7152. 8	1	4 U
6 P o 3S	20-	25 1F	353 F.	150D-	7150 8.	1	4 U
I RP S-	FF8N	25 1-	15- N8	1530-	7153DI-	1	4 U
L VT.	30. 8F	25 13	15D8.	153. 8	7158883	1	4 U
Go MO0	3D8FF	25N 3	15- NN	1508	7152 2-	1	4 U
6 YT- S	. . F	25NN-	15FD-	153D2	7158F0	1	4 U
o GpK0	N022	25NF.	15N88	1533	713F- -	1	4 U
C6 P P - 8K	FNN2	25NF	1588D	1538	715 3N	1	4 U
ERG3	3. DN0	25N8F	15- 20	1530	7158 22	1	4 U
I KTR 8	F011	25N- 8	15D2D	153. 0	7152D8	1	4 U
I MOI 0	FF. -	25N- 3	152DN	151. .	7153NI.	1	4 U
L pf T0	30F2-	25N2.	15D0F	153N	735 21F	1	4 U
P pVGT0	83- .	25N2D	158DD	1538	715 2	1	4 U
RpS 0	32F3D	25N8N	15- 1N	1531D	713F- 0	1	4 U
o 3.	DFF2	25N8D	15N- -	1503	7153D2	1	4 U
pY9 P 3	38FF1	25N83	15 F-	1500	7158883	1	4 U
SATI 0	2- DN	25N8	15- 20	1532	7150NN	1	4 U
GC9 3	3D- D8	25NI8	15F10	1538N	715 2D	1	4 U
RRL E	32888	25D N	15NIN	1532	7150 82	1	4 U
pCL 8	3- N F	25D D	152F8	151. F	715F	1	4 U
GAYpXRC3	3D- 10	25D F	15- DN	1530F	7152DN	1	4 U
I KTR0	F3. .	25D	15NN2	1522	7152. 0	1	4 U
GAL 6 86	3D23D	25DN	15FD2	153DN	715 23	1	4 U
GR6 X0	3N822	25DN8	1581N	1532-	7150F0	1	4 U
GI Yp-	3D- -	25DDD	15NFF	1500.	715 22	1	4 U
TXL G2T	. FNF	25DF0	15- 13	1531D	715 0.	1	4 U
pY9 S6	38F- .	25D8N	15FD	153DN	7158 3	1	4 U
K6 So 0	32FF	25D8F	150.	153DD	715F0N	1	4 U
pXP 3	3- . N0	25D8-	15F- -	153D8	7152 20	1	4 U
P - GD2- A	- 8- 8	25D83	15F-	153D8	7351. -	1	4 U

Gene ID	Gene Name	Score (d)	Numerator (r)	Denominator (s+s0)	Fold Change	adjusted *P* value (%)	Direction
L L p3.	3082F	25D- D	15220	15!N	71!3D	1	4 U
ERI YGI 31P	3. DD2	25D- 2	15!0F	15!-	71!3DN8	1	4 U
r AC1 S	01F8D	25!2N	15. .	15!22	71!FN8	1	4 U
XC1 Kp2	N- 18	25!2D	15F1N	15!F2	71!0D8	1	4 U
pMP RT3	380. D	25!20	15!28	15!- 2	71!8N8	1	4 U
9 YE3D	. 23.	25!0.	35!8N	15- 3N	71!D. D	1	4 U
Gr 0K	3NN00	25!08	15!F8	15!80	71!FF0	1	4 U
pEC XG	38. 02	25!02	15F. D	15!ND	71!F00	1	4 U
S1 X	28FN	25!00	15!DD	15!88	71!88	1	4 U
L MOP 3	30F12	25!88	15D02	15!. 8	71!F03	1	4 U
r ST	01F- F	25!80	15- 8-	15!00	73!213	1	4 U
9 YE3-	. 238	25!83	35F32	15- 28	71!D. 3	1	4 U
9 YE3Fp0	. 23N	25!D8	35!12	15- 1F	71!DN2	1	4 U
P MS9 33	81N-	25!D2	1!8	15!28	71!- 1F	1	4 U
I 6 L N 6	F32.	25!D0	15F10	15!F2	71!81F	1	4 U
pP T!L D	3- DDD	25!D3	15!3.	15!-	71!8FF	1	4 U
YRP 2	3FF0N	25F. F	1!N8	15!03.	73!38-	1	4 U
pTGS Y-	3803.	25FN0	15!30	15!2.	71!F- F	1	4 U
TpS 6 E0	33F. 8	25FD	15223	15!.	71!2. 8	1	4 U
P GE	83N	25FDD	15F33	15!FF	71!2F0	1	4 U
S 6 P L 2	0N32	25FD2	15- 13	15!1.	73!3. F	1	4 U
YRI 3D8	3FFDI	25!FF	15!1N	15!N-	71!F2D	1	4 U
T6 VR	. 80N	25FF8	15!- 8	15!- .	71!FF2	1	4 U
GAYpX!I 3	3D- 11	25FF2	15DD0	15!. D	71!23N	1	4 U
I 6 Kp-	8NI -	25FF0	1!NN	15!0-	71!F- 2	1	4 U
9 YE- 0p	. 2- F	25F80	15!8D	15!080	71!5 0-	1	4 U
SOS T0	- - 12	25F83	15 2.	15D8D	71!5 - -	1	4 U
S P MB	2- 03	25F8	15DFF	15!03	71!FDD	1	4 U
XEpY)6	NDF3	25F- .	15!1.	15!3-	71!21D	1	4 U
9 TI 0	. 01-	25F- .	15!D	15!8.	71!5 1-	1	4 U
GW6 pDI	3NN0.	25F- -	15!2D	15!1-	73!3N8	1	4 U
EC I KY0	3. 0-.	25F-	15!8N	15!82	71!F2-	1	4 U
S S P S 2	2182	25F2N	15DB2	15!. F	71!5 . 2	1	4 U
GS R 2K	3D8. 0	25F22	15!18	15!2.	71!2DD	1	4 U
T2L KET2	. - D2	25F22	15220	15!. 2	73!30N	1	4 U
Gp6 YS T3	3N2F2	25F20	15N23	15!00.	71!5 FD	1	4 U
I MOQ3	FD8.	25F0.	15NF8	15!02N	71!F. -	1	4 U
6 MS 2	DDI	25F00	15D- 0	15!018	71!5- 3N	1	4 U
To I p	. F- 0	25F0	15FD8	15!3NF	71!0. 3	1	4 U
6 Y6 p2	NND	25F3N	15 . D	15!2D	71!5 F0	1	4 U
C6 G3	F. - 0	25F32	15DD8	15!032	71!80F	1	4 U
L 6 TT	30118	25F3	15 02	15!08F	73!3N8	1	4 U
6 XL 3	- - F	25F10	15DD8	15!038	70!828	1	4 U
L I 6 p-	302- D	25F10	35I. F	15!21-	71!81N	1	4 U
f I p2F	033. 3	25F10	15FF.	15!3NF	71!2FD	1	4 U
EGS 00P 2	011F.	25F	15- 8N	15!0D	71!F80	1	4 U
EGo f 0	011N8	25!. 8	15 . N	15!2N	71!5 0	1	4 U
GMKp	3N0DF	25!. 8	15203	15!3N	71!20D	1	4 U
o MO6 2	NI N	25!. 3	15DIN	15!. D	71!5 2N	1	4 U
L L p02K	308- 1	25!N2	15F3N	15!3D0	71!3D8F	1	4 U
pY9 SP Kp	38F80	25!N3	15F20	15!3DF	71!5 - .	1	4 U
GpYV0	3N- N2	25!F.	15FF8	15!3NF	71!5 23	1	4 U
L VM3K	30. D0	25!F8	15!2N8	15!31N	71!5 . D	1	4 U
GTXE2	3NI 2F	25!F2	15DI.	15!3. .	71!0F8	1	4 U
TYYR- S T	33N23	25!F0	15- D	15!328	71!5 3N	1	4 U
S FHZB3- 8	0822	25!F	15!3D	15!- 8	71!NFN	1	4 U
S S T3-	2320	25!8D	15 . N	15!0N8	71!5DF	1	4 U
SL EL 2	2ND-	25!8F	15!820	15!38	71!8NN	1	4 U
S 3G	0322	25!80	15FF-	15!ND	71!21.	1	4 U
6 RO6 2	DF3	25!83	15. .	15!0N8	73!3I . F	1	4 U
o MO6 -	NI . 1	25!- F	15!2F3	15!310	71!21.	1	4 U
pAS 6 L 3	3- N31	25!- F	15- 8D	15!30.	71!2. .	1	4 U
I 0YT3	8DND	25!- 0	15!2-	15!383	71!3D8N	1	4 U
I 6 G	F3NI	25!- 3	15!288	15!3	71!308.	1	4 U
L AEETD6	30228	25!220	15- N0	15!2D	73!3!8	1	4 U
pY9 P 2	38FF0	25!80-	15!83N	15!3- D	71!5DF	1	4 U
6 P o 36	200	25!80-	15ND-	15!0- N	71!8. -	1	4 U
YKp-	3F282	25!80	35!10-	15!0. 3	71!8.	1	4 U
E4 KKF	01083	25!83D	15FF8	15!3N	71!2882	1	4 U
AP R 3	822-	25!832	15DF8	15!03N	71!3DD0	1	4 U
r GRT3	01D- 1	25!833	15F. 0	15!3. D	71!F. D	1	4 U
L E3O	30D N	25!83	15FN0	15!3. -	71!308-	1	4 U
S TP R N	2DDD	25!83	15F2N	15!3N0	73!2NF	1	4 U
o X8 3	DND0	25!81.	15- F2	15!320	71!5F8	1	4 U
C pY30-	D2FD	25. .	15!88-	15!38N	71!3013	1	4 U
SSP SNI	2311	25 . N	1!FF	15!3N	71!28	1	4 U
6 P 6 L EG3	0F.	25 . D	15FF0	15!3N	71!8FF	1	4 U
S 3Y	0323	25 . F	15F- N	15!3N8	71!23N	1	4 U
I XKXR	F2N	25 . F	15F- F	15!3N8	71!2N2	1	4 U
6 YT- 6	. . 8	25 . -	15!2FN	15!318	73!3N-	1	4 U
pY)S 9 TA3	38F0D	25- NN	1!3D	15!00F	71!828	1	4 U
EXL p0	3. 2- -	25- NF	15DID	15!012	71!0N8	1	4 U
pYATp	38F3-	25- N2	15!3D	15!- .	71!5- N2	1	4 U
Ao P 0	8- 12	25- D0	15!81F	15!3- F	71!2N8	1	4 U
SpOL 3	- 32D	25- D	15!- F	15!38D	71!8- 8	1	4 U
GGpR	3N8N2	25- FD	15!8. F	15!3D0	71!2. N	1	4 U
CRC33	D0- 3	25- F8	15!8. D	15!3D0	71!22D	1	4 U
S1 o	28F0	25- F3	15!8D8	15!3FF	71!30D	1	4 U
XQS J7GS o X)3	NF- D	25- 8F	15- - -	15!30N	71!F. .	1	4 U
EpL 0	3. N82	25- 8F	15!8N	15!3D	71!5 12	1	4 U
6 P P 2	203	25- 8	1!FN	15!3. D	71!5 F8	1	4 U
9 TI 30	. 3. N	25 - 0	15- 2F	15!30D	71!F80	1!20-	4 U
6 R9 YP 28	F. 8	25- -	15NI 8	15!02-	71!5 F2	1!20-	4 U
RXP 3	32- 8F	25- 2N	15F- 8	15!3NN	71!308-	1!20-	4 U
9 YE8	. 2- D	25- 20	35!2F	15!2N	71!F- N	1!20-	4 U
EL AL 0116	3. 88-	25- 23	15 - .	15!23	71!288	1!20-	4 U
I 6 L - 26	F1- 1	25- 2	15- N8	15!- 3	71!81N	1!20-	4 U
EWXGE0	010DN	25- 2	1F!88	15!. 3	71!0NN	1!20-	4 U
S 33 HZ3 F	3DND	25 0F	15F- 0	15!3ND	71!5 3-	1!20-	4 U
9 X 0F6	. 383	25 08	15!2N0	15!330	71!N8.	1!20-	4 U
o MO6 D	NI . 2	25 02	15N0F	15!0- 3	71!5 D	1!20-	4 U
I GET3	FDDF	25 00	15D- 8	15!03N	71!2F.	1!20-	4 U

Gene ID	Gene Name	Score (d)	Numerator (r)	Denominator (s+s0)	Fold Change	adjusted *P* value (%)	Direction
AR pp0	88F0	25-3N	15&-3	15!8N	7!5&-2	1!20-	4 U
CYp	D82D	25-38	3!10F	15!	7!5D	1!20-	4 U
pP CI Y6	3-D8-	25-1D	15F. D	15!18	7!5!20	1!20-	4 U
f S2o 30K	03312	25-1D	15!82	15!D-	7!5!. F	1!20-	4 U
WP YNF	01N8F	25-1F	15N8D	15!-	7!5-0F	1!20-	4 U
pP A06	3-D!1	25-18	15F03	15!N0	7!5&3F	1!20-	4 U
I TR6	FF3D	25-18	1!2NF	15!32	7!5&8-	1!20-	4 U
p9 P 0	381D8	25-1-	15- - 0	15!2	7!5-03	1!20-	4 U
S TP R8	2DD-	25-13	15D- .	15!00	7!5FFN	1!20-	4 U
GMP 2	3N0NF	25!. .	15NN8	15!0F	73!30-	1!20-	4 U
GfS 306 -	3DFFF	25!. D	1!2N-	15!32	7!5&D0	1!20-	4 U
6 9 Y3S 3	- N	25!. F	15FF3	15!. 8	7!5ND	1!20-	4 U
TYSo 0	33D8D	25!. -	15!D8	15!N8	7!5-2N	1!20-	4 U
ppp3Y386	38-. 0	25!. -	1!2F.	15!1.	7!5-8D	1!20-	4 U
Y4 RO3E3	3F. . .	25!. 2	15F1N	15!D	7!5!1D	1!20-	4 U
CY!P 3	D810	25!. 3	15!88	15!- F	7!5-23	1!20-	4 U
GS 6 YR 6 3D	3D8- D	25!NN	15F8N	15!. -	7!5!D!	1!20-	4 U
o AC3	DNI.	2-!N	15&33	15!883	7!5&3.	1!20-	4 U
WE)6	01. 2N	25!DN	15&82	15!F-	7!5N	1!20-	4 U
ES A6 TD	3. 1. 0	25!DD	15- - 3	15!23	73!3F3	1!20-	4 U
o 6 Kp-	DFN8	25!DF	15- - N	15!22	7!5!- D	1!20-	4 U
L L A	3080-	25!DF	15&NN	15!D-	7!5!. 2	1!20-	4 U
SMI3- 6 3	2. FF	25!DF	15F8-	15!. -	7!5F32	1!20-	4 U
RMr	328. N	25!D8	15!2-	150 3N	7!5 02	1!20-	4 U
9 X6 6 1- 1N	. 10D	25!D2	1!2- F	15!12	7!5!2	1!20-	4 U
f RI 211p3	032. 1	25!F.	15&- D	15!F0	7!5!. F	1!20-	4 U
P 4 Gp3	803D	25!F.	15FF.	15!. N	7!5!2D	1!20-	4 U
GRO2	3N0F2	25!8.	150N2	15!N-	73!5 0-	1!20-	4 U
6 Yo C6 p0N	. 0F	25!8.	1!2D.	15!32	7!5!82	1!20-	4 U
6 9 Y3K3	- NF	25!8N	15!1F	15!83	7!5 2.	1!20-	4 U
MP f -	32N -	25!8-	150 88	15!DF	7!5 . -	1!20-	4 U
GRS 6	3N880	25!- .	1!2- -	15!12	7!5NF-	1!20-	4 U
S RER6 p2	2. - 1	25!2N	15&- 8	15!F2	7!5-2N	1!20-	4 U
P RL 3p- F	81FD	25!2F	1!2D0	15!30	7!5&- 0	1!20-	4 U
TYXC 2	33D!1	25!2F	15&DN	15!D!	7!5!2F	1!20-	4 U
P S R	- F2-	25!28	15N8	150 8	7!5!02	1!20-	4 U
9 T9 N	. 0DI	25!28	3!&2F	15- F3	73!3ND	1!20-	4 U
S 33HB3 2	3DN-	25!20	1!21-	15!. 3	7!5 - 2	1!20-	4 U
J4 R	NN81	25!08	15F- 3	15!. 2	7!5 0-	1!20-	4 U
R o G	32- 80	25!00	150. F	15!N	7!5 D0	1!20-	4 U
r XL	01FD2	25!03	1!83	15!8-	7!5!D8	1!20-	4 U
6 Tp9 0	8F.	2-!20	150N0	15!N8	73!830	1!20-	4 U
EGo f 2	011NF	25!3.	15&23	15!3F	7!5!N-	1!20-	4 U
SMI3N6 3	2. DI	25!3N	15&. 2	15!D	7!5!F	1!20-	4 U
J6 L 0	NDN2	25!3F	15- - 2	15!22	7!5!2	1!20-	4 U
f AK3	033FF	25!1D	15&02	15!8N	7!5!8.	1!20-	4 U
G)pY3	3DI - F	25!1F	15- . D	15!8	7!5F- N	1!20-	4 U
Go 2pOP 06	3D80N	25!10	15-F	15!2.	7!5!3N	1!20-	4 U
SP 9 R3S	2- 33	25!13	15F1-	15!N2	7!5&DD	1!20-	4 U
GSC8	3D8F8	25!. .	15&23	15!F3	7!5!. -	1!20-	4 U
GSo)6)3	3D8DD	25!. 2	15F33	15!N8	7!5!2- D	1!&2F	4 U
9 SRo N	NNN8	25!. 0	15-F-	15!- 3	7!5!D8	1!&2F	4 U
L L p0	3082D	25!N	15FN0	15!D1D	7!5 - F	1!&2F	4 U
TMY	33FD	25!ND	15008	15!FN	7!5D 3	1!&2F	4 U
SRYX)3	2. 08	25!N8	15!D-	15!N2	7!5!DD	1!&2F	4 U
L YS 0	30F- 3	25!N-	15F8D	15!	7!5!F.	1!&2F	4 U
pER	38. 2.	25!N2	3!5NN	15!20	7!5DD	1!&2F	4 U
S SRP 0	23F2	25!N0	15-N8	15!- D	7!5FF.	1!&2F	4 U
EYpS 3	0112N	25!N0	15-F.	15!- 2	7!5!8D	1!&2F	4 U
XP 2	N230	25!N	15-0F	15!2	7!5&N8	1!&2F	4 U
AEo A3	8D82	25!N	1!2DN	15!38	73!022	1!&2F	4 U
TMS 381F00	31FDF	25!D	15!. D	15!00	70!D- F	1!&2F	4 U
I o 6 P 3	F2D	25!8.	15!1N	15!F-	7!5NN0	1!&2F	4 U
XGTY	NF. -	25!8.	15FNF	15!33	7!5!3F	1!&2F	4 U
6 TMO8	8F-	25!8N	1!21N	15!. 8	73!2F8	1!&2F	4 U
S3- HB3 2.	3NF8	25!8F	15-0-	15!2	7!5&2N	1!&2F	4 U
I CI 3	F2- 3	25!80	15010	15!F0	7!50FF	1!&2F	4 U
pSG9 D	3- F. .	25!- N	15023	15!D8	7!5F2.	1!&2F	4 U
pECG0	38. 0D	25!- F	1!21N	15!. 8	7!5!DF	1!&2F	4 U
p9 X6	381D	25!-	15F- 2	15!. N	73!00F	1!&2F	4 U
S VEo 2	- 828	25!-	15&F8	15!D-	7!50F-	1!&2F	4 U
AI o 6 0	82FF	25!2N	1!2N2	15!3N	7!5!- -	1!&2F	4 U
9 SRL K-	N 0-	25!2N	15&D0	15!DD	7!5!80	1!&2F	4 U
GYpO	3N8- F	25!2N	15F83	150 13	7!5!3.	1!&2F	4 U
SI o Y2	28F8	25!2D	15&1D	15!88D	7!5!33	1!&2F	4 U
GVpT0	3NND8	25!2F	150DD	15!N8	73!I. 3	1!&2F	4 U
CpO2	D- F.	25!2F	15F28	15!. F	7!5F- 0	1!&2F	4 U
J6 C3	NDD-	25!28	1!2. D	15!02	7!5!D0	1!&2F	4 U
YpGF9 6 2	3FN N	25!22	1!2ND	15!0	7!5!. .	1!&2F	4 U
SAG3	28- 8	25!0N	15-DD	15!- N	7!5!8D	1!&2F	4 U
XECK3	NDDD	25!0D	1!2F-	15!32	7!5&3F	1!&2F	4 U
p6 TL P	3- - . -	25!0F	15&3-	15!58.	7!5&28	1!&2F	4 U
I f P D	FN2F	25!0F	15F2.	15!. N	7!5&3.	1!&2F	4 U
RY0I 3	32FDF	25!08	15 F	150. N	7!5FF-	1!&2F	4 U
SMI386 3	2. FD	25!08	15-N	15!80	7!50FD	1!&2F	4 U
I OVP 3	FN8N	25!02	15-3.	15!2	7!5F0F	1!&2F	4 U
YSKEK0	3F2FD	25!03	1!283	15!1.	7!5 - D	1!&2F	4 U
S 3DHB3	0111	25!03	15-0D	15!22	7!5!28	1!&2F	4 U
J6 f I 3	NDNF	25!00	1!28F	15!33	7!5 30	1!&2F	4 U
XC1 KpF	N- 1N	25!00	15&2N	15!FD	7!5 - D	1!&2F	4 U
pATX0	3- N3D	25!3N	15-D2	15!- D	7!5!02	1!&2F	4 U
S9 L E0	2D2-	25!30	150. .	15!. 2	7!5!. 3	1!&2F	4 U
r S6 R	01F- 8	25!3	15!DD	150F	7!5!DF	1!&2F	4 U
L 6 ER 0	3032N	25!1.	15F33	15!3.	7!5FD	1!&2F	4 U
6 QpDp3	NDF	25!1D	15-2-	15!28	7!5 - N	1!&2F	4 U
EL AL - 8K	3. F33	25!1F	15 02	150NN	73!DDN	1!&2F	4 U
GfS 06 3-	3DN0.	25!1-	1!2NN	15!03	7!5!NF	1!&2F	4 U
GI Yp0	3D - N	25!12	15NN0	15!D8	7!5-2	1!&2F	4 U
9 6 R9 0	NN8N	25!12	15-3N	15!23	7!5&10	1!&2F	4 U
6 RCpET0	F22	25!10	15F1N	15!3.	7!5!2N	1!&2F	4 U
6 REOY0	D83	25!13	1!23	15!. D	7!5!D	1!&2F	4 U
CTX8	D8- .	25!. N	15&38	15!F3	7!5F. N	1!&2F	4 U

Gene ID	Gene Name	Score (d)	Numerator (r)	Denominator (s+s0)	Fold Change	adjusted *P* value (%)	Direction
TXO3T	. D88	2S8. D	15DD	1SI NF	71.5F2	1.82F	4 U
L 6 pDP 2	301D0	2S8. F	15088	1.5I N	71.208	1.82F	4 U
1 6 E-	F3. 3	2S8. F	15000	1.5I D	71.21.	1.82F	4 U
6 TP o 36 2	832	2S8. F	15D83	15028	71.5D- 2	1.82F	4 U
GITI R32	3NI0.	2S8. 8	1.5830	1.53F	71.8ND	1.82F	4 U
1 6 E3	F3NN	2S8. -	1.5F82	15D1-	71.5- 8	1.82F	4 U
pSO9 8	3- F. D	2S8. 2	15DD8	1.5I NF	71.033	1.82F	4 U
GL 6 P.	3NI F0	2S8. 0	1.502N	1.5I D8	71.2- -	1.82F	4 U
S03HZB2-	00. F	2.8N	150. -	1.5I . 0	71.8- N	1.82F	4 U
pP A3K	3- D0N	2.8NF	15DDD	1.5I ND	71.28	1.82F	4 U
Ep82X2	3. N21	2.8NF	15- 8.	1.58- -	71.8NIN	1.82F	4 U
TGp3	33N8D	2.8N-	15- 3	1.530.	71.03N	1.82F	4 U
EL AL 31.	3. - 83	2.8N-	15- 22	1.52F	73.88D	1.82F	4 U
I 2	8D. 1	2.8N0	1.5DF	1.502.	71.88F	1.82F	4 U
I CI D	F2F1	2.8N	1.52FN	1.53F	71.028	1.82F	4 U
T6 L 6 -	. - N	2.8DF	1.52F8	1.538	71.88F	1.82F	4 U
TS 6 E	. 82F	2.8D2	1.52D8	1.53D	71.8. 0	1.82F	4 U
pT6 S.	3830-	2.8F0	15 - 2	1.58-	71.28-	1.82F	4 U
SMI3F6 3	2. FN	2.8F	15 3N	1.520	71.203	1.82F	4 U
EYXL 0.	3. . 8N	2.888	15 - 2	1.50. .	73.8 12	1.8N8	4 U
XC1 0	N2. F	2.882	15 38	1.520	71.5 00	1.8N8	4 U
P 6 K0	- 8- .	2.8- .	15 8N	1.58- 8	71.030	1.8N8	4 U
L YCpYI	30F- N	2.8- N	150. 2	1.5I . 2	71.N28	1.8N8	4 U
KCR	3811	2.8- 8	1.581N	1.5F3	71.5- D	1.8N8	4 U
pP pR	3- DN8	2.8- -	1.58F8	1.53N	71.5 83	1.8N8	4 U
YR I 3- - 6	3FF82	2.8- -	1.52.	1.530-	71.5I 82	1.8N8	4 U
TMS 3113. 1. 2.	312F2	2.8- 2	15- DD	1.5880	71.5F- D	1.8N8	4 U
SGP S0	- 022	2.8- 2	150D0	1.5I ND	71.5 20	1.8N8	4 U
RL K	32822	2.8- 0	1.58. .	1.58. 3	71.80D	1.8N8	4 U
ERRX0	3. DFF	2.8- 3	15 3	1.50.	71.8.	1.8N8	4 U
S2	02N	2.8-	1.5F- N	1.501F	71.N02	1.8N8	4 U
J6 L 2	NDN-	2.82N	1.52- 0	1.581.	71.202	1.8N8	4 U
6 SEKT0	01-	2.82N	15 - -	1.58- 3	71.5F88	1.8N8	4 U
YS6 R0	3F2F-	2.82-	1.528F	1.533-	71.5 8F	1.8N8	4 U
GTS 2N6 0	3DN 3	2.822	1.520	1.531F	71.888	1.8N8	4 U
L Y6 G	30F2.	2.822	1.8N8	1.5ND	71.5 03	1.8N8	4 U
L 6 p3K	30122	2.820	15- 13	1.50N	71.5D8	1.8N8	4 U
GpYV3	3N- N0	2.820	1.588-	1.5DD	71.5 82	1.8N8	4 U
r pG2F	01D88	2.80N	1.520	1.510	71.5 N2	1.8N8	4 U
EL AL 33.	3. - 8.	2.80N	1.5F-	15018	71.5FF	1.8N8	4 U
SEG9	- 282	2.80N	15D1-	15008	71.5 0D	1.8N8	4 U
GpRG0	3N- - .	2.80N	1.5FD0	15038	71.5N1F	1.8N8	4 U
EL AL - 2	3. F1N	2.80F	150FF	1.5I N8	71.08N	1.8N8	4 U
RAI L	32282	2.808	150N0	1.5I .	71.5F2	1.8N8	4 U
YKL G3	3F22N	2.808	15- D0	1.583	71.5I N	1.8N8	4 U
GP pY	3D0- D	2.808	1.5F3	1.5I . 8	71.23F	1.8N8	4 U
RAI o	32283	2.80-	1.580	1.5DD	71.500	1.8N8	4 U
L 6 CAT0	33. . 3	2.802	15- 0F	1.52F	71.812	1.8N8	4 U
ESI D	3. 332	2.802	15- 1-	1.50.	73.5- 23	1.8N8	4 U
6 KS6 F	- 0	2.800	1.528	1.5D8	71.5I . 8	1.8N8	4 U
L E3L	30D D	2.83N	1.5NI.	1.508.	71.50.	1.8N8	4 U
P R6 JK8	813N	2.83D	1.522D	1.51N	71.50. .	1.8N8	4 U
So 08o	28N8	2.83	1.5F2-	1.501-	71.222	1.8N8	4 U
CCE8	DI D0	2.81.	1.582F	1.5D0	71.222	1.8N8	4 U
SOST30	- 2. N	2.81F	15- 0D	1.52N	71.0FD	1.8N8	4 U
f I p2FT0	033. 2	2.81F	1.581D	1.5F2	71.88F	1.8N8	4 U
6 Yo C6 p01	. 3N	2.81-	1.522	1.51D	71.50. F	1.8N8	4 U
GYpO0	3N8- D	2.812	1.5F23	1.5012	71.0D2	1.8N8	4 U
seUS1	3D2- 3	2.812	15 - 8	1.5I - 2	71.5 . -	1.8N8	4 U
YMKM2	3FD22	2.810	1.523F	1.510	71.8N2	1.8N8	4 U
XTN	N828	2.8NF	150- -	1.5I D	73.82-	1.8N8	4 U
L OY6 8	30. 13	2.8N8	15- 2	1.52.	71.0DD	1.8N8	4 U
6 Cp6 E-	- 1-	2.8N-	1.523	1.51D	71.8D-	1.8N8	4 U
YGpM2	3F. F2	2.8N0	15- 18	1.523	71.2. F	1.8N8	4 U
CTENP 0	D8N0	2.8N0	1.528D	1.53F	71.8- 3	1.8N8	4 U
6 9 Y3K38	- NN	2.8N	15DDN	1.582	70.820	1.8N8	4 U
Go I	3D881	2.8N	1.508D	1.5N2	73.NN	1.8N8	4 U
6 9 6 p32	- FF	2.8DN	150NF	1.5I . 2	71.22N	1.8N8	4 U
L AC2	300D8	2.8D	15- 1N	1.522	71.508	1.8N8	4 U
pYRp	38FNN	2.8D	1.58FF	1.5N-	71.0N8	1.8N8	4 U
EpL -	3. N88	2.8F.	15- 82	1.5I - D	71.50	1.8N8	4 U
6 P YK0	28F	2.8F.	1.528	1.5D-	71.NFN	1.8N8	4 U
6 REOY3	D81	2.8F8	1.8-	1.5I DF	71.5- N8	1.8N8	4 U
4 6 S6	01202	2.8F-	1.582	1.538	71.81F	1.8N8	4 U
f I o O-	033N8	2.8F-	1.508	1.5I D8	71.208	1.8N8	4 U
P 6 SE3	- 882	2.8F0	1.5F0-	1.501-	71.5 12	1.8N8	4 U
AI RK0	82DN	2.8F0	15- F0	1.583	71.8N2	1.8N8	4 U
f S So S0-	03321	2.8F	1.530	1.5FD	71.N2	1.8N8	4 U
p6 TTP	3- - . 1	2.8F	1.52N-	1.50F	71.222	1.8N8	4 U
L VML 3	30. . -	2.888	1.512	1.5I .	71.2D8	1.8N8	4 U
YMY3	3FD- 2	2.888	150. N	1.5I . N	71.30D	1.8N8	4 U
6 6 GG	0D	2.882	1.52D8	1.503	71.5F2.	1.8N8	4 U
9 TI F	. 01N	2.882	1.523N	1.531-	71.5- FD	1.8N8	4 U
Ko To A00	381-	2.8I8	1.581N	1.53FD	71.5- 2.	1.8N8	4 U
RE8A	32D- D	2.8I - 8	1.528-	1.53F	71.8FN0	1.8N8	4 U
XAY0	N20N	2.8I - 8	15 - D	1.5I - D	71.5N08	1.8N8	4 U
pP CI YK	3- D88	2.8I - 8	1.580-	1.5D0	71.50.	1.8N8	4 U
L Y6 p0	30F2N	2.8I - 3	1.52N	1.508	73.83.	1.8N8	4 U
ApCR	88. .	2.8I 23	1.5I . F	1.5I F8	71.5ND	1.8N8	4 U
L P I XS	3003N	2.8I 0D	1.52- .	1.538	71.I 3F	1.8N8	4 U
6 0L	8	2.8I 0D	1.581F	1.53FD	71.30N	1.8N8	4 U
SMITF6 0	2. . 8	2.8I 02	1.5F38	1.501-	71.5- F8	1.8N8	4 U
6 EI 2	33- D	2.8I 02	1.5- N-	1.53F	71.30N	1.8N8	4 U
KKMO3	3- 31	2.8I 00	1.5N- .	1.50N8	71.5 N-	1.8N8	4 U
6 RCpET-	F28	2.8I 00	1.5ND0	1.50NN	71.52N	1.8N8	4 U
I o T2	F2N-	2.8I 00	150- N	1.5I N0	73.0D	1.8N8	4 U
CpY6 Gp3	D- 81	2.8I 03	1.5- 1-	1.532-	71.32N	1.8N8	4 U
P P Y0	- FD-	2.8I 0	15- 3D	1.52N	71.22-	1.8N8	4 U
S 3QER I -	030-	2.8I 3.	1.52-	1.532	71.382	1.8N8	4 U
SP 9 T8	2- 1N	2.8I 3.	1.52. 0	1.52	71.F8F	1.8N8	4 U
S01HZB12	002-	2.8I 3N	1.5F. D	1.523	71.5 . N	1.8N8	4 U
Spf	- 32.	2.8I 3D	1.5- D8	1.58F	71.F1N	1.8N8	4 U

Gene ID	Gene Name	Score (d)	Numerator (r)	Denominator (s+s0)	Fold Change	adjusted *P* value (%)	Direction
GpMR3	3N- 8F	2Sl 3F	1SN83	1S0N0	71S2- 8	1SN8	4 U
TMS 0N22. 0	31D. 8	2Sl30	15- 3.	1S52.	71S01.	1SN8	4 U
L CS 0- 312	302. D	2Sl30	15F0N	1S01.	71S002	1SN8	4 U
S T3p2	2N03	2Sl33	152- 2	1S33-	71S38-	1SN8	4 U
R C I Y	32- 2D	2Sl3	1582N	1S3D	71S022	1SN8	4 U
G6 6 3	3DI83	2Sl1N	350ND	15- 0N	71SDID	1SN8	4 U
XC I KpD	N- 1.	2Sl1N	15 . F	1S5F8	71S812	350032	4 U
S 32HZE22	3N- F	2Sl18	15F13	150	71S8-	350032	4 U
seUS53	3D2- 0	2Sl1-	15- D.	1S58N	71S22	350032	4 U
S Vp04 3	- 812	2Sl12	152222	1S333	71S018	350032	4 U
o TI	D . .	2Sl10	15F83	150 3D	71S 82	350032	4 U
Y6 YK	3F02D	2Sl10	1501F	1SIF.	73S IF-	350032	4 U
L AE	3021-	05 . .	15D8	1508	71S D8	350032	4 U
P GA	83Nl	05 . .	152. .	1S222	71S883	350032	4 U
6 P 6 L EG8	0N2	05 . F	158. F	15I. .	71S003	350032	4 U
I MOR 2	FD81	05 . F	1S208	1S31N	71SF80	350032	4 U
pS MTS A0	3- FNN	05 . F	15D12	150 28	71S2F	350032	4 U
YR I 2.	3FDI 0	05 . 8	152F0	1S303	71SNl-	350032	4 U
S S P S 81	21FN	05 . -	150F0	1SI NN	71S NF	350032	4 U
TMS 8D088N	330. 2	05 . 2	15003	1SI D.	71SD8-	350032	4 U
9 T9 D	. 0F.	05 . 2	3S102	152- 0	73S2- D	350032	4 U
AKI 3	80. 2	05 . 0	1523	1S31-	71S0D-	350032	4 U
T6 EG0	. 80F	05 . 3	150D	15I.	71S83N	350032	4 U
9 YEFS	. 281	05 . 3	15DN8	150F2	73S8. 3	350032	4 U
S 2HZE8D	0- 02	05 NN	152DN	1S50D	71S 88	350032	4 U
GTS 06 2	3DN23	05 ND	15I. N	15IFF	1S13F	350032	4 U
R pY0	32F- 0	05 ND	152ND	1S32	71S080	350032	4 U
CI pE0	DI8-	05 NF	1S812	15IF.	71SI - N	350032	4 U
9 YEFK	. 2- .	05 NF	352N2	15 F2	71S0ND	350032	4 U
S . HZE2	0D0.	05 N-	15F2-	150 30	71S28	350032	4 U
f AK0	033FN	05 N	152- -	1S338	71SI . D	350032	4 U
P f Xp3	80DF	05 N	15 33	1S52N	71S 0D	350032	4 U
L Vo 33	30. 20	05 N	15 FD	152 0-	71S0D	350032	4 U
S Y0	- 3- 0	05 DN	15F- 3	15038	70SI 0D	350032	4 U
P f Xp3T	80DD	05 DN	1523.	1S31D	71S8-	350032	4 U
GVR pM	3NNF-	05 DD	152-	1S33-	71S 0-	350032	4 U
Apo KF	8F32	05 DF	15 2N	1S9- D	71S8N	350032	4 U
XC I 3	N2. -	05 DF	15F3-	150 1F	71S 1F	350032	4 U
o XI 36	DND-	05 DF	15 1F	1S52F	71S83-	350032	4 U
S GYp0	- 0DD	05 D-	15802	1S0DF	71S D8	350032	4 U
T6 L 6 3	. - NF	05 D0	1S230	1S518	71S080	350032	4 U
f I p2FT3	033. 0	05 FD	15 FN	1S38N	71S8- D	350032	4 U
L L YR3	30881	05 F8	15 F3	1S988	73S8- 0	350032	4 U
Cp X6 Kp3	D2- -	05 F8	15F- D	150 3N	71S08.	350032	4 U
I XI Xp3T	F2. .	05 F8	1S21F	1S512	73S808	350032	4 U
P AI K3	- D2F	05 F-	15NI N	150D2	71SFND	350032	4 U
GMS G8	3N0N3	05 F2	1S21D	1S51-	71S 3	350032	4 U
9 S EP 30	N - .	05 8.	15 8	1S580	71S00D	350032	4 U
Go 2pOP 0K	3D80.	05 8N	15 2.	1S5- N	71S 2.	350032	4 U
GRS 6 Xp	3N882	05 88	1S3FD	1S18F	71SN08	350032	4 U
AL O0MG	882N	05 88	15 F8	1S58D	71S28F	350032	4 U
p0YV3	3- - 08	05 8-	150. .	1S513	71S2D	350032	4 U
EKO38	3. 1FN	05 - .	15088	1SI ND	71S223	350032	4 U
GMS G0	3N0DN	05 - N	15N3	150D8	71S F8	350032	4 U
I 6 p	F3D0	05 - D	15F. 0	15028	71S0N8	350032	4 U
I 6 L 31D6	8N28	05 - F	15F1-	15018	71SF- N	350032	4 U
o MO6 3376 G8	NI NF	05 - 8	15 1-	1S52D	71S330	350032	4 U
9 TI D	. 01.	05 - 3	152N	1S50.	71S 0D	350032	4 U
p6 Yr 6	3- 88D	05 -	152D	1S30F	71S88N	350032	4 U
L 6 p- 9 -	301F8	05 2N	1521F	1S51-	71S23F	350032	4 U
S MI 26 3	2. N2	05 28	15DD	150F0	71S00F	350032	4 U
XI 22	N83D	05 28	158. .	1501-	73S I - F	350032	4 U
6 S ER3	03-	05 2-	15 N-	1S3F8	71S822	350032	4 U
S YXCpTP 0	- 3N2	05 20	152D8	1S50D	71S810	350032	4 U
S YV6 K	- 01.	05 0.	350	152- N	71S 2	350032	4 U
T3R CM0	. F. F	05 0F	1523	1S31F	73S - 8	350032	4 U
S 3QER I 8	0308	05 02	158- 2	1S3NF	71SF1N	350032	4 U
JP p0	NDND	05 02	152. F	1S328	71S202	350032	4 U
GE6 YP N	3NFF3	05 0	150ND	15I. N	71S02N	350032	4 U
6 Yo C6 p31	. 31	05 3.	1528.	1S502	71SF- D	350032	4 U
S VTP	- - F.	05 3F	150D0	15I. 2	71S3. -	350032	4 U
GE9 3DK	3NF. 3	05 38	152FN	1S30F	71S210	350032	4 U
pp6 pP S2	38- 0-	05 3-	150D8	15I. 2	71S1D	350032	4 U
CR 6 X8	D001	05 3-	15	1S52D	71SFN	350032	4 U
S 3HZE387RKT3	03F2	05 32	158D0	15I. F	71S23-	350032	4 U
EA9	3. 3D0	05 30	15- - -	1S582	71S 8F	350032	4 U
S 3QER I 3	0303	05 3	1523	1S51D	71SF3.	350032	4 U
o MO6 .	NI. -	05 1.	15 1.	15I- 3	71S28	350032	4 U
GEOD	3NDI83	05 1F	1508	1S1NF	71S - 2	350032	4 U
S 01HZE3. -	008N	05 1-	150N2	15I. D	71S00	350032	4 U
GTI R33	3NI 0F	05 1-	15 - D	1S58-	71S822	350032	4 U
TV. F	33N .	05 12	15 0.	15I- N	71S22N	350032	4 U
YS6 R3	3F2F2	05 12	15F3.	1S032	71SD .	350032	4 U
S T3p-	2N00	05 10	15 30	15I- 0	71S03.	350032	4 U
Y6 GCYp0	3F0F1	05N D	15 - 0	1S582	73S003	350032	4 U
EGp6 R3N	01318	05N 8	1528 8	1S502	71S2DN	350032	4 U
GpMR0	3N- 8D	05N -	152- D	15I0	71S2. .	350032	4 U
f L 6 E2	030- 2	05N 2	150F-	15I. 3	71S0D8	350032	4 U
RSM6 D	323- D	05N 3	158NF	15012	71S083	350032	4 U
6 P 6 L EGN	0NF	05NNF	158- -	15IN	71SF2.	350032	4 U
J4 R K	NN83	05NNF	152DN	1S323	71SD- 8	350032	4 U
pp X8	38- - .	05NN8	15 D8	1S5F2	71S0NF	350032	4 U
R4 P E. p3	32NI 2	05NN0	150D8	15I. 8	71S8. 0	350032	4 U
TL M0	. D28	05NN3	15 1F	1S9- 3	71SFN8	350032	4 U
YCL 6	3F- N2	05NN3	15F02	1503F	71SFDF	350032	4 U
S TAS 36	2D. 1	05NN3	152- D	15I0	71S2. -	350032	4 U
S P . 2	20. 8	05NDF	152.	1S52F	71SNDN	350032	4 U
L OY6 N	30. 12	05NDF	158D	15013	71S082	350032	4 U
6 S r Y06	02-	05ND8	150D8	15I. F	71S0N8	350032	4 U
S FHZE3D-	08- 8	05ND2	152- 8	15I0	71SIF-	35 F	4 U
YpT03p- -	3FD. 0	05ND2	15 8	1S58D	73S N	35 F	4 U
G6 S G	3DI8N	05ND2	1S210	1S518	71S08N	35 F	4 U

Gene ID	Gene Name	Score (d)	Numerator (r)	Denominator (s+s0)	Fold Change	adjusted *P* value (%)	Direction
L OY6 D	30. 10	05ND0	15Z3D	15I3	715-2	35-F	4 U
pY4 RA0	38NI N	05ND8	150D2	15I. 8	715R3	35-F	4 U
S TS6 0	2D-0	05ND8	15DF0	150FF	705-8F	35-F	4 U
L MK9 T0K	308FF	05ND	15Z1N	15I1D	71S22N	35-F	4 U
SSP SN0	2310	05ND	15- -.	15I8D	71S22F	35-F	4 U
AL XTXR3	8801	05NF.	15. . -	15I5D0	71I52	35-F	4 U
Ap6 G3	88N-	05NFD	15-N2	15IFN	71I588	35-F	4 U
XEX6 8	ND- -	05NFF	15I0N	15I- 8	71I50D3	35-F	4 U
pTP 3	38380	05NF8	150DN	15I. D	71I5 -	35-F	4 U
6 ET3	33D-	05NF-	15- 12	15I3- 3	73I5I. N	35-F	4 U
o EY6 3	N0DI	05NF-	15I2.	15I08N	71I50- D	35-F	4 U
S6 pR8	0NDF	05NF0	15- - -	15I888	71I50F-	35-F	4 U
TC6 TG2	. F0-	05NF	15Z1D2	15I523	71I5D00	35-F	4 U
S3P A6	2DI F	05N8.	15RN8	15D12	71I588-	35-F	4 U
Ar S0	8D0D	05N8N	15038	15I.D8	71I5I. 2	35-F	4 U
6 R9 YP 2D	DI1	05N8F	15- 28	15I580	71I5N00	35-F	4 U
TXbA	. DI0	05N8-	15I2-	15I08D	71I5 -	35-F	4 U
I RP S3	FF88	05N82	15F18	15I030	71I5F13	35-F	4 U
TMS 311818. 22	31- F3	05N80	15I00-	15I1DN	71I5FFD	35-F	4 U
GVP A3	3NN- 3	05N83	15I. .	15I1D	71I580	35-F	4 U
TP K0	. 8D-	05N- .	150. F	15I31-	71I588.	35-F	4 U
K2C6 E3	3222	05N- .	1580	15IN2	71I58- 8	35-F	4 U
pP 9 -	3- DD8	05N- N	15DD8	150D0	71I5 2D	35-F	4 U
pP CI YT	3- D8F	05N- D	15D0D	15088	71I502D	35-F	4 U
pYYO0	38DD8	05N- D	1583.	15IN0	71I5 DF	35-F	4 U
Gp6 YS	3N2F0	05N- D	15FF.	15028	71I53F	35-F	4 U
L AS ML	3002F	05N- -	15Z3D	15330	71I583N	35-F	4 U
R1 XK	32- 32	05N- -	158DB	15013	71I58- 0	35-F	4 U
pp6 p06	38- 3N	05N- 2	15I2.	15I2D	71I5022	35-F	4 U
p0YV3-	3- - 0.	05N- 0	15I2DD	15I22	71I5D	35-F	4 U
o Gp6 30K	N03N	05N-	15- 0N	15I83	71I52DD	35-F	4 U
TMS 311321DDF	311. .	05N2N	1508.	15I. 3	71I5F8N	35-F	4 U
EpE3	3. NDF	05N2F	15I2- 2	15I03	71I5N8-	35-F	4 U
AEr 3	8DBN	05N2F	1508-	15IN	71I503.	35-F	4 U
Gl Yp3	3D - D	05N22	15 D0	15I2- 2	71I5F0N	35-F	4 U
S VG3	- 80.	05N22	158- D	15I. 2	71I5038	35-F	4 U
pTOP S3	3800-	05N20	15213	15I1F	71I5223	35-F	4 U
pAY3	3- N0-	05N20	15 -	15I88	71I52FF	35-F	4 U
pMEAI	382N	05N20	15I2- -	15I03	71I58- 3	35-F	4 U
6 AKp3	2F-	05N20	15D1N	1508	71I52D3	35-F	4 U
6 RO6 NT0	DFF	05N23	3I5N8	15 3.	71I5F-	35-F	4 U
9 X6 6 3- F0	. 1ND	05N23	15- 3.	15I3- N	71I50D3	35-F	4 U
I YAL 3	FD2D	05N0N	150D	15I. 8	71I52. D	35-F	4 U
TMO	33FNI	05N0N	158DF	15D1-	71I5. D	35-F	4 U
Y6 KDF3	3F32N	05N0F	15I2DN	15I2-	71I50F3	35-F	4 U
9 XYYAT	. 3N0	05N08	15IFN	15I32	71I5883	35-F	4 U
S3- HH2D	3N 0	05N08	15IF3	15I30N	71I5082	35-F	4 U
P S T9 0	- F0.	05N00	150D2	15I. D	71I5 18	35-F	4 U
9 T9 8	. 0FD	05N0	3I5I2-	15I2FD	73I5F- 0	35-F	4 U
TVT3	33. 12	05N8.	1501N	15ID-	73I523-	35-F	4 U
CTXbY3	D882	05N8N	150. 0	15I31-	71I581F	35-F	4 U
6 SER2	03F	05N8D	150. -	15I31-	71I5FNF	35-F	4 U
XEL 06	ND- .	05N88	15F2.	1500D	71I5D88	35-F	4 U
G3pY0	3DI - D	05N8-	15288	15I50F	71I5 8F	35-F	4 U
TMS 22. 80-	33113	05N82	150- 3	15INF	71I5203	35-F	4 U
ECL 8	3. 08.	05N83	15I- -	15I83	73I58FF	35-F	4 U
SDHH3B1	08N0	05NI8	15Z- 2	15I500	71I503N	35-F	4 U
pT6 CT3	3830F	05NI2	150N0	15I513	71I5223	35-F	4 U
YAS 9	3F2. 8	05NI0	15Z0	15I33-	71I5033	35-F	4 U
L L pD	308- D	05NI3	3I5IFN	15- 3D	71I5 8.	35-F	4 U
S6 SR6 0P 3	0D. 2	05N	15002	15IN	15I588	35-F	4 U
K6 So 3	32F8	05D .	1501N	15ID-	71I58N	35-F	4 U
f I pL 0	0301F	05D F	15- 18	15I- 8	71I5838	35-F	4 U
6 P pYo	2- F	05D F	15Z- F	15I30-	71I5018	35-F	4 U
pTA9 o o 0	383N-	05D F	150N0	15I513	71I5102	35-F	4 U
TYYS 20	33DD-	05D 8	15R1-	15IN	71I5 1.	35-F	4 U
GVR0	3NN- D	05D -	15Z2	15I33N	71I500-	35-F	4 U
RMES o -	328. 8	05D -	15Z2N	15I52F	71I50- 0	35-F	4 U
TMS D0N2. 0	33820	05D 0	15- 0F	15I580	71I58F-	35-F	4 U
GTS D6 31	3D. N0	05DN	15- F0	15IFF	71I5838	35-F	4 U
SP S3- K	221F	05DNF	15I. F	15I1D	71I5022	35-F	4 U
pr YT2	3F13N	05DN-	150FN	15I. F	15IDF	35-F	4 U
CVpS	DF82	05DN3	15003	15I1D	71I583.	35-F	4 U
r AC1 K	01F8F	05DN3	150. 3	15I31-	71I5 2F	35-F	4 U
6 P XbMQ	220	05DD-	15F3D	15I000	71I5 1-	35-F	4 U
p6 O3	3- 8DI	05DDD	15- 80	15IF2	71I58.	35-F	4 U
L AC1 F	300D.	05DD8	15- F	15IFF	73I5FD2	35-F	4 U
Y6 K02	3F1. 0	05DD-	15ZN	15I3-	71I52- D	35-F	4 U
GTS 0F6 2	3DN1 -	05DD	15R0D	15I3.	72I5FN	35-F	4 U
P 6 YS	- 8D2	05DF-	15- 1.	15I3- N	73I50F	35-F	4 U
I 0Y	8DNF	05DF-	15Z1.	15I330	71I508F	35-F	4 U
EL AL 01-	3. 8F1	05DF-	15ZN8	15I52.	71I52- 0	35-F	4 U
SVVY3	- 82.	05DF0	15Z1N	15I533	71I5FF	35-F	4 U
AL O0	882D	05DF3	150F.	15I. D	71I5 32	35-F	4 U
GTS 3F6 D	3DF. 8	05DF3	15013	15IDI2	71I518-	35-F	4 U
P 4 GpF	802N	05D8.	15R2N	15I3. 8	71I52- -	35-F	4 U
TMS 311321NDF	31331	05D8.	15R2F	15I3. -	71I5N-	35-F	4 U
GSR0K	3DB. 1	05D8N	150F-	15I. F	71I580.	35-F	4 U
EKS 3P 0	3. 103	05D8D	15Z FD	15I522	73I5213	35-F	4 U
f P o o S2	0338N	05D8D	1508	15I. 3	73I5038	35-F	4 U
6 9 Y3K31	- ND	05D8F	15D0.	15I0F-	70I58F2	35-F	4 U
L E3T	30D F	05D8F	15R- 8	15I3. N	71I5ID2	35-F	4 U
o VL 6 X	N0N	05D8F	15-3-	15I38	71I5NN	35-F	4 U
6 Yo CAI - 1	. F8	05D8F	15Z. F	15I3- -	71I5F8	35-F	4 U
9 TI 31	. 3. F	05D88	15Z. 8	15I3- 2	71I5 82	35-F	4 U
SS T02	23- 0	05D88	1501.	15IDF	73I5FN	35-F	4 U
I 31	8DD	05D8-	15I- -	15I80	71I500-	35-F	4 U
EL AL 311	3. - - 3	05D80	15Z- 8	15I50F	71INID	05I. 8	4 U
SMT3D6 3	2. F.	05D- N	15F. D	15I08-	71I52-N	05I. 8	4 U
L 6 L P S0	3011D	05D- N	15Z28	15I500	71I3- D	05I. 8	4 U
pA6 9 3	3- NI F	05D- D	15Z30	15I33-	71I500-	05I. 8	4 U
EWXGE3	010DD	05D- D	15ZF0	15I320	71I5820	05I. 8	4 U

Gene ID	Gene Name	Score (d)	Numerator (r)	Denominator (s+s0)	Fold Change	adjusted *P* value (%)	Direction
Al RK3	82DD	05D- D	15ΩN8	15ß-	71ß0FD	05ß. 8	4 U
pTΧR3	383. 8	05D- F	15ΩßN	15ß0F3	71ß5F0-	05ß. 8	4 U
6 MO3	DD0	05D- F	15Ω2N	15ß2N	71ß8- 8	05ß. 8	4 U
I 6 L 016	F11.	05D- F	15- 13	15ß- F	71ß5.	05ß. 8	4 U
S 33HΨBB8	3DD0	05D- 8	15- NF	15ß0D	71ß0D	05ß. 8	4 U
ΧEC6 r	ND08	05D- -	15- 2F	15ß8.	71ß5F83	05ß. 8	4 U
S 4 O0	- 2N2	05D- 2	150. D	15ß1N	73ß0B0	05ß. 8	4 U
CYK31	D- NF	05D-	15Ω.	15ß- 0	71ß5FFF	05ß. 8	4 U
YpT03	3FD 3	05Ω2.	15Ω0DD	15ß2N	73ß0D-	05ß. 8	4 U
S S T0N	23- D	05Ω2N	15N-	15Ω1N	71ß5N82	05ß. 8	4 U
I TYE0	FF02	05Ω2N	150- .	15ß. 3	71ß5D10	05ß. 8	4 U
KEKP 33	3F2D	05Ω2N	15ΩN-	15ß-	73ß5F0D	05ß. 8	4 U
I 6 L 3F- 6	8. 0N	05Ω2F	15Ω23	15ß03	71ß5D- .	05ß. 8	4 U
R OR	32N- 2	05Ω2F	150. D	15ß1.	71ß0N0	05ß. 8	4 U
CCE6 3p	DI DF	05Ω28	15- 13	15ß- F	71ß5 DN	05ß. 8	4 U
GTΧE0	3NI 28	05Ω28	15ΩFD	15ß2-	71ß0ND	05ß. 8	4 U
po Vo Χp	3- . F8	05Ω2-	15Ω2N	15ß ND	73ß1- 3	05ß. 8	4 U
I TJ2F123	F832	05Ω20	15Ω. F	15ß- 8	71ß- -	05ß. 8	4 U
Eo GP D6	3. 218	05Ω23	15Ω- 8	15ß0F	71ß5F82	05ß. 8	4 U
S ERRK3	- 220	05Ω23	15Ω20-	15ß3.	71ß5NIF	05ß. 8	4 U
T6 L K3	. - . 3	05Ω23	150Ω12	15ß D-	71ß5N8	05ß. 8	4 U
AEG3	8D8F	05Ω2	15Ω83	15ß. 0	71ß5 D8	05ß. 8	4 U
r CTT2	01FFD	05Ω0-	15Ω2-	15ß NF	71ß1N0	05ß. 8	4 U
ppp3Y32T	38- ND	05Ω0-	15ΩF2	15ß22	73ß1. 2	05ß. 8	4 U
6 KS6 N	- -	05Ω02	15Ω- .	15ß0N	71ß8F-	05ß. 8	4 U
6 L MET0	F1F	05Ω03	15ΩD8	15ß2N	71ß5ß8	05ß. 8	4 U
9 Χ6 6 1. 00	. 183	05Ω0	15Ω80	15ß0.	71ß5Nß3	05ß. 8	4 U
S 6 YP F	0N N	05Ω8.	15Ω. .	15ß- D	71ß0N	05ß. 8	4 U
I 6 L 01S	F133	05Ω8.	15- -	15ßF0	71ß5 D0	05ß. 8	4 U
L 6 I K	33. 88	05Ω8.	15ΩF8	15Ω2-	71ß5 NN	05ß. 8	4 U
TMOT0	33FN2	05Ω8N	15ß- 0	15Ω	71ß1ß32	05ß. 8	4 U
Tpo R0	33D0 1	05Ω8N	150F	15ß. F	71ß0- 0	05ß. 8	4 U
EKS 3P 0K	3. 122	05Ω8N	150D8	15ß	71ß2DD	05ß. 8	4 U
TMR YI 2	33FDN	05Ω8F	15ΩN8	15ß- 0	71ß8N0	05ß. 8	4 U
ΧP 3	N231	05Ω8-	15ß. D	15Ω0	71ß5 FN	05ß. 8	4 U
I 6 L F8K	F1NI	05Ω8-	15- 10	15ß- N	73ß1F	05ß. 8	4 U
P P O- 2	- DI0	05Ω8-	15- DΩ	15ßD-	71ß0F2	05ß. 8	4 U
Χ6 6 L 8	N21-	05Ω82	150NF	15ß18	71ßD D	05ß. 8	4 U
TApY	. F1F	05Ω82	15ßN2	15ßFD	71ß8- 0	05ß. 8	4 U
I TJ- 0DI.	F8DI	05Ω80	15Ω2N	15Ω08	71ß5 F	05ß. 8	4 U
ACY2	82. N	05DI N	15F. 0	150ß8	71ß22.	05ß. 8	4 U
P P O0FK	- F. 3	05DI N	15Ω30	15ß38	71ß0FF	05ß. 8	4 U
EI 6 p0K	3. 038	05DI D	3522.	15ß. 8	73ßND	05ß. 8	4 U
SpAK3	- 1. .	05DI D	15- D	15ßF8	71ßFDD	05ß. 8	4 U
I 326 3	8DN2	05DI8	15- 00	15ß8F	71ß8. -	05ß. 8	4 U
TMS 31130D N2	. DF.	05DI0	15ßD0	15ßF-	71ß3. .	05ß. 8	4 U
pYP L N	38F12	05F. D	150Ω8	15ßND	71ß200	05ß. 8	4 U
KL p0	38- -	05F. D	150D	15ß12	71ß0D2	05ß. 8	4 U
SL 6 o p	2NF-	05F. 0	15ß02	15ß. -	73ß188	05ß. 8	4 U
I f P -	FN22	05FN	15- 0	15ß8F	71ß88-	05ß. 8	4 U
9 YEF6	. 2- N	05FNN	15 1.	15Ω2N	735 D	05ß. 8	4 U
L 6 YS 9 G	30333	05FND	15ΩNF	15ß- -	71ß380	05ß. 8	4 U
I L MP	FF- 8	05FNF	15FNN	150ßF	71ß228	05ß. 8	4 U
GATp	3D0. N	05FNF	15ΩN	15ß- 8	73ß8DN	05ß. 8	4 U
S 30HΨBB8	3N2-	05FN-	15- .	15ßN0	71ß5 D	05ß. 8	4 U
Gpo 9 3	3N- 3 N	05FN-	15ΩDN	15ß- 3	71ß5 F.	05ß. 8	4 U
TYYS DI	33N83	05FN2	150. 2	15ß1.	71ßD- 0	05ß. 8	4 U
KRS 0	38F0	05FN8	15Ω02	15ß0	71ß3N2	05ß. 8	4 U
S RER3	2. 20	05FD-	15023	15ßNF	71ß20.	05ß. 8	4 U
CGEp3	D8DN	05FD8	15D8F	150FD	71ß5 2.	05ß. 8	4 U
9 TI N	. 031	05FD8	150. D	15ß33	71ß832	05ß. 8	4 U
S 32HΨB8	3N2D	05FD-	15Ω. .	15ß- .	71ß2DF	05ß. 8	4 U
r AR EO	01F8N	05FD-	1500F	15ßN-	73ß1D	05ß. 8	4 U
ECI KY3	3. 0- N	05FD8	15Ω22	15ß0-	71ßN83	05ß. 8	4 U
K6 S A3	32F2	05FD	150F3	15ß. N	71ß8D-	05ß. 8	4 U
o GP 3DK3	N8NI	05FF.	1FFN2	150ßF	725ßD	05ß. 8	4 U
r P Y	01F8-	05FFN	15Ω8	15ß23	71ßFFD	05ß. 8	4 U
o MO6 F	NI. 0	05FFD	15ß00	15ß. F	71ß002	05ß. 8	4 U
TMS - 131. D	333F-	05FFD	15023	15ßND	71ß8. F	05ß. 8	4 U
L L P	30800	05FF-	15Ω. F	15ß- .	71ßN0	05ß. 8	4 U
T6 L 6 0	. - ND	05FF0	15ß32	15ß. 2	71ß80F	05ß. 8	4 U
L E36	30DNN	05FF3	15- -	15ßFD	71ß0- 2	05ß. 8	4 U
T6 L K2	. - , -	05FF3	15DD8	150. 3	71Ω22-	05ß. 8	4 U
f RI 803	03808	05FF	15 - D	15ßFN	71ß5 8-	05ß. 8	4 U
GΧYp6	3DF31	05F8.	15Ω. -	15ß- N	71Ω. 3	05ß. 8	4 U
P ΧY6 G2	- NND	05F8.	15Ω- 8	15Ω2	71ß0FD	05ß. 8	4 U
CTΧ0	D881	05F8.	15ß8F	15ß8.	71ß830	05ß. 8	4 U
TYp3	33D28	05F8N	1508	15ß. -	71ß1D	05ß. 8	4 U
STΧS0	2N32	05F8F	15ΩF.	15Ω2.	71ß5 - .	05ß. 8	4 U
SpRA8	- 332	05F88	15- 8.	15ßD2	71ßN. 8	05ß. 8	4 U
P pE	832D	05F82	15FD2	1508-	71ßI - .	05ß. 8	4 U
L E3A	30D. 3	05F82	15ßN0	1503.	71ßI. .	05ß. 8	4 U
ΧEC6 D	NI8N	05F82	15- NF	15ßN2	71ß2F-	05ß. 8	4 U
RMES o 2	328. -	05F82	15ΩD8	15ß-	71ß82	05ß. 8	4 U
ERI GI 33	3. D- 0	05F80	150- .	15ß. -	71ß- D	05ß. 8	4 U
pP A3S	3- D0.	05F83	15ΩN8	15ß- 8	71ßN. D	05ß. 8	4 U
Χ13NY3	N- DF	05F8	150. 8	15ß33	71ßFD	05ß. 8	4 U
6 P 6 L EGF	0N-	05F8	15Ω28	15ßN	71ß018	05ß. 8	4 U
CTC3	D8 - N	05F- F	150D0	15ß12	71ßFDN	05ß. 8	4 U
6 KS K3	- F	05F- F	150- 3	15ß. 3	71ßN8	05ß. 8	4 U
r WI	01DF8	05F- 2	15ΩN8	15ß- F	71ß82	05ß. 8	4 U
TC6 TGD	. F0D	05F- 2	15NI3	15Ω12	71ßD8N	05ß. 8	4 U
SP o 33	22- N	05F- 2	15ΩD	15ß- 2	71ß3. 8	05 18	4 U
ppT	38- F2	05F- 0	15- 0N	15ßF0	73ß D2	05 18	4 U
L VM8A	30. D8	05F- 3	15Ω8	15Ω20	71ßFFD	05 18	4 U
TYL p	33D2-	05F-	15- 32	15ß8D	71ßNDD	05 18	4 U
C4 Tp3	DF2N	05F2.	15Ω88	15Ω28	71ß02-	05 18	4 U
EI pX	3. 028	05F2N	15Ω- N	15Ω20	71ß38.	05 18	4 U
AKI -	80. F	05F2D	15- . D	15ßN	73ß820	05 18	4 U
Eo KG0	3. 0NI	05F2F	15F0N	15ß02N	71Ω2- F	05 18	4 U
I 4 E-	FNI D	05F28	150. D	15ß32	71ß8F0	05 18	4 U
R6 L pE	3218F	05F2-	15- 1F	15ß8-	71Ω23N	05 18	4 U

Gene ID	Gene Name	Score (d)	Numerator (r)	Denominator (s+s0)	Fold Change	adjusted *P* value (%)	Direction
pSPo3N	3-F1N	05F23	15DDF	1S18	71S1-N	05 18	4 U
I VR	FN0D	05F2	15-1D	1S388	71S 3-	05 18	4 U
pSPoKF	3-F-2	05F2	1500D	1S1NF	71SF-.	05 18	4 U
K6LKX	32NF	05F2	15 DN	1S2D0	70SFFF	05 18	4 U
KARPF	3-N2	05F0.	1S1NN	1S1D8	71S0. .	05 18	4 U
TXL63	. FDF	05F0F	15-1F	1S38-	71S3DFD	05 18	4 U
f VO	03N-D	05F02	1S2FF	1S32.	71SN13	05 18	4 U
YKLG2	3F2-1	05F02	1501.	1S1N	71S12D	05 18	4 U
6SEC0	01D	05F00	15DF-	150. 0	71S38D	05 18	4 U
pYLE0	38FN3	05F03	15023	1S1NN	70S2D8	05 18	4 U
GSR. 6	3D8. N	05F03	1S3F-	1S1F2	73S1-N	05 18	4 U
C6TRET0	F. 3.	05F0	15. .	1S3. 3	71S 83	05 18	4 U
RSYR6110-3	3201-	05F0	152. 8	1S383	71S1F	05 18	4 U
pRLE	380DF	05F3F	3S328	15-2-	7-3SF8	05 18	4 U
ITX8	F-21	05F3F	1S20D	1S308	71S 82	05 18	4 U
ERI6X5F	3. D88	05F3F	158-N	1501.	71S23D	05 18	4 U
XS6L0	N213	05F3-	15-2	1S3D	71S2FN	05 18	4 U
RYOR0	321D8F	05F30	150DD	1S31F	71S2N8	05 18	4 U
S6Gp8	0. 0-	05F30	152- -	1S320	71SN- -	05 18	4 U
pTST0	383-D	05F33	1503D	1S1N2	71S2F	05 18	4 U
XEL0K	ND81	05F1.	1S23	1S33.	71S- .	05 18	4 U
6SGT-	3N	05F1.	1508-	1S1. D	71S11N	05 18	4 U
Y6G5p3	3F0F2	05F1.	15-83	1S1D2	71S F-	05 18	4 U
6PL	22F	05F1N	1SF23	150- 0	71S2F.	05 18	4 U
I6L30. S	8ND	05F1F	150- .	1S1. F	70S12.	05 18	4 U
pMGER	382N2	05F18	15D8F	150.	71S08-	05 18	4 U
6P6LEG2	0N8	05F1-	15038	1S1N2	71S2D	05 18	4 U
f R1F. .	03FF2	05F12	1S1F8	1S1F2	71S2N	05 18	4 U
XP0	N233	05F12	1S203	1S302	71S 12	05 18	4 U
6R9o	F-D	05F12	152. F	1S380	71S08F	05 18	4 U
APR0	8228	05F10	1SN80	1S230	73S820	05 18	4 U
S6SR63S	0DN8	05F10	150- -	1S1. -	71S F3	05 18	4 U
T4L	33ND	05F10	15DI-	150D	71S212	05 18	4 U
K6R93	32N	058. N	15-DN	1S3N-	73SF3N	05 18	4 U
C1G0	FN-1	058. N	15DFN	150. F	71S0F-	05 18	4 U
p6KpS-T	3- - - N	058. D	150NN	1S333	71S2ND	05 18	4 U
ApK-3T0	88ND	058. F	152- 8	1S322	71S008	05 18	4 U
ppIXKp3	38- - 0	058. 8	150ND	1S333	71S1. D	05 18	4 U
YR13-8	3FF88	058. 2	150N0	1S31.	71S0N8	05 18	4 U
L L p3-	30820	058.	1S808	15012	71S000	05 18	4 U
SMT360	2. D2	058.	15DD3	150DN	71S2- 2	05 18	4 U
SGP6	- 020	058.	1583-	1S3. N	71S200	05 18	4 U
YMKM-	3FD2-	058.	1S20D	1S30F	71S - 8	05 18	4 U
S8HB32	0- DD	058N	1S20	1S302	71S2N-	05 18	4 U
RXp6T-	32- DI	058NN	1S21-	1S33D	71S8F8	05 18	4 U
COVTE0	DF- F	058ND	1SF8	15083	71S28D	05 18	4 U
EJp3	3. 288	058NF	15022	1S1.	71SNN-	05 18	4 U
9T9-	. 0FF	058N-	150. 3	1S332	71S880	05 18	4 U
f KEK3F	031F-	058N2	1SF1F	15028	70S2DN	05 18	4 U
EES0N	013F2	058N0	1S1DD	1S1FN	71S3EN	05 18	4 U
SP8.	20D-	058N3	15-2-	1S3FN	71SF1-	05 18	4 U
9To T0	. 020	058N	152F2	1S1- 3	71SFDF	05 18	4 U
SpRAN	- 33F	058N	15080	1S1. N	71S2N0	05 18	4 U
STAS2K	2D. D	058DN	15- .	1S3D-	7150	05 18	4 U
T3EP3	. - F.	058DD	1520.	1S30N	73S31N	05 18	4 U
SXPAS	2DIN	058DF	15-F3	1S3D	71S0N8	05 18	4 U
6R9YP8D	D8F	058DF	15-N8	1S3NN	70S8F2	05 18	4 U
6pMP	N-F	058D8	3S12	15-	70S3F8	05 18	4 U
AIS6K3	8283	058D2	150N0	1S31.	71SF1F	05 18	4 U
CYYp3	D8-3	058D0	15-30	1S3F	71SNN2	05 18	4 U
pSMTSA	3-FND	058D0	15-F2	1S3N	71S1DF	05 18	4 U
ERI6X5N	3. D8F	058D0	1528N	1S32.	71S2. 8	05 18	4 U
ASGSY	823D	058F.	1522N	1S320	73S3N8	05 18	4 U
AYC	8F8D	058FN	1S380	1S18.	71S 20	05 18	4 U
MOAY3	3- - 31	058FF	15- N	1S3D8	73S1-	05 18	4 U
TXLG3	. FN2	058F8	150DD	1S31N	71S018	05 18	4 U
SoYPT3	2F80	058F-	18-	15033	71S 0-	05 18	4 U
E6S3	3N 1N	058F0	1501F	1S1N	71S2.	05 18	4 U
pYYO3	38DD-	058F0	1S802	1501-	71S3F	05 18	4 U
EL AL - 86	3. F31	058F	1SFF8	150F	71S20D	05 18	4 U
To I pT0	. F- -	058F	152F	1S3-	71S0D0	05 18	4 U
GMO3D	3N233	0588N	15-38	1S3F0	71S00	05 18	4 U
L VMBP	30. D-	0588N	150FF	1S31-	71S2. 8	05 18	4 U
SOST3	- 2. 8	0588N	1SFDF	150F-	71S D-	05 18	4 U
RPYC3	320ND	0588D	15F0F	150- 8	70SN2-	05 18	4 U
AL SR	8832	0588	15-2-	1S3D	71S 00	05 18	4 U
XX3F	N228	0588	15-1.	1S3F	71S 88	05 18	4 U
S3QERID	030D	0588	1508F	1S3	71S2N8	05 18	4 U
GSRD6	3D8. F	0580	150. F	1S33F	71S823	05 18	4 U
XI- Y	N80D	0588	1S203	1S30F	71S 18	05 18	4 U
6RMF	D2.	058- .	1S1DD	1S1F.	71S2D8	05 18	4 U
6YoCAI-	. F-	058- .	150- N	1SL. D	71S038	05 18	4 U
AREpP3	88DI	058- N	1508N	1S313	71S838	05 18	4 U
SOHB2F	- - 0.	058- D	153- F	1S18D	71SD 2	05 18	4 U
TMS31130. . - 1	. . . .	058- F	150D-	1S31N	71S1F8	05 18	4 U
GE931	3NFNF	058- 8	150. 0	1S338	73S3- F	05 18	4 U
I L RT2	FF2D	058- 2	1S3F0	1S1F-	715 -	05 18	4 U
S0HB31	02- .	058- 2	15NN2	1S2- D	71S D8	05 18	4 U
GTS. 6.	3NI30	0582.	1523N	1S308	71S2- .	05 18	4 U
L E3K	30DN	0582N	15- . N	1S3. F	71S3- 2	05 18	4 U
EL AL 320S	3. - D-	0582N	150ND	1S332	7150. D	05 18	4 U
SMT863	2. . 3	0582D	152. .	1S38D	71S3. 8	05 18	4 U
I6L2P	F128	0582D	1SFN-	150D	73S0D8	05 18	4 U
C6TRE30	F. 1D	0582F	150N8	1S333	71SF80	2S8D-	4 U
Ppp-	830F	0582-	15-2.	1S1D2	71S N-	2S8D-	4 U
ASL0	823F	0582-	150D2	1S31N	71S3. 2	2S8D-	4 U
CTXpY0	D88F	0582-	15-88	1S3D	71S010	2S8D-	4 U
PpAp0	8330	05822	150FD	1S318	73S0N-	2S8D-	4 U
f R10. 8	032N-	05820	1S3N-	1S1D2	73S0D	2S8D-	4 U
XI M3	N222	0582	1S3NN	1S1D-	71S80D	2S8D-	4 U
L 6p-98	301FF	0580.	15080	1S3	71S2D8	2S8D-	4 U
6Po3K	202	0580N	1523D	1S308	71S2DD	2S8D-	4 U

Gene ID	Gene Name	Score (d)	Numerator (r)	Denominator (s+s0)	Fold Change	adjusted *P* value (%)	Direction
TKo	. 80.	0580N	1501O	1SI N	71SF23	2SID	4 U
YG4 3	3F. FN	0580N	1S38N	1SIF2	71SNN-	2SID	4 U
TYYS 2K	33DN-	0580D	1SIDB	1SIFN	71S00D	2SID	4 U
Y6 G6 2	3F0- F	0S802	1S28-	1SI-	71SI N	2SID	4 U
P XM0	- ND	0S800	152- N	1S52N	71SFND	2SID	4 U
f GWXL -	03N2-	0S803	15- 2	1SIDB	71SIDI2	2SID	4 U
WKp8	01DN2	0S803	15- 80	1SID	71S F3	2SID	4 U
pEC3Y	38. 00	0583N	1521F	1S003	71S2DB	2SID	4 U
KARP -	3- N8	0583D	15I-	1SI8F	735 -	2SID	4 U
GGS 8P	3N8DD	0583D	158F0	15002	71S080	2SID	4 U
P R6 GA3T2	818D	0583D	15 - N	1SIDN	715 8	2SID	4 U
6 YGX	318F	0583F	150.	1S38	71S2ND	2SID	4 U
pTA9 o C3	383D8	0S838	1521N	1S500	71S280	2SID	4 U
ETY-	3. 2NI	0583-	150F.	1SI1D	7150F.	2SID	4 U
ETA-	3. 2FN	0583-	15030	1SIN-	71S2F8	2SID	4 U
ACI TF	82ND	0S832	15DIN	150N0	71S28.	2SID	4 U
SMpf 0	- 12.	0S833	15- N	1SI. 3	71SI. 0	2SID	4 U
SP. .	20. N	0S833	15082	1SI13	71SID	2SID	4 U
AI AL p3	82F2	0S833	15F0D	1508	7150B	2SID	4 U
SMI- 6 0	2. N8	0581.	152D-	1SI- .	71S00.	2SID	4 U
6 YpS0	3120	0581.	1508N	1S512	715 D8	2SID	4 U
p6 pTR	3- 830	0581N	1502N	1SI. 8	735 0F	2SID	4 U
AI RK2	82D	0581D	1S20	1S50D	71S002	2SID	4 U
9 YE3F	. 23D	0581D	15DD	1S21D	735 F0	2SID	4 U
E4 GS 8	010D2	0581D	152D8	1S38	7150F2	2SID	4 U
YS R3	3F2D-	0581F	15- 12	1SIF3	71S - 8	2SID	4 U
KRS 3	38F3	0581-	150N2	1S332	73S ID-	2SID	4 U
6 I 6 p3T3	2DI	0581-	150. -	1S33D	71S2. -	2SID	4 U
6 P 6 L 30	0- D	0S812	150. 0	1S33D	71S003	2SID	4 U
TMS - - 3NF.	330F-	0S810	15- 20	1SID2	715 . F	2SID	4 U
SF	0830	058	150F	1SI1-	71SDB3	2SID	4 U
L 6 pYA0	301. D	058	152- N	1S52.	71SF08	2SID	4 U
XT9	N8- 0	05 . D	1503-	1SINF	7130F.	2SID	4 U
Y4 RO0	3DI11	05 . -	150F0	15318	1SIDI2	2SID	4 U
9 TI 8	. 01D	05 . -	15F1-	150- 0	73S DD	2SID	4 U
L I CAN	30281	05 . -	158D0	1500.	71S2F8	2SID	4 U
pECAY-	38. 3F	05 . -	15- 1F	1SIF2	715 10	2SID	4 U
o r SR3	N0NI	05 . 0	150N	1S33F	715 F-	2SID	4 U
ERRE2	3. DDB	05 . 3	150D	1S31N	71S013	2SID	4 U
o 6 6 M	DFN0	05 . 3	15I. .	1SI N	73S2ND	2SID	4 U
I 6 L - . 6	F18-	05 .	1523-	1S50F	71S2DB	2SID	4 U
L VT0	30. - .	05 N	15I F	1SIF-	71S0F8	2SID	4 U
6 TP o 0	83D	05 N	15- D8	15I. 3	71SFN	2SID	4 U
o MO6 8	NI. 3	05 N	15- 0N	1SID0	71S812	2SID	4 U
SS T3.	232D	05 NN	15NF0	152- D	73SF3F	2SID	4 U
L AXG0	300NF	05 NN	1523N	1S0N	71SI 32	2SID	4 U
L L p2	308- F	05 ND	15FDD	150D0	71S8F-	2SID	4 U
KT9	380.	05 ND	1582-	15038	70SI F-	2SID	4 U
G3 116 0	3DI23	05 ND	15D -	1523.	71S820	2SID	4 U
pYXS 9 TA0	38F0N	05 N8	15- 08	1SIDB	71S 0N	2SID	4 U
CY6 L P 0	D- DN	05 N2	1521.	1S30-	73SIFF	2SID	4 U
GEMR 3	3NDBD	05 N	152DD	1S380	71S - D	2SID	4 U
STP R3-	2DF1	05 D	15022	1SI. -	73SID	2SID	4 U
RS YR6 1108FK	32038	05 DD	152- F	15I-	71SN2D	2SID	4 U
CpRL K	D280	05 DF	150ND	1S33F	71S208	2SID	4 U
EL AL 320A	3. - DF	05 DF	1500	1SI N	15I. .	2SID	4 U
Eo V3	3. 233	05 D2	15 D-	15I. 0	71SIDD	2SID	4 U
pC1	3- NN2	05 DB	152F3	15I- F	71SF0N	2SID	4 U
S D	08N8	05 D	15 03	1SIDB	73SI. D	2SID	4 U
L AI 0S	300D0	05 D	1522F	1S32F	71S8F.	2SID	4 U
SSP S NN6	2331	05 F.	150. 8	15I0	71S01D	2SID	4 U
6 P 6 L 02	08F	05 F.	1S22D	1S88	73SI00	2SID	4 U
GAGR 3	3D- 31	05 FN	1523-	1S30D	715 33	2SID	4 U
6 P 6 L EG	0ND	05 FN	15-	1SIF0	71S20.	2SID	4 U
YR I 3FF	3FFF-	05 FF	1501-	1SIN2	73SI22	2SID	4 U
6 SGT3	3ND	05 F8	15 2.	1SIDN	71S 80	2SID	4 U
po TP 6 2	3- . - N	05 F-	1528-	15I- -	71S0N	2SID	4 U
pL So T3	3802.	05 F-	15I- 0	1SI8N	735 3	2SID	4 U
KS TFK	3- 8-	05 F2	1S20D	1S222	73SI2.	2SID	4 U
S RX6 2	2N 8	05 F0	152. 8	1SIF3	71S08-	2SID	4 U
GTS 086 0D	3DDD-	05 F0	15 1-	1SIF-	71S00.	2SID	4 U
YXj9 -	3F8N2	05 F3	1523D	1S30.	70SI38	2SID	4 U
L S 6 L	303DN	05 F3	152. 0	1S38.	71S - F	2SID	4 U
K6 E1 2	3- 10	05 8N	150.	1S33N	71S 1D	2SID	4 U
C6 K6 Y6 pT3	FN8-	05 8D	1521D	1S308	71SI. -	2SID	4 U
6 YCT4 3	. 1N	05 88	150. N	1S303	71S822	2SID	4 U
ATEP 3	8833	05 8-	15210	1S302	71S 28	2SID	4 U
Eo KG3	3. 0D	05 82	152F	15I- D	715 3	2SID	4 U
pS P o K3N	3- F2N	05 80	15I. -	1SI1D	71SN33	2SID	4 U
9 P ATS 0	N FN	05 83	150D0	1S333	71SI18	2SID	4 U
I S AY36	F0DF	05 83	15823	1503D	73SD- F	2SID	4 U
TMS D200D0	33F- .	05 83	3512-	15 00	71SF88	2SID	4 U
EL KXL 3	3. - 1N	05 8	152D0	1S380	71SDDF	2SID	4 U
SP 9 T3	2- 1-	05 - .	15008	1SI. 0	71S01.	2SID	4 U
L VM 6	30. ND	05 - F	15008	1SI. 0	71SD1D	2SID	4 U
6 S6 6 0	33F	05 - F	152. 8	1SIF3	715 8-	2SID	4 U
So R3	2F- 3	05 - -	1523N	1SI2	73SI1.	2SID	4 U
SP 9 38	22N0	05 - 0	1533N	1SI- N	715 - N	2SID	4 U
9 To T0.	. 0- 3	05 - 3	1521D	1S30F	7130. 2	2SID	4 U
TMS 88- 010	330N	05 2.	1508	1SI12	71SFN2	2SID	4 U
f R1 - F.	03- ND	05 2N	158- N	15008	71S28-	2SID	4 U
CYAL 3	D . 0	05 2D	15 0N	1SIDF	71S203	2SID	4 U
9 YE38	. 23F	05 28	3538	15 3D	71SD8-	- S23D	4 U
pp6 p0K	38- 3.	05 28	152.	1S3F	71SI. .	- S23D	4 U
S - HZ8.	0- F.	05 28	1502-	1SI. F	73SI1N	- S23D	4 U
I KR3	F010	05 22	15 1.	1S3FN	71SIF2	- S23D	4 U
6 TP o 36 3	833	05 22	1S280	15I- 8	71SF- F	- S23D	4 U
TMS 3113238- 3	313N-	05 23	15 - 2	1SIN0	71SF83	- S23D	4 U
AV6 0	8DD0	05 23	158- 8	1500-	71S2N-	- S23D	4 U
CL I C	D01F	05 23	15 1D	1SIFD	71S8. N	- S23D	4 U
EL AL 321	3. - DI	05 23	15 . F	1501-	71S . F	- S23D	4 U
S6 Gp-	0. 02	05 0.	1S22N	1S32.	71S83-	- S23D	4 U

Gene ID	Gene Name	Score (d)	Numerator (r)	Denominator (s+s0)	Fold Change	adjusted *P* value (%)	Direction
GEO30	3NDE.	05-0.	1503	15INO	715 D	-523D	4 U
pTEp	38003	05-0.	15-2	15I0DD	715-08	-523D	4 U
K6 SA0	32F-	05-0N	15880	1500D	7152-	-523D	4 U
YAS QT	3F2. F	05-0N	15I2D	15I8D	715I00	-523D	4 U
C6 GF	F. - N	05-0D	15-1.	15IF.	715 2F3	-523D	4 U
CMI XL -	D0. 2	05-02	1532	1530.	715 2- D	-523D	4 U
pTORS 3	38022	05-03	150N	1533.	7150 82	-523D	4 U
R EI -	32D83	05-3.	15-02	15ID8	715D -	-523D	4 U
pRTX6Yp2	380FD	05-3.	1580 2	1503F	72522.	-523D	4 U
S RER6 p2K	2. - 3	05-3.	15I. N	15IN0	715 .	-523D	4 U
L GR	30DD0	05-3N	1528	15I- 8	715 IDD	-523D	4 U
P GC2	83N-	05-3N	15FD-	150D	735N0N	-523D	4 U
P I R6 8	- NI-	05-3N	15020	15I. F	735 I1D	-523D	4 U
XECK2	NI20	05-3F	15-8	15INF	71502	-523D	4 U
ETY31	3. 2DD	05-3F	150D8	1533-	7352. 8	-523D	4 U
6 Tp9 2	8DI	05-3F	1521-	1530F	715 - 8	-523D	4 U
TMS 3113. 02DN	312FF	05-38	15IDF	15ID2	735 ID8	-523D	4 U
S EXI	- 20F	05-3-	1523.	15320	7152 1N	-523D	4 U
6 QpD	NO8	05-3-	152. 2	15IF2	7152. D	-523D	4 U
CTG	D8D8	05-30	150. -	15I00	715 2.	-523D	4 U
S6 L 9 0R3	0N- N	05-30	15F3-	15088	715N18	-523D	4 U
SO2S T3	- 2. 0	05-33	15-F.	15I. -	715F2D	-523D	4 U
Y6 KDK	3F32D	05-3	15 -	15IN2	7150F0	-523D	4 U
XEC6 8	NO8F	05-3	152- -	15I- 2	71508	-523D	4 U
4 KA0A0	01282	05-1.	150. -	15I00	715N	-523D	4 U
Rp Y3	32F- 3	05-1N	150F2	1531.	7150 80	-523D	4 U
KL pF	38- .	05-1N	152N0	1538.	715I2-	-523D	4 U
L I 6 p8	302- N	05-18	1583N	15038	7152 0F	-523D	4 U
S2HZ8N	0- 0-	05-18	150N2	1533N	715 3D	-523D	4 U
L XEI	30- D8	05-1-	15020	15I. F	715I13	-523D	4 U
MTI L T0K	32. 3D	05-12	152NF	15IF3	71520	-523D	4 U
YRI 381	3FF8.	05-12	15D8	150. 8	715D-3	-523D	4 U
pEC1 Y	38. 01	05-	15002	15I. 2	7150- D	-523D	4 U
9 SRJ30	NN 2	052. .	152FN	1583 82	71 5FFN	-523D	4 U
GTS 3F6 0	3DF. 1	052. N	1533	15032	7350 2F	-523D	4 U
XI RCY3	N2D0	052. N	150N2	1533N	7152 2N	-523D	4 U
RS YR6 11230	32081	052. N	152- 3	15I- 0	7150N8	-523D	4 U
SXK0	2DI0	052. 0	15-F	15I. 0	715-N2	-523D	4 U
GCSP	3D- DI	052. 0	1522-	15I-	715IN	-523D	4 U
6 R9 GF	D0.	052. 3	1581N	15030	7152	-523D	4 U
R6 6 T6 P T3	32120	052.	1582D	15I8D	7152 8N	-523D	4 U
SP 0-	202-	052.	15 N	15- 3	7350 12	-523D	4 U
SML L P F	- 13F	052N	15022	15I. D	735D- 0	-523D	4 U
SP D K	20N8	052NF	1521.	1530.	705N8F	-523D	4 U
P L P	-. F.	052N8	1503	15INN	7152 8.	-523D	4 U
MP f 0	32N 0	052N2	1583 2	15038	7153- .	-523D	4 U
Eo KG-	3. 0N0	052N2	15F. F	150. 0	7150N2	-523D	4 U
I 6 Kp8	8NI 8	052N	1583D	15D3D	7150- F	-523D	4 U
p4 YC	3F11F	052D.	1533	15I- F	7150 13	-523D	4 U
p6 TL 0	3- - . 0	052D0	15I. 2	15IN8	715 N0	-523D	4 U
GE2C6 T0	3NF31	052D0	1502	15I. D	7150 18	-523D	4 U
6 RMB	D22	052D	15-02	15IDN	715FN-	-523D	4 U
WTG	01. 13	052D	152. 2	15IFF	715F22	-523D	4 U
pL Ap6 3	380- 3	052F.	15-D0	15I. .	7150 3D	-523D	4 U
GMS G2	3N0D	052FD	15-08	15IN	7150 13	-523D	4 U
TMS 311323N0F	31001	052F8	1500-	15I. 8	715IF	-523D	4 U
L GT2	30DFF	052F8	15I0F	15I82	715 2	-523D	4 U
p6 L Y3	3- - . D	052F8	15 - N	15IN	715 F.	-523D	4 U
ERS	3. DB1	052F8	15F0-	150F-	715- 3F	-523D	4 U
6 9 Y3S 2	- . 1	052F-	15F0	150F0	735FFN	-523D	4 U
SP 0- N	202D	052F-	1522	15I- 3	715IF.	-523D	4 U
CJK8	DB02	052F2	1510	1530N	735N2-	-523D	4 U
GTS MD6 3	3NI3N	052F0	152DB	1558D	735IN	-523D	4 U
TpOR	33DB2	052F0	152N	15IF3	715 DF	-523D	4 U
SMTN6 0	- 110	052F3	15 . 8	1503	715IF3	-523D	4 U
XI3Y3	N- N0	052F3	152DF	1558.	715N83	-523D	4 U
Yo MQ	3F8- 2	052F	1503-	15I. 3	715I02	-523D	4 U
6 Ep33K	33NN	052F	1520D	1532.	7152.	-523D	4 U
TMS 311818NIF	31- 8-	052F	15 - .	153.	715812	-523D	4 U
S6 GE	0. 2-	052F	15082	15I1D	7150 1D	-523D	4 U
6 Sr Y3S	022	0528.	15033	151.	7152 0-	-523D	4 U
TMS 311320N 3	310. -	0528.	1532-	15I8D	715I.	-523D	4 U
L MS G3	308D8	0528.	1508	15IF	735I. 3	-523D	4 U
ER6 p	3. DI.	0528.	15ID	15IDF	715I. 2	-523D	4 U
po TP K3	3- . - .	0528N	15080	15I1D	15IN	-523D	4 U
L 6 CAP - K	33. NF	0528N	158- 3	1502	715 D0	-523D	4 U
o GP 3DK33	N8N0	0528N	152- -	15I- F	7152 1N	-523D	4 U
GpGK3	3N- . 1	0528N	152- 8	15I- F	7152- D	-523D	4 U
EGp6 R33	011. N	0528D	153. -	15IN0	7153 D-	-523D	4 U
6 P 6 L EG3N	0DD	0528F	15 . 2	1501.	7152 D8	-523D	4 U
9 pR6 2	. 0. 2	0528	15IDB	15ID-	715F1.	-523D	4 U
P EP 3	83. 2	0528	152DN	15IF3	715 N	-523D	4 U
SMI36 3	2. D0	0528	15F8N	150N	7152N8	-523D	4 U
L 6 1	33. 80	0528	150D0	1533F	715 8-	-523D	4 U
S6 TS YT	0N0-	0583	1508N	1533	7152 - F	-523D	4 U
GVE33	3NND8	052- .	1502D	1513	7352F0	-523D	4 U
SMT86 0	2. . 0	052- .	15F02	150F8	7153D	-523D	4 U
P o YG30	- N- 3	052- .	1500	15I. -	735 1D	-523D	4 U
Rp V0Y	32F8D	052- .	1518	1532	735INN	-523D	4 U
L E06	30D .	052- N	15 DF	15012	7150. 3	-523D	4 U
C6 KYA	FND8	052- N	15D	1522F	71 3F00	-523D	4 U
GAYpXRA3	3D2. D	052- N	150- F	1518	7152 2F	-523D	4 U
GVRL	3NNF2	052- D	15N0.	1582	715N- 3	-523D	4 U
ECI K2	3. 0- F	052- D	15 - . 3	1501.	71 5F0N	-523D	4 U
So T3	2F0N	052- F	1508F	1531.	7320F	-523D	4 U
L 6 I I	33. 8F	052- 8	1508	1532N	715 - 0	-523D	4 U
GEV9 3	3NDF1	052- 8	15-08	15IN8	735 0F	-523D	4 U
SMYXR	- 1- .	052- 8	1521F	1532	715 D2	-523D	4 U
GAL 6 2P	3D21D	052- 2	1583F	1500	715D N	-523D	4 U
SGEF	- 0N8	052- 3	15D80	1521-	735INF	-523D	4 U
f RI FF0	03F22	052-	15-FN	150	735I8D	-523D	4 U

Gene ID	Gene Name	Score (d)	Numerator (r)	Denominator (s+s0)	Fold Change	adjusted *P* value (%)	Direction
4 o L 9 3	01 - F8	7 - 50 DF	71 5 - 3 -	1 S I . D	71 5 F 3 .	3 5 - F	P H w n
S o 6 P T	28 N	7 - 50 - .	71 5 DF 8	1 S N	71 5 F 08	3 5 - F	P H w n
Yp 4 GP 3	3F . 3 -	7 - S I D -	71 5 - 2 .	1 S 18	71 S 8 D	3 5 - F	P H w n
pGL P -	38 N F N	7 - S I F F	71 5 20 .	1 S I D	71 S F . .	3 5 - F	P H w n
YpYP 0	3F N 8 F	7 - S I -	71 5 2 38	1 S I D N	71 S D N 0	0 S I . 8	P H w n
9 YES 6 p 2	. - 8 .	72 5 . 82	71 S F - 3	1 S F 0	71 S 8 N N	0 S I . 8	P H w n
pVS Y 0	3F 12 F	72 5 . 2 D	71 5 20 8	1 S I N 2	71 S D F 0	0 S I . 8	P H w n
S 3 H Z B 3 N 0	03 D D	72 5 . 2 F	71 5 - 20	1 S 3	71 5 D	0 S I . 8	P H w n
pGL K -	38 N - D	72 5 N N 2	71 5 2 F -	1 S I . -	71 5 0 F	0 5 . 18	P H w n
EL pYGGF	3 . F . 1	72 5 N - 0	71 S 888	1 S 3 - 8	71 S N I .	0 5 . 18	P H w n
GR YR p 28	3N 03 N	72 5 D - D	71 5 20 -	1 S I N D	71 S F 28	2 S B D -	P H w n
TMS 0 N - . 2 .	31 N 1	72 5 F 8 D	71 5 D I -	1 S 3 . 0	73 5 0 -	2 S B D -	P H w n
R X E 3	32 - D F	72 5 F 1 .	71 5 2 - .	1 S I . D	71 S F 2 N	2 S B D -	P H w n
TVG L P 3	33 . 03	72 5 F 18	71 5 - 3 .	1 S 3 F	71 S D I -	2 S B D -	P H w n
E 6 YG 0	3N D 0	72 5 B D 0	71 S 0 F 0	1 S I D 2	71 5 23	2 S B D -	P H w n
S 3 H Z B 3 D	0023	72 5 8 8 -	71 5 - N -	1 S 2 F	71 5 FN	2 S B D -	P H w n
G S 6 L p 2	3 D 80 N	72 5 8 8	71 5 22 -	1 S I . -	71 S 83 D	2 S B D -	P H w n
ERI YGI 3 N	3 . D 23	72 5 8 - D	71 S F 2 N	1 S 3 N	73 S 3 . -	2 S B D -	P H w n
f R I F - F	03 F 0 -	72 5 8 - 2	71 S 3 D -	1 S I - .	71 S 0 FN	2 S B D -	P H w n

Add. Table 4: SJi gJDncgatl y JfIdrdgagdeTrdxxd yi dgdxys dab ddgyawdyh dacs ot.hnytmxadrxyG n l ycg yG nU

Gene ID	Gene Name	Score (d)	Numerator (r)	Denominator (s+s0)	Fold Change	adjusted *P* value (%)	Direction
CALD1	2825	50825	. 0B7-	. 0128	4 0L35	.	p T
G NC2	12- 71	50811	. 08U3	. 0177	4 079	.	p T
6 6 G F	1U555	50853	. 0921	. 0l-	4 0723	.	p T
Np 6 E2	13. . .	50878	. 0791	. 0 85	4 0652	.	p T
CRL18A1	U93.	50- 37	. 0823	. 0128	4 0721	.	p T
MPNG F2	- U21	50 - 8	. 05U	. 0 97	4 0L15	.	p T
DXYSLU	515.	50633	. 0837	. 0153	4 07. 7	.	p T
FAOL6	18979	505U3	. 0835	. 0158	4 0LB7	.	p T
CFOM	7L2U	50823	. 089-	. 0l - 2	4 0L8	.	p T
OMXF2	3. 57	505. 3	. 0B1	. 0129	4 0738	.	p T
FSHZU	2. . 8-	505. 2	. 0- 37	. 0122	4 0LB7	.	p T
OXE 8	3737	50737	. 0832	. 0171	4 07. 8	.	p T
SNXE 2	18573	50758	. 0812	. 0179	4 0- U9	.	p T
CLG X	L8U	50753	. 0858	. 0U19	4 02U9	.	p T
MAX	- 132	50U3-	. 0927	. 0132	4 0B1-	.	p T
BCA6	2. - 75	50U- 5	. 0895	. 0l - 3	4 0- 97	.	p T
LREL2	11- 8U	50U75	. 0897	. 0179	4 0- 29	.	p T
6 PE 6	1UU95	50UU-	. 0525	. 0 98	4 0L! -	.	p T
FIG X2	19U77	5029 7	. 0B9	. 0179	4 07U2	.	p T
LRE	11- 8.	5022U2	. 0811	. 0155	4 0- 83	.	p T
CRLUA1	U98U	502U	10 U1	. 0193	4 0- 71	.	p T
XFNM	1599.	50185	. 0725	. 0 82	4 0L21	.	p T
PG ILI6 1	552.	5087	. 0- 19	. 0119	4 0713	.	p T
A6 OXFL2	- UU	50l - 5	. 0B- U	. 0178	4 0728	.	p T
SLIFU	18. U-	50l -	. 0B99	. 0155	4 072-	.	p T
XDOMNV	17355	50171	. 0- 58	. 0128	4 071-	.	p T
G SNVU	1233-	50171	. 0B7-	. 0175	4 0LIU	.	p T
SXANC	18U- 2	5017	. 0892	. 0137	4 0788	.	p T
6 ID1	1U75-	50UU2	. 0B25	. 0171	4 0f1	.	p T
DACFU	7555	50 83	. 0B5	. 0173	4 0L- 2	.	p T
MVL6 2	- 199	50 83	. 0893	. 0l3-	4 0717	.	p T
6 RE 7	1U- . U	50 - 3	. 05U-	. 0l. -	4 0B89	.	p T
C6 6 2	U9. 1	50 53	. 0B5U	. 0179	4 0L78	.	p T
FOMV1I1	19277	50 29	. 0555	. 0l1	4 0L57	.	p T
FCMF	19112	50 18	. 0S8-	. 0113	4 0L! -	.	p T
HFNAU	8232	50 . 8	. 0- 39	. 0lU-	4 0B1-	.	p T
G OC271. U	12U93	50 . U	. 0B1	. 0l - 2	4 0778	.	p T
XDLIG 3	17333	70991	. 0799	. 0l	4 05. 7	.	p T
FXG 7	19855	70988	. 0535	. 0115	4 0525	.	p T
FG PG 2. . A	19557	70931	. 0739	. 0 9-	4 077-	.	p T
G ENA5	129. 1	709- -	. 0527	. 0l. -	4 0559	.	p T
OLF8D2	3182	70958	. 0752	. 0 91	4 0777	.	p T
SHRE 2	135- -	7095-	. 0511	. 0l. U	4 0L93	.	p T
CRL5A1	U991	7095	. 0583	. 0119	4 0B- 2	.	p T
OPG	3. U5	7095	. 0B2U	. 0l7-	4 0l72	.	p T
XALLD	1779.	7097-	. 077U	. 0 9	4 05U-	.	p T
I6 HVA	853U	709U3	. 0873	. 0132	4l02 32	.	p T
S6 AI2	181UU	7092	. 05U7	. 0l. 8	4 0L23	.	p T
MSFL1	- 33-	709. 9	. 0B99	. 0l - U	4 07 - 8	.	p T
XRD6 L1	15293	709. 8	. 05U7	. 0l. 9	4 058	.	p T
CRL1A2	U93U	70882	. 093-	. 02	4 0818	.	p T
CRL5A2	U992	70881	. 09- 7	. 0198	4 0827	.	p T
ZPV1	211- -	7083U	. 0- . 8	. 0125	4 0L75	.	p T
N6 M77A	1- - 5U	70831	. 051	. 0l. 5	4 0LB5	.	p T
XRD6	1529-	708- 8	. 05U8	. 0111	4 0L-	.	p T
DSP	518.	70875	. 05. U	. 0l. 7	4 0752	.	p T
SCO5	131- 5	708U-	. 0- 2U	. 0129	4 0282	.	p T
FHY1	19Ul1	70828	. 0- 9-	. 0177	4 0B2	.	p T
DZIXIL	5233	70828	. 07. 3	. 0 87	4 075-	.	p T
F6 MAIX-	19315	7082-	. 0B7-	. 0155	4 0B9U	.	p T
APVXI	U- 7	70811	. 0881	. 0l8U	4 0B. 3	.	p T
XRSF6	15U8U	708. 5	10 2-	. 0217	4 0B. U	.	p T
XLKU	152. U	70891	. 0l7-	. 0 9U	4 0l19	.	p T
VO6	15. .	70887	. 0582	. 0122	4 0- 87	.	p T
HFNA1	823.	70882	. 0888	. 0l8-	4 0799	.	p T
G IN1. . HO	127- U	70838	. 0B	. 0173	4 02U3	.	p T
DACF1	755U	708- -	. 0B1U	. 0l5	4 0- . U	.	p T
CDH11	UU78	70878	. 051	. 0l. 3	4 0- 1	.	p T
FP AD1	19159	7087-	. 0f1	. 0 8-	4 05U7	.	p T
SPNXI6 M	137. .	70875	. 0- 99	. 0173	4 023-	.	p T
ACFA2	2. 2	70U8	. 08. 2	. 0l - 9	4 02- 9	.	p T
MV6 1	- 2. 2	70U7	. 0- 21	. 0lU1	4 0- 1-	.	p T
FNXC1	2. . U8	70U2	. 05. U	. 0l. -	4 02 7	.	p T
IOMVXU	87. 5	70U1	. 0- U9	. 0lU5	4 0LU-	.	p T
ANHOAX28	92-	7027	. 0f- -	. 0 99	4 0719	.	p T
IFXNIX	83- 1	7022	. 0519	. 0l1	4 0LU2	.	p T
LG RD1	93U9	7019	. 0L81	. 0 81	4 0l38	.	p T
S1. . A1.	13. 25	7012	. 0- 1	. 0129	4 0295	.	p T
OXN127	3U- 3	7011	. 0531	. 0121	4 02 7	.	p T
BIG	2. - 3U	708. U	. 0551	. 0113	4 02- 9	.	p T
CRL1A1	U932	70- 95	. 0979	. 02. 2	4 099U	.	p T
FHVS2	1928.	70 9	. 08U5	. 0138	4 0B92	.	p T
ADAG FS-	287	70 - 9	. 0U1-	. 0 - 8	4 0- 2	.	p T
CYN- 1	7528	70 - 7	. 082U	. 0l3-	4 0l3	.	p T
DKKU	79U2	70- 53	. 057	. 0l1-	4 0L55	.	p T
XNKCDVX	15- 52	70- U8	. 0589	. 0123	4 0L52	.	p T
XNNE 1	15337	70- UU	. 0- 95	. 0l5	4 057	.	p T
XLSU	15215	70- 27	. 0- 51	. 0171	4 02- 2	.	p T
LAG A7	9789	70- 1-	. 0775	. 0 9-	4 0712	.	p T
G ANBPLD1	1212.	70- 15	. 059-	. 0129	4 05- 1	.	p T
G G XI7	125U2	70 . 7	. 0B13	. 0l5-	4 0 - 9	.	p T
LIG S2	9- 87	70 . U	. 0779	. 0 93	4 0l51	.	p T
MVI6	- U89	70 . 2	. 0- 53	. 0l7U	4 07. -	.	p T
G NB11	123U9	7093	. 0595	. 0129	4 0299	.	p T
C5orf- 2	25. 9	7093	. 0- 21	. 0lU5	4 02- 9	.	p T

Gene ID	Gene Name	Score (d)	Numerator (r)	Denominator (s+s0)	Fold Change	adjusted *P* value (%)	Direction
DC6	7- U7	7(6539	. (8331	. (19	4 (L81	.	p T
ISG 1	8- 9-	7(6539	. (8337	. (1- 9	4 (2-	.	p T
XCSK5	17- 93	7(63U	. (L1 2	. 0 - -	4 (L29	.	p T
NANNPS2	1- 27.	7(658	. (8	. (135	4 (221	.	p T
KC6 G V7	8927	7(653	. (-93	. (15U	4 (-73	.	p T
SNXE	1857-	7(675	. (-39	. (179	4 (1- 3	.	p T
A6 FE N1	35.	7(677	. (- . 9	. (1U7	4 (-31	.	p T
ISLN	8- 97	7(672	. (8L19	. (1- U	4 (713	.	p T
G G XI9	125U-	7(625	. (L7U	. (3-	4 (1. 3	.	p T
FXG i 2	1985U	7(618	. (599	. (1L2	4 (72-	.	p T
CYS1	7529	7(618	. (-31	. (179	4 (791	.	p T
XDLIG 7	17335	7(6. 3	. (718	. (9U	4 (223	.	p T
SPNXI6 O1	137. 2	7(79U	. (718	. (9U	4 (2. 7	.	p T
LFVX2	118- 3	7(785	. (793	. (111	4 (235	.	p T
XXAXDCU	15727	7(733	. (L72	. (3-	4 (L-2	.	p T
G YL9	1295-	7(731	. (-77	. (177	4 (U1-	.	p T
XXIC	15779	7(731	. (55-	. (127	4 (518	.	p T
CRL- AU	U99-	7(7- 8	. (597	. (1UU	4 (851	.	p T
G ENA8	129. U	7(7- -	. (-83	. (157	4 (783	.	p T
OS6	3558	7(7-	. (799	. (112	4 (-1U	.	p T
CMH	U5- 2	7(752	. (67-	. (12U	4 (2. -	.	p T
Fp VV-	2. 251	7(77-	. (- - -	. (15	4 (L5-	.	p T
G G X2	125U8	7(777	. (-89	. (155	4 (759	.	p T
CRL- A1	U997	7(7U5	. (85	. (1- 9	4 (-75	.	p T
XNICKLP1	15- 23	7(725	. (823	. (1- 7	4 (71U	.	p T
SXR6 1	1875-	7(718	. (921	. (2. 9	4 (753	.	p T
G POU	12235	7(712	. (73	. (1. 3	4 (295	.	p T
C1S	21UU	7(7. U	. (-U-	. (177	4 (257	.	p T
MOM	- U71	7(7. 1	. (272	. 0 55	4 (651U	.	p T
G DMC	12218	7(L8-	. (L93	. 0 91	4 (157	.	p T
NVG S1	1- UL8	7(L85	. (788	. (111	4 (228	.	p T
ADAG 12	273	7(L87	. (712	. 0 97	4 (633	.	p T
SLC2AU	138UI	7(LB2	. (255	. 0 58	4 (23	.	p T
M6 1	- - 79	7(L- 9	. (89	. (2. 7	4 (957	.	p T
OAS1	- 972	7(L- 7	. (-85	. (153	4 (L5-	.	p T
G OC7297	1271.	7(L59	. (633	. (1L2	4 (8U5	.	p T
xdTI01	13U72	7(L53	. (799	. (115	4 (7. U	.	p T
SOCD	1373.	7(L5U	. (7- 9	. (1. 8	4 (615	.	p T
F6 S1	19382	7(L52	. (L9U	. 0 9	4 (-1. UU	.	p T
LIG S1	9- 8U	7(L7U	. (L17	. 0 38	4 (781	.	p T
Lp G	11839	7(L72	. (88U	. (2. U	4 (-U5	.	p T
PBC2	5323	7(LU	. (25U	. 0 58	4 (285	.	p T
LCAF	95U-	7(L2	. (LB9	. 0 88	4 (218	.	p T
MPZ1	- L2-	7(LI-	. (LB7	. 0 83	4 (L-	.	p T
FVE 15	19. - 8	7(LI7	. (291	. 0 - 3	4 (288	.	p T
PMHA2	5U- -	7(LI 5	. (L91	. 0 91	4 (-1 0 - 5	.	p T
C1N	21UI	7(LI U	. (-12	. (172	4 (275	.	p T
SMNX2	13778	7(LI 1	. (9. 7	. (21	4 (7- -	.	p T
C1orf1546 VL1	21- U	7(293	. (-5	. (151	4 (79U	.	p T
CLIXU	1821	7(29	. (LB5	. 0 83	4 (2- 7	.	p T
A6 EA1	357	7(289	. (-U	. (173	4 (-1 0 - 9	.	p T
6 ID2	1U753	7(288	. (L-2	. 0 87	4 (-1 0 - 5U	.	p T
KIAA17- 2	9. 83	7(288	. (738	. (111	4 (7 5	.	p T
CRXZ2	7. U9	7(282	. (-2	. (175	4 (65U8	.	p T
XXAXDC1A	15721	7(281	. (853	. (2	41(-1. 5U	.	p T
OADD75V	- 88U	7(28	. (622	. (122	4 (28U	.	p T
AOXAF7	7. 7	7(239	. (L-	. 0 87	4 (23-	.	p T
XG PXA1	15271	7(23U	. (588	. (1U8	4 (613	.	p T
NHRu	1- 572	7(259	. (753	. (1. 3	4 (-1 0 93	.	p T
SPNXI6 H1	137. U	7(25-	. (-52	. (15U	4 (8. 7	.	p T
CRL- A2	U995	7(257	. (-53	. (157	4 (6- U	.	p T
NME 8	1- 731	7(279	. (LB5	. 0 88	4 (-1 7	.	p T
XLE DC1	15227	7(279	. (L8	. 0 89	4 (728	.	p T
ANSI	1. 5-	7(2UI	. (LB5	. 0 89	4 (89-	.	p T
BOLLU	2. - - 3	7(225	. (283	. (- 8	4 (L2-	.	p T
XCRLCP	17- 83	7(227	. (632	. (1U5	4 (752	.	p T
XDOMNA	17357	7(219	. (-99	. (1- -	4 (2U5	.	p T
CRL12A1	U9- 7	7(218	. (81U	. (19U	4 (853	.	p T
D6 AuV5	5. 18	7(21-	. (L59	. 0 85	4 (L83	.	p T
G MAX5	12U78	7(21U	. (BU	. (13U	4 (8- 9	.	p T
IKVIX	87U8	7(21U	. (288	. (- 8	4 (617	.	p T
6 D6	1L282	7(2. 8	. (658	. (1UU	4 (2-1	.	p T
V6 C2	15- 2	7(195	. (7. 7	. 0 9-	4 (781	.	p T
HIMA	3837	7(195	. (7- 5	. (111	4 (233	.	p T
XNNE2	15335	7(191	. (6- 9	. (1U-	4 (-19	.	p T
CYFHU	75U5	7(18-	. (622	. (125	4 (1- 8	.	p T
XDOMNL	1735-	7(185	. (815	. (195	4 (L83	.	p T
NAV2U	1- . 92	7(181	. (791	. (113	4 (8. 1	.	p T
XDX6	17381	7(18	. (597	. (172	4 (62-	.	p T
C17orfU3	1892	7(139	. (729	. (1. U	4 (789	.	p T
LNXI	113U5	7(139	. (288	. (- 9	4 (235	.	p T
SPG A5A	13UI3	7(135	. (-1	. (17-	4 (293	.	p T
CRL8A2	7. . 2	7(13	. (-95	. (1- 3	4 (-29	.	p T
SKAX2	13- U7	7(13	. (755	. (1. 9	4 (-1 89	.	p T
G AX7K7	12. - 5	7(157	. (L25	. 0 38	4 (L98	.	p T
XED6	1- . 23	7(15U	. (- 8	. (1- 1	4 (6. 9	.	p T
DAV2	7579	7(173	. (77-	. (1. 3	4 (139	.	p T
ASX6	1122	7(1UB	10. 58	. (25-	4 (-92	.	p T
CCDC8.	UI. .	7(1U-	. (-. 3	. (173	4 (272	.	p T
SLC2A17	13829	7(1U-	. (757	. (11	4 (23	.	p T
G ANCKS	12111	7(1U	. (7- -	. (11U	4 (L91	.	p T
PHD2	57. U	7(129	. (7-	. (111	4 (253	.	p T
DLC1	79U-	7(128	. (L- -	. 0 37	4 (178	.	p T
XBNLU	1- . 18	7(123	. (L5U	. 0 8-	4 (215	.	p T
6 AXILU	1U - -	7(125	. (LL9	. 0 82	4 (2LU	.	p T
ONASX	3787	7(122	. (7- -	. (11U	4 (121	.	p T

Gene ID	Gene Name	Score (d)	Numerator (r)	Denominator (s+s0)	Fold Change	adjusted *P* value (%)	Direction
CLPC11A	U882	70119	. 0- . 1	. 017-	4 058	.	p T
XHLDV1	17979	70111	. 017	. 0 8U	4 0277	.	p T
C3orf1.	2582	701. 3	. 0772	. 01. 8	4 05- 9	.	p T
PON1	5U9-	701. 5	. 08U5	. 02. U	4 0 U1	.	p T
SHUXE D2A	13528	701. 2	. 07- 7	. 011U	4 0L28	.	p T
XXMVX1	15772	701. 2	. 0U35	. 0 91	4 07UU	.	p T
XLE DC2	15225	70 9U	. 0521	. 0123	4 0-21	.	p T
LHMK	9- 72	70 92	. 0539	. 0171	4 01. 3	.	p T
PFB1	5318	70 89	. 0281	. 0 - 9	4 0U73	.	p T
OE YLF2	3- 7-	70 59	. 0335	. 0191	4 0-13	.	p T
SLM6 11	18. 2-	70 58	. 07- 3	. 0115	4 0182	.	p T
G YLK	12958	70 5-	. 0-38	. 01- 3	4 01- 5	.	p T
KINNPL	9182	70 5-	. 0U99	. 0 98	4 0273	.	p T
RLMG L2V	1U913	70 55	. 0781	. 0119	4 0-77	.	p T
CFSK	7U5U	70 75	. 0BU5	. 0182	4 0789	.	p T
FSXR2	2. 12.	70 71	. 0UU5	. 0 8U	4 0-17	.	p T
IFOA11	8311	70 7	. 0BUI	. 0181	4 0955	.	p T
XNDG 1	15591	70 U3	. 0783	. 0121	4 0787	.	p T
M6 DC1	- - 55	70 U-	. 0-3	. 01- -	4 0B31	.	p T
C1WF6 M5	2125	70 U7	. 057	. 01U7	4 0-	.	p T
CRL1. A1	U9- 1	70 2-	. 0937	. 0272	41073	.	p T
CAC6 A2D1	239U	70 25	. 0292	. 0 3U	4 02U8	.	p T
ADAG FS17	23U	70 27	. 0B12	. 0133	4 0B17	.	p T
SOIX1	13737	70 18	. 0713	. 01. 7	4 0-U2	.	p T
C9orf125	2- 87	70 . 8	. 0712	. 01. U	4 0157	.	p T
p ACA	2. U2U	70 . -	. 0U87	. 0 9-	4 02. 7	.	p T
PCG 2	5U1-	70 . 7	. 0U17	. 0 38	4 0U3U	.	p T
MVL6 5	- 2. .	70 . 2	. 0-12	. 0 5U	4 01U9	.	p T
HG C6 1	8. . 5	UD995	. 0-12	. 0 5U	4 0555	.	p T
FG PG 75A	19- 1.	UD987	. 0BU-	. 0185	4 07- 8	.	p T
ONPG 1	3792	UD939	. 0559	. 017	4 0B2U	.	p T
MREM2	- - 97	UD93	. 0285	. 0 32	4 0U- 7	.	p T
SXR6 2	18753	UD93	. 0U- 2	. 0 91	4 0753	.	p T
C11orf9-	1383	UD9- 5	. 055	. 01U9	4 021U	.	p T
6 PMH	1UU51	UD959	. 0593	. 0151	4 0U19	.	p T
VP6 D-	178U	UD95-	. 0122-	. 0 53	4 05- 5	.	p T
NPCK	1- U95	UD952	. 0U- 7	. 0 92	4 0LB3	.	p T
SSC5D	18533	UD973	. 0- - -	. 01- 9	4 0785	.	p T
AKAX12	7- 5	UD97-	. 073	. 0119	4 0 - 8	.	p T
LPXNP1	9- . 3	UD977	. 0235	. 0 3	4 0- - -	.	p T
ADAG FS5	28U	UD972	. 0- . 5	. 0157	4 01U9	.	p T
CRL1- A1	U9- 8	UD972	. 0715	. 01. 5	4 0U17	.	p T
KDPLC2	89- 8	UD9U8	. 0U52	. 0 89	4 0729	.	p T
XNKD1	15- - .	UD9U5	. 0U55	. 0 9	4 0188	.	p T
ANL7C	99-	UD923	. 0518	. 01U2	4 02. 2	.	p T
ACF6 1	217	UD925	. 073	. 0U2	4 0789	.	p T
DDN2	7- 37	UD919	. 0715	. 01. -	4 0L2-	.	p T
HRE A114AS1	8. 8-	UD9. 3	. 0571	. 01U8	4 0788	.	p T
Q 6 F2	2. 911	UD9. 2	. 07UI	. 01 1	4 0-75	.	p T
XF XND	15932	UD9. 2	. 0592	. 0152	4 0519	.	p T
XFOIN	15922	UD89-	. 0U55	. 0 91	4 0595	.	p T
CMHNU	U5- 5	UD89	. 0757	. 0113	4 0135	.	p T
HAVX7	3- 85	UD888	. 0U- 8	. 0 95	4 01. -	.	p T
FG PG 2	19552	UD888	. 0U21	. 0 8U	4 05- 8	.	p T
LAG V1	9791	UD888	. 0B2U	. 0 53	4 0U1 1	.	p T
6 CN6 A. . 271	1U2. 7	UD883	. 07U-	. 0112	4 0113	.	p T
SSX6	1858U	UD839	. 0625	. 01U5	4 02U2	.	p T
ONX	35UB	UD83-	. 097	. 027U	4 0-71	.	p T
XNRS1	15312	UD832	. 0U- 2	. 0 9U	4 0 9-	.	p T
IFOA1	83. 9	UD83	. 0UB	. 0 9-	4 0777	.	p T
CD99	U298	UD8- 9	. 0U1 U	. 0 38	4 0L99	.	p T
CPS1	U575	UD8- 3	. 075U	. 0113	4 01. 1	.	p T
CCDC8	U 99	UD8- -	. 05U8	. 01U9	4 0133-	.	p T
G F1G	12393	UD8- 5	. 0B- 8	. 0199	4 0 31	.	p T
XNDG -	15- . 2	UD851	. 0U79	. 0 91	4 0BU8	.	p T
VHLHP71	15. 3	UD851	. 0- 79	. 01- 9	4 0 93	.	p T
SXRCK1	1875U	UD873	. 0- 95	. 0181	4 08. 2	.	p T
PON2	5U93	UD875	. 0- . U	. 0153	. 0 11	.	p T
CG FG U	U837	UD8UB	. 07- 3	. 0122	4 0L9U	.	p T
HPYL	3879	UD8U5	. 0797	. 0129	4 0B23	.	p T
C6 6 1	U9. .	UD8U1	. 0815	. 021U	4 0179	.	p T
FQ ISF2	2. 238	UD823	. 0- . U	. 0153	4 0187	.	p T
LRC1. . 12997.	9999	UD82	. 0U88	. 01. 1	4 05. -	.	p T
LSX1	11853	UD8. 3	. 0U- 8	. 0 93	4 0 9U	.	p T
ACSL7	189	UD8. -	. 0U 2	. 0 39	4 0199	.	p T
CRL5AU	U99U	UD8. -	. 0B2-	. 01U8	4 0895	.	p T
SHUXE D2V	13529	UD8. 7	. 07-	. 0121	4 05. -	.	p T
SALL7	13. - 3	UD8	. 0- - 7	. 0135	4 09U8	.	p T
SRVX	1823-	UD899	. 028	. 0 37	4 0158	.	p T
IFOA5	831-	UD899	. 07U	. 011U	4 05-	.	p T
CFSV	7U7-	UD895	. 07UB	. 0115	4 0 - 2	.	p T
Q ISX1	2. 893	UD89U	. 0U17	. 0 8U	4 0-97	.	p T
NVG SU	1- U7.	UD891	. 02U8	. 0 - U	4 0139	.	p T
M.6 A	- - 13	UD89	. 0U15	. 0 8U	4 02- 9	.	p T
Z6 MF- 9	21783	UD888	. 0 -	. 0137	4 0-U2	.	p T
KLM3	92. 9	UD88-	. 0U88	. 01. 2	4 0758	.	p T
LNNCU2	11337	UD885	. 0782	. 0123	4 0U78	.	p T
C9orf5U	2329	UD885	. 0 - 9	. 0133	4 0725	.	p T
LNCH2	11313	UD885	. 0271	. 0 - 7	4 0253	.	p T
CRG X	7. 2.	UD3U	. 0838	. 02UU	4 0B. 9	.	p T
M5F	- 335	UD8- -	. 0B3-	. 02. -	4 05. -	.	p T
Q ISX2	2. 898	UD8- -	. 0982	. 02- 1	4 0559	.	p T
ZMKU-	21191	UD8- U	. 05U1	. 0171	4 0 85	.	p T
SBPX1	18827	UD8- 2	. 0U2-	. 0 83	4 0 -	.	p T
uDX2	8383	UD8- 1	. 07U1	. 0115	4 077	.	p T
MRE W1	- 319	UD8-	. 0B- 5	. 02. 7	4 0799	.	p T

Gene ID	Gene Name	Score (d)	Numerator (r)	Denominator (s+s0)	Fold Change	adjusted *P* value (%)	Direction
SCAN6 A13	13173	UB58	. (57	. (177	4 (128	.	p T
NAV3L1	1- 1U8	UB58	. (771	. (113	4 (731	.	p T
NASAU	1- 27-	UB53	. (U85	. (1. U	4 (185	.	p T
6 FG	1UB5U	UB55	. (U29	. 0 88	4 (821	.	p T
LG CD1	9323	UB73	. (799	. (1UU	4 (75-	.	p T
OLIXN2	315-	UB72	. (798	. (1UU	4 (U1-	.	p T
ZMHE7	21181	UBUB	. (798	. (1UU	4 (258	.	p T
SF- OAL2	18- 13	UBU-	. (733	. (128	4 (835	.	p T
LRC1. . 1U2891	1. 297	UB25	. (1- 1	. 0 7U	4 (7U	.	p T
DXF	51UB	UB25	. (873	. (2. 1	4 (1- 7	.	p T
AXCDD1	8. 9	UB22	. (588	. (158	4 (18U	.	p T
uAO1	8337	UB19	. (7. 3	. (1. 9	4 (7. 7	.	p T
Sp LM	18337	UB18	. (- 8	. (18	4 (975	.	p T
PIM5A2	57- 8	UB13	. (28U	. 0 3-	4 (U	.	p T
C12orf3.	18U	UB. 8	. (715	. (112	4 (535	.	p T
LREL1	11- 82	UB. 8	. (597	. (1-	4 (- U	.	p T
6 E6	1UB7U	UB. 3	. (U77	. 0 9U	4 (78-	.	p T
AFMJ	1173	UD- 92	. (731	. (128	4 (19-	.	p T
EO	2. 953	UD- 9	. (U5-	. 0 93	4 (791	.	p T
6 HS	1U752	UD- 88	. (252	. 0 - 8	4 (257	.	p T
BPOMC	2. - 53	UD- 83	. (U8U	. (1. 7	4 (297	.	p T
ZPV2	211- 8	UD- 33	. (U72	. 0 9U	4 (- 9	.	p T
IFOVL1	83U9	UD- 33	. (- 32	. (18U	4 (522	.	p T
CRL8A1	7. . 1	UD- 37	. (B72	. (2. . 2	4 (959	.	p T
ANHOPMF.	9- 5	UD- 3U	. (7. 8	. (111	4 (2. 1	.	p T
C21orfU7	229-	UD- 3	. (232	. 0 37	4 (- 0 - 2	.	p T
G F1E	12398	UD- 9	. (58	. (158	4 (- 0 - 3	.	p T
G YR1V	12932	UD- 7	. (U12	. 0 85	4 (212	.	p T
PMPG X2	5U- 7	UD- 59	. (722	. (115	4 (788	.	p T
XDLIG U	17337	UD- 58	. (7- 3	. (128	4 (1- 3	.	p T
IFOVU	83U2	UD- 53	. (62-	. (177	4 (7UB	.	p T
SLC12A7	13- - -	UD- 5-	. (292	. 0 8	4 (19U	.	p T
ACBN2A	2U7	UD- 55	. (2- 7	. 0 32	4 (2U2	.	p T
LRC1. . 1U 83-	1. 11.	UD- 73	. (538	. (159	4 (233	.	p T
G AG DC2	12. . . 3	UD- 73	. (U72	. 0 97	4 (13U	.	p T
MKVX9	- 719	UD- 72	. (188	. 0 52	4 (755	.	p T
LXCAF2	11- 95	UD- U9	. (231	. 0 37	4 (172	.	p T
C5orf1U	2733	UD- U9	. (U- -	. (1. 1	4 (587	.	p T
LNIOU	113U	UD- U8	. (782	. (1U2	4 (11U	.	p T
CD2. .	1228	UD- U5	. (1U7	. 0 92	4 (1. -	.	p T
SXSV1	1879.	UD- 27	. (13U	. (1. U	4 (7-	.	p T
G ENA3	129. 2	UD- 2	. (U17	. 0 83	4 (717	.	p T
XFX6 21	15959	UD- 18	. (7- U	. (128	4 (132	.	p T
C13orf51	2. . .	UD- 12	. (728	. (118	4 (2U3	.	p T
KLM12	9198	UD- 11	. (U7	. 0 97	4 (283	.	p T
CPLM2	U738	UD- . 8	. (U7-	. 0 9-	4 (1 UU	.	p T
MAG 3A1	- 115	UD- . 3	. (2- 1	. 0 32	4 (73U	.	p T
LAY6	9528	UD-	. (199	. (111	4 (218	.	p T
XFOMN6	15921	UD-	. (198	. (1 1	4 (598	.	p T
SY6 DIO1	18851	UB599	. (B7-	. (2. 3	4 (8UU	.	p T
SCHIX1	13133	UB587	. (5. 8	. (172	4 (121	.	p T
NPCWL	1- U9-	UB58	. (131	. 0 78	4 (198	.	p T
OOF5	3. 32	UB533	. (75-	. (128	4 (1U7	.	p T
MOM3	- U- .	UB533	. (127	. 0 9	4 (1 85	.	p T
MRER1	- 312	UB53	. (1U2	. 0 9U	4 (1 . -	.	p T
MAG 2. A	- . . 9	UB53	. (7. 1	. (112	4 (1 89	.	p T
Q DN8-	2. 85-	UB5- 3	. (B. 3	. (198	4 (2UU	.	p T
ZMKG 2	212. -	UB5- 5	. (U35	. (1. 5	4 (7. 2	.	p T
LRC571731	11281	UB5- 7	. (752	. (123	4 (B31	.	p T
G F1P	12391	UB5-	. (587	. (1- 7	4 (1. 2	.	p T
KLM2	92. 7	UB559	. (731	. (1U2	4 (177	.	p T
LAG A1	978-	UB553	. (U1 3	. 0 8-	4 (2U	.	p T
G AX7K5	12. - -	UB55-	. (279	. 0 3	4 (15-	.	p T
CPNCAG	15U-	UB557	. (173	. 0 98	4 (B32	.	p T
DZIX1	523-	UB552	. (1B2	. (1. 5	4 (29	.	p T
OLIS1	3153	UB55	. (729	. (121	4 (79-	.	p T
uAG U	8387	UB55	. (122	. 0 91	4 (275	.	p T
SLC2- A1.	138. 1	UB573	. (U- 5	. (1. U	4 (7- U	.	p T
NRN1	1- 37U	UB575	. (U1 5	. 0 8-	4 (257	.	p T
CFHNC1	7L25	UB572	. (- 3	. (188	4 (927	.	p T
XKD2	15. 31	UB572	. (157	. (1	4 (1U-	.	p T
SLCU- A1	1388.	UB5U-	. (159	. (1. 2	4 (529	.	p T
OLIS2	3158	UB5U5	. (795	. (17	4 (5U7	.	p T
G IFM	12731	UB5U2	. (U1 U	. 0 8-	4 (U1 8	.	p T
6 XN2	1U- 72	UB52-	. (188	. (11	4 (25-	.	p T
OuV2	312.	UB52-	. (8U-	. (2U3	4 (978	.	p T
ZMA6 D5	21137	UB522	. (2- U	. 0 35	4 (152	.	p T
OXC-	3ULU	UB519	. (7U5	. (127	4 (583	.	p T
C6 NIX1	U925	UB519	. (223	. 0 - 5	4 (175	.	p T
C6 IHU	1895	UB51-	. (771	. (125	4 (199	.	p T
SOG S2	1378U	UB517	. (U2-	. 0 9U	4 (73U	.	p T
SFAND8	18- - 1	UB517	. (23U	. 0 38	4 (139	.	p T
X2NY1	17725	UB517	. (252	. 0 32	4 (1- 1	.	p T
Np 6 E1F1	1- 999	UB517	. (5. 9	. (175	4 (0 95	.	p T
uAZM	838-	UB512	. (U12	. 0 89	4 (2U5	.	p T
HSXV2	82UU	UB5. 3	. (5- 7	. (1- 1	4 (1U9	.	p T
6 KD2	1U78-	UB5. -	. (18-	. (11	4 (783	.	p T
CRL15A1	U9- 3	UB5. 5	. (725	. (121	4 (1	.	p T
CD278	U2U3	UB5. 7	. (U31	. (1. -	4 (U	.	p T
HPO1	38. 9	UB5. 2	. (7. 7	. (115	4 (2. 2	.	p T
G YR1D	12937	UB5. 2	. (297	. 0 87	4 (577	.	p T
M2N	538-	UB799	. (U12	. 0 89	4 (2- 5	.	p T
XPLI2	17813	UB793	. (725	. (121	4 (189	.	p T
ALDH1L2	51-	UB79U	. (721	. (121	4 (5U	.	p T
LIG SUL	9- 8-	UB789	. (U51	. (1. 1	4 (279	.	p T
HHIXL1	38- U	UB735	. (U5	. (1. 1	4 (- . 5	.	p T

Gene ID	Gene Name	Score (d)	Numerator (r)	Denominator (s+s0)	Fold Change	adjusted *P* value (%)	Direction
ZCLH12V	211. U	U735	. 019-	. 0 5-	4 0 82	.	p T
AVCA-	72	U7- 1	. 739	. 1L8	. 0 19	.	p T
G F 1L	1239-	U75-	. 617	. 179	4 0 1. -	.	p T
ANAXLU	883	U75-	. LB2	. 1. 8	4 0 97	.	p T
ADAG FS12	231	U751	. 25-	. 0 37	4 091	.	p T
XNKCA	15- 79	U751	. 77-	. 129	4 0 . 5	.	p T
MAS	- 18.	U772	. 29	. 0 87	4 0 U	.	p T
VG Xl	1571	U771	. 19-	. 0 53	4 0B98	.	p T
ORLOA3V	3283	U7	. L- 3	. 1. 3	4 0558	.	p T
CLIX7	L822	U7	. LB3U	. 1. 8	4 0 1. 7	.	p T
LOALS1	9- 18	U723	. 72U	. 127	4 0 51U	.	p T
C2. orf1. U	22U7	U725	. B. 3	. 2. -	4 0519	.	p T
G PIS2	1228-	U713	. L- 7	. 1. 3	4 01-	.	p T
MAG 7UA	- . 7.	U71-	. LB3U	. 1. 9	4 01-	.	p T
KA6 K2	8818	U71U	. L7	. 1	4 0221	.	p T
AKAX1U	7- -	U712	. 25-	. 0 35	4 0198	.	p T
SLAG M9	13- 52	U7. -	. L51	. 1. U	4 083U	.	p T
HSXO2	8275	U7. 2	. 2- U	. 0 33	4 0729	.	p T
FG PG 7U	19- . 8	U L99	. 238	. 0 82	4 0LL5	. 013	p T
POML-	5LB3	U L9-	. 9- 35	. 199	4 0293	. 013	p T
C1. orf1.	1- 81	U L95	. 63-	. 013	4 0 82	. 013	p T
G AOPL2	11991	U L9U	. L- U	. 1. 3	4 0281	. 013	p T
MAF7	- 191	U L89	. 189	. 0 5-	4 0115	. 013	p T
HIC1	3832	U L8-	. L79	. 1. U	4 0277	. 013	p T
C2. orf197	2258	U L85	. L1 1	. 0 89	4 0L1 1	. 013	p T
IDU	8U12	U L85	. LLL9	. 1	4 0259	. 013	p T
CECL12	7U98	U L87	. L8	. 112	4 0123	. 013	p T
SXAFS2L	18U89	U L82	. 7. 7	. 119	4 023U	. 013	p T
G G Xl1	12529	U L81	. 81-	. 271	410 3-	. 013	p T
FXSF1	19837	U L38	. L85	. 117	4 051	. 013	p T
G AXlV	12. UU	U L32	. L71	. 1. 1	. 0 . U	. 013	p T
LRC1. . 1U182-	1. 22.	U L32	. 231	. 0 8	4 07. 7	. 013	p T
A6 FEN2	351	U L3	. 2L-	. 0 3	4 0 73	. 013	p T
KLK7	92- -	U L- -	. L 9	. 0 92	4 0 78	. 013	p T
XPAK1	178. -	U L59	. 28	. 0 8U	4 0 93	. 013	p T
ANHOAX2.	918	U L51	. 238	. 0 8U	4 0 8U	. 013	p T
DRCK11	5. 87	U L73	. L55	. 1. -	.	. 013	p T
SXPCC1	187. 7	U L71	. 2- 1	. 0 38	4 0272	. 013	p T
SXHK1	18718	U L7	. L- 7	. 1. 9	4 071-	. 013	p T
6 p AK1	1L3- 3	U LL9	. L U	. 0 91	4 0 58	. 013	p T
FG PG 2. 7	195- .	U LLU	. L95	. 119	4 0L33	. 013	p T
CRL3A1	7. . .	U L29	. 6L5	. 1- 1	4 052U	. 013	p T
MZD3	- 8L-	U L25	. 6. 1	. 151	4 019U	. 013	p T
HRG PN1	8. 32	U L21	. 27U	. 0 3U	4 6. 1	. 013	p T
DSF	5189	U L21	. 752	. 1L-	4 0 . 3	. 013	p T
ADAG 19	251	U LL2	. 232	. 0 82	4 0 L8	. 013	p T
O6 O11	3271	U L18	. 751	. 1L-	4 0 1	. 013	p T
SMNX7	13779	U L1U	. 68	. 135	4 0297	. 013	p T
VACH2	1L- -	U LL1	. 19	. 0 53	4 0 - U	. 013	p T
LRC28- . - 8	1. 952	U L 9	. 159	. 0 78	4 0521	. 013	p T
FIG XU	19U75	U L 9	. 68	. 135	4 0 - -	. 013	p T
PM6 V2	5LB8	U L -	. 712	. 125	4 0711	. 013	p T
IFOV1	8323	U L 7	. L U	. 0 92	4 02- 7	. 013	p T
MAG 1. 1V	5825	U L U	. 718	. 123	4 6. 7	. 013	p T
X7HAU	177U-	U L U	. 23	. 0 82	4 0928	. 013	p T
ANXC2	1. L2	U293	. 25	. 0 3-	4 07L2	. 013	p T
SOK1	13735	U293	. 722	. 128	4 0 . -	. 013	p T
Z6 M1 . Xl	21U9.	U292	. 77U	. 1L5	4 01U1	. 013	p T
KCFD12	8979	U291	. LB-	. 117	4 0 2-	. 013	p T
MRSV	- - 3-	U291	. B5U	. 229	. 0 95	. 013	p T
G G Xl1U	125U1	U29	. B77	. 22-	4 081U	. 013	p T
SLIF2	18. U5	U289	. L- 5	. 111	4 0239	. 013	p T
PD6 NA	5ULB	U28-	. L1	. 0 97	4 0592	. 013	p T
CDN1	U72U	U281	. 223	. 0 - 9	4 025-	. 013	p T
LZFS1	119U7	U238	. 221	. 0 - 8	4 0735	. 013	p T
CDH1U	UL5.	U233	. L8U	. 113	4 078-	. 013	p T
MAG - 9A	- . 85	U232	. 258	. 0 39	4 0273	. 013	p T
IOMVX3	87. 9	U232	. 723	. 1U1	4 0297	. 013	p T
VG XN2	155-	U231	. 2. 5	. 0 - U	4 0LB8	. 013	p T
XLE 6 C1	152UU	U231	. L-	. 1	4 0559	. 013	p T
XN6 X	15- 88	U23	. 798	. 152	4 01U1	. 013	p T
SPC2UA	1323.	U23	. L72	. 1. 5	4 0531	. 013	p T
C12orf35	18U7	U2- -	. 758	. 17	4 0LB7	. 013	p T
SFOCU	18- 8.	U2- U	. 2U1	. 0 31	4 0LB7	. 013	p T
CNISXLD2	718U	U2- 2	. L7-	. 1. -	4 07. 1	. 013	p T
XLPKHO2	1513-	U253	. 258	. 0 39	4 0522	. 013	p T
IFOAB	8325	U25-	. LB5	. 115	4 0722	. 013	p T
CRL7A2	U985	U25	. 7. 3	. 125	4 0LL-	. 013	p T
FSXA6 18	2. 1. 5	U279	. L71	. 1. 5	4 0L25	. 013	p T
LDV2	9537	U278	. 231	. 0 8U	4 0 - 1	. 013	p T
AH6 AK2	7U1	U273	. 755	. 17	4 08U2	. 013	p T
Dp SXl	5213	U27-	. 6	. 157	4 0 27	. 013	p T
CXE G 1	71LB	U275	. 717	. 128	4 0132	. 013	p T
XLD1	15152	U27U	. 25-	. 0 39	4 0L2-	. 013	p T
DDE 7U	73. 2	U272	. 781	. 178	4 028U	. 013	p T
C- orf137	2575	U271	. LU19	. 0 98	. 0 1-	. 013	p T
PG E2RS	55L8	U2L8	. 717	. 128	4 02. 8	. 013	p T
KLKXl	923U	U2U-	. L5-	. 1	4 0852	. 013	p T
PDILU	5LLU	U2U	. 9- 18	. 191	41 0289	. 013	p T
PG Xl	5529	U228	. 77-	. 1L8	4 0 15	. 013	p T
CCDC88A	Ul1.	U225	. 292	. 0 9	4 0192	. 013	p T
CDK6 1A	U7. 9	U225	. 2LU	. 0 32	4 0L5	. 013	p T
LHMXL2	9- 77	U219	. LU7	. 1. 7	4 018	. 013	p T
XCDH18	17- . 8	U213	. 285	. 0 89	4 0 8U	. 013	p T
XLPKHH2	15187	U2. 9	. 233	. 0 8-	4 0 . 3	. 013	p T
SXANCL1	18U- U	U2. 9	. 9- 19	. 19U	4 0 9U	. 013	p T

Gene ID	Gene Name	Score (d)	Numerator (r)	Denominator (s+s0)	Fold Change	adjusted *P* value (%)	Direction
CCNL1	Ul9-	U2. 9	. 072-	. 0UUU	4 0328	. 013	p T
A6 KH	- 73	U2. 3	. 0L3	. 011-	4 0135	. 013	p T
XP6 K	17822	U2. 3	. 0258	. 0 8	4 05U5	. 013	p T
LRC328835	11559	U2	. 07- U	. 0175	4 02U	. 013	p T
XANBA	17553	U0I99	. 0U -	. 0 9-	4 028-	. 013	p T
CAX6 5	283-	U0I99	. 0718	. 0UU1	4 0I91	. 013	p T
XRFPM	15U89	U0I98	. 0282	. 0 88	4 02- U	. 013	p T
IOM2	8U9-	U0I97	. 0L25	. 0L . 2	4 0I17	. 013	p T
p C6 2	2. 7U-	U0I9U	. 0735	. 0179	4 059-	. 013	p T
SY6 XR	188- 7	U0I9U	. 0232	. 0 85	4 0IU8	. 013	p T
M6 DC7	- - 58	U0I9U	. 0UI3	. 0 99	4 0I17	. 013	p T
XLAF	15128	U0I9	. 0813	. 0255-	4 0U79	. 013	p T
uAG 2	838U	U0I9	. 0LUL2	. 0L . 7	. 0 . U	. 013	p T
IMMR1	8ULU	U0I8-	. 02. 2	. 0 - 7	4 0212	. 013	p T
MAF1	- 188	U0I87	. 056. 9	. 0I-	4 0IU	. 013	p T
LRC1. . 283221	1. UB3	U0I8	. 0UB3U	. 0113	4 09. 3	. 013	p T
N6 M35	1- - 3.	U0I39	. 021	. 0 - -	4 0I1-	. 013	p T
NME2	1- 7- 5	U0I33	. 0UI8	. 0I	4 0UI	. 013	p T
LNNC13	11359	U0I3-	. 0537	. 0181	4 0752	. 013	p T
BS6 L1	2. 37.	U0I3-	. 0562-	. 0I - -	4 0291	. 013	p T
LY9-	11899	U0I - 3	. 0UB7	. 0118	4 0I - 3	. 0UI7	p T
G F1V	12389	U0I - 5	. 0732	. 0179	4 0 87	. 0UI7	p T
XHACFN2	179. -	U0I - U	. 02- 2	. 0 8U	4 0I39	. 0UI7	p T
SXNY2	1878U	U0I - 1	. 0751	. 0I7U	. 0 U	. 0UI7	p T
KLM	92. 8	U0I55	. 0273	. 0 38	4 0IUB	. 0UI7	p T
PM6 V1	5UB3	U0I51	. 0L5	. 0111	4 0I79	. 0UI7	p T
CXZ	71U9	U0I7-	. 0L8-	. 0I2U	4 0UI8	. 0UI7	p T
XYOR1	1- . 7U	U0I75	. 02- -	. 0 85	4 0UB3	. 0UI7	p T
FHVS1	19239	U0IU5	. 0L92	. 0I25	4 05UB	. 0UI7	p T
SXNY1	18782	U0IU7	. 072	. 0IU7	4 0I. 1	. 0UI7	p T
ADAG FS1	2- 9	U0IU2	. 0732	. 0I51	4 0I1-	. 0UI7	p T
A6 OXF2	- U	U0IUI	. 0L99	. 0I23	4 09. 8	. 0UI7	p T
NHRW	1- 57U	U0IU	. 0I22-	. 0 32	4 0 81	. 0UI7	p T
CAB2	2977	U0I29	. 0I27-	. 0 39	. 0 88	. 0UI7	p T
XCSK3	17- 99	U0I23	. 0I38	. 0 53	4 02- 1	. 0UI7	p T
CCDC82	UI. 2	U0I21	. 0LB-	. 0I2	4 0I13	. 0UI7	p T
XLAC9	15127	U0I15	. 0L52	. 0I1U	4 0 35	. 0UI7	p T
G S6	12332	U0I. -	. 0L58	. 0I15	4 02. 7	. 0UI7	p T
CYX2p 1	75. U	U0I. U	. 0I23-	. 0 89	. 0 . 1	. 0UI7	p T
A6 KNDL5	- 95	U0I. 2	. 0582	. 0I88	4 0 58	. 0UI7	p T
G PFN6 L	12U 9	U0 9-	. 0L27	. 0I. 5	4 087	. 0UI7	p T
G MOP8	12U5.	U0 97	. 057	. 0I35	4 029	. 0UI7	p T
OAS-	- 978	U0 97	. 0LB8	. 0122	4 025-	. 0UI7	p T
CM	U5- 8	U0 9	. 0L81	. 0I2U	4 0 27	. 0UI7	p T
DCLK2	7- 29	U0 89	. 0257	. 0 82	4 0UI	. 0UI7	p T
6 PMG	1UL5U	U0 85	. 02-	. 0 87	4 05. 1	. 0UI7	p T
NOS2	1- 5. 2	U0 81	. 0625	. 0I31	4 0 3	. 0UI7	p T
NRCK2	1- 3U-	U0 81	. 0277	. 0 39	4 02-	. 0UI7	p T
HYG AI	8289	U0 8	. 0LB2	. 0I21	4 0 - 3	. 0UI7	p T
BG Xl	2. - 85	U0 8	. 0L9	. 0123	4 0B- 2	. 0UI7	p T
M1UA1	538U	U0 38	. 0LB3	. 0I22	4 0722	. 0UI7	p T
HRE A7	8. 9.	U0 33	. 023-	. 0 9	.	. 0UI7	p T
SFK13V	18- 91	U0 3U	. 0283	. 0 9U	4 0 15	. 0UI7	p T
LRC7. 1. 93	111- 7	U0 - U	. 02. 7	. 0 - 3	4 071U	. 0UI7	p T
ANNDCU	1. 7-	U0 - 1	. 0U- 7	. 0119	4 0L. 7	. 0UI7	p T
LRC1. . 1289. 5	9881	U0 - 1	. 0I13	. 0 U8	4 0U- 1	. 0UI7	p T
S1. . A7	13. UU	U0 -	. 07U5	. 0172	4 0775	. 0UI7	p T
F6 MSM1	19372	U0 -	. 02U-	. 0 33	4 0L95	. 0UI7	p T
HRE AU	8. 89	U0 59	. 0737	. 0155	. 0 U-	. 0UI7	p T
N6 M22	1- - U9	U0 57	. 0UI2	. 0L . 2	4 0292	. 05- U	p T
H19	3- - U	U0 5U	. 0557	. 0182	4 0IU2	. 05- U	p T
6 NX2	1UB11	U0 5U	. 02. -	. 0 - 8	4 0BU7	. 05- U	p T
MG RD	- - 75	U0 52	. 0553	. 018U	4 0 81	. 05- U	p T
OAVANAXL1	- 857	U0 51	. 029-	. 0 93	4 0 55	. 05- U	p T
G GX3	12573	U0 51	10 1-	. 0LUU	4 02- 8	. 05- U	p T
Q F1X	2. 9U8	U0 5	. 0L38	. 0127	4 0291	. 05- U	p T
FSHZ2	2. . 85	U0 7-	. 0LUU	. 0L. 9	. 0 79	. 05- U	p T
ACFVL2	2. 7	U0 72	. 0L29	. 0L. 8	4 022-	. 05- U	p T
SC6 UV	13192	U0 71	. 0712	. 0U-	4 0I2	. 05- U	p T
Sp LM2	18335	U0 71	. 05U8	. 0133	4 0B. -	. 05- U	p T
D6 AuV7	5. 13	U0 71	. 028	. 0 92	4 078-	. 05- U	p T
VACP2	1U- 7	U0 7	. 055	. 0181	4 0229	. 05- U	p T
MSC6 1	- 3- 5	U0 U9	. 0755	. 0I5	4 07- 8	. 05- U	p T
XNKDU	15- - 2	U0 U8	. 0U77	. 0I1U	4 0I- 9	. 05- U	p T
ORLIG 7	329U	U0 UB	. 0UIU	. 0I. U	4 0U73	. 05- U	p T
XHLDAU	17978	U0 UB	. 0U21	. 0L. -	4 0I- 9	. 05- U	p T
FQ SO1	2. 28.	U0 UB	. 0297	. 0 93	4 083	. 05- U	p T
NASL11V	1- 2- 3	U0 U-	. 0759	. 0151	4 071U	. 05- U	p T
MU	539.	U0 U2	. 063-	. 0I9	4 0I39	. 05- U	p T
CRL7A1	U987	U0 U	. 0U9-	. 0UUI	4 078	. 05- U	p T
CAB1	297U	U0 29	. 0755U	. 0I5	. 0 79	. 05- U	p T
BPOMV	2. - 5-	U0 27	. 0271	. 0 8	4 0I9	. 05- U	p T
ANSP	1. 52	U0 18	. 0281	. 0 9U	4 0875	. 05- U	p T
XLAp	15129	U0 18	. 0579	. 0182	4 0839	. 05- U	p T
VCAF1	17UI	U0 17	. 0L2-	. 0L. 8	4 08- 9	. 05- U	p T
WKI	1- . 57	U0 1U	. 0225	. 0 35	4 0I38	. 05- U	p T
SYDP1	18871	U0 . -	. 0153	. 0 52	4 02. 2	. 05- U	p T
M6 DCUV	- - 53	U0 . 7	. 0231	. 0 9	4 0L58	. 05- U	p T
G AX3DU	12. 32	U0 . 2	. 02. U	. 0 - 8	4 0 5-	. 05- U	p T
CSNX2	7233	U0 . 1	. 0725	. 0172	4 0I99	. 05- U	p T
RLMG L2A	1U91-	U	. 02U9	. 0 8	4 0BUU	. 05- U	p T
G RED1	12- . U	U	. 07-	. 015U	4 0 UI	. 05- U	p T
CDKL5	U7. 8	2099	. 0LUL2	. 0111	4 07. U	. 05- U	p T
LAFS2	952-	2098	. 021U	. 0 31	4 0I98	. 05- U	p T
CCDCU	U 5U	2095	. 07- 5	. 0155	. 0 2-	. 05- U	p T
DAXKU	753.	2095	. 0257	. 0 85	4 09- 3	. 05- U	p T

Gene ID	Gene Name	Score (d)	Numerator (r)	Denominator (s+s0)	Fold Change	adjusted *P* value (%)	Direction
CDK-	UL99	2099	. 0793	. 0- -	4 0138	. 65- U	p T
DRCK7	5. 83	2099	. 0299	. 0	4 071-	. 65- U	p T
ADXNH	U7-	20988	. 0U	. 0	4 0 77	. 65- U	p T
G G D	12522	2098-	. 0L31	. 0127	4 0 . 8	. 65- U	p T
NMXL14AS1	1- 75U	20982	. 02L5	. 0 39	4 0287	. 65- U	p T
FOMVN1	19278	20981	. 0235	. 0 92	4 079-	. 65- U	p T
LXH6 2	113. .	20933	. 0225	. 0 35	4 0 3U	. 65- U	p T
LRC7. 11- 7	111- 8	2093-	. 02LU	. 0 38	4 0L3U	. 65- U	p T
CLD6 11	L358	2093U	. 0577	. 018U	. 0 L2	. 65- U	p T
LAG C1	979-	209- 8	. 0L38	. 0123	4 0719	. 65- U	p T
IOMVX-	87. 8	209- 7	. 0L95	. 01LU	4 0 - 2	. 65- U	p T
G G P	12527	209- 7	. 0L- U	. 0122	. 0l 7	. 65- U	p T
LNNC15	1135-	20953	. 0B1	. 0227	41 0L1U	. 65- U	p T
S1. . A2	13. Ul	20953	. 0B15	. 0272	4 0L81	. 65- U	p T
Op LXI	3- L8	2095U	. 0L 7	. 0l . U	4 0 55	. 65- U	p T
Z6 M521	21525	2095U	. 07. U	. 01U-	4 0Ul	. 65- U	p T
FG PG 119	19759	20979	. 0737	. 0l - 1	4 02U	. 65- U	p T
6 AG XF	1U 5-	20978	. 0L85	. 01U1	4 0251	. 65- U	p T
KDPLC1	89- 3	20978	. 029	. 0 98	4 0581	. 65- U	p T
LRC1. . 129L93	9972	20973	. 0229	. 0 38	4 05- 7	. 65- U	p T
MRE L1	- 3. 5	20975	. 01L5	. 0117	4 0L- 7	. 65- U	p T
Op CY1VU	3- U	20977	. 0212	. 0 32	4 0781	. 65- U	p T
KIAA. 7. 8	9. 23	209L9	. 0279	. 0 85	. 0 - 7	. 65- U	p T
CILX	L311	209L8	. 08LB	. 0285	4 07-	. 65- U	p T
OLIXN1	315U	209U-	. 027	. 0 82	4 02L5	. 65- U	p T
6 NXI	1LB1.	209U-	. 028U	. 0 93	4 0173	. 65- U	p T
XDLIG 2	1733U	209U-	. 0l 5U	. 0 52	4 0623	. 65- U	p T
MAu723. 9	- 53.	209LU	. 02- 8	. 0 92	4 0l-	. 0858	p T
LPXNPL1	9- . 8	209LU	. 0753	. 0l 5-	4 0lU-	. 0858	p T
A2G	5	209L2	. 07U-	. 0179	4 0l11	. 0858	p T
CDKL1	U7. 7	20929	. 0221	. 0 35	4 0l83	. 0858	p T
ADG	UU-	20928	. 0599	. 02. 7	4 0298	. 0858	p T
MAu7113.	- 55.	20928	. 0l33	. 0 -	4 0l91	. 0858	p T
PD6 1	5LU7	2092-	. 073U	. 0l - 1	4 0 97	. 0858	p T
AMAXILL1	LB.	20925	. 0231	. 0 92	4 028-	. 0858	p T
FG PG 213	19532	20927	. 0L2	. 0l 1	4 0B85	. 0858	p T
CAND-	2898	2092	. 0L2-	. 0l 11	4 0 51	. 0858	p T
CAXZV	2891	2092	. 0lU-	. 0 73	4 0728	. 0858	p T
ACFV	2. U	20919	. 0l97	. 0 - 3	4 0-58	. 0858	p T
ADC	U. 1	20913	. 0258	. 0 89	4 061-	. 0858	p T
VACP1	1U- U	20915	. 02L9	. 0 82	4 0772	. 0858	p T
FQ ISF1	2. 233	20915	. 0238	. 0 95	4 0l33	. 0858	p T
PXV71L2	5583	20917	. 0L. U	. 0l. U	4 0 - 5	. 0858	p T
XAE 1	1753.	20912	. 0758	. 0153	4 0- . 9	. 0858	p T
MZD1	- 829	209. 9	. 0L8-	. 0lUU	4 023	. 0858	p T
OX6 G V	3U52	209. 8	. 02- 1	. 0 9	4 02. 1	. 0858	p T
NAVUIL1	1- 119	209. 3	. 02U-	. 0 81	4 0778	. 0858	p T
ADDU	U21	209. 3	. 078U	. 0l- -	4 0 72	. 0858	p T
HSXA12V	8218	209. -	. 0L57	. 0122	4 0lUB	. 0858	p T
ICAG 7	8U U	209. 7	. 021	. 0 32	4 0l97	. 0858	p T
M2NL1	5383	209. 7	. 0LU-	. 0l1-	4 0 81	. 0858	p T
OLI2	315.	209. U	. 0lU5	. 0 7-	4 0L1 -	. 0858	p T
LRC1. . 1U727.	1. U7.	209. 1	. 0LB3	. 0lU	41 0l11	. 0858	p T
6 I6 u2	1U7- 2	209	. 0L8	. 0lUl	4 05. 2	. 0858	p T
A6 EA2XU	3- .	209	. 0L73	. 0l2	4 0L1- 9	. 0858	p T
XIFE2	15. 59	20898	. 0L27	. 0112	4 0-55	. 0858	p T
X7HA2	177U5	20897	. 02- 8	. 0 92	4 0B- 1	. 0858	p T
RDZ7	1U897	20897	. 0255-	. 0 89	4 05. 2	. 0858	p T
A6 KNDUB	3. .	20892	. 0LU7	. 0115	4 0L98	. 0858	p T
OXE3	373U	20891	. 0L12	. 0l. 8	4 0L9	. 0858	p T
NRVR1	1- 3Ul	20888	. 0219	. 0 3-	4 07- -	. 0858	p T
CSDC2	72LU	2088-	. 0199	. 0 - 9	4 0711	. 0858	p T
MRS	- - 35	20882	. 0- L2	. 0219	. 0 91	. 0858	p T
GMAX2	12U77	20838	. 0788	. 0l - 9	41 02. 8	. 0858	p T
PVMI	529U	20833	. 02U-	. 0 82	. 0 28	. 0858	p T
AASS	23	2083-	. 0235	. 0 9-	4 0215	. 0858	p T
SF5	18- 15	20832	. 02- 7	. 0 92	4 07- 7	. 0858	p T
MKVX3	- 713	208- 8	. 0Ul3	. 0l 11	4 0751	. 0858	p T
LRC- 751- -	11U83	208- 3	. 0L5U	. 0l2U	4 071	. 0858	p T
XDP1V	17328	208- U	. 0l95	. 0 - 8	. 0 51	. 0858	p T
G G X2UV	1257.	208- U	. 071U	. 0177	4 0137	. 0858	p T
LRC1. . 1U 33-	1. . 99	208- 1	. 0198	. 0 - 9	4 0232	. 0858	p T
NAV3V	1- 1UB	20858	. 07 7-	. 0l5-	4 028	. 0858	p T
CSNXI	723-	20853	. 02U	. 0 81	4 0 2U	. 0858	p T
FOMVI	19273	2085-	. 07 7	. 0157	4 0922	. 0858	p T
C1WF6 M	212-	2085-	. 02 2U	. 0 38	4 0979	. 0858	p T
SFR6 1	18313	2085-	. 0L23	. 0115	4 025-	. 0858	p T
MG 6 LU	- - UB	20857	. 0l51	. 0 5U	4 0L73	. 0858	p T
6 RFCHU	1U597	2085U	. 0Ul3	. 0111	4 0L1 -	. 0858	p T
SACS	13. 58	2085	. 02- 1	. 0 92	4 0 83	. 0858	p T
ARCU	33.	20879	. 0735	. 0l - 3	. 0 91	. 0858	p T
ACF6 U	21-	20873	. 0279	. 0 83	4 072-	. 0858	p T
DKMZXS8- K152.	7912	20873	. 0l33	. 0 - 2	4 0L- -	. 0858	p T
MVL6 1	- 198	20872	. 0773	. 0153	4 023-	. 0858	p T
DSPL	5181	20871	. 0L75	. 0121	4 0L55	. 0858	p T
SHUKVXI	13523	2087	. 02-	. 0 92	4 0122	. 0858	p T
FNR	2. . U7	208LB	. 0L3U	. 0Ul1	4 05LB	. 0858	p T
XFH1N	15929	208U7	. 0l. 9	. 0 U8	4 0 89	. 0858	p T
PONU	5L98	208U7	. 059	. 02. 8	4 0l72	. 0858	p T
SPNXI6 P1	13U93	208Ul	. 02L2	. 0 82	4 02- 2	. 0858	p T
XLRD2	152. 9	208U	. 07L9	. 0155	4 052U	. 0858	p T
FG PG 158	195. 2	20823	. 0518	. 018U	4 0- UB	. 0858	p T
A6 EA2	358	20823	. 0L72	. 0121	4 0l8U	. 0858	p T
MG R2	- - U9	20823	. 0B. 1	. 0278	. 0 - 5	. 0858	p T
LNCH1	1131-	20825	. 0l57	. 0 55	4 0L91	. 0858	p T
DXYSL2	5179	2082U	. 0LU	. 0113	4 0l. U	. 0858	p T

Gene ID	Gene Name	Score (d)	Numerator (r)	Denominator (s+s0)	Fold Change	adjusted *P* value (%)	Direction
G G XU	1257-	20822	. 0- U3	. 022-	4 .0737	10 9-	p T
HRE A3	8. 9U	20821	. 0588	. 02. 9	4 .0 73	10 9-	p T
G F1A	12388	20821	. 0U5 -	. 0IU	4 .0 25	10 9-	p T
NR VRU	1- 3UU	20819	. 02. U	. 0 32	4 .0 13	10 9-	p T
6 DPL1	1U239	20819	. 0I82	. 0 - 5	4 .0U3-	10 9-	p T
KNF13	9U19	20813	. 09- 2	. 0U72	4 .0I1	10 9-	p T
6 CKAX5L	1UIU3	2081-	. 0I21	. 0 7U	4 .0UI7	10 9-	p T
NCA6 2	1- U- 7	20815	. 0252	. 0 89	4 .0 29	10 9-	p T
LNN6 7CL	118UI	20811	. 0L2U	. 0I15	. 0 75	10 9-	p T
LRC28U8- 3	1. 8U7	208. 9	. 072	. 0I5	4 .0- 71	10 9-	p T
DRCK-	5. 89	208. 8	. 02- 1	. 0 9U	4 .0UI1	10 9-	p T
AKFU	5. 2	208. -	. 0L5-	. 0I23	4 .0I91	10 9-	p T
F6 MNSM2A	1932-	208. -	. 0758	. 0I - U	4 .078-	10 9-	p T
C1UbrfUU	187-	208. 7	. 075	. 0I-	4 .0I-	10 9-	p T
CASF	29U7	20893	. 02L5	. 0 87	4 .0I19	10 9-	p T
XNICKLP2	15- 28	20893	. 0U53	. 0I28	4 .02	10 9-	p T
N6 M75	1- - 55	2089-	. 02- 7	. 0 97	4 .0I99	10 9-	p T
FG PG 1U2P	1973-	20897	. 0UI5	. 0I1U	4 .0288	10 9-	p T
ZMKU- L1	21192	20892	. 0UL3	. 0I21	4 .0I15	10 9-	p T
G YR5A	12981	20889	. 0277	. 0 83	4 .03	10 9-	p T
XF XNO	15935	2088-	. 0I7-	. 0 52	4 .0272	10 9-	p T
CSDA	72U2	20885	. 073-	. 0I31	4 .0227	10 9-	p T
F6 MNSM A	193UU	20882	. 0212	. 0 3-	4 .0517	10 9-	p T
CDC17V	UU -	2088	. 0I- 8	. 0 - 1	4 .0 58	10 9-	p T
G RVKL2V	125- -	20839	. 027-	. 0 89	4 .0 31	10 9-	p T
Z6 M5U2	215UU	20837	. 0238	. 0I	4 .0L2	10 9-	p T
DXX7	512-	2083U	. 07. 1	. 0I75	4 .0L5-	10 9-	p T
C8orf7	2- U9	2083U	. 087	. 02- 3	4 .0- . -	10 9-	p T
F VE5	19. 33	2083	. 0I58	. 0 53	4 .0L9-	10 9-	p T
HSUSFUA1	81- -	2083	. 0I- 8	. 0 - 1	4 .0588	10 9-	p T
A6 R-	3U9	208- 9	. 0I 7U	. 0 52	4 .0I17	10 9-	p T
XPCAG 1	1781.	208- 3	. 0233	. 0I	. 0I52	10 9-	p T
FOMVU	1927-	208- 3	. 0751	. 0I - U	4 .079U	10 9-	p T
C6 F6 AXU	U97.	208- 5	. 0UB2	. 0IU5	. 0 18	10 9-	p T
C1WF6 M	2121	208- 7	. 0272	. 0 88	4 .02- 7	10 9-	p T
C1WF6 M8	2123	208- 2	. 02. -	. 0 35	4 .0I15	10 9-	p T
DIR2	7839	208-	. 02- 3	. 0 93	4 .029U	10 9-	p T
PYA2	5332	20859	. 0783	. 0I33	4 .02U3	10 9-	p T
G MAX7	12U73	20859	. 0BU2	. 02- 5	4 .0 . 8	10 9-	p T
HAS2	331.	2085-	. 0I73	. 0 5U	4 .0UI77	10 9-	p T
G YR1P	12935	20855	. 028U	. 0I. U	4 .0UL5	10 9-	p T
CCDCU-	U 53	20857	. 0I98	. 0 32	4 .0UI71	10 9-	p T
HRE A9	8. 97	2085	. 0UL8	. 0I2U	4 .0I1-	10 9-	p T
p SF	2. 599	20878	. 025-	. 0 9U	4 .0257	10 9-	p T
MHAD1	- LB9	20878	. 0IU	. 0 73	4 .0I3-	10 9-	p T
SC6 2V	1319.	2087-	. 02. 9	. 0 3-	4 .021	10 9-	p T
6 F5P	1UB73	20871	. 02- U	. 0 9-	4 .0252	10 9-	p T
S6 AI1	181U2	2087	. 0UI2	. 0I17	4 .0799	10 9-	p T
CRNI6	7. 79	2087	. 02- 1	. 0 95	4 .0 83	10 9-	p T
AFXI 1V	1188	2087	. 0L 9	. 0I1U	4 .0UI1	10 9-	p T
SFUOAL2	18- 1.	2087	. 022-	. 0 82	4 .0I87	10 9-	p T
KNF5	9U73	208U8	. 08- 7	. 0UI-	4 .0 - 5	10 9-	p T
6 KEU2	1U5. U	208U5	. 0L8	. 0IU9	410I29	10 9-	p T
ACRF9	1- 3	208U7	. 0257	. 0 9U	4 .021	10 9-	p T
S1XN2	13. 73	208LU	. 0255	. 0 9U	4 .0 7-	10 9-	p T
DND7	51- 1	208UI	. 0U9-	. 0I75	410 28	10 9-	p T
VHG F2	15. 9	208UI	. 02U5	. 0 8-	4 .0 - 2	10 9-	p T
PFHP1	531U	20829	. 0277	. 0 9	4 .0775	10 9-	p T
XANX7	17551	20829	. 0I- 7	. 0 -	4 .0L U	10 9-	p T
OuC1	312-	20829	. 0L39	. 0IU9	4 .0539	10 9-	p T
XNPLX	15- 17	20823	. 0I. 8	. 0 7	. 0 59	10 9-	p T
NALV	1- 195	2082-	. 0275	. 0 9	4 .05	10 9-	p T
G F1H	12397	20827	. 0U 3	. 0I1U	4 .0I2	10 9-	p T
CH25H	U585	20827	. 07- 8	. 0I32	. 0 13	10 9-	p T
KNF17	9UI5	2082U	. 098-	. 0U- 2	4 .0 95	10 9-	p T
CHN6 A3	U- - 3	2082U	. 022	. 0 81	4 .0U- 5	10 9-	p T
A6 EA8L2	3- -	2082	. 09UI	. 0U72	4 .0288	10 9-	p T
ORLOA8P	3289	20819	. 0252	. 0 9U	4 .0I8	10 9-	p T
SPNX16 P2	13U98	20818	. 07. 1	. 0I78	4 .0L9-	10 9-	p T
KNF1- X2	9UI8	2081-	. 083	. 0L2	4 .0 U2	10 9-	p T
C1orf57	2211	20815	. 02U9	. 0 88	4 .0U-	10 9-	p T
CC6 R	UI39	2081U	. 08UI	. 0U -	4 .0783	10 9-	p T
CDK6 1C	U711	20812	. 07	. 0I78	4 .0 75	10 9-	p T
HSD13V11	8182	20812	. 0L2	. 0I18	4 .0 UI	10 9-	p T
SLC1- A3	13- 95	208. 8	. 0I8	. 0 - -	. 0 53	10- 72	p T
NXS- KAU	1- 898	208. 8	. 02- 8	. 0 99	. 0 U2	10- 72	p T
CRL17A1	U9- -	208. 8	. 07 7U	. 0I- 7	4 .0 92	10- 72	p T
6 PDD9	1UL5.	208. 8	. 0297	. 0I. 9	4 .0277	10- 72	p T
ANHOPM7	9- 7	208. 5	. 02U7	. 0 8-	4 .0I78	10- 72	p T
KA6 K7	882.	208. 1	. 0595	. 02 2	4 .0- 12	10- 72	p T
MLIXI1L	- U99	20- 99	. 02. 8	. 0 33	4 .0778	10- 72	p T
OSFXI	3538	20- 98	. 062U	. 0I97	4 .0 51	10- 72	p T
G PM2A	122- 9	20- 9-	. 02- U	. 0 98	4 .027U	10- 72	p T
LNXI2	113U8	20- 92	. 0UI-	. 0I18	4 .0531	10- 72	p T
XCDHOA8	17- 52	20- 91	. 0I9-	. 0 3U	4 .0IU-	10- 72	p T
IWCutSCHIXI	8- 73	20- 91	. 02 91	. 0I. 8	4 .0I12	10- 72	p T
XID1	17982	20- 91	. 0LB1	. 0IU8	. 0 . U	10- 72	p T
G PCRG	122U-	20- 89	. 02. 9	. 0 38	.	10- 72	p T
CFIM	7U2-	20- 83	. 0292	. 0I. 9	4 .0I93	10- 72	p T
IFOV-	83U-	20- 8-	. 05U8	. 02	4 .02- 7	10- 72	p T
CYLD	77- 9	20- 8-	. 0215	. 0 8	. 0 5-	10- 72	p T
KLM9	9211	20- 8U	. 0U- 1	. 0IU7	4 .0I79	10- 72	p T
XDP3V	1737-	20- 82	. 0227	. 0 8U	4 .0I79	10- 72	p T
Z6 M88.	2138U	20- 81	. 0217	. 0 8	4 .0L51	10- 72	p T
F6 C	1931.	20- 8	. 058	. 021-	4 .0UI3	10- 72	p T
MRSL2	- - 38	20- 3-	. 07. U	. 0I51	4 .0532	10- 72	p T

Gene ID	Gene Name	Score (d)	Numerator (r)	Denominator (s+s0)	Fold Change	adjusted *P* value (%)	Direction
SOCV	137-9	20.35	.02.57	.0.95	4.01.98	10.72	p T
GAMV	11955	20.35	.02.97	.01.1	4.01.9-	10.72	p T
Z6M.99	21--U	20.37	.01U.3	.0.51	4.01.71	10.72	p T
LRC1. . 5. 58. -	1. 757	20.3U	.07.25	.01.59	4.07.22	10.72	p T
KLM.	919-	20.32	.01U-	.01.18	4.01-.2	10.72	p T
ORLOA-L1.	3281	20.31	.01.-	.01.17	4.05.28	10.72	p T
ONID1	35. 2	20.-9	.01. -	. 0 7	. 0 21	10.72	p T
CDHN2	ULB.	20.-8	.02.27	.0.87	4.05-.5	10.72	p T
SLCU8A2	13891	20.-3	.02U.5	.0.88	4.01. 1	10.72	p T
PGE2	55UB	20.-3	.02.13	.0.81	4.01.71	10.72	p T
6 RFCH7	1U595	20.--	.01.1 8	.01.1-	4. 0 . 8	10.72	p T
NCVFV2	1-U-3	20.--	.02.25	.0.85	. 0 3	10.72	p T
RDZ2	1U892	20.-7	.06.25	.01.93	4.01.3-	10.72	p T
LRC328. - 1	115. -	20.-1	.01.81	.01.7U	4.07.9U	10.72	p T
6 N6 1	1UB. 8	20.-1	.01U.2	.01.25	4.02U.9	10.72	p T
SXAFA9	18U.85	20.-1	.01U.2	. 0 5	4.01.28	10.72	p T
GNAS	12-U.9	20.59	.01.87	.01.77	. 0 - 3	10.72	p T
XFX6 17	15957	20.59	.01U-2	.01U-	4.02.32	10.72	p T
up 6	881.	20.53	.07.1U	.01.5-	. 0 82	10.72	p T
NRNA	1-375	20.53	.02U.8	. 0 9	4.02. U	10.72	p T
CILX2	UB12	20.5-	.07.38	. 01.8	4.08.78	10.72	p T
BDN	2. - 57	20.5U	.02.9U	. 01.1	4.01.97	10.72	p T
F6 MAIX8	1931-	20.73	.02.32	.01. U	4. 0 - 2	10.72	p T
CDH2	UL5-	20.73	.07.85	.01.8U	41.0. 18	10.72	p T
NASD1	1-251	20.7U	.06-	.02.12	4. 0 1-	10.72	p T
p VP2W2XI	2. UBU	20.U-	.02U.9	. 0 91	4.01. 5	10.72	p T
SGAD9	18. - 2	20.U-	.01- 2	. 0 - 2	. 0 8U	10.72	p T
EYLF1	2. 99-	20.U7	. 02U	. 0 83	4.01.1 8	10.72	p T
D6 AuC18	5. U2	20.U7	.01.39	. 0 - 8	4. 0 - 8	10.72	p T
LRC7. . 7- 7	111UI	20.U	.01.97	. 0 37	4. 0 97	10.72	p T
XPN1	17827	20.28	.0U.79	.01.UU	4. 0 .8U	10.72	p T
Np 6 E1	1-998	20.2-	.02.97	.01.12	4.0B2U	10.72	p T
MAG 2. C	-. 11	20.25	.01.28	.01.25	4. 0 9-	10.72	p T
LANX-	9513	20.25	.01.U.5	.01.28	4.01.88	10.72	p T
XpNO	1-. . -	20.2U	.01.28	. 0 79	4.07. 7	10.72	p T
MAVX5	58. 5	20.21	.07.UI	.01.- 7	4. 0 .UB	10.72	p T
C1Ubrf15	18UB	20.18	.01.17	. 01.2	4. 0 .81	10.72	p T
ADAGFSL2	289	20.13	.02.31	.01. 7	4.09.35	10.72	p T
PHDU	57. 7	20.13	.01.93	. 0 35	4.01.29	10.72	p T
SDC1	1322-	20.15	.07.78	.01.31	4.08.13	10.72	p T
FSC22DU	2. . - 9	20.15	.01.2U	.01.2U	4.01.- 7	10.72	p T
XC6 E	17-87	20.15	. 02U	. 0 88	4.01.1 9	10.72	p T
MAG 7UV	-. 71	20.11	.02-.8	.01. U	4.01.1 1	10.72	p T
CHSF12	U-39	20.11	.02. 2	. 0 33	4.01U-	10.72	p T
NC6 1	1-UB7	20.1	.01U.7	. 01.2	4.01.2U	10.72	p T
MAG 89A	- 1U.9	20. . 9	.01U.7	.01.28	.01.- 7	10.72	p T
CECL2	77. U	20. . 3	.06.98	.02.29	. 0 8	10.72	p T
G1AF	127U	20. . -	.07.- 8	. 01.8	4.06.1-	10.72	p T
KC6 ul 5	889-	20. . 5	.01.12	. 0 7U	4.0BUU	10.72	p T
6 XHXU	1U-2-	20. . U	.02. U	. 0 38	4.01.1 -	20.7	p T
LRC1. . 19. 9U.9	1. U-U	20. . 1	.01.73	.01.UU	4.01.93	20.7	p T
IM1-	8UL5	2069.9	.01.27	.01.27	4.01.51	20.7	p T
PGIL16 2	5521	2069.8	.01.U.5	.01.29	4.01.UU	20.7	p T
CXP	7. 98	2069.8	.06.25	.02. .2	4.01.9U	20.7	p T
LRC1. . 1U . . .	1. . . . 5	2069.3	.0- 8	.02.53	4.02.93	20.7	p T
IL7N	8523	2069.7	.02.75	.0.95	4. 0 .3U	20.7	p T
CRE3A1	7. 39	2069.U	.07.59	.01.33	4.01.83	20.7	p T
ZCCHC11	21121	2069.2	.02.1-	. 0 8U	4.01.U.U	20.7	p T
C- orf175	25UU	2069	.01. 1	.01.1-	4. 0 .88	20.7	p T
XLAOL1	1512-	2068.9	.02.12	.0.82	4. 0 . .2	20.7	p T
AMAXI	U-8	2068.9	.01.8-	. 0.32	4.06	20.7	p T
CSXO7	72-8	2068.8	.01.U.9	.01.U.1	4.06.2	20.7	p T
CD99XI	UU.	2068.8	.02.12	.0.82	4.08.95	20.7	p T
A6 KS-	329	2068.3	.07.13	.01.- 1	4. 0 - 3	20.7	p T
p VFD2	2. 717	2068.3	.02.13	.0.87	41.0. U.9	20.7	p T
GAOPH1	1199.	2068.5	.01. 2	.01.13	4.02.25	20.7	p T
FXSUIU	198U	2068.5	.02.39	.01. 8	4.01	20.7	p T
CHSF11	U-38	2068.5	.02-.7	.01. 2	4. 0 - 79	20.7	p T
ANHOAXI.	91.	2068.U	.02.37	.01. -	4.02.53	20.7	p T
ORXC	3U.	2068	.01.89	. 0 3U	4.07.5U	20.7	p T
C9orfU	231-	2068	.01.81	. 0 3	4.06.25	20.7	p T
KAF6 AL1	88U	2063.9	.02.77	.0.95	4.07. 3	20.7	p T
VACH1	1U-5	2063.9	.01- U	. 0 - U	4.02.U.9	20.7	p T
LVH	9529	2063.9	.01- 9	. 0 - 5	4.01-.5	20.7	p T
IODCC7	8L.9U	2063.9	.02.95	.01.17	4.01.72	20.7	p T
FFC2U	2. 153	2063.9	.02U.9	. 0 9U	4.01.99	20.7	p T
HRRKU	8. 38	2063.8	.02.71	.0.97	4.02U.9	20.7	p T
P6 FXD1	553.	2063.3	.02. 1	.0.38	4.01.39	20.7	p T
RLMGL1	1U.915	2063.3	.01.3-	. 0 - 8	4.02U.8	20.7	p T
LG6A	93UI	2063.-	.02.1-	.0.87	4.01.5-	20.7	p T
GYH9	12977	2063.-	.02. 8	.0.81	4.01.-U	20.7	p T
HIBPX2	39-7	2063.-	.02.8U	. 01.1	4.07-	20.7	p T
XAXXA	1751-	2063.5	.02.92	.01.17	4.08. -	20.7	p T
MHRDU	-UB3	2063.1	.07. 7	.01.53	4.01.72	20.7	p T
CLPCUV	UB93	206.-8	.01.38	.01.73	4. 0 . 9	20.7	p T
ADCY3	UI7	206.-3	.02.3U	.01. -	4.06. 2	20.7	p T
FOMVN2	19279	206.-U	.02.9-	.01.15	. 01.U7	20.7	p T
IL11	8751	206.-	.02U	. 0 9	41.02.9U	20.7	p T
ANPO	89.	206.-	.06.15	.01.18	4.01.U.U	20.7	p T
QDN-U	2. 8UB	2065.-	.01.32	.0.-3	4. 0 11	20.7	p T
VHLHP22	15. 7	2065.5	. 01.5	.01.UB	. 0 . 8	20.7	p T
AS6S	111U	2065.7	.01.1 1	.01.18	4.07.98	20.7	p T
OAL6FL2	- 919	2065.7	.01.8-	.01.51	4. 01.2	20.7	p T
QIXM	2. 892	2067.9	.02. .3	.0.81	4.01.31	20.7	p T
SFE2	1837-	2067.9	.02.98	.01.13	4.01.-1	20.7	p T
GF2A	12399	2067.8	.01.9-	.01.55	4. 0 37	20.7	p T

Gene ID	Gene Name	Score (d)	Numerator (r)	Denominator (s+s0)	Fold Change	adjusted *P* value (%)	Direction
Dp SX-	52U8	2067 8	. 0U8U	. 0151	. 0 72	207	p T
Z6 MfU8	217- 9	2067-	. 0185	. 0 3U	4 02U3	207	p T
AMAXIL2	UB1	2067 7	. 0LL2	. 0UU1	4 0217	207	p T
V6 IXLL	15- -	2067 U	. 02U5	. 0 9U	4 0- 2	207	p T
6 XC2	1U- 13	2067	. 0233	. 0I . 9	4 0U1U	207	p T
OAVNV2	- 8- 8	2067	. 015-	. 0 - 2	4 0559	207	p T
XNN5L	15359	2065 2	. 0228	. 0 9	4 0815	207	p T
XCDHV17	17- U7	2065 I	. 0L5U	. 0U9	4 0213	207	p T
MRE 6 U	- 31.	2065 9	. 0222	. 0 88	4 0UU	207	p T
LRC1. . 5. 35. 3	1. 5U7	2062 8	. 02U3	. 0 97	4 0511	207	p T
LRC175- 97	1. - 72	2062	. 0U1U	. 0127	4 0- 98	207	p T
CLIC7	UB15	2061 8	. 025-	. 0I . 2	4 0555	207	p T
p 6 C5V	2. 791	2061 8	. 0L82	. 0152	41 0B93	207	p T
CLD6 5	UB37	2061 3	. 0F11	. 0I - U	. 0 87	207	p T
LRC- 5U 35	11787	2061	. 0UI2	. 0127	4 0 7	207	p T
CX6 P8	711-	2061	. 0183	. 0 35	4 0 29	207	p T
FMXI	192U5	205. 8	. 0I8U	. 0I 1U	. 0 5-	207	p T
PNG 6	5- 3.	205. 7	. 0I-	. 0 - 7	4 0LB	U0I - 7	p T
BCL	2. - 7-	205. U	. 0273	. 0 99	4 0251	U0I - 7	p T
XCDHV1-	17- U-	205. U	. 0LB5	. 0I5	4 0 - 9	U0I - 7	p T
ANHOAXUI	929	205. 2	. 0I73	. 0 59	4 0L75	U0I - 7	p T
XXXLCC	155UU	205. 1	. 0I9-	. 0 39	4 0LB-	U0I - 7	p T
F6 AX	193. 9	205. 1	. 0I53	. 0 - U	. 0 72	U0I - 7	p T
KNF72X	9U7-	207 99	. 0LU	. 0U2	4 0I7	U0I - 7	p T
CUbrf- 7	2723	207 99	. 0I7U	. 0 53	4 0295	U0I - 7	p T
FSXA6 2	2. 1. 3	207 93	. 0I39	. 0 32	4 0I93	U0I - 7	p T
OLO1	3178	207 9-	. 02	. 0 8	4 02U3	U0I - 7	p T
XLPKHO1	15135	207 95	. 0278	. 0 99	4 0 9	U0I - 7	p T
SY6 2	18873	207 97	. 02- U	. 0I . -	. 0 27	U0I - 7	p T
FGPG 113	19758	207 97	. 0218	. 0 88	4 07. 8	U0I - 7	p T
NAX2V	1- 225	207 9U	. 0I31	. 0 - 9	4 0L- 2	U0I - 7	p T
SLCU9A1U	139. U	207 9	. 0139	. 0 32	4 05L2	U0I - 7	p T
CUbrf53	272U	207 83	. 0I88	. 0 3-	. 0 23	U0I - 7	p T
ZSQ IG 7	218U7	207 83	. 0L78	. 0I 7	4 0231	U0I - 7	p T
XLSCN7	15219	207 83	. 0LI 1	. 0121	. 0 UI	U0I - 7	p T
NAXOPM2	1- 228	207 8-	. 0159	. 0 - 7	4 0 72	U0I - 7	p T
CYX23C1	7788	207 87	. 0L85	. 0151	4 0795	U0I - 7	p T
FVC1D2	19. 21	207 87	. 0E7U	. 0 98	4 052-	U0I - 7	p T
ANSV	1. 5.	207 8U	. 0I31	. 0 - 9	4 0- 82	U0I - 7	p T
6 IXAL7	1U73.	207 8U	. 0LL8	. 0U-	4 0BU9	U0I - 7	p T
VFVD19	1- 71	207 82	. 0I17	. 0 7-	4 0895	U0I - 7	p T
ZVFV1	21. - .	207 81	. 02. 1	. 0 81	4 0- U9	U0I - 7	p T
MLNF2	- - 2U	207 81	. 0I3	. 0 - 8	4 0I58	U0I - 7	p T
XDOMA	1735.	207 81	. 022	. 0 89	4 0I93	U0I - 7	p T
xdT0I.	13U71	207 38	. 0232	. 0I 1	4 0219	U0I - 7	p T
XFOIS	1592U	207 3U	. 07	. 0I - 2	. 0 - 9	U0I - 7	p T
XAVXC7L	17778	207 32	. 0228	. 0 92	4 0 98	U0I - 7	p T
NAVAC1	1- 177	207 3	. 0I9	. 0 33	4 09. 1	U0I - 7	p T
CF6 6 V1	7UL2	207 - 9	. 02U9	. 0 93	4 0L29	U0I - 7	p T
FHSD3A	19U 5	207 - 3	. 0277	. 0I	4 0I82	U0I - 7	p T
BXSU-	2. 315	207 - 5	. 02. 8	. 0 87	4 028-	U0I - 7	p T
XFFO11X	1599-	207 - 7	. 0182	. 0 37	4 05L5	U0I - 7	p T
FCPAL3	19. 92	207 - 2	. 02U	. 0 9U	4 0I25	U0I - 7	p T
CH6 1	U- 71	207 - 1	. 02- -	. 0I . 8	4 0- 8	U0I - 7	p T
CEorf53	77UB	207 - 1	. 02- 2	. 0I . -	. 0 31	U0I - 7	p T
XXXIN1UL	15783	207 58	. 0277	. 0 98	4 075-	U0I - 7	p T
MuuU- . UI	- 51U	207 58	. 0235	. 0I 12	4 0 . 1	U0I - 7	p T
LOALS3	9- 23	207 58	. 0 . 5	. 0227-	4 0L29	U0I - 7	p T
MY6	- 823	207 5-	. 0UI1U	. 0123	4 0 83	U0I - 7	p T
ZCCHC9	211UB	207 55	. 0I2-	. 0 51	4 02UI	U0I - 7	p T
Q DN71	2. 813	207 57	. 0I9	. 0 33	4 0585	U0I - 7	p T
SXO2.	18717	207 57	. 0222	. 0 9	4 0I33	U0I - 7	p T
OLS	3135	207 5U	. 02U9	. 0 98	4 0I31	U0I - 7	p T
SFE3	18351	207 5U	. 0I33	. 0 32	4 0 22	U0I - 7	p T
IL1-	87- 2	207 5	. 0157	. 0 - U	4 0I- 3	U0I - 7	p T
XXAX2V	15719	207 79	. 0L23	. 0LU7	4 0 . -	U0I - 7	p T
SFG 6 2	1831.	207 73	. 0731	. 0I 9U	4 052	U0I - 7	p T
SLC2. A1	1332.	207 7-	. 0199	. 0 81	41 0I71	U0I - 7	p T
ID1	8UI.	207 7U	. 0F12	. 0I - 9	4 0 17	U0I - 7	p T
XXXIN15A	15792	207 72	. 02. 3	. 0 85	4 0 93	U0I - 7	p T
G AF6 U	121U9	207 71	. 0728	. 0L35	4 0958	U0I - 7	p T
A6 OXFL7	- U5	207 7	. 0583	. 0227	. 0 31	U0I - 7	p T
XOG 5	1789-	207 7	. 021	. 0 8-	. 0 8	U0I - 7	p T
CCDC1. 2A	2982	207 U9	. 0253	. 0I . 5	4 02U9	U0I - 7	p T
NASONM2	1- 258	207 U9	. 0229	. 0 97	4 07- -	U0I - 7	p T
HPCQ 2	38. 8	207 U-	. 0297	. 0L21	4 0728	U0I - 7	p T
XXAX2A	15718	207 U-	. 023U	. 0I12	. 0IU9	U0I - 7	p T
ACAA2	11-	207 U5	. 0289	. 0119	4 0 - U	U0I - 7	p T
CLIX2	UB2.	207 U5	. 0I- U	. 0 - 3	4 07- -	U0I - 7	p T
G YL12V	12978	207 U7	. 0I3U	. 0 31	4 0B. U	U0I - 7	p T
CRO-	U953	207 U7	. 0I21	. 0 5	4 0L2U	U0I - 7	p T
LRC1. . 12398U	93- 9	207 U2	. 0197	. 0 8	4 0L5U	U0I - 7	p T
LRC1. . 128252	98. 1	207 U2	. 0L38	. 0I5-	4 0229	U0I - 7	p T
IL1NAX	8787	207 U2	. 0223	. 0 97	4 0L5	U0I - 7	p T
LIE 1L	9315	207U	. 0I- 3	. 0 - 9	. 0 . 8	U0I - 7	p T
CNYAV	72. 9	207 29	. 0- 87	. 0282	. 0 71	U0I - 7	p T
LNNC8A	1181U	207 29	. 0191	. 0 39	4 0535	U0I - 7	p T
ZYE	21873	207 23	. 025U	. 0I . 7	4 0278	U0I - 7	p T
M.6 C	- - 19	207 2U	. 0I7-	. 0 -	4 07- 3	U0I - 7	p T
KLHL28	927.	207 21	. 0I9-	. 0 81	4 0B59	U0I - 7	p T
HREA-	8. 92	207 18	. 07U2	. 0138	4 0 11	U0I - 7	p T
PLKU	5783	207 13	. 0175	. 0 -	4 0725	U0I - 7	p T
CRL11A1	U9- 2	207 17	. 02U7	. 0 93	41 0 37	U0I - 7	p T
LRCUB519-	11. 5U	207 1U	. 0UI2	. 0129	4 072U	U0I - 7	p T
XLFX	15221	207 12	. 0LI 7	. 0I2-	4 0 . 8	U0I - 7	p T
SINXA	13- 1.	207. 9	. 0239	. 0I1-	. 0 15	U0I - 7	p T

Gene ID	Gene Name	Score (d)	Numerator (r)	Denominator (s+s0)	Fold Change	adjusted *P* value (%)	Direction
REF	1771-	20Ø. 9	. Ø138	. 0 37	4 ØBU8	UØ1 - 7	p T
LRC1. . 129- 35	99- 9	20Ø. 8	. ØE. 3	. 0 8-	4 Ø1 - U	UØ1 - 7	p T
ADAG FS9	283	20Ø. 8	. ØU 9	. Ø128	4 0 2-	UØ1 - 7	p T
XLA2O5	1511U	20Ø. 5	. ØE. 1	. 0 87	4 Ø73-	7Ø718	p T
ANL15	988	20Ø. 7	. ØE1U	. 0 89	4 ØE25	7Ø718	p T
VAO2	1U- 9	20Ø. U	. ØU 5	. Ø123	4 Ø887	7Ø718	p T
XCDH3	17- 11	20Ø. U	. ØE99	. Ø127	4 0- 7-	7Ø718	p T
OYXC	3- 5U	20Ø. 1	. Øl- U	. 0 - 8	. ØU37	7Ø718	p T
FFC3A	2. 18U	20Ø. 1	. ØE19	. 0 91	4 ØEU2	7Ø718	p T
XDP7DIX	173UB	20Ø. 1	. Ø132	. 0 32	4 ØE8	7Ø718	p T
A6 EA5	3- U	20Ø	. ØE21	. 0 92	4 ØU77	7Ø718	p T
F6 6 I2	193- -	20U.98	. Ø619	. ØE1-	. 0 97	7Ø718	p T
G ALL	12. . 5	20U.98	. Ø7. U	. Ø1 - 8	. 0 73	7Ø718	p T
CCI6	UI25	20U.98	. ØU77	. 0 -	4 Ø65U	7Ø718	p T
Q VX5	2. 38U	20U.93	. ØUL9	. ØU71	4 0 9-	7Ø718	p T
FFC28	2. 1- U	20U.9-	. ØIUL2	. 0 55	4 ØL21	7Ø718	p T
CRL13A1	U9- 9	20U.9-	. Ø677	. ØE23	4 0 77	7Ø718	p T
CECN3	7715	20U.9-	. ØL9U	. Ø1 - 7	4 Ø875	7Ø718	p T
SRCSU	18239	20U.97	. ØU- 7	. Ø152	4 0 U	7Ø718	p T
SALL1	13. - 7	20U.9U	. 0 93	. 0 71	4 Ø7 - 9	7Ø718	p T
Z6 M535	2153.	20U.92	. Ø1 - 8	. 0 3	4 0 . -	7Ø718	p T
CALp	28U.9	20U.91	. ØE- -	. Ø111	4I1 0 U.9	7Ø718	p T
SOFV	13797	20U.91	. Ø18	. 0 35	4 Ø1 - 7	7Ø718	p T
CAC6 A1C	2385	20U.91	. Ø187	. 0 33	4 0 99	7Ø718	p T
6 AALADL1	1U U2	20U.91	. Ø111	. 0 7-	4 ØL. -	7Ø718	p T
CLPC2V	UB9U	20U.9	. ØE32	. Ø117	4 Ø119	7Ø718	p T
SLCU8A5	13897	20U.88	. ØE73	. Ø1. U	4IØE9U	7Ø718	p T
XFXNV	159- 9	20U.83	. ØE29	. 0 9-	4 0 29	7Ø718	p T
G YL12A	12973	20U.83	. ØEU-	. 0 99	4 Ø7U2	7Ø718	p T
CHSYU	U- 9U	20U.83	. ØIUI	. 0 55	4 0-21	7Ø718	p T
Z6 M555	21579	20U.8-	. Ø187	. 0 33	4 Ø7UB	7Ø718	p T
XXG 1K	15732	20U.87	. ØL5U	. Ø178	4 ØB25	7Ø718	p T
XIQ IL7	15. - 7	20U.8U	. ØE35	. Ø115	4 0 89	7Ø718	p T
SYXL2	18831	20U.82	. Ø155	. 0 - 5	4 Ø137	7Ø718	p T
ADAG FS1-	235	20U.38	. ØL2-	. ØUB	4 Ø635	7Ø718	p T
C- orf2. 7	255U	20U.38	. Ø121	. 0 51	. 0 . 2	7Ø718	p T
G A6 1A1	12. 17	20U.38	. ØU 8	. Ø129	4 Ø1	7Ø718	p T
C1orf12U	2173	20U.38	. ØI3	. 0 31	4 ØE83	7Ø718	p T
PDA2N	5UE2	20U.35	. Ø135	. 0 37	4 Ø129	7Ø718	p T
KIAA. 922	9. 51	20U.35	. ØE5-	. Ø1. 8	4 ØUI2	7Ø718	p T
IL8	85U.5	20U.37	. Ø1U7	. 0 5-	4 Ø1 - 9	7Ø718	p T
LPXNPL2	9- . 9	20U.3U	. ØL38	. Ø159	4 0- U7	7Ø718	p T
XHC2	1791U	20U.32	. Ø17U	. 0 -	4 ØUI9	7Ø718	p T
SLCU5V7	138- 7	20U- 9	. Ø183	. 0 39	4 Ø77U	7Ø718	p T
XLK2	152. 2	20U- 9	. Ø712	. ØI37	4 ØL98	7Ø718	p T
PBI2A	5328	20U- 8	. ØE82	. ØU19	4 ØE7-	7Ø718	p T
ADAG FS1.	23.	20U- -	. ØUL9	. Ø17U	4 ØLLU	7Ø718	p T
O6 XFAV	32- 7	20U- -	. Ø188	. 0 39	4 ØL1 U	7Ø718	p T
NAV27	1- . 9U	20U- U	. ØE21	. 0 9U	4 Ø59U	7Ø718	p T
SFAND9	18- - 2	20U- 2	. ØIU7	. 0 53	4 ØI75	7Ø718	p T
C6 F6 1	U9U2	20U- 1	. ØE12	. 0 9	4 ØE13	7Ø718	p T
OAS3	- 979	20U-	. ØE2-	. 0 9-	4 Ø177	7Ø718	p T
Q LS	2. 9. 1	20U-	. ØUIU	. ØUL2	4 ØE93	7Ø718	p T
CNPVUL2	7153	20U.59	. ØEU	. 0 98	4 ØE81	7Ø718	p T
KX6 AU	929U	20U.59	. Ø15-	. 0 - -	4 Ø7U5	7Ø718	p T
FVE 18	19. - 9	20U.58	. Ø152	. 0 - 5	4 0 - 5	7Ø718	p T
G G XI.	12528	20U.5-	. Ø7- 5	. Ø198	4 0-91	7Ø718	p T
XNDG 8	15- . U	20U.55	. ØI3	. 0 32	. 0 75	7Ø718	p T
CYXIV1	7738	20U.51	. Ø757	. ØI9U	4 Ø1 - 9	7Ø718	p T
LRC1. . 288- 15	1. 7. -	20U.5	. ØE. 8	. 0 89	4 0 83	7Ø718	p T
VUOALFL	1UL2	20U.5	. ØEUB	. Ø1. 1	4 Ø898	7Ø718	p T
SLCU9A17	139. 7	20U.78	. ØI82	. 0 38	4 ØB52	7Ø718	p T
CRNR1C	7. 52	20U.73	. ØE2U	. 0 95	4 ØL22	7Ø718	p T
LRC28UL92	1. 395	20U.7-	. ØU7-	. Ø178	. 0 . 2	7Ø718	p T
D6 G 1X7-	5. - 3	20U.7-	. ØE. 3	. 0 88	. ØI7U	7Ø718	p T
NAVUI	1- 1. 2	20U.75	. Ø728	. Ø18U	4 0-77	7Ø718	p T
ANNDC7	1. 73	20U.77	. ØUI	. ØUL2	4 0 18	7Ø718	p T
MaI225U-	- 75-	20U.72	. Ø183	. Ø1 - 5	4 ØL58	7Ø718	p T
LAG VU	9797	20U.71	. Ø658	. ØEL8	. 0 U9	7Ø718	p T
HPY1	3873	20U.7	. ØUI2	. ØUUU	4 ØLUB	7Ø718	p T
XF6	159U9	20U.U9	. Ø6- 3	. ØE272	. 0 38	7Ø718	p T
O6 O2	3277	20U.UU	. Ø139	. 0 33	. 0 79	7Ø718	p T
CYV5NU	775U	20U.U2	. Ø155	. 0 - 3	4 Ø7. 3	7Ø718	p T
DLE5	79- 2	20U.U2	. ØU29	. Ø171	4 Ø6U9	7Ø718	p T
SLC27AU	13351	20U.UI	. Ø6. 1	. ØE15	4 0-52	7Ø718	p T
NOL1	1- 739	20U.UI	. ØE32	. Ø113	. Ø1. 1	7Ø718	p T
ABXN1A	1U 8	20U.28	. Ø13U	. 0 37	4 0 3-	7Ø718	p T
XDP2A	173UI	20U.28	. ØUI3	. ØU1-	. ØE23	7Ø718	p T
SRE13	18UI1	20U.28	. ØU1 -	. ØUI1	. Ø1. U	7Ø718	p T
G YH1.	129UI	20U.28	. Ø197	. 0 87	4 Ø6U-	7Ø718	p T
LRC- 7U- 5.	11UU-	20U.23	. Ø7. 9	. Ø13-	4 Ø1 1	7Ø718	p T
DPXDC3	739U	20U.25	. ØEUU	. Ø1	4I1 0 73	7Ø718	p T
Z6 MF2U	21753	20U.25	. ØE1U	. 0 92	4 ØE-	7Ø718	p T
SLC1- AU	13- 91	20U.27	. ØL97	. Ø1 - 9	4I1 ØU72	7Ø718	p T
CC6 D2	UI - U	20U.2U	. ØE8	. Ø121	. 0 28	7Ø718	p T
KIM2- V	9152	20U.22	. Ø155	. 0 - 3	4I1 Ø1. 2	7Ø718	p T
MHL2	- U8U	20U.21	. ØUE7	. ØUL9	4 ØE. 1	7Ø718	p T
FFCUB	2. 135	20U.2	. Ø1 - 9	. 0 3U	4 ØUI5	7Ø718	p T
LRN	11- 39	20U.2	. Ø1UB	. 0 59	4 0 92	7Ø718	p T
Cp V6	7U- 9	20U.I9	. 0 82	. 0 U5	4 0 U7	7Ø718	p T
AFXI. A	1187	20U.I3	. Ø189	. 0 82	4 ØB52	7Ø718	p T
CRL1UA1	U9- 5	20U.I-	. ØU 8	. ØUUU	4 Ø655	7Ø718	p T
CAG K26 1	2878	20U.I-	. Ø7- 1	. Ø199	4 ØL57	7Ø718	p T
HAXL6 U	33. 2	20U.I5	. . Ø5U	. ØE29	4 ØLU2	7Ø718	p T
G XZLU	12- U5	20U.I5	. Ø139	. 0 33	4 ØLUB	7Ø718	p T
C5orf7-	2793	20U.IU	. ØU2	. ØUU8	4 ØB8U	7Ø718	p T

Gene ID	Gene Name	Score (d)	Numerator (r)	Denominator (s+s0)	Fold Change	adjusted *P* value (%)	Direction
DRCK5	5. 88	20UI2	. (Q1	. 0 91	4 (B5-	70f18	p T
LRC28UI7U	1. 383	20UI2	. (Il1U	. 0 79	4 (Q89	70f18	p T
NAI17	1- 192	20UI	. (Q51	. (I. 9	4I(Q2	70f18	p T
SDXN	13273	20UI 9	. (ILBU	. (I- 1	. (Il9-	70f18	p T
ORLOA8A	3288	20UI 8	. (Q79	. (I. 8	4 0 7	70f18	p T
MAG 79A	- . 57	20UI 8	. (QUU	. (I. 1	4 0 21	70f18	p T

Add. Table 5: Statistically over-represented annotation terms, according to DAVID, of differently expressed genes between metabolic cluster Mc1 and Mc2

Annotation Cluster 1		Enrichment Score: 12.55	Count	P_Value	Benjamini
	SP_PIR_KEYWORDS	signal	139	3.60E-19	1.40E-16
	UP_SEQ_FEATURE	signal peptide	139	6.30E-19	9.00E-16
	GOTERM_CC_FAT	extracellular region part	71	1.60E-18	4.00E-16
	SP_PIR_KEYWORDS	Secreted	83	6.40E-14	1.30E-11
	GOTERM_CC_FAT	extracellular region	99	6.70E-14	8.30E-12
	SP_PIR_KEYWORDS	disulfide bond	113	5.50E-12	7.30E-10
	UP_SEQ_FEATURE	disulfide bond	109	2.30E-11	1.70E-08
	GOTERM_CC_FAT	extracellular space	43	7.10E-09	3.50E-07
	SP_PIR_KEYWORDS	glycoprotein	137	1.30E-08	1.00E-06
	UP_SEQ_FEATURE	glycosylation site:N-linked (GlcNAc...)	129	1.70E-07	8.40E-05
Annotation Cluster 2		Enrichment Score: 10.65	Count	P_Value	Benjamini
	GOTERM_CC_FAT	extracellular region part	71	1.60E-18	4.00E-16
	GOTERM_CC_FAT	extracellular matrix	34	4.40E-12	3.70E-10
	SP_PIR_KEYWORDS	extracellular matrix	26	2.70E-11	2.70E-09
	GOTERM_CC_FAT	proteinaceous extracellular matrix	31	7.30E-11	4.50E-09
	GOTERM_CC_FAT	extracellular matrix part	11	3.90E-04	6.40E-03
Annotation Cluster 3		Enrichment Score: 8.78	Count	P_Value	Benjamini
	GOTERM_BP_FAT	cell adhesion	46	8.80E-11	9.00E-08
	GOTERM_BP_FAT	biological adhesion	46	9.10E-11	6.20E-08
	SP_PIR_KEYWORDS	cell adhesion	27	5.90E-07	3.90E-05
Annotation Cluster 4		Enrichment Score: 7.45	Count	P_Value	Benjamini
	GOTERM_BP_FAT	vasculature development	25	1.60E-09	6.70E-07
	GOTERM_BP_FAT	blood vessel development	23	2.50E-08	7.50E-06
	GOTERM_BP_FAT	angiogenesis	17	1.70E-07	2.90E-05
	GOTERM_BP_FAT	blood vessel morphogenesis	20	2.20E-07	3.50E-05
Annotation Cluster 5		Enrichment Score: 6.23	Count	P_Value	Benjamini
	GOTERM_BP_FAT	regulation of locomotion	22	1.60E-09	8.10E-07
	GOTERM_BP_FAT	regulation of cell migration	19	3.60E-08	9.30E-06
	GOTERM_BP_FAT	regulation of cell motion	19	2.80E-07	4.10E-05
	GOTERM_BP_FAT	positive regulation of locomotion	13	1.60E-06	2.00E-04
	GOTERM_BP_FAT	positive regulation of cell migration	11	2.60E-05	2.30E-03
	GOTERM_BP_FAT	positive regulation of cell motion	11	6.00E-05	4.30E-03
Annotation Cluster 6		Enrichment Score: 6.11	Count	P_Value	Benjamini
	GOTERM_BP_FAT	regulation of response to external stimulus	23	6.00E-12	1.20E-08
	GOTERM_BP_FAT	regulation of inflammatory response	13	9.60E-08	2.00E-05
	GOTERM_BP_FAT	negative regulation of defense response	9	9.20E-07	1.20E-04
	GOTERM_BP_FAT	negative regulation of inflammatory response	7	5.10E-05	3.90E-03
	GOTERM_BP_FAT	negative regulation of response to stimulus	11	7.20E-05	4.90E-03
	GOTERM_BP_FAT	negative regulation of response to external stimulus	8	1.10E-04	6.00E-03
Annotation Cluster 7		Enrichment Score: 5.56	Count	P_Value	Benjamini
	GOTERM_MF_FAT	polysaccharide binding	18	8.00E-08	4.00E-05
	GOTERM_MF_FAT	pattern binding	18	8.00E-08	4.00E-05
	GOTERM_MF_FAT	glycosaminoglycan binding	17	1.20E-07	3.00E-05
	GOTERM_MF_FAT	heparin binding	12	2.20E-05	1.60E-03
	SP_PIR_KEYWORDS	heparin-binding	9	5.00E-05	1.80E-03
	GOTERM_MF_FAT	carbohydrate binding	20	5.00E-04	2.30E-02
Annotation Cluster 8		Enrichment Score: 5.22	Count	P_Value	Benjamini
	GOTERM_CC_FAT	actin cytoskeleton	22	1.20E-06	5.10E-05
	GOTERM_MF_FAT	cytoskeletal protein binding	30	4.40E-06	7.40E-04
	SP_PIR_KEYWORDS	actin-binding	18	1.30E-05	6.50E-04
	GOTERM_MF_FAT	actin binding	22	1.90E-05	1.90E-03
Annotation Cluster 9		Enrichment Score: 4.96	Count	P_Value	Benjamini
	GOTERM_BP_FAT	cytoskeleton organization	27	4.40E-06	4.70E-04
	GOTERM_BP_FAT	actin cytoskeleton organization	18	1.10E-05	1.10E-03
	GOTERM_BP_FAT	actin filament-based process	18	2.60E-05	2.40E-03
Annotation Cluster 10		Enrichment Score: 4.2	Count	P_Value	Benjamini
	INTERPRO	EGF-like calcium-binding	14	1.40E-07	9.10E-05
	INTERPRO	EGF-like calcium-binding, conserved site	14	1.40E-07	9.10E-05
	INTERPRO	EGF-type aspartate/asparagine hydroxylation conserved site	14	1.60E-07	5.20E-05
	SMART	EGF_CA	14	1.10E-06	1.80E-04
	INTERPRO	EGF	14	3.60E-06	7.90E-04
	INTERPRO	EGF-like, type 3	17	4.90E-06	7.90E-04
	SP_PIR_KEYWORDS	egf-like domain	18	5.10E-06	2.90E-04
	INTERPRO	EGF-like region, conserved site	21	6.00E-06	7.80E-04
	INTERPRO	EGF-like	16	3.10E-05	3.40E-03
	UP_SEQ_FEATURE	domain:EGF-like 1	12	3.60E-05	1.00E-02
	UP_SEQ_FEATURE	domain:EGF-like 3; calcium-binding	7	9.60E-05	2.00E-02
	INTERPRO	EGF calcium-binding	9	1.50E-04	1.30E-02
	SMART	EGF	16	2.40E-04	1.90E-02
	UP_SEQ_FEATURE	domain:EGF-like 2	9	4.40E-04	6.20E-02
	UP_SEQ_FEATURE	domain:EGF-like 5; calcium-binding	6	8.90E-04	9.40E-02
	UP_SEQ_FEATURE	domain:EGF-like 4	7	1.20E-03	1.10E-01
	UP_SEQ_FEATURE	domain:EGF-like 6; calcium-binding	5	1.60E-03	1.20E-01
	UP_SEQ_FEATURE	domain:EGF-like 4; calcium-binding	5	4.40E-03	2.00E-01
	UP_SEQ_FEATURE	domain:EGF-like 2; calcium-binding	6	6.10E-03	2.30E-01
	UP_SEQ_FEATURE	domain:EGF-like 7; calcium-binding	4	1.70E-02	4.10E-01
	UP_SEQ_FEATURE	domain:EGF-like 10; calcium-binding	3	2.80E-02	5.00E-01

Add. Table 6: Statistically over-represented annotation terms, according to DAVID, of differently expressed genes between metabolic cluster Mc1 and Mc3

Annotation Cluster 1		Enrichment Score: 39.49	Count	P_Value	Benjamini
	SP_PIR_KEYWORDS	signal	270	8.60E-56	3.90E-53
	UP_SEQ_FEATURE	signal peptide	270	3.10E-55	6.70E-52
	SP_PIR_KEYWORDS	extracellular matrix	77	4.20E-54	9.60E-52
	GOTERM_CC_FAT	extracellular matrix	90	3.40E-50	1.10E-47
	GOTERM_CC_FAT	proteinaceous extracellular matrix	86	5.30E-49	8.50E-47
	GOTERM_CC_FAT	extracellular region part	132	5.90E-41	6.30E-39
	SP_PIR_KEYWORDS	Secreted	166	3.00E-40	4.60E-38
	GOTERM_CC_FAT	extracellular region	191	1.40E-37	1.10E-35
	SP_PIR_KEYWORDS	glycoprotein	272	5.90E-33	6.70E-31
	GOTERM_CC_FAT	extracellular matrix part	42	4.00E-29	2.60E-27
	UP_SEQ_FEATURE	glycosylation site:N-linked (GlcNAc...)	251	8.10E-27	8.70E-24
	SP_PIR_KEYWORDS	disulfide bond	197	1.20E-25	1.10E-23
	UP_SEQ_FEATURE	disulfide bond	192	3.90E-25	2.80E-22
Annotation Cluster 2		Enrichment Score: 29.11	Count	P_Value	Benjamini
	GOTERM_BP_FAT	cell adhesion	98	1.40E-33	3.20E-30
	GOTERM_BP_FAT	biological adhesion	98	1.60E-33	1.80E-30
	SP_PIR_KEYWORDS	cell adhesion	61	2.00E-22	1.50E-20
Annotation Cluster 3		Enrichment Score: 19.86	Count	P_Value	Benjamini
	GOTERM_CC_FAT	extracellular matrix part	42	4.00E-29	2.60E-27
	GOTERM_CC_FAT	basement membrane	27	2.90E-18	1.60E-16
	SP_PIR_KEYWORDS	basement membrane	17	2.20E-14	9.20E-13
Annotation Cluster 4		Enrichment Score: 17.3	Count	P_Value	Benjamini
	GOTERM_BP_FAT	extracellular matrix organization	34	2.50E-23	1.90E-20
	GOTERM_BP_FAT	extracellular structure organization	36	1.50E-18	4.70E-16
	GOTERM_BP_FAT	collagen fibril organization	14	3.40E-12	7.00E-10
Annotation Cluster 5		Enrichment Score: 15.2	Count	P_Value	Benjamini
	GOTERM_BP_FAT	vasculature development	47	4.80E-21	2.70E-18
	GOTERM_BP_FAT	blood vessel development	44	5.30E-19	2.40E-16
	GOTERM_BP_FAT	blood vessel morphogenesis	34	2.70E-13	6.60E-11
	GOTERM_BP_FAT	angiogenesis	25	2.40E-10	2.80E-08
Annotation Cluster 6		Enrichment Score: 11.76	Count	P_Value	Benjamini
	GOTERM_CC_FAT	extracellular matrix part	42	4.00E-29	2.60E-27
	GOTERM_MF_FAT	extracellular matrix structural constituent	28	1.00E-18	5.80E-16
	SP_PIR_KEYWORDS	hydroxylation	24	2.10E-17	1.30E-15
	GOTERM_CC_FAT	collagen	19	4.50E-17	2.10E-15
	SP_PIR_KEYWORDS	collagen	25	2.50E-15	1.30E-13
	INTERPRO	Collagen triple helix repeat	23	4.60E-14	5.40E-12
	SP_PIR_KEYWORDS	trimer	14	2.60E-13	9.90E-12
	SP_PIR_KEYWORDS	triple helix	14	4.50E-12	1.50E-10
	SP_PIR_KEYWORDS	hydroxylysine	14	4.50E-12	1.50E-10
	UP_SEQ_FEATURE	region of interest:Triple-helical region	12	3.80E-11	1.30E-08
	SP_PIR_KEYWORDS	hydroxyproline	14	6.50E-11	2.00E-09
	SP_PIR_KEYWORDS	pyroglutamic acid	9	1.00E-04	1.30E-03
	GOTERM_CC_FAT	anchoring collagen	5	2.20E-04	2.90E-03
	UP_SEQ_FEATURE	domain:VWFA 1	5	1.50E-03	5.70E-02
	UP_SEQ_FEATURE	domain:VWFA 2	5	1.90E-03	6.70E-02
Annotation Cluster 7		Enrichment Score: 11.42	Count	P_Value	Benjamini
	GOTERM_BP_FAT	skeletal system development	50	5.60E-19	2.10E-16
	GOTERM_BP_FAT	bone development	21	7.20E-09	7.10E-07
	GOTERM_BP_FAT	ossification	20	1.30E-08	1.20E-06
Annotation Cluster 8		Enrichment Score: 11.3	Count	P_Value	Benjamini
	GOTERM_BP_FAT	cell motion	55	7.40E-15	2.10E-12
	GOTERM_BP_FAT	cell migration	37	5.60E-12	9.60E-10
	GOTERM_BP_FAT	localization of cell	37	1.20E-10	1.70E-08
	GOTERM_BP_FAT	cell motility	37	1.20E-10	1.70E-08
Annotation Cluster 9		Enrichment Score: 10.46	Count	P_Value	Benjamini
	INTERPRO	EGF-like calcium-binding, conserved site	28	7.10E-18	5.90E-15
	INTERPRO	EGF-like region, conserved site	45	7.40E-17	4.60E-14
	INTERPRO	EGF-like calcium-binding	27	8.10E-17	3.10E-14
	SP_PIR_KEYWORDS	egf-like domain	38	6.20E-16	3.80E-14
	INTERPRO	EGF-type aspartate/asparagine hydroxylation conserved site	25	1.30E-14	2.60E-12
	INTERPRO	EGF calcium-binding	22	1.60E-14	2.70E-12
	INTERPRO	EGF-like, type 3	34	1.80E-14	2.50E-12
	SMART	EGF_CA	27	7.60E-14	1.50E-11
	INTERPRO	EGF	25	6.90E-12	7.20E-10
	INTERPRO	EGF-like	31	9.30E-12	8.60E-10
	UP_SEQ_FEATURE	domain:EGF-like 3; calcium-binding	14	7.00E-11	2.20E-08
	UP_SEQ_FEATURE	domain:EGF-like 2; calcium-binding	16	2.60E-10	6.90E-08
	UP_SEQ_FEATURE	domain:EGF-like 1	22	2.80E-10	6.80E-08
	UP_SEQ_FEATURE	domain:EGF-like 5; calcium-binding	13	1.10E-09	2.40E-07
	UP_SEQ_FEATURE	domain:EGF-like 4; calcium-binding	12	4.00E-09	7.80E-07
	SMART	EGF	31	8.40E-09	8.40E-07
	UP_SEQ_FEATURE	domain:EGF-like 6; calcium-binding	9	8.00E-07	1.30E-04
	UP_SEQ_FEATURE	domain:EGF-like 4	11	1.60E-05	1.80E-03
	UP_SEQ_FEATURE	domain:EGF-like 2	13	2.70E-05	2.70E-03
	UP_SEQ_FEATURE	domain:EGF-like 3	12	2.90E-05	2.70E-03
	UP_SEQ_FEATURE	domain:EGF-like 7; calcium-binding	7	1.90E-04	1.10E-02
Annotation Cluster 10		Enrichment Score: 9.06	Count	P_Value	Benjamini
	UP_SEQ_FEATURE	domain:VWFC	12	1.00E-12	4.40E-10
	INTERPRO	von Willebrand factor, type C	13	5.10E-09	3.90E-07
	SMART	VWC	13	1.30E-07	6.40E-06

Add. Table 7: Gene set enrichment analysis (GSEA) result for Gene Ontology (GO) gene sets. Metabolic cluster Mc1 was compared with Mc2 and Mc3.

NAME	SIZE	ES	NES	NOM p-val	**FDR q-val**	FWER p-val	RANK AT MAX	LEADING EDGE
COLLAGEN	23	0.7818	2.0623	0.0011	0.0020	0.0070	2064	tags=70%, list=9%, signal=77%
EXTRACELLULAR_MATRIX	96	0.6880	2.0895	0.0000	0.0020	0.0050	2225	tags=49%, list=10%, signal=54%
PROTEINACEOUS_EXTRACELLULAR_MATRIX	94	0.6915	2.1008	0.0000	0.0025	0.0040	2225	tags=49%, list=10%, signal=54%
EXTRACELLULAR_MATRIX_PART	55	0.7282	2.1274	0.0000	0.0040	0.0040	2129	tags=51%, list=10%, signal=56%
INTEGRIN_BINDING	30	0.7220	1.9686	0.0000	0.0080	0.0270	3129	tags=63%, list=14%, signal=74%
CELL_SUBSTRATE_ADHESION	37	0.6891	1.9336	0.0000	0.0109	0.0420	3380	tags=57%, list=15%, signal=67%
EXTRACELLULAR_MATRIX_STRUCTURAL_CONSTITUENT	26	0.6938	1.9012	0.0000	0.0110	0.0550	1226	tags=46%, list=6%, signal=49%
CELL_MATRIX_ADHESION	36	0.6843	1.9120	0.0000	0.0112	0.0470	3380	tags=56%, list=15%, signal=66%
CELL_MATRIX_JUNCTION	16	0.7306	1.8324	0.0000	0.0257	0.1290	2484	tags=56%, list=11%, signal=63%
BASEMENT_MEMBRANE	35	0.6546	1.8215	0.0010	0.0268	0.1380	2684	tags=43%, list=12%, signal=49%
TRANSMEMBRANE_RECEPTOR_PROTEIN_KINASE_ACTIVITY	51	0.6166	1.8115	0.0000	0.0276	0.1540	3983	tags=49%, list=18%, signal=60%
AXON_GUIDANCE	22	0.6824	1.7839	0.0000	0.0323	0.1990	933	tags=27%, list=4%, signal=28%
BASAL_LAMINA	19	0.6938	1.7897	0.0020	0.0330	0.1900	2684	tags=42%, list=12%, signal=48%
SKELETAL_DEVELOPMENT	99	0.5846	1.7745	0.0000	0.0338	0.2130	2762	tags=37%, list=13%, signal=43%
REGULATION_OF_CELL_MIGRATION	27	0.6465	1.7558	0.0000	0.0393	0.2490	2952	tags=44%, list=14%, signal=51%
BASOLATERAL_PLASMA_MEMBRANE	31	0.6225	1.7124	0.0000	0.0539	0.3680	2798	tags=42%, list=13%, signal=48%
BLOOD_COAGULATION	42	0.6010	1.7209	0.0000	0.0543	0.3420	3903	tags=48%, list=18%, signal=58%
ADHERENS_JUNCTION	21	0.6590	1.7162	0.0000	0.0549	0.3610	2484	tags=48%, list=11%, signal=54%
HEMOSTASIS	47	0.5966	1.7230	0.0000	0.0556	0.3340	3903	tags=47%, list=18%, signal=57%
COAGULATION	43	0.5950	1.7030	0.0000	0.0570	0.4060	3903	tags=47%, list=18%, signal=57%
SULFURIC_ESTER_HYDROLASE_ACTIVITY	16	0.6727	1.6963	0.0010	0.0584	0.4200	3141	tags=50%, list=14%, signal=58%
LIPID_HOMEOSTASIS	16	0.6690	1.6824	0.0010	0.0611	0.4790	3348	tags=44%, list=15%, signal=52%
ANATOMICAL_STRUCTURE_FORMATION	52	0.5763	1.6844	0.0000	0.0618	0.4690	5237	tags=52%, list=24%, signal=68%
WOUND_HEALING	53	0.5772	1.6865	0.0000	0.0623	0.4610	4715	tags=51%, list=22%, signal=65%
BONE_REMODELING	28	0.6094	1.6632	0.0010	0.0668	0.5410	3983	tags=39%, list=18%, signal=48%
TISSUE_REMODELING	29	0.6081	1.6635	0.0000	0.0691	0.5410	3983	tags=38%, list=18%, signal=46%
EXTRACELLULAR_REGION_PART	322	0.5296	1.6665	0.0000	0.0696	0.5260	4482	tags=39%, list=21%, signal=49%
REGULATION_OF_BODY_FLUID_LEVELS	56	0.5625	1.6467	0.0000	0.0728	0.6060	4183	tags=45%, list=19%, signal=55%
TRANSMEMBRANE_RECEPTOR_PROTEIN_TYROSINE_KINASE_ACTIVITY	43	0.5705	1.6498	0.0000	0.0750	0.5920	3856	tags=42%, list=18%, signal=51%
POSITIVE_REGULATION_OF_CELL_DIFFERENTIATION	23	0.6161	1.6470	0.0000	0.0751	0.6060	2762	tags=43%, list=13%, signal=50%
GLYCOSAMINOGLYCAN_BINDING	30	0.5890	1.6322	0.0040	0.0806	0.6740	3108	tags=40%, list=14%, signal=47%
HOMEOSTASIS_OF_NUMBER_OF_CELLS	19	0.6164	1.6235	0.0071	0.0826	0.7060	1949	tags=37%, list=9%, signal=40%
POLYSACCHARIDE_BINDING	32	0.5863	1.6326	0.0020	0.0830	0.6730	3108	tags=38%, list=14%, signal=44%
CELL_MIGRATION	92	0.5447	1.6261	0.0000	0.0830	0.6990	2952	tags=35%, list=14%, signal=40%
MUSCLE_DEVELOPMENT	89	0.5369	1.6113	0.0000	0.0831	0.7460	5238	tags=46%, list=24%, signal=60%
RUFFLE	27	0.5885	1.6170	0.0000	0.0839	0.7260	3309	tags=37%, list=15%, signal=44%
TISSUE_DEVELOPMENT	135	0.5301	1.6127	0.0000	0.0840	0.7360	5011	tags=42%, list=23%, signal=54%
ATP_DEPENDENT_HELICASE_ACTIVITY	22	0.6085	1.6190	0.0050	0.0844	0.7200	6660	tags=68%, list=30%, signal=98%
REGULATION_OF_CYTOSKELETON_ORGANIZATION_AND_BIOGENESIS	28	0.5915	1.6140	0.0010	0.0849	0.7330	2952	tags=36%, list=14%, signal=41%
HEPARIN_BINDING	22	0.5979	1.6041	0.0020	0.0870	0.7710	3108	tags=41%, list=14%, signal=48%
ACTIN_BINDING	72	0.5291	1.5901	0.0000	0.0880	0.8240	4089	tags=38%, list=19%, signal=46%
CELL_CORTEX_PART	23	0.5909	1.5937	0.0030	0.0885	0.8110	3160	tags=35%, list=14%, signal=41%
REGULATION_OF_ORGANELLE_ORGANIZATION_AND_BIOGENESIS	37	0.5654	1.5914	0.0010	0.0886	0.8210	2952	tags=32%, list=14%, signal=37%
PROTEIN_COMPLEX_BINDING	54	0.5464	1.5850	0.0010	0.0887	0.8400	3232	tags=39%, list=15%, signal=46%
REGULATION_OF_RESPONSE_TO_EXTERNAL_STIMULUS	15	0.6496	1.5822	0.0092	0.0895	0.8460	3525	tags=53%, list=16%, signal=64%
ANGIOGENESIS	44	0.5509	1.5856	0.0010	0.0899	0.8380	5625	tags=52%, list=26%, signal=70%
EXTRACELLULAR_REGION	423	0.5050	1.5985	0.0000	0.0901	0.7930	4482	tags=37%, list=21%, signal=45%
MUSCLE_CELL_DIFFERENTIATION	20	0.6121	1.5939	0.0061	0.0904	0.8090	5130	tags=60%, list=23%, signal=78%
INTEGRIN_COMPLEX	19	0.6200	1.5960	0.0040	0.0908	0.8040	4500	tags=58%, list=21%, signal=73%
ACTIN_POLYMERIZATION_AND_OR_DEPOLYMERIZATION	23	0.5846	1.5773	0.0010	0.0924	0.8600	2848	tags=35%, list=13%, signal=40%
NEURON_PROJECTION	19	0.6090	1.5706	0.0060	0.0933	0.8780	5094	tags=58%, list=23%, signal=75%
CALMODULIN_BINDING	25	0.5821	1.5712	0.0030	0.0944	0.8760	7178	tags=64%, list=33%, signal=95%
SODIUM_CHANNEL_ACTIVITY	16	0.6191	1.5722	0.0061	0.0950	0.8740	1909	tags=38%, list=9%, signal=41%
VASCULATURE_DEVELOPMENT	51	0.5379	1.5645	0.0010	0.0975	0.9000	5188	tags=49%, list=24%, signal=64%
KINASE_INHIBITOR_ACTIVITY	25	0.5854	1.5627	0.0040	0.0978	0.9010	3734	tags=40%, list=17%, signal=48%
ECTODERM_DEVELOPMENT	79	0.5307	1.5594	0.0050	0.0990	0.9090	5011	tags=42%, list=23%, signal=54%
PROTEIN_KINASE_INHIBITOR_ACTIVITY	24	0.5865	1.5561	0.0050	0.1004	0.9140	3734	tags=42%, list=17%, signal=50%
ENERGY_RESERVE_METABOLIC_PROCESS	15	0.6309	1.5537	0.0082	0.1009	0.9160	5542	tags=60%, list=25%, signal=80%
ACTIN_FILAMENT_BINDING	23	0.5747	1.5501	0.0030	0.1009	0.9250	4089	tags=48%, list=19%, signal=59%
NEGATIVE_REGULATION_OF_DNA_BINDING	16	0.6063	1.5511	0.0112	0.1018	0.9240	4951	tags=56%, list=23%, signal=73%
EXTRACELLULAR_STRUCTURE_ORGANIZATION_AND_BIOGENESIS	29	0.5641	1.5443	0.0261	0.1046	0.9410	2999	tags=41%, list=14%, signal=48%
ACTIN_CYTOSKELETON	122	0.4982	1.5355	0.0000	0.1114	0.9560	3302	tags=30%, list=15%, signal=35%
CARBOHYDRATE_BIOSYNTHETIC_PROCESS	45	0.5400	1.5369	0.0030	0.1115	0.9540	5302	tags=44%, list=24%, signal=59%
ORGAN_MORPHOGENESIS	136	0.4979	1.5320	0.0000	0.1137	0.9580	6037	tags=48%, list=28%, signal=66%
METALLOENDOPEPTIDASE_ACTIVITY	27	0.5639	1.5297	0.0131	0.1144	0.9600	5134	tags=44%, list=23%, signal=58%
STRUCTURAL_CONSTITUENT_OF_CYTOSKELETON	55	0.5283	1.5242	0.0030	0.1187	0.9670	5240	tags=44%, list=24%, signal=57%
EPIDERMIS_DEVELOPMENT	70	0.5233	1.5215	0.0060	0.1205	0.9680	5011	tags=40%, list=23%, signal=52%
TRANSMEMBRANE_RECEPTOR_PROTEIN_SERINE_THREONINE_KINASE_SIGNALING_PATHWAY	47	0.5270	1.5184	0.0020	0.1226	0.9710	5843	tags=49%, list=27%, signal=67%
SERINE_HYDROLASE_ACTIVITY	44	0.5325	1.5073	0.0060	0.1352	0.9810	2788	tags=30%, list=13%, signal=34%
SULFUR_COMPOUND_BIOSYNTHETIC_PROCESS	16	0.5972	1.4970	0.0215	0.1419	0.9870	2772	tags=31%, list=13%, signal=36%
PHOSPHORIC_DIESTER_HYDROLASE_ACTIVITY	39	0.5283	1.4978	0.0020	0.1428	0.9870	4367	tags=41%, list=20%, signal=51%
CORTICAL_CYTOSKELETON	19	0.5744	1.4985	0.0071	0.1439	0.9850	3160	tags=32%, list=14%, signal=37%
NEGATIVE_REGULATION_OF_BINDING	17	0.5775	1.4941	0.0153	0.1441	0.9880	4951	tags=53%, list=23%, signal=68%
METALLOPEPTIDASE_ACTIVITY	46	0.5251	1.4996	0.0010	0.1444	0.9850	5789	tags=46%, list=26%, signal=62%
MYOBLAST_DIFFERENTIATION	17	0.5818	1.4862	0.0295	0.1479	0.9900	3890	tags=47%, list=18%, signal=57%
GROWTH_FACTOR_BINDING	32	0.5301	1.4874	0.0220	0.1480	0.9900	5197	tags=50%, list=24%, signal=66%
DENDRITE	16	0.5891	1.4885	0.0163	0.1486	0.9900	4156	tags=44%, list=19%, signal=54%
GENERATION_OF_A_SIGNAL_INVOLVED_IN_CELL_CELL_SIGNALING	27	0.5619	1.4894	0.0151	0.1490	0.9900	5004	tags=44%, list=23%, signal=58%
REGULATION_OF_INTRACELLULAR_TRANSPORT	22	0.5552	1.4797	0.0190	0.1556	0.9910	4825	tags=41%, list=22%, signal=52%
RAS_GTPASE_ACTIVATOR_ACTIVITY	26	0.5449	1.4743	0.0130	0.1628	0.9920	6320	tags=46%, list=29%, signal=65%
RECEPTOR_COMPLEX	56	0.5100	1.4702	0.0040	0.1630	0.9940	4969	tags=45%, list=23%, signal=58%
SERINE_TYPE_PEPTIDASE_ACTIVITY	43	0.5200	1.4686	0.0100	0.1635	0.9940	2788	tags=28%, list=13%, signal=32%
STRUCTURAL_CONSTITUENT_OF_MUSCLE	32	0.5360	1.4709	0.0090	0.1639	0.9930	5250	tags=44%, list=24%, signal=58%
PROTEIN_PROCESSING	45	0.5146	1.4720	0.0020	0.1640	0.9930	4954	tags=36%, list=23%, signal=46%
ENDOPEPTIDASE_ACTIVITY	111	0.4832	1.4645	0.0000	0.1681	0.9940	5238	tags=35%, list=24%, signal=46%
HELICASE_ACTIVITY	45	0.5127	1.4631	0.0070	0.1687	0.9950	8005	tags=62%, list=37%, signal=98%
PROTEASE_INHIBITOR_ACTIVITY	40	0.5187	1.4584	0.0050	0.1723	0.9960	681	tags=18%, list=3%, signal=18%
REGULATION_OF_MYELOID_CELL_DIFFERENTIATION	18	0.5734	1.4591	0.0234	0.1731	0.9950	1949	tags=33%, list=9%, signal=37%
PATTERN_BINDING	38	0.5131	1.4517	0.0110	0.1774	0.9970	4908	tags=42%, list=22%, signal=54%
PEPTIDASE_ACTIVITY	164	0.4698	1.4527	0.0000	0.1777	0.9970	5789	tags=37%, list=26%, signal=49%
REGULATION_OF_SECRETION	33	0.5276	1.4532	0.0120	0.1789	0.9960	5004	tags=42%, list=23%, signal=55%
AMINE_BIOSYNTHETIC_PROCESS	15	0.5867	1.4486	0.0346	0.1810	0.9970	8286	tags=80%, list=38%, signal=129%

NAME	SIZE	ES	NES	NOM p-val	**FDR q-val**	FWER p-val	RANK AT MAX	LEADING EDGE
OXIDOREDUCTASE_ACTIVITY_ACTING_ON_NADH_OR_NADPH	25	0.5327	1.4416	0.0221	0.1921	0.9990	6672	tags=64%, list=31%, signal=92%
NEGATIVE_REGULATION_OF_CELLULAR_COMPONENT_ORGANIZATION_AND_BIOGENESIS	26	0.5243	1.4385	0.0190	0.1958	0.9990	2745	tags=31%, list=13%, signal=35%
POSITIVE_REGULATION_OF_TRANSCRIPTION_FROM_RNA_POLYMERASE_II_PROMOTER	57	0.4909	1.4355	0.0040	0.1998	1.0000	4266	tags=35%, list=20%, signal=43%
TRANSPORT_VESICLE	29	0.5150	1.4181	0.0180	0.2030	1.0000	4937	tags=38%, list=23%, signal=49%
REGULATION_OF_NUCLEOCYTOPLASMIC_TRANSPORT	19	0.5413	1.4151	0.0322	0.2031	1.0000	4825	tags=37%, list=22%, signal=47%
DNA_HELICASE_ACTIVITY	22	0.5435	1.4325	0.0332	0.2036	1.0000	6302	tags=55%, list=29%, signal=77%
ELECTRON_CARRIER_ACTIVITY	75	0.4780	1.4185	0.0020	0.2040	1.0000	5315	tags=44%, list=24%, signal=58%
NEGATIVE_REGULATION_OF_TRANSCRIPTION_FROM_RNA_POLYMERASE_II_PROMOTER	78	0.4714	1.4165	0.0000	0.2042	1.0000	7409	tags=46%, list=34%, signal=70%
KERATINOCYTE_DIFFERENTIATION	15	0.5781	1.4152	0.0462	0.2048	1.0000	6886	tags=53%, list=32%, signal=78%
TUBE_DEVELOPMENT	18	0.5542	1.4104	0.0445	0.2050	1.0000	1962	tags=33%, list=9%, signal=37%
COPPER_ION_BINDING	15	0.5645	1.4189	0.0324	0.2052	1.0000	1565	tags=27%, list=7%, signal=29%
NUCLEOTIDE_BIOSYNTHETIC_PROCESS	19	0.5430	1.4090	0.0456	0.2056	1.0000	4828	tags=42%, list=22%, signal=54%
MEMBRANE_FUSION	27	0.5163	1.4128	0.0320	0.2058	1.0000	3927	tags=37%, list=18%, signal=45%
TRANSFORMING_GROWTH_FACTOR_BETA_RECEPTOR_SIGNALING_PATHWAY	36	0.5086	1.4288	0.0130	0.2063	1.0000	7420	tags=56%, list=34%, signal=84%
PROTEIN_BINDING_BRIDGING	59	0.4886	1.4106	0.0070	0.2065	1.0000	7526	tags=46%, list=34%, signal=70%
REGULATION_OF_CELL_DIFFERENTIATION	55	0.4901	1.4189	0.0040	0.2070	1.0000	2911	tags=29%, list=13%, signal=33%
PROTEIN_DNA_COMPLEX_ASSEMBLY	37	0.4978	1.4111	0.0171	0.2071	1.0000	8969	tags=68%, list=41%, signal=114%
CONTRACTILE_FIBER_PART	23	0.5362	1.4196	0.0332	0.2076	1.0000	1468	tags=26%, list=7%, signal=28%
SERINE_TYPE_ENDOPEPTIDASE_ACTIVITY	39	0.5094	1.4268	0.0190	0.2080	1.0000	2788	tags=28%, list=13%, signal=32%
RESPONSE_TO_HYPOXIA	27	0.5217	1.4289	0.0100	0.2083	1.0000	7014	tags=59%, list=32%, signal=87%
AXONOGENESIS	43	0.5047	1.4210	0.0070	0.2087	1.0000	3671	tags=30%, list=17%, signal=36%
ACTIN_FILAMENT	17	0.5527	1.4200	0.0515	0.2088	1.0000	4742	tags=35%, list=22%, signal=45%
RNA_DEPENDENT_ATPASE_ACTIVITY	15	0.5695	1.4246	0.0483	0.2099	1.0000	7365	tags=73%, list=34%, signal=111%
ENZYME_INHIBITOR_ACTIVITY	115	0.4685	1.4211	0.0000	0.2107	1.0000	4713	tags=34%, list=22%, signal=43%
REGULATION_OF_ANATOMICAL_STRUCTURE_MORPHOGENESIS	23	0.5341	1.4227	0.0272	0.2119	1.0000	3035	tags=35%, list=14%, signal=40%
CELL_CELL_ADHESION	81	0.4783	1.4215	0.0020	0.2120	1.0000	6050	tags=44%, list=28%, signal=61%
CELL_PROJECTION_PART	18	0.5419	1.3966	0.0406	0.2174	1.0000	6415	tags=56%, list=29%, signal=79%
POSITIVE_REGULATION_OF_RNA_METABOLIC_PROCESS	102	0.4592	1.3983	0.0010	0.2175	1.0000	4266	tags=32%, list=20%, signal=40%
ENZYME_LINKED_RECEPTOR_PROTEIN_SIGNALING_PATHWAY	135	0.4501	1.3957	0.0000	0.2175	1.0000	4274	tags=34%, list=20%, signal=42%
CELL_JUNCTION	76	0.4747	1.3998	0.0050	0.2183	1.0000	6471	tags=47%, list=30%, signal=67%
NEGATIVE_REGULATION_OF_TRANSCRIPTION	167	0.4474	1.4007	0.0000	0.2183	1.0000	7227	tags=43%, list=33%, signal=64%
BIOGENIC_AMINE_METABOLIC_PROCESS	16	0.5563	1.4015	0.0427	0.2184	1.0000	4828	tags=44%, list=22%, signal=56%
CELLULAR_MORPHOGENESIS_DURING_DIFFERENTIATION	49	0.4909	1.3987	0.0090	0.2186	1.0000	3035	tags=27%, list=14%, signal=31%
LEADING_EDGE	42	0.4842	1.3966	0.0190	0.2191	1.0000	3309	tags=29%, list=15%, signal=34%
PHOSPHOLIPID_BINDING	39	0.4973	1.3925	0.0240	0.2224	1.0000	4460	tags=38%, list=20%, signal=48%
POSITIVE_REGULATION_OF_TRANSCRIPTIONDNA_DEPENDENT	100	0.4568	1.3902	0.0010	0.2253	1.0000	4266	tags=32%, list=20%, signal=40%
ANATOMICAL_STRUCTURE_MORPHOGENESIS	356	0.4361	1.3832	0.0000	0.2258	1.0000	5963	tags=39%, list=27%, signal=53%
CELL_SURFACE	72	0.4643	1.3855	0.0040	0.2264	1.0000	7241	tags=49%, list=33%, signal=72%
RESPONSE_TO_WOUNDING	178	0.4479	1.3821	0.0080	0.2264	1.0000	6311	tags=41%, list=29%, signal=57%
RECEPTOR_SIGNALING_PROTEIN_SERINE_THREONINE_KINASE_ACTIVITY	34	0.4972	1.3887	0.0150	0.2267	1.0000	5214	tags=41%, list=24%, signal=54%
ACTIN_CYTOSKELETON_ORGANIZATION_AND_BIOGENESIS	101	0.4543	1.3869	0.0010	0.2268	1.0000	3500	tags=30%, list=16%, signal=35%
POSITIVE_REGULATION_OF_JNK_ACTIVITY	18	0.5382	1.3834	0.0455	0.2271	1.0000	4705	tags=44%, list=22%, signal=57%
POSITIVE_REGULATION_OF_TRANSCRIPTION	120	0.4520	1.3875	0.0010	0.2273	1.0000	6739	tags=43%, list=31%, signal=62%
TUBE_MORPHOGENESIS	15	0.5559	1.3856	0.0462	0.2278	1.0000	1962	tags=33%, list=9%, signal=37%
REGULATION_OF_TRANSCRIPTION_FACTOR_ACTIVITY	36	0.4904	1.3838	0.0200	0.2278	1.0000	4951	tags=39%, list=23%, signal=50%
CELL_PROJECTION	98	0.4512	1.3749	0.0040	0.2311	1.0000	2978	tags=27%, list=14%, signal=31%
GTPASE_ACTIVATOR_ACTIVITY	56	0.4723	1.3791	0.0100	0.2311	1.0000	6484	tags=45%, list=30%, signal=63%
DNA_DEPENDENT_ATPASE_ACTIVITY	19	0.5307	1.3755	0.0676	0.2316	1.0000	4923	tags=47%, list=23%, signal=61%
EXTRACELLULAR_SPACE	233	0.4436	1.3766	0.0000	0.2326	1.0000	3568	tags=28%, list=16%, signal=33%
NEGATIVE_REGULATION_OF_MULTICELLULAR_ORGANISMAL_PROCESS	30	0.5084	1.3773	0.0311	0.2329	1.0000	4878	tags=40%, list=22%, signal=51%
REGULATION_OF_ANGIOGENESIS	25	0.5071	1.3756	0.0302	0.2330	1.0000	5625	tags=44%, list=26%, signal=59%
NEGATIVE_REGULATION_OF_CELL_DIFFERENTIATION	27	0.5095	1.3679	0.0340	0.2434	1.0000	1501	tags=26%, list=7%, signal=28%
REGULATION_OF_NEUROTRANSMITTER_LEVELS	22	0.5257	1.3657	0.0493	0.2463	1.0000	4964	tags=45%, list=23%, signal=59%
TRANSCRIPTION_INITIATION_FROM_RNA_POLYMERASE_II_PROMOTER	18	0.5264	1.3646	0.0487	0.2470	1.0000	5685	tags=56%, list=26%, signal=75%

Add. Table 8: Gene set enrichment analysis (GSEA) result for Gene Ontology (GO) gene sets. Metabolic cluster Mc1 was compared with Mc2.

NAME	SIZE	ES	NES	NOM p-val	FDR q-val	FWER p-val	RANK AT MAX	LEADING EDGE
INTEGRIN_BINDING	30	0.7361	2.0381	0.0000	0.0110	0.0110	2319	tags=60%, list=11%, signal=67%
CELL_MATRIX_JUNCTION	16	0.7521	1.9300	0.0000	0.0360	0.0460	1814	tags=56%, list=8%, signal=61%
ADHERENS_JUNCTION	21	0.6979	1.8518	0.0000	0.0620	0.1030	1814	tags=48%, list=8%, signal=52%
PROTEINACEOUS_EXTRACELLULAR_MATRIX	94	0.5694	1.7481	0.0050	0.0954	0.2720	5379	tags=55%, list=25%, signal=73%
EXTRACELLULAR_MATRIX	96	0.5696	1.7493	0.0050	0.1095	0.2680	3162	tags=45%, list=14%, signal=52%
COLLAGEN	23	0.6382	1.7129	0.0384	0.1243	0.3630	6011	tags=78%, list=28%, signal=108%
TRANSMEMBRANE_RECEPTOR_PROTEIN_KINASE_ACTIVITY	51	0.5924	1.7532	0.0010	0.1253	0.2550	3358	tags=45%, list=15%, signal=53%
EXTRACELLULAR_MATRIX_STRUCTURAL_CONSTITUENT	26	0.6175	1.7028	0.0051	0.1254	0.3980	2994	tags=50%, list=14%, signal=58%
EXTRACELLULAR_MATRIX_PART	55	0.5969	1.7696	0.0130	0.1265	0.2220	5379	tags=58%, list=25%, signal=77%
GROWTH_FACTOR_BINDING	32	0.6009	1.6675	0.0010	0.1309	0.5230	5615	tags=66%, list=26%, signal=88%
CELL_SUBSTRATE_ADHESION	37	0.5911	1.6695	0.0000	0.1383	0.5160	3072	tags=46%, list=14%, signal=53%
LIPID_HOMEOSTASIS	16	0.6659	1.6505	0.0020	0.1391	0.5820	2598	tags=44%, list=12%, signal=50%
SERINE_TYPE_ENDOPEPTIDASE_ACTIVITY	39	0.5827	1.6553	0.0000	0.1393	0.5630	3056	tags=36%, list=14%, signal=42%
BASEMENT_MEMBRANE	35	0.5880	1.6724	0.0060	0.1458	0.4990	5379	tags=54%, list=25%, signal=72%
NEGATIVE_REGULATION_OF_DNA_BINDING	16	0.6452	1.6274	0.0031	0.1503	0.6830	3270	tags=44%, list=15%, signal=51%
BASOLATERAL_PLASMA_MEMBRANE	31	0.5887	1.6307	0.0000	0.1532	0.6660	1814	tags=35%, list=8%, signal=39%
SERINE_HYDROLASE_ACTIVITY	44	0.5650	1.6203	0.0000	0.1541	0.7100	3056	tags=34%, list=14%, signal=40%
PROTEIN_COMPLEX_BINDING	54	0.5525	1.6153	0.0010	0.1541	0.7320	3878	tags=43%, list=18%, signal=52%
SERINE_TYPE_PEPTIDASE_ACTIVITY	43	0.5853	1.6741	0.0000	0.1565	0.4930	3056	tags=35%, list=14%, signal=40%
HEMOSTASIS	47	0.5537	1.6083	0.0000	0.1582	0.7580	2123	tags=36%, list=10%, signal=40%
CELL_MATRIX_ADHESION	36	0.5787	1.6323	0.0000	0.1606	0.6600	3072	tags=44%, list=14%, signal=52%
EPIDERMIS_DEVELOPMENT	70	0.5423	1.5873	0.0010	0.1666	0.8300	3565	tags=37%, list=16%, signal=44%
NEURON_PROJECTION	19	0.6006	1.5887	0.0030	0.1711	0.8270	2527	tags=42%, list=12%, signal=48%
TRANSMEMBRANE_RECEPTOR_PROTEIN_TYROSINE_KINASE_ACTIVITY	43	0.5487	1.5957	0.0040	0.1735	0.8050	3358	tags=40%, list=15%, signal=47%
REGULATION_OF_MAPKKK_CASCADE	19	0.6113	1.5904	0.0091	0.1757	0.8230	3372	tags=42%, list=15%, signal=50%
NEGATIVE_REGULATION_OF_BINDING	17	0.6147	1.5664	0.0061	0.1798	0.8970	3270	tags=41%, list=15%, signal=48%
MUSCLE_DEVELOPMENT	89	0.5286	1.5750	0.0000	0.1826	0.8690	4652	tags=47%, list=21%, signal=60%
COAGULATION	43	0.5457	1.5666	0.0010	0.1857	0.8950	2123	tags=35%, list=10%, signal=39%
BLOOD_COAGULATION	42	0.5462	1.5666	0.0010	0.1924	0.8950	2123	tags=36%, list=10%, signal=39%
ECTODERM_DEVELOPMENT	79	0.5244	1.5467	0.0020	0.2059	0.9310	3173	tags=34%, list=15%, signal=40%
STRUCTURAL_CONSTITUENT_OF_CYTOSKELETON	55	0.5388	1.5494	0.0040	0.2068	0.9260	5410	tags=45%, list=25%, signal=60%
ACTIVATION_OF_PROTEIN_KINASE_ACTIVITY	24	0.5706	1.5224	0.0071	0.2084	0.9700	2429	tags=38%, list=11%, signal=42%
CELL_MIGRATION	92	0.5099	1.5270	0.0010	0.2102	0.9640	2625	tags=34%, list=12%, signal=38%
KINASE_INHIBITOR_ACTIVITY	25	0.5648	1.5227	0.0020	0.2134	0.9700	5182	tags=44%, list=24%, signal=58%
SKELETAL_DEVELOPMENT	99	0.4977	1.5271	0.0080	0.2156	0.9640	4851	tags=42%, list=22%, signal=54%
REGULATION_OF_BODY_FLUID_LEVELS	56	0.5194	1.5323	0.0010	0.2168	0.9560	2123	tags=34%, list=10%, signal=37%
PROTEIN_KINASE_INHIBITOR_ACTIVITY	24	0.5736	1.5351	0.0030	0.2175	0.9530	5182	tags=46%, list=24%, signal=60%
TRANSFORMING_GROWTH_FACTOR_BETA_RECEPTOR_SIGNALING_PATHWAY	36	0.5409	1.5151	0.0060	0.2186	0.9780	7287	tags=58%, list=33%, signal=87%
TRANSMEMBRANE_RECEPTOR_PROTEIN_SERINE_THREONINE_KINASE_SIGNALING_PATHWAY	47	0.5338	1.5276	0.0010	0.2205	0.9620	7287	tags=57%, list=33%, signal=86%
STRUCTURAL_CONSTITUENT_OF_MUSCLE	32	0.5553	1.5352	0.0040	0.2242	0.9530	2760	tags=41%, list=13%, signal=46%
EXTRACELLULAR_REGION_PART	322	0.4756	1.5086	0.0030	0.2281	0.9810	6443	tags=46%, list=29%, signal=64%
WOUND_HEALING	53	0.5178	1.5040	0.0020	0.2328	0.9810	2935	tags=38%, list=13%, signal=43%
EXTRACELLULAR_STRUCTURE_ORGANIZATION_AND_BIOGENESIS	29	0.5388	1.5001	0.0313	0.2359	0.9840	4817	tags=48%, list=22%, signal=62%
LIPID_TRANSPORT	28	0.5511	1.4774	0.0080	0.2488	0.9940	7203	tags=54%, list=33%, signal=80%

Add. Table 9: Gene set enrichment analysis (GSEA) result for Gene Ontology (GO) gene sets. Metabolic cluster Mc3 was compared with Mc1 and Mc2.

NAME	SIZE	ES	NES	NOM p-val	**FDR q-val**	FWER p-val	RANK AT MAX	LEADING EDGE
EXTRACELLULAR_MATRIX_PART	55	0.7515	2.1854	0.0000	0.0020	0.0040	1682	tags=47%, list=8%, signal=51%
COLLAGEN	23	0.8417	2.2165	0.0000	0.0040	0.0040	1682	tags=70%, list=8%, signal=75%
EXTRACELLULAR_MATRIX	96	0.6787	2.0428	0.0000	0.0055	0.0170	1682	tags=43%, list=8%, signal=46%
PROTEINACEOUS_EXTRACELLULAR_MATRIX	94	0.6836	2.0553	0.0000	0.0063	0.0160	1682	tags=43%, list=8%, signal=46%
INTEGRIN_BINDING	30	0.7168	1.9587	0.0000	0.0098	0.0330	2692	tags=50%, list=12%, signal=57%
EXTRACELLULAR_MATRIX_STRUCTURAL_CONSTITUENT	26	0.7268	1.9400	0.0000	0.0113	0.0440	1997	tags=54%, list=9%, signal=59%
BASEMENT_MEMBRANE	35	0.6598	1.8425	0.0000	0.0345	0.1170	703	tags=31%, list=3%, signal=32%
BASAL_LAMINA	19	0.6669	1.7255	0.0000	0.1232	0.3500	703	tags=32%, list=3%, signal=33%
CELL_MATRIX_ADHESION	36	0.5977	1.6720	0.0000	0.1718	0.5340	2695	tags=39%, list=12%, signal=44%
CELL_SUBSTRATE_ADHESION	37	0.5963	1.6740	0.0010	0.1877	0.5230	2695	tags=38%, list=12%, signal=43%
PROTEASE_INHIBITOR_ACTIVITY	40	0.5840	1.6425	0.0000	0.2111	0.6390	1497	tags=20%, list=7%, signal=21%

Add. Table 10: Integrated pathway analysis result from comparison of the metabolic clusters Mc1 compared to Mc2

Pathway	Total	Expected	Hits	P.Value	Metabolite hits	Gene hits
Tyrosine metabolism	80	1.9872	8	0.00066125	L-Tyrosine	*AOC3, ALDH1A3, AOX1, ADH1C, MAOA, MAOB, PNMT*
Glycerolipid metabolism	72	1.7885	7	0.0017364		*AKR1B1, AKR1B10, ALDH2, AGPAT4, PPAP2A, PPAP2B, PNLIPRP3*
Fatty acid metabolism	83	2.0617	7	0.003944		*ACSL4, ACSL1, ACAA2, ADH1A, ADH1B, ADH1C, ALDH2*
Glycolysis / Gluconeogenesis	91	2.2604	7	0.0065727	Beta-D-glucose, Acetate	*ADH1A, ADH1B, ADH1C, ALDH2, ALDH1A3*
Ether lipid metabolism	51	1.2668	5	0.0078844		*LPCAT2, ENPP2, PLD1, PPAP2A, PPAP2B*
Glycerophospholipid metabolism	119	2.956	8	0.0082917	Glycerophosphocholine, Phosphocholine	*LCAT, LPCAT2, PPAP2A, PPAP2B, PLD1, AGPAT4*
Arachidonic acid metabolism	100	2.484	7	0.010899		*CYP2U1, ALOX5, GPX3, GGT5, PTGS2, PTGIS, AKR1C3*
Nicotinate and nicotinamide metabolism	39	0.96876	4	0.014869		*AOX1, NNMT, NAMPT, NT5E*
D-Glutamine and D-glutamate metabolism	9	0.22356	2	0.01955	Glutamate	*GLS*
Phenylalanine metabolism	29	0.72036	3	0.033755	L-Tyrosine	*AOC3, ALDH1A3*
Drug metabolism - cytochrome P450	127	3.1547	7	0.035916		*AOX1, ALDH1A3, ADH1A, ADH1B, ADH1C, GSTP1, FMO2*
Mucin type O-Glycan biosynthesis	32	0.79488	3	0.043479		*ST3GAL2, GALNTL2, GALNT12*

Add. Table 11: Integrated pathway analysis result from comparison of the metabolic clusters Mc1 compared to Mc3

Pathway	Total	Expected	Hits	P.Value	Metabolite hits	Gene hits
Glycerophospholipid metabolism	119	2.5977	9	0.0009	Glycerophosphocholine, Phosphocholine	*LCAT, PLA2G5, LPCAT2, PPAP2A, PPAP2B, PLD1, AGPAT4*
Ether lipid metabolism	51	1.1133	5	0.0045		*PPAP2A, PPAP2B, PLA2G5, PLD1, LPCAT2*
D-Glutamine and D-glutamate metabolism	9	0.19646	2	0.0153	Glutamate	*GLS*
Glycosaminoglycan biosynthesis - chondroitin sulfate	14	0.30561	2	0.0360		*XYLT1, CHSY3*

Paper III

Is not included due to copyright